CORA Cork Open Research Archive
Cartlann Taighde Oscailte Chorcaí

Title	Immune and stress factors in the pathophysiology of the mdx mouse model of Duchenne Muscular Dystrophy
Authors	Manning, Jennifer
Publication date	2014
Original Citation	Manning, J. 2014. Immune and stress factors in the pathophysiology of the mdx mouse model of Duchenne Muscular Dystrophy. PhD Thesis, University College Cork.
Type of publication	Doctoral thesis
Rights	© 2014, Jennifer Manning. - http://creativecommons.org/licenses/by-nc-nd/3.0/
Download date	2026-11-02 14:45:01
Item downloaded from	https://hdl.handle.net/10468/1902



UCC
University College Cork, Ireland
Coláiste na hOllscoile Corcaigh

Ollscoil na hÉireann
THE NATIONAL UNIVERSITY OF IRELAND

Coláiste na hOllscoile, Corcaigh
UNIVERSITY COLLEGE CORK



Immune and stress factors in the pathophysiology of the *mdx* mouse model of Duchenne Muscular Dystrophy

Thesis presented by
Jennifer Manning, BSc (Hons)
Department of Physiology

Under the supervision of
Dr. Dervla O'Malley

Head of Department
Professor Ken D. O'Halloran

for the degree of
Doctor of Philosophy
April, 2014

Table of Contents

Table of Figures ..... ***VI***

List of Tables ..... ***IX***

List of Abbreviations ..... ***X***

Declaration ..... ***XII***

Acknowledgements ..... ***XIII***

Publications arising from this thesis ..... ***XV***

Abstract ..... ***XVI***

Chapter 1: Introduction ***1***

1.1 Duchenne Muscular Dystrophy ***2***

1.2 Dystrophin ***3***

1.2.1 The Dystrophin Gene 3

1.2.2 The Dystrophin Protein 4

1.2.2.1 Structure 4

1.2.2.2 Function 5

1.3 The Role of Dystrophin in the Pathogenesis of DMD ***7***

1.3.1 Mechanical Hypothesis 7

1.3.2 Calcium Hypothesis 7

1.3.3 Inflammation Hypothesis 8

1.4 Pathophysiological Changes Induced by Loss of Dystrophin ***10***

1.4.1 Striated Skeletal Muscle 10

1.4.2 Diaphragm 12

1.4.3 Cardiac Muscle 12

1.4.4 Smooth Muscle 13

1.5 The mdx mouse model as a model of DMD ***15***

1.5.1 Emulating the human disease severity in *mdx* mice 15

1.6 Inflammatory Mediators in DMD ***16***

1.6.1 Interleukin-6: A Myokine Released from Damaged Muscle 16

1.6.2 Mechanism of action of IL-6 17

1.7 The occurrences of co -morbidities in DMD ***19***

1.7.1 Depression in DMD 19

1.7.2 Anxiety in DMD 21

1.7.3 Stress in DMD 22

1.8 Current therapeutic strategies for DMD ***25***

1.8.1 Genetic therapy 26
1.8.2 Pharmaceutical Interventions targeting inflammation in DMD 30
1.9 Conclusions 33
1.10 Thesis Layout and Rationale 34

Chapter 2: Methods 35
2.1 Ethical Approval and Animal License 36
2.2 Animals 36
2.3 In vivo Studies 37
2.3.1 Stress Induced Defecation 37
2.3.2 Behavioural Tests 37
2.4 Collecting and Processing Tissue 41
2.4.1 Histology 42
2.4.2 Imaging Techniques 44
2.5 Biochemical Analysis 46
2.5.1 Protein Quantification 46
2.5.2 Enzyme Linked Immunosorbent Assay (ELISA) 49
2.5.3 Western Blot 51
2.6 High Performance Liquid Chromatography (HPLC) 55
2.7 Organ Baths 59
2.7.1 Colon Organ Baths 59
2.7.2 Diaphragm Organ Baths 62
2.8 Statistical Analysis of Data 65
2.9 Reagents 65

Chapter 3: Investigating the potential benefits of amitriptyline in treating inflammation and mood in mdx mice 66
3.1 Introduction 67
3.1.1 Mood Disorders in Duchenne Muscular Dystrophy 67
3.1.2 Amitriptyline as a potential pluripotent anti-depressant 68
3.1.3 Hypothesis 69
3.1.4 Specific Study Aims 69
3.2 Methods 70
3.2.1 Animals and experimental design 70
3.2.2 Techniques 71
3.3 Results 72

Part 1: Assessing mdx behaviours and skeletal inflammation ***72***

3.3.1 Behavioral phenotype of *mdx* mice 72

3.3.2 *Mdx* striated skeletal muscle exhibit histological signs of regeneration and infiltration of mononuclear cells 78

3.3.3 IL-6 ELISA for Homogenized Muscle 81

3.4 Part 2 ***82***

Intervention Study - The effects of amitriptyline on mdx behaviour and inflammation ***82***

3.4.1: The effects of amitriptyline on *mdx* behaviour and inflammation 82

3.4.2 Amitriptyline alters amine levels in several brain regions of *mdx* mice 86

3.4.3 Amitriptyline reduces histopathological changes in *mdx* mice 88

3.4.4 Amitriptyline lowers IL-6 levels in plasma of treated *mdx* mice 91

3.5 Discussion ***92***

3.5.1 The behavioural profile of *mdx* mice 92

3.5.2 Altered expression of monoamines in *mdx* brain 94

3.5.3 Histopathological changes in *mdx* skeletal muscle 97

3.5.4 Interleukin-6 - a key modulator of inflammation in DMD? 98

3.6 Conclusions ***99***

Chapter 4: The role of IL-6 and Urocortin 2 in dysfunction of the diaphragm in the mdx mouse ***100***

4.1 Introduction ***101***

4.1.1 Dytrophin deficiency in the diaphragm 101

4.1.2 Diaphragm dysfunction in the *mdx* mouse 101

4.1.3 Investigating Potential Therapies 102

4.1.4 Hypothesis 104

4.1.5 Specific Study Aims 104

4.2 Methods ***105***

4.2.1 Animals and study protocol 105

4.2.2 Techniques: ***106***

4.3 Results part one: Diaphragm function in WT and mdx mice ***108***

4.3.1 Diaphragm function in WT and *mdx* mice 108

4.3.2 Repeated Stimulation 118

Part Two: Effect of monoclonal IL-6R antibodies and/or a CRFR 2 agonist (Urocortin 2) on mdx diaphragm muscle function ***122***

4.4.1 Diaphragm Function with intervention studies compared to saline treated *mdx* mice 122

4.4.2 Repeated Muscle Stimulation 132
4.4.3 Blocking IL-6 signalling in *mdx* mice significantly lowers IL-6 protein in diaphragm muscle 136
4.5 Discussion ***138***
4.5.1 Isometric contractile properties of *mdx* muscle 141
4.5.2 Effect of intervention on *mdx* isometric contractile properties 142
4.5.3 Isotonic contractile shortening of *mdx* muscle compared to WT controls 144
4.5.4 Effect of interventions on *mdx* isotonic contractile shortening properties 144
4.5.5 Isotonic mechanical work production of *mdx* muscle compared to WT controls 145
4.5.6. Effect of intervention on work production 145
4.5.7 Isotonic shortening velocity and power production in *mdx* mice compared to WT controls and the change in shortening velocity following treatments 146
4.5.8 Repeated stimulation in *mdx* muscle – Isotonic Fatigue Protocol 147
4.5.9 Effect of repeated stimulation on velocity and power production 148
4.6 Conclusions ***149***

Chapter 5: The role of IL-6 and CRF in gastrointestinal dysfunction in the mdx mouse ***150***
5.1 Introduction ***151***
5.1.2 Interleukin-6 and GI function 151
5.1.3 The role of the stress hormone - CRF in GI dysfunction in the *mdx* mouse 152
5.1.4 Interaction between IL-6 and the CRF family of proteins 153
5.2 Methods ***156***
5.2.1 Animals and Experimental Design 156
5.2.2 Techniques 158
Part One: Characterisation of distal colon physiology in mdx and WT mice ***159***
5.3.1 Mdx faecal wet weight or water content does not differ from WT controls 159
5.3.2 Alterations in *mdx* colonic morphology 162
5.3.3 Functional differences in *mdx* colon contractility 166
5.3.4 Summary of results Part 1 172
Part Two: Effect of blocking IL-6R signalling in the absence or presence of a CRFR2 agonist on mdx mouse colonic pathophysiology **174**
5.4.1 Faecal output in *mdx* mice was not changed by intervention treatments 174
5.4.2 The effects of interventions on colonic motility in *mdx* mice 176
5.4.3 *Mdx* colonic length following interventions 181
5.4.4 Interventions change the amplitude of contraction in *mdx* mice 184

5.4.5 Intervention studies change the frequency of contractions in *mdx* mice when compared to saline *mdx* mice 188

5.4.6 Intervention studies change levels of IL-6 and IL-6 receptor in the colon of treated mice compared to saline controls 190

5.5 Discussion ***191***

5.5.1 Faecal output changes in *mdx*mice 195

5.5.2 Faecal output changes in *mdx* mice and a role for IL-6 signalling and Urocortin 2 in transit time 196

5.5.3 Faecal composition is not changed in *mdx* mice 197

5.5.4 Morphological changes in *mdx* mice 198

5.5.4.1 Morphological changes in *mdx*mice by blocking IL-6 signalling and CRFR2 agonism 199

5.5.5 Colonic contractile changes in *mdx* to exogenous stimuli 200

5.5.6 Conclusions 204

Chapter 6: Summary and Conclusions ***206***

6.1 Summary of Results 207

6.2 Limitations 210

6.3 Future Studies 211

6.4 Implications 211

Chapter 7: Bibliography ***212***

Appendix ***237***

GAPDH 238

IL-6R 240

IL-6 243

Loading control example 245

Table of Figures

Chapter 1:	**Introduction**	
Figure 1.1:	Dystrophin Protein Structure	4
Figure 1.2:	Dystrophin Associated Protein Complex (DAPC)	6
Figure 1.3:	Hypotheses of pathology in DMD	9
Figure 1.4:	Interleukin-6 Receptor signalling	18
Figure 1.5:	A schematic representing the interaction of the inflammatory response, stress hormones and the HPA axis	25
Figure 1.6:	Antisense nucleotides as a therapy for DMD	29
Chapter 2:	**Methods**	
Figure 2.1:	A diagram detailing the dimensions of the open field arena	40
Figure 2.2:	Novel Object Recognition Test still images from video recording of trials	40
Figure 2.3:	Representative image of the technique used to score striated skeletal muscle for myo-phagocytosis	44
Figure 2.4:	Representative image of colon scored for muscle layer thickness	45
Figure 2.5:	Schematic of a PVDF membrane containing immobilised proteins which have been separated by electrophoresis	50
Figure 2.6:	Schematic of an Enzyme Linked Immunosorbent Assay in a 96 well plate well	52
Figure 2.7:	Schematic of the colon organ bath set-up	61
Figure 2.8:	Protocol for diaphragm organ bath	62
Figure 2.9:	Schematic of the diaphragm organ bath set-up	64
Chapter 3:	**Investigating the potential benefits of amitriptyline in treating inflammation and mood in the *mdx* mouse**	
Figure 3.1:	Open Field Behavioural Analysis	73
Figure 3.2:	Open Field Behavioural Analysis	74
Figure 3.3:	Novel Object Recognition Test Analysis	76
Figure 3.4:	Tail Suspension Behavioural Analysis	76
Figure 3.5:	Pathohistological Analysis of skeletal muscle inflammatory markers	79
Figure 3.6:	ELISA analysis of IL-6 in homogenised skeletal muscle of the forelimb	80
Figure 3.7:	Open Field Behavioural Analysis of amitriptyline treated *mdx* mice compared to saline *mdx* controls	82
Figure 3.8:	Novel Object Recognition Behavioural Analysis of amitriptyline treated *mdx* mice compared to saline *mdx* controls	84
Figure 3.9:	Tail Suspension behavioural Analysis of amitriptyline treated *mdx* mice compared to saline controls	84
Figure 3.10:	Pathohistological Analysis Tail Suspension behavioural Analysis of amitriptyline treated *mdx* mice compared to saline *mdx* controls	88

Figure 3.11:	ELISA analysis of IL-6 in plasma Analysis of amitriptyline treated *mdx* mice compared to saline *mdx* controls	89
Chapter 4:	**The role of IL-6 and Urocortin 2 in dysfunction of the diaphragm in the *mdx* mouse**	
Figure 4.1:	Twitch Kinetics of WT and *mdx* mice diaphragm	108
Figure 4.2:	Peak Specific Force of WT and *mdx* mice diaphragm	109
Figure 4.3:	Load-Shortening Relationship in WT and *mdx* diaphragm	112
Figure 4.4:	Mechanical Work Production in WT and *mdx* diaphragm	113
Figure 4.5:	Load-Shortening Velocity relationship in WT and *mdx* diaphragm	115
Figure 4.6:	Load - Power relationship in WT and *mdx* diaphragm	116
Figure 4.7:	Shortening-Time relationship in WT and *mdx* diaphragms during repeated muscle stimulation	118
Figure 4.8:	Velocity-Time relationship comparing WT and *mdx* diaphragm during repeated muscle stimulation	119
Figure 4.9:	Power-Time relationship comparing WT and *mdx* diaphragms during repeated muscle stimulation	120
Figure 4.10:	Twitch Kinetics in *mdx* diaphragm with and without drug interventions	122
Figure 4.11:	Specific Peak Force in *mdx* diaphragm with and without drug interventions	123
Figure 4.12:	Load-Shortening Relationship in *mdx* diaphragms with and without interventions	126
Figure 4.13:	Mechanical Work Production in *mdx* diaphragms with and without interventions	127
Figure 4.14:	Shortening Velocity Relationship in *mdx* diaphragms with and without interventions	129
Figure 4.15:	Mechanical Power Production in *mdx* diaphragms with or without intervention	130
Figure 4.16:	Muscle Shortening-Time relationship in *mdx* diaphragms with or without intervention	132
Figure 4.17:	Velocity-Time relationship in treated *mdx* diaphragms with or without intervention	133
Figure 4.18:	Power-Time relationship in treated *mdx* diaphragms with or without intervention	134
Figure 4.19:	Western Blot Densitometry analysis of IL-6 and IL-6 receptor expression in *mdx* diaphragms	136
Chapter 5:	**The role of IL-6 and CRF in gastrointestinal dysfunction in the *mdx* mouse**	
Figure 5.1:	Analysis of faecal weight and water content between WT and *mdx* mice	159
Figure 5.2:	Analysis of faecal boli excreted between *mdx* and WT mice	160
Figure 5.3:	Colon Morphology in *mdx* and WT mice	162
Figure 5.4:	Histological analysis of colon layer thickness	164
Figure 5.5:	Amplitude change induced by addition of compounds to in vitro colon preparations in untreated *mdx* and WT mice	166
Figure 5.6:	Amplitude change induced by addition of compounds to in vitro colon preparations in untreated *mdx* and WT mice	167

Figure 5.7:	Effect of amplitude change on reaction to TTX blocked colonic contractibility	170
Figure 5.8:	Frequency of Contractions evoked by IL-6 and CRF	172
Figure 5.9:	Faecal water content with or without intervention	174
Figure 5.10:	Analysis of faecal boli excreted	176
Figure 5.11:	Analysis of faecal treatment times after treatment with Urocortin 2	177
Figure 5.12:	Analysis of faecal transit times after treatment with anti IL-6R and Urocortin 2	178
Figure 5.13:	Faecal output comparing all treatments	179
Figure 5.14:	Colon length measured with or without drug intervention	181
Figure 5.15:	Colon length measured with or without interventions	182
Figure 5.16:	Treated *mdx* mice compared to saline in the addition of compounds; IL-6, CRF or IL-6+CRF	185
Figure 5.17:	Contractile properties of *mdx* treated mice	186
Figure 5.18:	Frequency of Contraction	188
Figure 5.19:	Western Blot protein analysis	190

List of Tables

Chapter 2:	**Methods**	
Table 2.1:	PBS and Harris' Haematoxylin Recipe	43
Table 2.2:	Lysis Buffer Recipe	47
Table 2.3:	Bradford Assay Standard Curve dilutions of Bovine Serum Albumin	47
Table 2.4 and 2.5:	Running and Transfer Buffer Recipe for Western Blot	48
Table 2.6:	Table of antibodies used in Western Blot Technique including host animal, dilution and incubation time and temperature and blocking solution	53
Table 2.7 and 2.8:	Resolving and Stacking Gel Recipe	54
Table 2.9:	HPLC Buffer Recipe	56
Table 2.10:	HPLC Internal Standards	57
Table 2.11:	Equation and Legend to determine $A_{unk,}$ Amount of Amine in sample (ng/g of tissue)	58
Table 2.12:	Krebs' Physiological Solution	60
Chapter 3:	**Investigating the potential benefits of amitriptyline in treating inflammation and mood in the *mdx* mouse**	
Table 3.1	Treatment groups and timeline	69
Table 3.2:	HPLC monoamine analysis of areas important in depression and anxiety in WT	85
Table 3.3:	HPLC monoamine analysis of areas important in depression and anxiety in *mdx*	86
Chapter 4:	**The role of IL-6 and Urocortin 2 in dysfunction of the diaphragm in the *mdx* mouse**	
Table 4.1:	Experimental groups & details of intervention protocol	105
Table 4.2:	Diaphragm preparation properties and isometric kinetic values WT and *mdx* mice	110
Table 4.3:	Diaphragm preparation properties and isometric kinetic values for saline and treated *mdx* mice	124
Chapter 5:	**The role of IL-6 and CRF in gastrointestinal dysfunction in the *mdx* mouse**	
Table 5.1:	Experimental groups and N numbers & a timeline of injection and in vivo experimentation	156

List of Abbreviations

5-HIAA	5-Hydroxyindoleacetic acid
5HT	Serotonin
ACTH	Adrenocorticotropic hormone
AEEC	Animal Experimentation Ethics Committee
BMD	Becker's Muscular Dystrophy
BSA	Bovine serum albumin
Ca^{2+}	Calcium ions
CK	Creatine kinase
CNS	Central nervous system
CRF	Corticotrophin Releasing Factor
DA	Dopamine
DAPC	Dystrophin associated protein complex
dH_20	Deionised water
DMD	Duchenne Muscular Dystrophy
DOPAC	3,4-Dihydroxyphenylacetic acid
ECG	Electrocardiogram
ECL	Enhanced Chemiluminescence
EDL	Extensor Digitorum Longus
EDTA	Ethylenediaminetetraacetic acid
EEG	Electroencephalography
EGG	Electrogastrography
ELISA	Enzyme Linked Immunosorbant Assay
FTC	Filter topped cages
GAPDH	Glyceraldehyde 3-phosphate dehydrogenase
GCPR	G-coupled protein receptors
GI	Gastrointestinal
H&E	Haematoxylin & Eosin
H_2SO_4	Sulphuric acid
HPA	Hypothalamic-pituitary-adrenocortical
HPLC	High Performance Liquid Chromatography
HVA	Homovanillic acid
IBD	Inflammatory bowel disease
IBS	Irritable bowel syndrome
I-CAM1	Intercellular Adhesion Molecule 1
Iκ-B	Inhibitor of Kappa B
IL-1	Interleukin 1
IL-6	Interleukin 6
IL-6R	Interleukin-6 receptor
iNOS	Inducible nitric oxide synthase

IVC	Individually ventilated cages
Krebs	Krebs' physiological saline solution
L_O	Optimum length
LPS	Lipopolisaccharide
mdx	C57BL/10ScSn-*Dmd*^{mdx}/J
MMC	Migrating motor complexes
mV	Millivolt
NA	Noradrenaline
NaCl	Saline
NFκB	Kappa-light-chain-enhancer of activated B cells
NOR	Novel Object Recognition
PBS	Phosphate buffered saline
PBS-T	Phosphate Buffered Saline - Tween
PFA	Para formaldehyde
PMO	Phosphorodiamidate morpholino oligomers
PVDF	Polyvinylidene fluoride
ROS	Reactive oxygen species
SDS	Sodium dodecyl sulfate
SNRI	Serotonin noradrenaline reuptake inhibitor
TCA	Tricyclic antidepressant
TGF β1	Transforming growth factor β1
TNF	Tumour Necrosis Factor
TST	Tail suspension test
TTX	Tetrodotoxin
UCC	University College Cork
WT	Wild type

Declaration

This dissertation has not been submitted in whole or in part for any other degree, diploma or qualification at University College Cork or elsewhere. All work presented in this thesis is original and entirely my own.

_____

Jennifer Manning

April 2014

Acknowledgements

To Dr. Dervla O'Malley, my supervisor, without whom this thesis would not be, thanks for everything. I am forever grateful to you and to Prof. O'Halloran; similarly, for taking me into the Department of Physiology and for the support I've received from day one, thank you both.

To the staff and members of Muscular Dystrophy Ireland for the funding, support and opportunity to present my findings directly to you each year, I sincerely thank you all.

To the staff of the physiology, anatomy & neuroscience, pharmacology department and especially the staff of the BSU, thanks for putting up with me and facilitating my project.

To the PhD students in the Physiology Department, I've been so lucky to have had the best coffee breaks and never ending offers of help and encouragement. Thank you all, you're a great bunch of scientists and great friends. For fear of leaving someone out, I won't name anyone… but you know who you are, and you guys are very special to me!

To Diane and Mr. Fehily and all the staff at Roman House in the past ten years – without the support and your kind encouragement, I wouldn't have gotten this far.

To my Ventures in 11th Cork Cloghroe Scout Group I've never made a better decision and the past two years has been great, thanks for keeping me sane while driving me mad!!!

Janelle, I hope you are happy with yourself! Your stubborn insistence is the reason for this train…. On a track, in a tunnel or something?! Let's stick to science actually… Thanks Janelle. And to Elaine, Locko… Thanks you for understanding and walking with me in this, there's light at the end of the tunnel, you are next!!!!!!

For all the friends I know who don't do science (not sure what that is about), thanks for your patience over the past few years, and especially for not asking is it finished yet…

To my family, extended and especially my own family for putting up with my singing at the kitchen table while writing at all hours, thank you.

To my sister Laura, your wisdom is admirable and its always you I turn to for practical advice "stop thinking" is the usual response and you are always right!

My brother, David thanks for your never ending banter and occasional challenging science conversations. Best siblings I could have asked for.

And to Ian, you… are my favourite.

To my parents,

I couldn't possibly even begin to thank you enough for all the support and patience,

I dedicate this thesis to you.

Publications arising from this thesis

Abstracts

"Investigating emotional disturbances and muscle damage in an animal model of Duchenne Muscular Dystrophy and possible correlations."

Irish Journal of Medical Science, 2010

"*Gastrointestinal Contractile Activity in the mdx mouse, a Model of Duchenne Muscular Dystrophy: A Role for Interleukin-6 in Pathophysiology?"*

Irish Journal of Medical Science, 2012

"The role of interleukin-6 in gastrointestinal contractile activity in a mouse model of Duchenne Muscular Dystrophy."

IUPS, Birmingham 2013

Papers

"Old drug, new use: Can Amitriptyline improve mood & reduce skeletal muscle inflammation in a mouse model of Duchenne Muscular Dystrophy?"

The Boolean, UCC (Vol 3) 2012

"Amitriptyline is efficacious in ameliorating muscle inflammation and depressive symptoms in the mdx mouse model of Duchenne muscular dystrophy."

Experimental Physiology, June 2014

Abstract

Duchenne Muscular Dystrophy (DMD) is a fatal multi-system neuromuscular disease caused by loss of dystrophin. The loss of dystrophin from membranes of contractile muscle cells and the dysregulation of the DAPC, induces chronic inflammation due to tissue necrosis and eventual replacement with collagen which weakens muscular force and strength. Patients are wheel chair bound by their teen years and premature death is typically due to respiratory failure.

However, different isoforms of dystrophin are present in other tissues, including smooth muscle and neurons although the consequences for loss of dystrophin in these tissues are poorly understood. Indeed, under-diagnosed features of DMD include mood disorders such as depression and anxiety and dysfunction of the gastrointestinal tract.

The first study in the thesis examined mood in the dystrophin-deficient *mdx mouse* model of DMD and examined the effects of the tri-cyclic antidepressant, amitriptyline on behaviours. Amitriptyline had anti-depressant and anxiolytic effects in the *mdx* mice possibly through effects on stress factors such as corticotrophin-releasing factor (CRF). This anti-depressant also reduced skeletal muscle inflammation and caused a reduction in circulating interleukin (IL)-6 levels.

In the second and third studies, we specifically blocked IL-6 signalling and used Urocortin 2, CRFR2 agonist to investigate their potential as therapeutic targets in *mdx* mice pathophysiology. Isometric and isotonic contractile properties of the diaphragm, were compared in *mdx* mice treated with anti IL-6 receptor antibodies (anti IL-6R) and/or Urocortin 2. Deficits in force production, work and power detected in *mdx* mice were improved with treatment.

In study three I investigated contractile properties in gastrointestinal smooth muscle. As compared to wild type mice, *mdx* mice had slower faecal transit times, shorter colons with thickened muscle layers and increased contractile activity in response to recombinant IL-6. Blocking IL-6 signalling resulted in an increase in colon length, normalised faecal output times and a reduction in IL-6-evoked contractile activity.

Interestingly, *mdx* mice treated with Urocortin 2 also had beneficial results in gastrointestinal function.

The findings from these studies indicate that for both diaphragm and gastrointestinal function in a dystrophin-deficient model, targeting of IL-6 and CRFR2 signalling has beneficial therapeutic effects.

Chapter 1: Introduction

1.1 Duchenne Muscular Dystrophy

Duchenne Muscular Dystrophy (DMD) is a fatal X-chromosome linked recessive disorder caused by the truncation or deletion of the dystrophin gene (Bulfield 1984). It is a multi–system disorder with manifestations in striated and smooth muscle and the nervous system (Torelli et al. 1999). DMD is the most frequently occurring type of muscular dystrophy, its incidence worldwide is 1 in every 3,500 live male births (Emery & Muntoni 2003) and has the most severe symptoms of the muscular dystrophies.

The most obvious and debilitating characteristic is the progressive weakening of skeletal muscles resulting in severe disability and premature death (Yiu & Kornberg 2008). This is due to a loss of the functional protein dystrophin, which acts to anchor the extracellular matrix to the actin cytoskeleton and is associated with a protein complex called the hetero-oligomeric protein complex named the dystrophin associated protein complex (DAPC) which spans the sarcolemma. In DMD, disruptions in the reading frame result in loss of dystrophin, whereas in Becker's Muscular Dystrophy (BMD) an in-frame deletion results in a truncated protein and a milder form of the disease (Koenig et al. 1989). Myofibres are the contractile cell type in muscle responsible for movement (Podhorska-Okolow et al. 1998) and in the absence of dystrophin, a muscle contraction mechanically stresses the plasma membrane, inducing damage to the myofibres (Gumerson & Michele 2011).

Clinical presentation of DMD occurs between 3 and 5 years of age with motor delay or abnormal gait as key indicators. Such phenotypical presentation of the disease is the first step in diagnosing DMD in young patients who exhibit developmental delays (Essex & Roper 2001). Affected boys have difficulty in running, they tend to walk on their toes, fall frequently, cannot jump (Manzur et al. 2007) and exhibit pseudo - hypertrophy of the calf muscles (Cros et al. 1989). In the past, the classical diagnostic test for DMD was to test raised serum enzyme levels, such as lutamic-oalacetic transaminase, glutamic-pyruvic transmaine, aldolase and most known creatine kinase (CK) levels (Dubowitz 1976) and was used as an early biomarker of the disease. However, genetic testing (Ashton et al. 2008; den Dunnen & Beggs 2006) now complements this assay as a definitive diagnostic test. Molecular diagnosis of the disease along with muscle biopsy to test for the presence

or absence of dystrophin at a cellular level (Itto et al. 2013; Sang-Jun et al. 2013; Essex & Roper 2001) is now commonly used. Patients are usually wheelchair-bound by age twelve (Wagner 2008) and have an average life expectancy of just over twenty years, with cardiomyopathy later in the disease (Yiu & Kornberg 2008). Although, therapeutic strategies such as ventilators are raising life expectancy and improving the quality of life for boys affected with the disease (Yiu & Kornberg 2008) there is currently no effective cure for DMD.

1.2 Dystrophin

1.2.1 The Dystrophin Gene

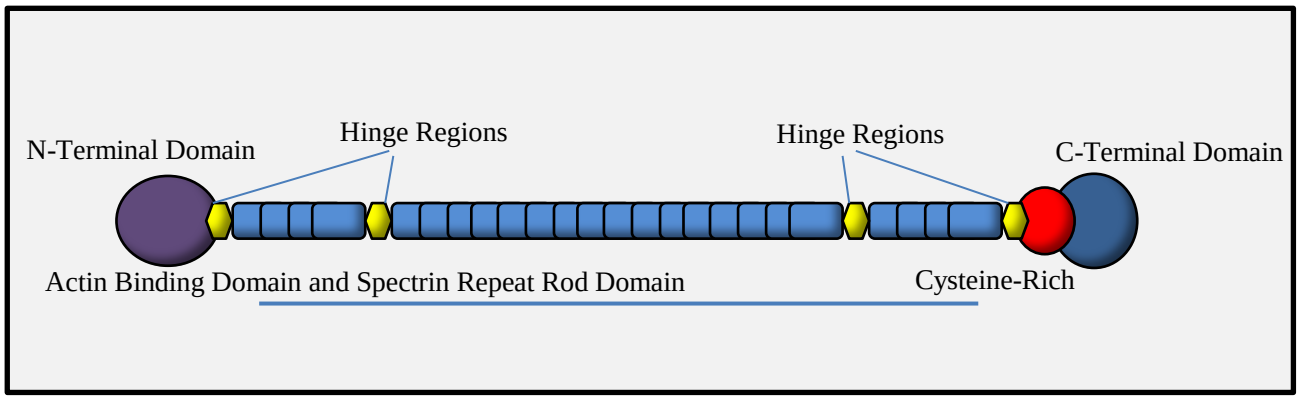
DMD is an X-chromosome linked recessive disorder caused by mutations in the dystrophin gene at Xp21. The dystrophin gene consists of 2.6 million base pairs and contains 79 exons. Introns make up 99.4% of the gene. It is the largest human gene corresponding to 0.1% of the entire human genome (Passamano et al. 2012). Its relatively large size makes it susceptible to genetic rearrangements and mutations. A third of all cases of DMD result from mutations which arise spontaneously (Muntoni et al. 2003). Approximately 65% of patients suffering from DMD have intragenic out-of-frame deletions, 10% have duplications of one or more exons of the gene and the remaining 25% have various point mutations (Aartsma-Rus et al. 2006). Frame-shift deletion of the dystrophin gene results in DMD, as seen in 90% of cases (Koenig et al. 1989). Other mutations of the gene result in BMD, where a truncated dystrophin protein is translated. In this case, some function is restored to the DAPC (Muntoni et al. 1994; Koenig et al. 1989; Hu et al. 1991; Feng et al. 2013; Wang et al. 2013; Lochmüller & Bushby 2013).

The dystrophin protein has 7 different promoter sites, resulting in different isoforms of the protein. The most common isoform is the Dp427 m-isoform, found in skeletal muscle (Monaco et al. 1986; Koenig et al. 1987), other variants of 427kD length in humans include Dp427-l, -c and –p, expressed in lymphoblastoid cells (Nishio et al. 1994), cortical (Nudel et al. 1989) and purkinje cells (Byers et al. 1993) respectively. A shorter protein named Dp260 is expressed in the retina (Kameya et al. 1997; Ervasti 2007). Dp140 isoform is found in the central nervous system (CNS) and kidney (Kameya et al. 1997), Dp116 in Schwann cells (Byers et al. 1993), Dp71 and Dp40 (Tinsley et al. 1993) expressed ubiquitously.

1.2.2 The Dystrophin Protein

1.2.2.1 Structure

Translation of the dystrophin gene results in a rod-shaped cytoskeletal protein (see Figure 1.1). Its long m - isoform (which is not present in DMD) is composed of 3,685 amino acid residues with a molecular weight of 427kD (Hoffman et al. 1987). Dystrophin protein is found on the cytoplasmic surface of cell membranes in muscle (Ervasti 2004). It comprises of a carboxyl end, which binds to the DAPC of the sarcolemma, and an amino end which binds to the cytoskeletal actin (Chamberlain et al. 1997). The protein is made up of 4 distinct domains: the N-terminal globular domain which consists of 240 amino acids; the second rod-shaped domain consisting of 24 homologous spectrin-like repeats with around 109 amino acids, the third, a cysteine rich domain with binding sites which have uncertain physiological significance, and the fourth, a C-terminus of 420 amino acids, which binds to proteins of the DAPC; providing a link between individual fibre contractile components and the extracellular matrix (Blake et al. 1996). This structure facilitates the function of dystrophin which is described below.



<u>Figure 1.1:</u> Dystrophin Protein Structure
Comprised of a carboxyl end (C-Terminal Domain which binds to proteins of the DAPC) the second rod-shaped domain consisting of 24 homologous spectrin-like repeats with around 109 amino acids, the third, a cysteine rich domain and an amino end (Actin Binding Domain). Adapted from (Hoffman et al. 2003).

1.2.2.2 Function

In muscle, the structure of the dystrophin protein facilitates the essential protection of the sarcolemma against mechanical stress due to repeated contractions, through the link between the sub-sarcolemmal cytoskeletal actin and the extra cellular matrix (Petrof et al. 1993) through the DAPC in the sarcolemma. Destabilization of this hetero-oligomeric protein complex, in the absence of dystrophin leads to progressive damage of the muscle fibres and the compromised membrane due to these stretch induced tears (Deconinck & Dan 2007). This subsequently results in mechanical damage of muscle fibres, loss of cell integrity and eventual necrosis.

Regeneration of muscle fibres does occur initially but when this regenerative capacity is exhausted, fibrosis predominates and fatty tissue infiltrates result in muscle weakness and loss of functional contractile myofibres (Cros et al. 1989).

As dystrophin has significant interactions with the DAPC it is not surprising that its absence affects the proteins of the complex. The expression of proteins of the DAPC is changed in DMD an example being the de-localization of the syntrophin-dystrobrevin sub complex (Compton et al. 2005; Matsumura et al. 1992), the change which suggests a role for dystrophin in the organisation of the complex (Ervasti & Campbell 1991).

Phosphorylation of dystrophin affects its affinity to bind actin and syntrophin (a protein in the DAPC) which has led to the hypothesis that dystrophin has a part in intracellular signalling (Michele & Campbell 2003; Lapidos et al. 2004) and it has been demonstrated that dystrophin has a role in the control of signalling molecules such as proteins involved in intra-cytoplasmic calcium homeostasis and nitric oxide synthesis (Davies & Nowak 2006).

Dystrophin Associated Protein Complex (DAPC)

The DAPC is primarily a mechano-transducer, translating physical signals from extra-cellular matrix to changes in gene expression in the nucleus. Moreover, contractile force is communicated outward to the interfiber connective space where there is evidence that the DAPC is involved in transmembrane signalling (Lapidos et al. 2004). Disruption to the complex of proteins disturbs cell signalling pathways, and cellular defence mechanisms which are regulated by signalling cascades (Petrof, Shrager, et al. 1993; Rando 2001) such as reactive oxygen species (ROS) (Menazza

et al. 2010) and Kappa-light-chain-enhancer of activated B cells (NFκB) activation (Evans et al. 2010). The DAPC describes the association of dystrophin with a number of other proteins, including dystroglycans, sarcoglycans, dystrobrevins, syntrophins and sarcospan (Waite et al. 2009) (see Figure 1.2). Mutations in the DAPC can cause other muscular dystrophies, for instance, a mutation in any of the sarcospan-SG proteins results in limb-girdle type muscular dystrophies (Duclos et al. 1998). Abnormal expression of dystroglycan results in Fukuyama congenital muscular dystrophy, muscle–eye–brain disease, Walker–Warburg syndrome, congenital muscular dystrophies type 1C and 1D, and limb-girdle muscular dystrophy 2I (Godfrey et al. 2011). Mutations in components of the extra-cellular matrix associated with the DAPC can also cause muscular dystrophies, e.g. congenital muscular dystrophy (MDC1A) is caused by mutations in the LAMA2 gene that encodes the laminin a2-chain. Mutations in collagen VI genes cause Ullrich syndrome and Bethlem myopathy (Kanagawa & Toda 2008).

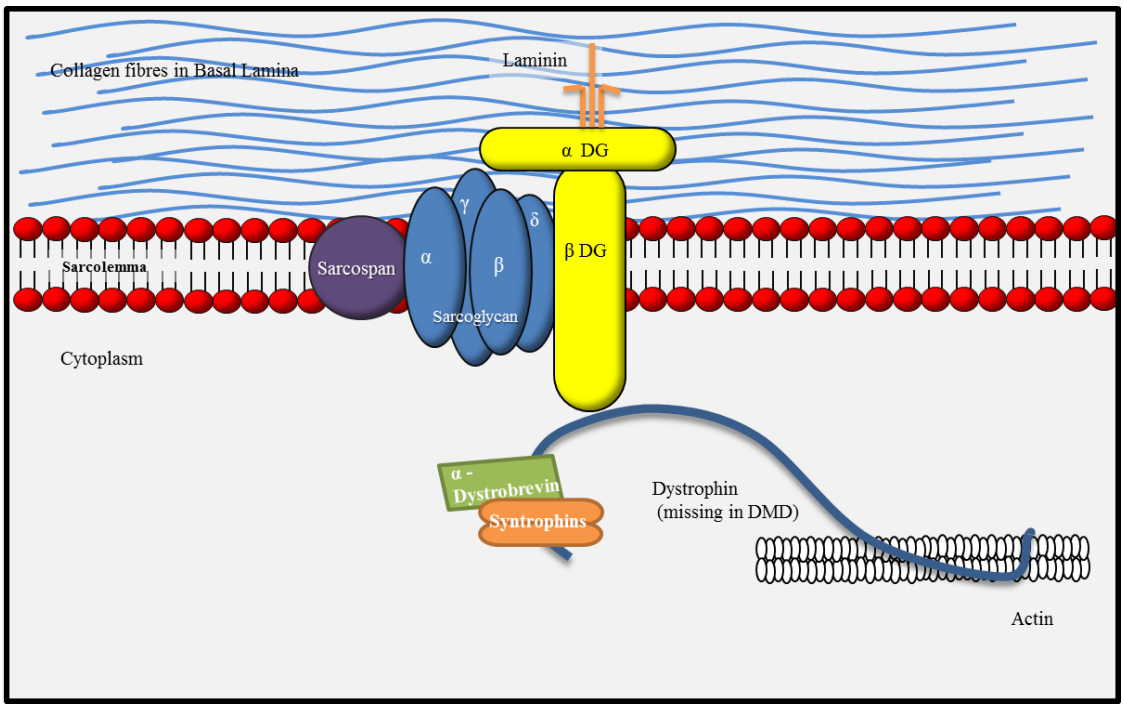


Figure 1.2: Dystrophin Associated Protein Complex (DAPC)
The DAPC comprises proteins bound to dystrophin on the subsarcolemmel side of the membrane including α-dystrobrevin, and membrane bound proteins; sarcospan, α-, β-, γ-, δ-sarcoglycan, α-, β-dystroglycans and laminin. Dystrophin anchors the extracellular collagen matrix to intra cellular cytoskeletal actin through the complex. Adapted from (Ervasti 2004).

1.3 The Role of Dystrophin in the Pathogenesis of DMD

There are three main hypotheses for the role of dystrophin in DMD, the mechanical, calcium and inflammatory hypothesis (Summarised in Figure 1.3).

1.3.1 Mechanical Hypothesis

As dystrophin functions to protect muscle fibres from the mechanical stress of contraction, loss of this protein causes increased sarcolemmal fragility making them susceptible to mechanical damage (Moens et al. 1993). Indeed, in the dystrophin-deficient *mdx* mouse, its myofibres are more susceptible to contraction- and stretch-induced damage manifesting as sarcolemmal tears (Moens et al. 1993). The degree of mechanical damage has been correlated to muscle fibre diameter and weight bearing capacity of the muscle. Thus, larger weight bearing muscles, such as the proximal muscles of the leg are the first to show signs of weakness and fatigue in DMD (Petrof et al. 1993). It is noteworthy to note that this models disease profile is age dependant. In contrast, muscle fibres of smaller diameter which bear less weight such as the distal foot muscles undergo less mechanical damage, and are spared until later in the pathogenesis of the disease (Boland et al. 1995).

1.3.2 Calcium Hypothesis

The calcium hypothesis explains the destructive effects of excessive calcium ions (Ca^{2+}) in cells through tears in the sarcolemma. Indeed, altered Ca^{2+} homeostasis has been implicated as a contributor to DMD pathophysiology with evidence of Ca^{2+} accumulation and hyper-contracted fibres in muscle biopsies of patients (Deconinck & Dan 2007; Zeiger et al. 2010). Increased intracellular Ca^{2+} (Mallouk et al. 2000) seen in DMD can be detrimental to the fibre as prolonged increases in Ca^{2+} concentrations in skeletal muscle fibres leads to activation of cytosolic proteases, which exacerbate the damage and can lead to fibre necrosis (Spencer et al. 1995). Moreover, twice the normal Ca^{2+} levels have been observed in *mdx* myofibres (Vandebrouck et al. 2002). The *mdx mouse* model has shown that normal physiological control of Ca^{2+} homeostasis is lost, has leaky Ca^{2+} channels (Fong et al. 1990; Turner et al. 1993) and abnormal mitochondrial Ca^{2+} handling (Ruegg et al. 2002).

In contrast, the extra-ocular muscles are spared in DMD and this may be due to superior control of Ca^{2+} homeostasis in these muscles (as well as a reduced load-bearing function) (Zeiger et al. 2010). In control animals, extra-ocular eye muscles have increased numbers of mitochondria (Felder et al. 2005) with associated enhanced abilities for Ca^{2+} uptake (Zeiger et al. 2010).

1.3.3 Inflammation Hypothesis

Of particular interest in this project is the hypothesis based on immune activation and inflammation which has been proposed as the reason for the particularly severe pathology caused by loss of dystrophin in DMD. Chronic inflammation characterises DMD, with elevations in levels of cytokine and chemokine activation, leukocyte adhesion and complement system activation (Porter et al. 2002). Changes in the profiles of pro-inflammatory cytokines such as Tumour Necrosis Factor (TNF) (Abdel-Salam et al. 2009), Interleukin 1 (IL-1) and Interleukin 6 (IL-6) (Porter et al. 2002) are detected early in the disease and the inflammatory response worsens with disease progression.

NFκB activation through the phosphorylation of Inhibitor of Kappa B (Iκ-B) kinases can be due to pro-inflammatory cytokines including IL-6 and TNF (Karin & Delhase 2000) and NFκB activated in patients with DMD (Kumar & Boriek 2003) even before pathophysiological changes are apparent and it is seen to be active in *mdx mouse* muscle too (Messina et al. 2011). In its active state, it can promote transcription of genes encoding various detrimental components of the inflammatory response; including chemokines, cytokines and adhesion molecule cells (Acharyya et al. 2007; Baldwin, Jr. 2001). The molecular mechanism underpinning the inflammatory pathogenesis in DMD is not fully understood, but NFκB activation has been implicated (Messina et al. 2011). However, there is discord in the literature with regard to the activation as NFκB activation as it diminishes with age, whereas the cytokine profile up-regulates (Messina et al. 2011).

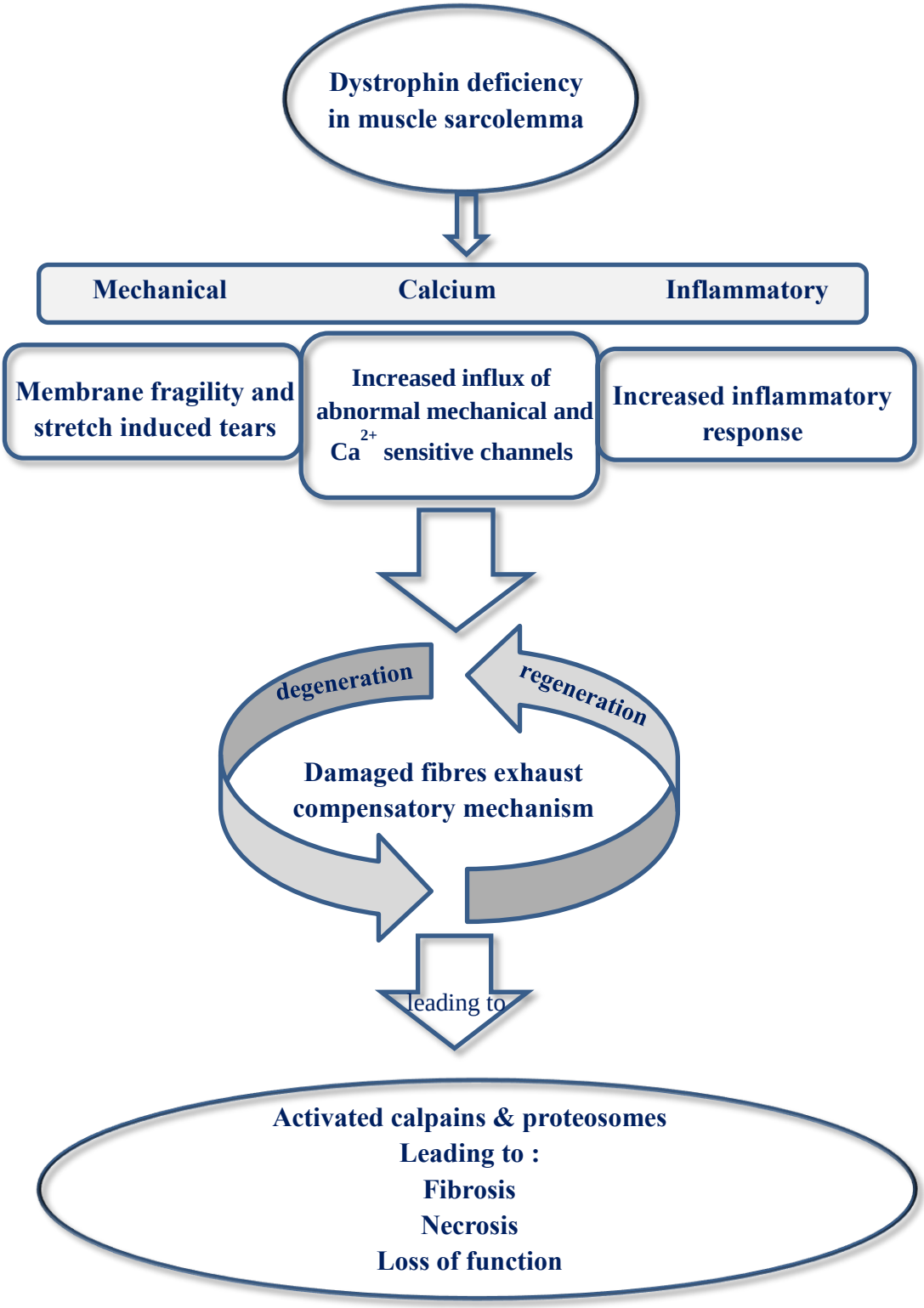


Figure 1.3: Hypotheses of pathology in DMD
Sarcolemmal integrity loss, calcium deregulation and an activated inflammatory process exasperate the pathology caused by dystrophin deficiency, leading to muscle fibre regeneration primarily and eventual fibrosis and necrosis and loss of functional muscle fibres.

1.4 Pathophysiological Changes Induced by Loss of Dystrophin

Despite the striated muscle weakness and necrosis being the primary pathophysiological changes in patients with DMD, it is a multi-system disorder affecting both smooth muscle and nervous system tissue in patients.

To understand the pathology of DMD and investigate potential therapeutic strategies, a preclinical model is required. The dystrophin-deficient *mdx mouse* was first identified in 1984 by Bulfield et al (Bulfield 1984) and is genetically comparable to the human form of DMD, that is, it lacks full length dystrophin. It does however diverge in severity in symptoms to the human condition. The phenotypical changes in skeletal, cardiac and smooth muscle in the rodent model differ to some extent as compared to the human disease. However, the *mdx mouse* has been the first step towards developing the therapies which are currently utilized in patients with DMD.

1.4.1 Striated Skeletal Muscle

The most obvious and pronounced effects of dystrophin deficiency in patients are apparent in skeletal muscle. Dystrophin comprises 0.002% of total skeletal muscle protein (Hoffman et al. 1987). In the human disease, weight bearing muscles are affected first, with weakness in the proximal lower and then upper limbs, which is followed by weakness of distal lower and then upper limbs (Barohn et al. 1998). DMD is characterised by pseudo-hypertrophy of the calf muscles (Schreiber et al. 1987), which is caused by muscle destruction, necrosis of fibres and some subsequent fibre regeneration by satellite cells, resulting in larger but significantly weaker muscle tissue. Eventually the necrosis overrides the muscles' ability to regenerate and terminal loss of function occurs (Cros et al. 1989).

Due to the degeneration and regeneration of myofibres and the associated activation of satellite cells, cell nuclei, which are normally peripherally located in the cells move to the middle of the fibres, and as such acts as a useful marker of muscle cell regeneration in histological analysis of DMD muscle (Mosqueira et al. 2013). Skeletal muscle centralised nuclei have been used as an indicator for dystrophic features in a variety of *mdx* muscles (Bulfield 1984) such as the *soleus* (Nakae et al. 2008), *tibialis anterior, extensor digitorum longus* (Baltgalvis et al. 2009) and the *gluteus* (Payne et al. 2006). *Mdx* skeletal muscle similarly progresses through

continuous degeneration and regeneration of fibre repair, starting at 2 weeks, peaking at 12 months and continuing for the life of the mouse but the severity of fibrosis and loss of function is less than that noted in human patients (Dangain & Vrbova 1984; Coulton et al. 1988). A chronic inflammatory response, as evidenced by infiltration of inflammatory cells such as macrophages, is also characteristic of DMD and *mdx mouse* peripheral skeletal muscles (Grounds et al. 2008).

Revertant Fibres

Although DMD is characterised by lack of dystrophin, residual dystrophin can be detected in up to 50% of DMD patients who express revertant fibres containing dystrophin (Thanh et al. 1995; Yokota et al. 2006). These revertant dystrophin expressing fibres exist due to the splicing machinery bypassing the mutation which causes the disease and restores a physical dystrophin protein, although these revertant fibres only comprise 1-7% of all fibres (Hoffman et al. 1990; Nicholson et al. 1993), having little benefit on muscle function. However, revertant fibres are also expressed in *mdx* mice (Hoffman et al. 1990).

Interestingly, revertant fibres do not produce an immune response which has led to the hypothesis that dystrophin replacement would be a possible therapeutic intervention in the disease (Fall et al. 2006). In humans, there has been conflicting conclusions regarding a correlation between the amount of revertant fibres and phenotypic severity of DMD (Nicholson et al. 1993), with a study concluding that numbers of revertant dystrophin positive fibres do not correlate to phenotypic severity and furthermore that these levels of dystrophin-positive revertant fibres do not change in individuals as the disease progresses (Arechavala-Gomeza et al. 2010).

1.4.2 Diaphragm

The diaphragm as a striated respiratory muscle, in constant use and is therefore affected dramatically by dystrophin deficiency. Patients with DMD exhibit diaphragm weakness in their early teens (De Bruin et al. 1997), where diaphragm muscle is thickened (De Bruin et al. 1997) due to accumulation of adipose and connective tissue. There is a reduction in force production due to these changes, however few studies in human patients have been undertaken to test this (Beck et al. 2006). This loss of force production leads to hypoventilation and hypercapnia in patients (Simonds et al. 1998). Indeed, respiratory failure is the most common cause of premature death in DMD, although artificial ventilation has led to improvements in life expectancy of patients with advanced respiratory weakness (Baydur et al. 1990).

In comparison, disease progression in the diaphragm of the *mdx mouse* most closely relates to the human condition with extensive fibrosis (Stedman et al. 1991) (Gosselin & Williams 2006), which is morphologically evident from 12 weeks of age and continues until death, although it is not as severe as the human condition (Huang et al. 2009). Force production is reduced in the diaphragm from an early age in *mdx* mice (Bates et al. 2013; Gehrig et al. 2008) with loss of mechanical work capabilities (Stevens & Faulkner 2000).

The diaphragm most closely relates to the human disease and is utilised in studies, such as our study (Study 2) to firstly, characterise dystrophin deficiency pathology and secondly, to pre-clinically investigate potential therapies.

1.4.3 Cardiac Muscle

In cardiac muscle fibres, dystrophin is present on the sarcolemma, but is also found in the T-tubules (Torelli et al. 1999), which function in the transmission of excitation coupling, but not force generation (Kaprielian et al. 2000). Loss of dystrophin protein affects cardiac muscle by inducing arrhythmias and conduction irregularities. This is in part due to cardiac fibrosis, which is irregular in area but correlates to electrocardiogram (ECG) irregularities and ventricular dysfunction (Romfh & McNally 2010). These irregularities progress in the course of the disease (Nigro et al. 1990), although most symptoms are subclinical or masked to some degree due to the physical inactivity of the patients (Nigro et al. 1990). Nonetheless, cardiac

damage is evident in one third of patients by age fourteen and in 100% of patients over eighteen years of age (Nigro et al. 1990).

Mdx mice, similar to the human disease, exhibit myocardial damage. At three months of age *mdx* mice have altered metabolic processing associated with increased oxygen consumption, decreased cardiac efficiency and increased cell membrane fragility (Khairallah et al. 2007). At six months heart-to-body weight ratios suggest the *mdx* heart is hypertrophied compared to wild type controls indicating cardiac dysfunction in aged mice. This is also reflected in changes in electrocardiography (ECG) readings (Bia et al. 1999; Stuckey et al. 2012). From nine months, fibrosis is evident histologically and by fifteen months myocardial interstitial fibrosis is detectable in the endocardium, myocardium and epicardium of the ventricular wall and septum (Marques et al. 2009).

1.4.4 Smooth Muscle

1.4.4.1 Vascular

Dystrophin is also expressed normally in the tunica media of blood vessels, but is absent in vessels from *mdx* mice causing a loss of neurovascular control (Ito et al. 2006). Abnormalities can lead to functional ischemia which may cause or exasperate the damage to myofibres due to abnormal blood flow (Engel & Hawley 1977). Because nitric oxide (NO) signalling is mediated though the DAPC (Ennen et al. 2013), and NO signalling plays a vital role in vascular health (see review (Jin & Loscalzo 2010)) loss of dystrophin in the vascular smooth muscle can cause shear stress and abnormal basal tone of the muscle (Ito et al. 2006).

1.4.4.2 Gastrointestinal

Although less abundant than either skeletal or cardiac muscle, dystrophin is found in smooth muscle cells of the gut. Differing from skeletal muscle it appears less frequently (Byers et al. 1991). Its role in gastrointestinal (GI) function can be gauged by symptoms such as GI hypo-motility of the system observed in patients resulting in acute gastric dilatation and pseudo-obstructions, which can be fatal (Dinan et al. 2003). GI symptoms including vomiting, pseudo-obstructions, diverticulum in the

colon in addition to functional abnormalities such as delayed gastric emptying time in the oesophagus and stomach (Leon et al. 1986).

Symptoms such as constipation, hard stools and reduced colonic transit time were hypothesised to be due to immobility and weakening of the skeletal muscle abdominal walls. However, in a cohort of patients with DMD, it was found that a proportion of the patients had a GI dysfunction regardless of whether they were wheelchair-bound or not and this was found to be distinct from the severity of the skeletal dysfunction in the disease (Borrelli et al. 2005).

Studies indicate that weakening of skeletal muscle is a definitive marker of DMD pathogenesis whereas abnormal electrogastrography (EGG) features may elude a to an equally important role of smooth muscle involvement in the DMD pathogenesis (Borrelli et al. 2005). Smooth muscle pathology is described in autopsied stomach tissue of a patient with DMD (Barohn et al. 1988). GI symptoms become evident in the late stages of the disease (~15 years) (Boland et al. 1996).

Investigations into the GI manifestations which arise clinically in patients have been explored in *mdx* mice. Faecal output was markedly reduced in *mdx* mice, however wet and dry weights were not changed (Mulè et al. 2010). In ilium preparations, higher amplitudes, or contractions were also reported in *mdx* mice, at 8-12 weeks of age (Baccari et al. 2007). Migrating motor complexes (MMC) characteristic of the fasting period originate proximally and propagate distally in both control and *mdx* mice at 4 months, however *mdx* mice had a higher frequency of spontaneous dysregulated MMCs (Tameyasu et al. 2004). Mice aged between 12-18 months underwent functional tests, gastric emptying after 20 minutes did not significantly change compared to WT mice, and transit rate was determined to be reduced however, without any evidence of small intestine length differences (Tameyasu et al. 2004).

1.5 The *mdx* mouse model as a model of DMD

Because the *mdx mouse* pathology is not as severe and does not progress comparatively to human DMD except for the diaphragm muscle, several optimisation tactics have been employed to make the *mdx mouse* a more physiologically analogous model of DMD.

1.5.1 Emulating the human disease severity in *mdx* mice

1.5.1.1 Exercise

Exercising *mdx* mice potentiates dysfunction associated with loss of dystrophin by increasing stretch-induced micro lesions which exacerbate myofibre necrosis and cause muscle strength deterioration (Moens et al. 1993), running causes damage to triceps, gastrocnemius and quadriceps muscles with an associated increase in plasma CK levels (Pierno et al. 2007).

1.5.1.2 Genetic Modification

The *mdx*52 (exon 52 knockout) mouse (Arakia et al. 1997) expels all reverent dystrophin fibres, which are advantageous in dystrophin replacement studies especially when expression of induced dystrophin is to be quantified. Despite evidence of increased hypertrophy in the *mdx*52 limb muscles, the disease phenotype remained similar to the *mdx mouse* (Bulfield 1984; Grounds et al. 2008).

1.5.1.3 Utrophin

The protein, utrophin exhibits 80% homology and shares structural and functional similarities with dystrophin and can interact with the same proteins that dystrophin binds within the cytoskeleton protein complexes (Matsumura et al. 2011). Under normal circumstances when dystrophin is expressed, utrophin is down-regulated in adult muscle and restricted to the myotendinous and neuromuscular junctions (Blake et al. 1996). However, with the loss of dystrophin, as is the case in *mdx* mice, utrophin can replicate the stabilizing function of dystrophin (Keep 2000) thereby preserving muscle function (Rybakova et al. 2006; Tinsley et al. 1998). Utrophin does however, differ from dystrophin in its pattern of localisation being found at the myotendinous junction and neuromuscular junction in adult tissue, whereas

dystrophin predominates in the sarcolemma of muscle fibres (Lewis & Ohlendieck 2010). Knockout mice lacking both dystrophin and utrophin were created by crossing *mdx* and utrophin-knockout mice. The protective role of utrophin in *mdx* mice (Deconinck et al. 1997) is evident in these mice as they are phenotypically the most comparable to the human DMD condition, exhibiting variability in myofibre size, hypertrophy by connective tissue replacement and the infiltration of macrophages. Life expectancy is also reduced to less than 20 weeks due to post weaning weight loss, joint contractures and kyphosis.

Increased expression of utrophin restores plasma membrane integrity and rescues dystrophin-deficient muscle in *mdx* mice (Gilbert et al. 1999) but in DMD muscle, while utrophin is up-regulated and redistributed to the sarcolemma, levels are not sufficient to prevent disease progression (Love et al. 1989).

Both revertant dystrophin expression and a high rate of cycling regeneration have meant that some characteristics of DMD such as the extent of skeletal muscle hypertrophy do not appear in the *mdx* mouse. Exacerbating the disease in *mdx* mice has produced useful information about the nature of dystrophin deficiency in patients with DMD and the *mdx mouse* remains an economical and useful model of the disease.

1.6 Inflammatory Mediators in DMD

1.6.1 Interleukin-6: A Myokine Released from Damaged Muscle

IL-6 is considered both a pro- and anti-inflammatory cytokine. Moreover, it is a myokine and is released from muscle fibres when contracted (McKay et al. 2009; Jonsdottir et al. 2000). IL-6 increases after eccentric exercise which causes ultra-structural damage and is unchanged following concentric exercise, motion which does not cause structural damage (Jonsdottir et al. 2000; Pedersen & Febbraio 2008) evidence it is indeed released from muscle undergoing fibre damage. IL-6 is seen to increase in the plasma of healthy people after muscle contraction (Pedersen & Febbraio 2008) and is elevated in the case of muscle damage (Croisier et al. 1999), making it an interesting marker and effector to look at in the context of DMD.

In other diseases associated with immune activation such as irritable bowel syndrome (IBS) and rheumatoid arthritis elevated levels of cytokines, including IL-6 are detected in blood plasma and in intestinal tissue (in IBS) (Desreumaux 2000) .

It is released during the acute reactive phase of inflammation from tissues, in response to activated cells of the immune system, including leukocytes (Chrousos 1995). It is also elevated in inflammatory diseases, such as Crohn's Disease, a smooth muscle inflammatory disease, which can be worsened by psychological- or immune- stress (Gustot et al. 2005).

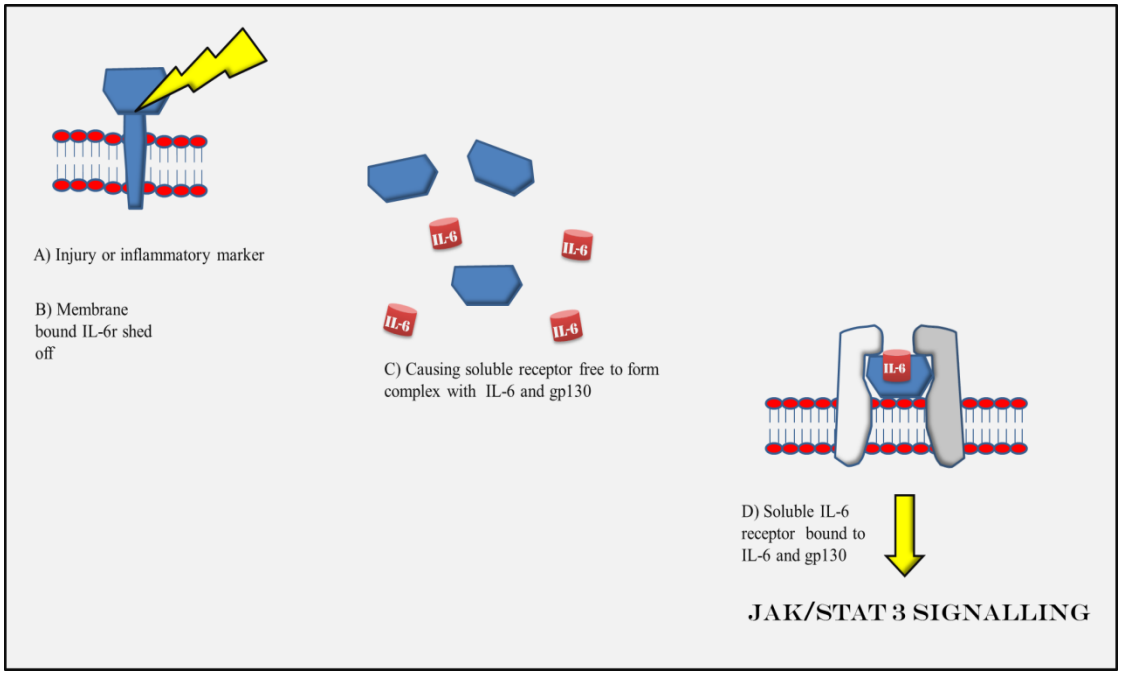
Indeed, patients with DMD, in which there is a chronic inflammatory response, have elevated plasma levels of pro-inflammatory cytokines including; IL-1, TNF and IL-6 (Chahbouni et al. 2010). IL-6 is also increased in patients with major depression and anxiety, and can be causative or a consequence of hypothalamic-pituitary-adrenocortical (HPA) axis activation (see Figure 1.4 for schematic interaction between stress and immune activation) (Frommberger et al. 1997; Bob et al. 2010; Voorhees et al. 2013).

1.6.2 Mechanism of action of IL-6

The family of cytokines to which IL-6 belongs to are grouped by their interaction with the non-specific signal propagating membrane bound Gp130 molecules (Erta et al. 2012), this Gp130 complex is ubiquitously expressed in tissues (Taga 1997). Firstly, IL-6 must bind to its specific receptor (Lust et al. 1992). This 80kDa receptor exists in two forms; a soluble and transmembrane form. The transmembrane form of the IL-6 receptor (IL-6R) is expressed in a variety of cell types but primarily expressed in leukocytes (Lust et al. 1992). The soluble receptor can be found in bodily fluids due to differential splicing of the membrane bound protein (Rose-John 2012).

Therefore, in the pro-inflammatory environment due an assault or injury, cells can shed this membrane bound receptor (Rose-John 2012) as is the case in the shedding of neutrophils (Deleo 2013), attracting IL-6 and propagating signalling through the Gp130 complex (the complex formed between IL-6 and its receptor consists of two IL-6 molecules, two IL-6 80kDa receptors and two Gp130 proteins, see Figure 1.4).This results in transcription of signalling cascades in tissues or cells though the JAK/STAT pathway and is primarily proinflammatory (Rose-John 2012; Hirano et

al. 1989; Yamasaki et al. 1988). Signalling in this way would not happen in the presence of IL-6 in a normal (devoid of soluble IL-6R) physiological state. Thus, trans-signalling can be carefully controlled in a distinct biological environment.



<u>Figure 1.4</u>: Interleukin-6 Receptor signalling

A) Shedding of the membrane bound receptor occurs in a mechanical injury or pathological state from cells expressing the receptor

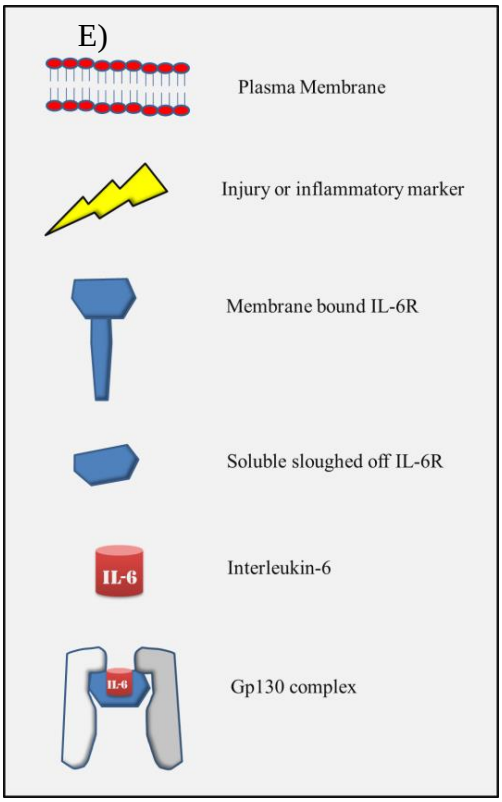
B) This causes an increase in soluble receptor available to form a complex with IL-6 and gp130

C) When a complex is formed, signalling occurs through the JAK/STAT3 signalling pathway

D) Causing a pro inflammatory response.

E) Figure Legend

Adapted from (Erta et al. 2012)



1.7 The occurrences of co -morbidities in DMD

1.7.1 Depression in DMD

Depression is hypothesised to be largely under-diagnosed in DMD, as compared to other central neurobiological deficits, such as cognitive deficits and evidence of intellectual disability (Sang-Jun et al. 2013). Symptoms such as apathy, fatigue, sleep disturbances and other classical symptoms are thought to result from a decline in motor abilities and sickness behaviour, caused by the disease (Fitzpatrick et al. 1986; Yiu & Kornberg 2008). However, DMD patients often show psychological symptoms like fatigue, apathy, high anxiety levels and depressive signs (Rubinsztein et al. 1998; Roccella et al. 2003; Angelini & Tasca 2012) Moreover, fatigue worsens muscle symptoms by increasing the apathy of the patients and reducing their mobility suggesting that the emotional status of the patient directly interacts with the course of the disease (Angelini & Tasca 2012).

Depression is a multi-faceted disease and has several key hypotheses to describe its pathophysiology. Brain regions which are involved in various hypothesis of depression include the limbic HPA axis. The HPA axis includes projections from brain areas involved in emotion; amygdala, hippocampus, to the hypothalamus which excretes a plethora of chemical signals which interact with the pituitary gland or peripherally in the adrenal glands, modulating the stress response (Chesnokova & Melmed 2002).

1.7.1.1 Amines regulating mood, the classical hypothesis of depression

"The Monoamine Hypothesis of Depression" is one of the most established and studied theories of major depression (Hirschfeld 2000). This hypothesis states that there is an imbalance or deficiency of monoamine neurotransmitters, notably serotonin (5HT), noradrenaline (NA) and dopamine (DA) and this hypothesis is supported by the antidepressant effects of tricyclic antidepressants and monoamine oxidase inhibitors, which elevate the levels of these neurotransmitters and alleviate the symptoms of depression (Hirschfeld 2000).

1.7.1.2 Inflammation causing depression

Studies which show that major depression and immune dysregulation coexist have caught our attention given the inflammatory profile of DMD patients. In a meta-analysis study, Dowlati et al, found a significant increase in TNF and IL-6 in depressed patients when compared to controls. Both these are released during infection or tissue injury, and as previously stated, are elevated in muscular dystrophy patients (Dowlati et al. 2010), although it is not known whether they contribute to depressive symptoms in DMD (Chahbouni et al. 2010). Nonetheless, it is known that blood-borne cytokines can cross the blood brain barrier and have effects on behaviours such as "sickness behaviour" (Larson & Dunn 2001; Dunn et al. 2005).

In 1991, the macrophage theory of depression was first hypothesised. It was proposed that IL-1β and other macrophage derived cytokines were responsible for depression, because of the potent effect they have on the HPA axis. Further evidence supporting this hypothesis was published in 1994, (Strik et al. 2001) when depressed patients exhibited a significantly higher production of Interleukin-18 and IL-6 in culture supernatant of mitogen stimulated peripheral blood mononuclear cells than normal controls.

This "macrophage hypothesis of depression" is relevant in inflammatory disease as noted in ulcerative colitis and Crohns disease where patients exhibit depression and anxiety (Robertson et al. 1989). Indeed, macrophage derived IL-6 is shown to be dysregulated in inflammatory diseases including Crohn's disease and rheumatoid arthritis (Nishimoto & Kishimoto 2004). In support of this hypothesis, a study compared an inflammatory arthritis (rheumatoid) with a non-inflammatory arthritis (osteoarthritis) and found a significantly higher percentage of depressive and anxiolytic symptoms in the chronic inflammatory arthritis group, even though both disease are similar in terms of pain and disability (Francisco et al. 2010).

Cytokines have been shown to modulate hippocampal neurogenesis as astroglia expression of IL-6 decreased overall neurogenesis by 63% in the hippocampal dentate gyrus in a transgenic murine model (Vallières et al. 2002). Studies on plasma of depressed patients showed a significantly higher concentration of IL-6 and TNF than control patients (O'Brien et al. 2007). Studies have indicated

that (along with other cytokines) IL-6 can activate the limbic - HPA axis, which is seen in a number of depressed patients, and several studies indicate that tricyclic antidepressants improve "sickness behaviour" in animal models of depression better than selective serotonin reuptake inhibitors (Dunn et al. 2005). This may be an important therapeutic route in treating both mood disorders and inflammation in DMD.

Interaction of these hypotheses

Neurogenesis is implicated as a contributing factor in the pathophysiology of depression, due in part to stress causing a reduction in dentate gyrus neuron birth rate (Jacobs et al. 2000), due to glucosteroids release by the stress responses. Also, monoamines, notably 5HT, can enhance neurogenesis in this brain area and therefore may be important in the treatment of depression. This relatively new theory may serve to help elucidate the full mechanisms of antidepressant action and indeed the pathogenesis of depression in diseases which have monoamine dysregulation and increased cytokine expression from chronic inflammatory diseases. However, It is not known if neurogenesis is reduced due to these deficiencies in DMD but hippocampal reductions in neurogenesis has indeed been seen in *mdx* brain, and rescuing this deficiency can reduce pathology in the mice (Deng et al. 2009).

1.7.2 Anxiety in DMD

It is noteworthy to mention that there is a high prevalence of comorbidity between depression and anxiety. Anxiety covers a broad range of disorders including panic disorder, social anxiety disorder, post-traumatic stress, obsessive compulsive disorder, and generalised anxiety disorder (Lydiard 1991) (for review see Lydiard 1991). A study of DMD patients indeed conclude anxiety type disorders occur in DMD patients (Fitzpatrick et al. 1986). Pharmacological treatments for anxiety disorders such as selective serotonin reuptake inhibitors and tricyclic antidepressants are also used for the treatment of depression (Lydiard 1991), and a cohort of patients have used pharmacological interventions to alleviate anxiety in DMD (Bushby et al. 2010) especially during late stages of the disease to help improve the quality of life of patients.

1.7.3 Stress in DMD

In the CNS, psychological stress can activate the HPA axis. In DMD, stress-related psychological and physical stress is apparent (Sabharwal 2014). Indeed a recent review reveals that not only psychological stress but physical autonomic dysfunction due to depression of the sympathetic nervous system has been identified in DMD, further indicating that the physical disease can influence the mental state of the patient (Sabharwal 2014).

This biological response is beneficial during an episode of physiological stress, with advantages including preservation of homeostasis and induction of glucose metabolism (Karalis et al. 1997). In the central nervous system, the stress response describes the activation of the HPA axis, this initially causes the secretion of Corticotrophin Releasing Factor (CRF) from the paraventricular nucleus of the hypothalamus, which drives the release of adrenocorticotropic hormone (ACTH) secretion from the pituitary gland (Vale et al. 1981), and the stimulation of glucosteroids from the adrenal glands, including cortisol (Ferenc 1986) (see Figure 1.5).

However, chronic stress shares symptoms with depression and anxiety, with chronic activation of the HPA pathway known to worsen the state of inflammatory disease (Gerber & Bale 2012). Indeed, interactions have been seen between depression, stress and pro-inflammatory cytokines (Connor & Leonard 1998). Long term stimulation of the HPA axis and secretion of the key stress hormone, CRF from the paraventricular nucleus of the hypothalamus is associated with mood disorders such as anxiety and a variety of other different behavioural changes (Bale & Vale 2004). Furthermore, CRF stimulates the sympathetic nervous system in the peripheral system and the cardiovascular system (Dunn & Berridge 1990) and can stimulate colonic motility (Taché et al. 1993). Stress is a known contributor in the pathogenesis of inflammatory diseases (O'Malley, et al. 2010), and it may be a contributing factor to the disease progression in DMD.

CRF initiates its effects though G-coupled protein receptors (GCPR), of which there are two subtypes, CRFR1 and CRFR2 (Bamberger & Bamberger 2000; Chen et al. 1993). CRF has a high affinity for both CRFR1 and CRFR2 (Coste et al. 2001).

Proteins of the same family with high homology to CRF have also been discovered, named Urocortin 1, Urocortin 2 and Urocortin 3. Urocortin 1 has a high affinity for the CRFR1 subtype, whereas Urocortin 2 had a high affinity for the CRFR2 subtype (Reyes et al. 2001), more so than CRF, and Urocortin 3 is specific to CRFR2 also (Martinez et al. 2004).

These receptor subtypes have opposing functions, for example CRFR1 mediates visceral nociception whereas CRFR2 can reduce visceral nociception. CRFR1 has been implicated in pro-inflammatory processes, potentially though lymphocytes (Kravchenco & Furalev 1994), whereas in the periphery CRFR2 has anti-inflammatory functions (Hinkle et al. 2007), causing apoptosis of macrophages (Tsatsanis et al. 2005) and has been found to modulate IL-6 levels following inflammation (Venihaki et al. 2001).

1.8.3.1 Urocortin 2 – beneficial in dystrophin deficiency

Interestingly, Urocortin 2, which is expressed in skeletal muscle (Kishimoto et al. 1995), signals through the CRFR2 subtype has significant beneficial effects on muscle. Urocortin 2 has been shown to improve muscle physiology in a range of pathological conditions. These include preventing nerve damage, immobilisation atrophy. It can act through modulating muscle mass and it has been hypothesised this mechanism may be through the interaction of corticosteroids released from the adrenocortex (Hinkle et al. 2003) in response to CRFR1 agonism and the stress response (Hinkle et al. 2004) in a protective manner, reducing the catabolic action of corticosteroids.

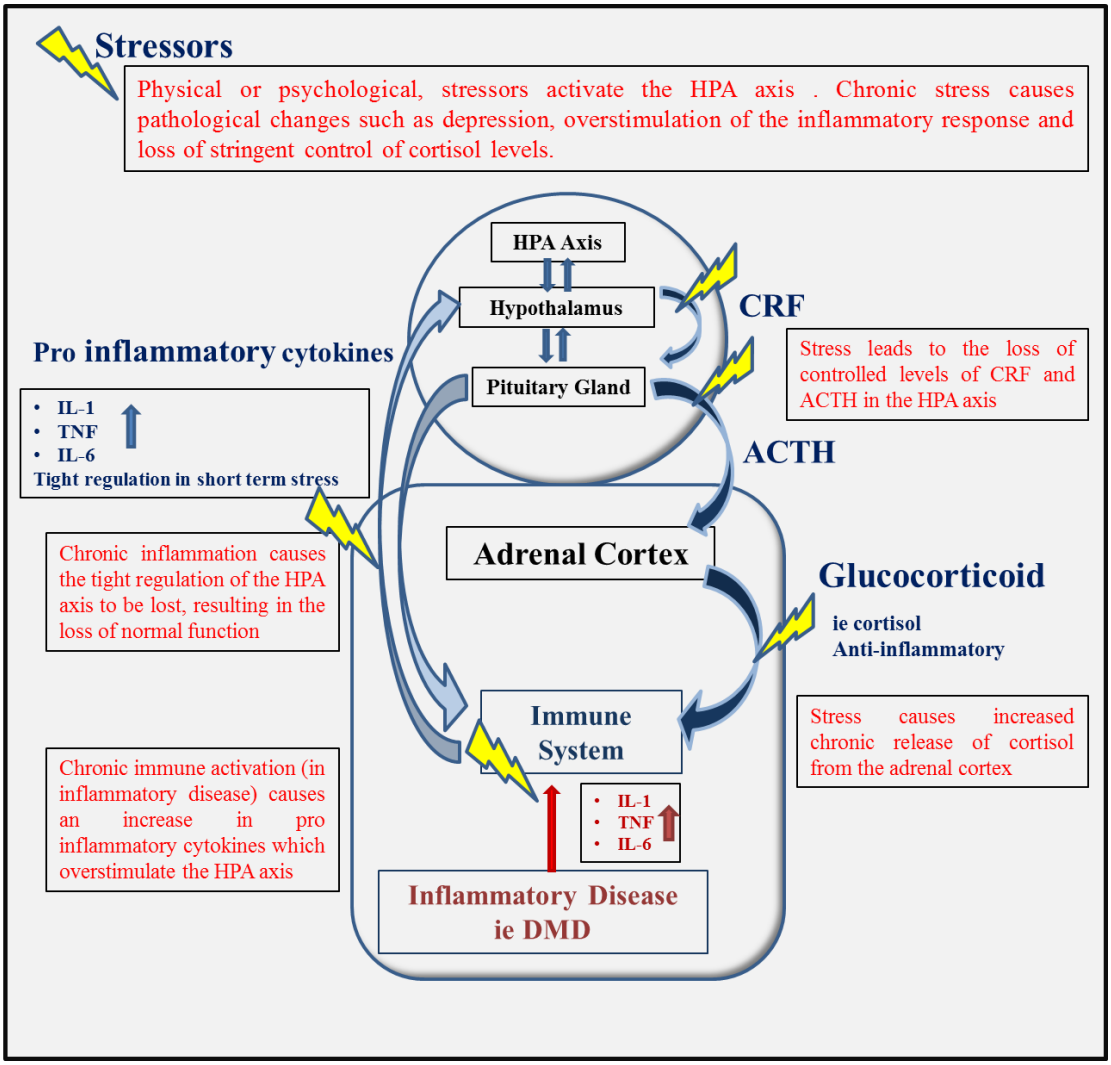
Moreover, this beneficial effect of Urocortin 2 has been investigated in *mdx* mice where it caused a reduction in CK levels and an increase in muscle mass (Hall et al. 2007). CRFR2 agonism in diaphragm has been beneficial in slowing the progression of the disease, increasing specific force production in the diaphragm and showing histopathological changes, such as fibrosis and inflammation. Molecular gene expression characteristic of DMD, including immune cell genes were also altered in treated *mdx* mice (Hinkle et al. 2007).

1.8.3.2 The CRF Stress Response and IL-6

There is significant interaction in the body between the CRF system and cytokines. IL-6, which signals through Gp130 in response to psychological, physical and inflammatory stress on the body (Karalis et al. 1997) has a major role in the modulation and control of acute and chronic inflammation. Its interaction with the HPA axis can control the circulating levels of IL-6 in the body i.e. IL-6 stimulates the release of glucocorticoid levels which then inhibits IL-6 levels (Venihaki et al. 2001).

Of particular interest in this project, is the peripheral interaction between CRFR2 agonists and IL-6. Previous studies have demonstrated that Urocortin 2 can induce IL-6 gene transcription in rodent aortic smooth muscle cell lines, and this is modulated through the CRFR2 receptor (Kageyama et al. 2006). Moreover, urocortin 2 modulates IL-6 levels in stromal cell lines in a time dependent manner (Zoumakis et al. 2000). CRFR2 agonists can cause anti-inflammatory effects in vitro by inducing macrophage apoptosis (Tsatsanis et al. 2005) but CRFR2 agonism also induces the release of IL-6 through NFκB, ERK and p38 MAP kinase proinflammatory signalling pathways in cardiomyocytes; however its role is not fully elucidated (Huang et al. 2009).

CRF antagonism increases IL-6 levels in plasma in psychological stress models (Ando et al. 1998) and in rodents, during an inflammatory insult, IL-6 is necessary for the CRF-stimulated stress response and whats more, it regulates its own mRNA levels (Vallières & Rivest 1999). What we lack understanding in is the interaction between IL-6 elevation and the CRFR2 activation in muscle, and even more so in DMD, especially when CRFR2 agonism has been shown to benefit *mdx* muscle function (Hall et al. 2007; Reutenauer-Patte et al. 2012).



<u>Figure 1.5:</u> A schematic representing the interaction of the inflammatory response, stress hormones and the HPA axis

Stress - be it psychological or physical causes activation of the stress response. Proinflammatory cytokines can be produced in the peripheral system and have central nervous system effects, such as activating the HPA axis and instigating a stress response - which in itself can modulate the pro inflammatory cytokine profile in the periphery. Adapted from (Glaser & Kiecolt-glaser 2005)

1.8 Current therapeutic strategies for DMD

1.8.1 Genetic therapy

1.8.1.1 Experimental Exon Skipping Therapy

Exon skipping is a promising genetic strategy which can restore semi-functional dystrophin by coding the protein after the nonsense mutation. The use of antisense oligonucleotides to induce skipping of the selected exons resulted in some restoration of a functional dystrophin protein (Goyenvalle et al. 2004) (see Figure 1.6 for schematic view of process). However, the practical application of this technique has initially been problematic.

Although this strategy did rescue dystrophin expression for 4 weeks in *mdx* mice in both *tibialis anterior* and *extensor digitorum longus* muscles, the effect was localised and temporary (Goyenvalle et al. 2004). Restoration of dystrophin expression in *mdx* mice resulted in an immune response to the new protein (Lu et al. 2003). Moreover, low expression levels were a problem with weekly intra venous administration of 2'-O-methyl phosphorothioates inducing dystrophin expression only in small areas of the diaphragm, *gastrocnemius* and intercostal muscles but never exceeding more than 5% of normal levels (Lu et al. 2005).

Nonetheless, optimisations of delivery techniques in the *mdx mouse* have been more promising toward an effective delivery to patients with DMD. Increased dystrophin expression was found following both local intramuscular and systemic administration using 2-O-methyl-modified bases, which are widely used to alter pre-mRNA processing (Fletcher et al. 2006). These studies suggest that antisense oligoribonucleotides may result in a rescued dystrophin transcription and a functional gene being produced. However, dystrophin expression was only induced for short periods of time and at very low levels (Fletcher et al. 2006).

An alternative strategy using recombinant adeno-associated virus vector also showed positive effects in *mdx* mice, restoring muscle function and normal life expectancy when given systemically for a year. After 18 weeks of treatment, dystrophin was detected in the diaphragms and reduced centralised nuclei were detected. A two-fold increase in force producing capacity was also found in treated

mice and improved resistance to contraction induced injury (Gregorevic et al. 2006; Nakamura & Takeda 2011).

Another method to induce exon skipping is using unmodified phosphorodiamidate morpholino oligomers (PMO); these differ from antisense oligoribonucleotides in design and can be transfected into cultured cells with higher efficacy (Lu et al. 2005). Furthermore, regular weekly intra venous injections of PMOs targeting mouse dystrophin exon 23 induced up to 50% of normal levels of dystrophin in body-wide skeletal muscles in the *mdx* mice, decreased CK levels, improved muscle strength significantly and improved muscle pathology (Winter et al. 2009).

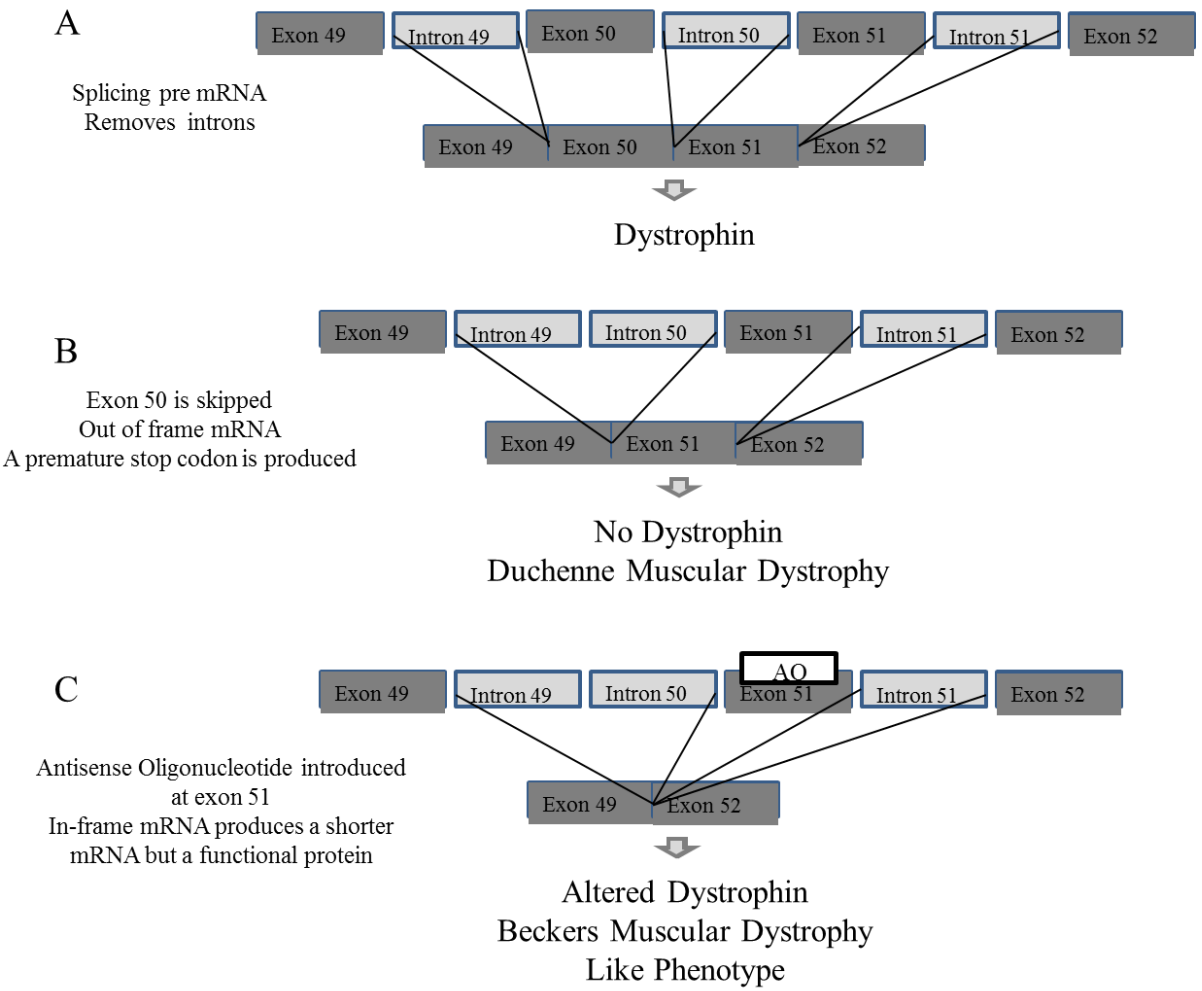
Due to the large percentage of DMD patients (up to 13%) with a nonsense mutation in exon 51, this is the most researched method of rescuing dystrophin through exon skipping (Lu et al. 2011). In a proof of concept study, four patients showed functional expression of dystrophin when given an intramuscular injection of antisense oligonucleotide named PRO051, showing this compound of clinical relevance (van Deutekom et al. 2007). A study to assess the safety, side effects and clinical relevance of systemically administered PRO051, this time by weekly subcutaneous injection in 12 patients showed an increase of dystrophin expression and few adverse side effects. Furthermore, PRO051 resulted in dystrophin expression in 60-100% of muscle fibres in 10 out of the 12 patients. Furthermore, this trial also showed modest increase in distance walked after twelve weeks of treatment (Goemans et al. 2011) indicating the potential for functional improvement.

1.8.1.2 Utrophin up regulation

An alternative strategy rather than trying to replace missing dystrophin would be to overexpress the compensatory structural protein, utrophin. Indeed, this strategy has been explored both pharmacologically and by using gene therapy. One study compared the efficacy of dystrophin versus utrophin in immune-immature neonatal *mdx* mice and concluded that both dystrophin and utrophin were mostly equivalent in ameliorating the development of dystrophic characteristic such as muscle necrosis and weakness in these neonates (Ebihara et al. 2000). Thus, in immune-competent adult *mdx* mice, up-regulation of utrophin would be a logical approach to genetic therapy for DMD. Consistent with this theory, increased utrophin expression in *mdx* mice reduced the numbers of centrally nucleated myofibres and the degree of

necrosis (Gilbert et al. 1999). Expression of Ca^{2+} channels, which are associated with fibre necrosis, was also normalised but other pathological characteristics remained; namely no increase in muscle force production (Squire et al. 2002). Additionally, an artificial zinc finger transcription factor to upregulate utrophin at promoter region A resulted in lower levels of inflammatory cell infiltration and fewer centralised myonuclei (Di Certo et al. 2010).

Using the compound heregulin which induces up regulation of utrophin, it was observed that *mdx* mice exhibited a reduction in fibre necrosis in *extensor digitorum longus* and *tibialis anterior* muscles and a significant reduction in centralised nuclei, giving some credence to this therapeutic tactic (Krag et al. 2004). However, a caveat to these studies are the absence of functional tests such as limb grip strength or mobility, specific forces from diaphragm or cardiac muscle to further validate utrophin as an adequate replacement for dystrophin.



<u>Figure 1.6:</u> Antisense nucleotides as a therapy for DMD
A – Splicing pre mRNA removes introns. B – in DMD Exon 50 is skipped and a premature stop codon is produced. C – When an Antisense Oligonucleotide is introduced at exon 51 protein is produced, which can restore some function in DMD.

1.8.2 Pharmaceutical Interventions targeting inflammation in DMD

1.8.2.1 Corticosteroids

Steroidal therapies such as prednisolone, prednisone or deflazacort, a derivative of prednisolone, are commonly prescribed for DMD patients and thus far are the only efficacious pharmacological intervention shown to slow the progression of the disease (Yiu & Kornberg 2008). The mechanisms of action of these drugs have been investigated and have demonstrated a metabolic effect of prednisone, slowing muscle necrosis in patients (Rifai et al. 1995). In *mdx* mice myogenic repair was enhanced and muscle differentiation was improved by deflazacort (Anderson et al. 2000). Importantly, prednisone and prednisolone have anti-inflammatory effects in *mdx* mice inducing a reduction in expression of macrophages, $CD4^+$ and $CD8^+$ T lymphocytes (Wehling-Henricks et al. 2004) and eosinophils (Marques et al. 2009) in skeletal muscle.

Functionally, prednisolone increases the specific force of skeletal muscle but not muscle function following eccentric contraction injury and had no influence on fibre regeneration. Nonetheless, the decline in forelimb grip strength was delayed by this treatment and the life expectancy of *mdx* mice was lengthened (Baltgalvis et al. 2009), although the *mdx mouse* does not mimic the shortened life-span to the extent a human patient does, therefore it seems this effect is not a directly transferable observation.

Deflazacort can attenuate skeletal muscle pathology, attenuating dystrophic phenotype and may act to reduce apoptosis (Lim et al. 2004). A recent study has shown that using steroid treatment in long term studies (> 100 days) causes an increase in cardiac fibrosis and subsequently is associated with a decrease in cardiac health, with similar results in skeletal muscle (Sali et al. 2012). This raises the question as to whether *mdx* mice are an appropriate positive control in long term pharmacological studies or if steroidal treatment benefits can "wear off", or even provide detrimental side effects in the longer term. The therapeutic efficacy of steroid treatments in DMD is limited, intermittent and is associated with a high

occurrence of side effects such as obesity, cataracts and a short stature (Schara & Mortier 2001) meaning that better treatment strategies are continually being sought.

1.8.2.2 Synergistic therapy-steroid co-treatment

Combination treatment with steroid and various compounds has been an important research area of pharmacological interventions for DMD. It is hoped that the synergistic effects of combined therapies may reduce dosages of corticosteroids required and thereby reduce the occurrence of unwanted side-effects from this palliative care.

Co-administration of arginine butyrate, a butric acid salt of the amino acid arginine, with prednisone resulted in a two-fold change in expression of an array of genes important in disease progression by controlling inflammation, fibrosis, muscle growth and regeneration through several signaling pathways. This was more effective than prednisone alone, providing protection against DMD pathology in *mdx* mice (Lim et al. 2004).

When taurine, an amino acid which can modulate sarcolemmal excitability and calcium handling is co-administered with prednisone in *mdx* mice the improvement in forelimb strength in *mdx* mice was enhanced as compared to either treatment alone. The mechanical threshold of the extensor digitorum longus myofibres was also improved, although this strategy did not lower CK levels nor improve histologically scored skeletal muscle pathology (Cozzoli et al. 2011).

An alternative strategy examined the importance of nutrition in treatment. A combination of four nutritive supplements in addition to steroid treatment (prednisone) produced the best overall results in a study investigating the effectiveness of creatine monohydrate, conjugated linoleic acid, alpha-linoic acid and beta-hydroxyl- methylbutryte in DMD pathology. Grip strength was found to be improved in *mdx* mice whereas muscle fatigue and numbers of centralised myonuclei were decreased (Payne et al. 2006).

1.8.2.3 Anti-inflammatory and anti-fibrotic reagents

Several therapeutic strategies tackling the inflammatory aspects of dystrophin deficiency have been investigated; thus far the results have been mostly disappointing. The precise mechanisms of fibrosis in *mdx* mice are largely unknown but are thought to be due to pro-inflammatory cytokines, and indeed *mdx* mice have raised pro-inflammatory profiles including transforming growth factor β1(TGF β1) (Andreetta et al. 2003), IL-6 (Kostek et al. 2012), TNF (Radley et al. 2008) and IL-1β (Huang et al. 2009). Immunostaining for NFκB in these fibres was reduced in green tea supplemented *mdx* mice (Grange 2011) and inhibition of NFκB improves whole body tension development (Siegel et al. 2009).

Moreover, pyrolidine dithiocarbamate, an inhibitor of NFκB nuclear activation reduced the number of necrotic myofibres in an age-independent manner (Carlson et al. 2005). Curcumin, another NFκB inhibitor improved membrane integrity and muscle strength, decreased CK activity and levels of the pro-inflammatory cytokines, TNF and IL-1 and inducible nitric oxide synthase (iNOS) which causes NFκB mediated inflammation (Pan et al. 2008).

mdx mice treated with a trimethylated xanthine derivative, Pentoxifylline – which had previously reduced TGFβ1 and type 1 collagen in a rat model of biliary fibrosis, was not effective in *mdx* mice nor did it reduce collagen metabolism (Gosselin & Williams 2006). Halofuginone which blocks TGFβ, stimulated collagen synthesis in four week old mice (Turgeman et al. 2008) and another drug targeting TGFβ, Pirfenidone attenuates fibrosis in interstitial pulmonary fibrosis but did not display effectiveness in targeting DMD fibrosis (Van Erp et al. 2006).

Blockade of TNF reduced inflammation over a longer treatment protocol, resulted in reduced necrosis, lower CK levels and increased duration of voluntary exercise (Radley et al. 2008). Blocking IL-6 was seen to increase inflammation in histological sections, contrary to the group's hypothesis, immunohistochemistry found Intercellular Adhesion Molecule 1 (I-CAM1) staining increased also, as ICAM1 is expressed where leukocyte infiltration occurs, but no changes in muscle function or other mRNA levels of TNF was found (Kostek et al. 2012).

1.9 Conclusions

Duchenne Muscular Dystrophy is primarily a skeletal muscle wastage disease; however from reviewing the literature it is clear it is not only a multi-level but a multi system disease, affecting striated muscle, the CNS, vasculature and smooth muscle.

Despite advances in genetic therapies, there is currently no cure for DMD. Therefore, developing treatments to slow the progression of the disease or palliative care to reduce the suffering of patients is an important area of research in DMD to improve quality of life of patients. However, these options so far are limited. But not only do these studies go about testing the efficacy of compounds, but they importantly provide insight into the specific mechanisms of pathology in DMD, furthering the understanding of this disease.

The *mdx mouse* model has been utilized to test these interventions pre-clinically and has proven most useful in gaining knowledge about dystrophin deficiency pathology and this is somewhat transferrable to the human disease, despite its less severe phenotype.

1.10 Thesis Layout and Rationale

- Study One: Investigating the potential benefits of amitriptyline in treating inflammation and mood in *mdx* mice

- Study Two: The role of IL-6 and Urocortin 2 in diaphragm dysfunction in *mdx* mice

- Study Three: The role of IL-6 and CRF in gastrointestinal dysfunction in *mdx* mice

In the first study (Chapter Three), I studied the efficacy of the tri-cyclic antidepressant amitriptyline in reducing inflammation and its effects on potential psychological deficits in *mdx* mice. As discussed in chapter three, amitriptyline's mechanism of action is still to be fully elucidated but it can provide anti-inflammatory beneficial therapy to a variety of tissues. We were interested in its effect on IL-6, a major component of the immune response to muscle damage, especially as DMD is an inflammatory disease.

In studies two and three the physiological benefits of neutralizing IL-6 signaling and activating CRFR2 were investigated. In study 2 (Chapter Four) we focused on the diaphragm, due to DMD being primarily a skeletal muscle disease and the diaphragm most closely relating to the human condition. And, similarly in study 3 (Chapter Five) the colon of *mdx* mice was studied due to the apparent dysfunction in the smooth muscle and a potential role for IL-6 and CRFR2 agonism in inflammatory bowel environments. Each results chapter therefore, has a specific hypothesis and aims included.

Chapter 2: Methods

2.1 Ethical Approval and Animal License

All animal experiments were approved and performed according to Animal Experimentation Ethics Committee (AEEC) regulations by the ethical committee in University College Cork (UCC). An animal license was acquired from the Department of Health and Children (Personal license number: REF /B100/4229) for behavioural testing and intervention studies.

2.2 Animals

Dystrophin-deficient C57BL/10ScSn-Dmd^{Mdx}/J (*mdx, dystrophic*) and C57BL/10ScSn wild type (WT) controls purchased from Jackson Laboratories (Bar Harbor, Maine, U.S.A, http://www.jax.org/) were used for the studies. Breeding colonies of both *mdx* and WT were established and maintained in the Biological Services Unit, University College Cork. For the amitriptyline intervention studies (Chapter 3) mice were housed in individually ventilated cages (IVCs). The animals were moved to filter topped cages (FTCs) shortly before initiation of treatment or 13-15 days before starting behavioural experiments (untreated groups). For other studies (Described in Chapter 4 and 5) mice were housed in FTCs. Weaned mice were housed in groups no greater than 4 per cage, and kept under an artificial light/dark cycle provided with light between 06:00 and 18:00 hours, with free access to drinking water and standard chow. Regular health screens (see FELASA criteria, http://www.felasa.eu/) confirmed that the animals in the IVCs and FTCs were not suffering from any infections. Male mice were used for all studies between 6-12 weeks.

2.3 *In vivo* Studies

2.3.1 Stress Induced Defecation

The anxiolytic environment of a brightly-lit exposed cage was used to measure stress-induced defecation in control and *mdx* mice, which acted as a marker of GI transit times (Julio-Pieper et al. 2010). Mice were transferred from home cages to brightly-lit individual cages (15cm x 13cm x 28cm) lined with absorbent paper and the number of faecal boli excreted during a 90 minute period was recorded. Faecal pellets were removed at 15 minute intervals and stored to prevent water loss and copraphagia. Pellet number per mouse was recorded in 15 minute intervals for a total of 90 minutes. Pellets were then weighed to calculate the wet weight and desiccated in an oven at 60 ^{o}C for 16 hours to calculate the dry weight. The water content was subsequently calculated as a difference in weight after they were desiccated compared to start wet weight.

Equation: $\mathbf{100 \times (wet\ weight - dry\ weight) \div wet\ weight}$

2.3.2 Behavioural Tests

All behavioural experiments were carried out between 8:00-13:00. Room temperature was maintained at 22±1°C. Mice were taken from the holding room to the testing room 30 minutes prior to the start of the experiment to allow the time for habituation.

2.3.2.1 Open Field

The open-field arena used for assessing anxiety in rodents (Prut & Belzung 2003; Dunn et al. 2005) was a brightly illuminated white square chamber measuring 60cm x 60cm, with walls of 60cm in height (see Figure 2.1). Mice from different experimental groups were tested in a random order. The open field arena was cleaned with water and wiped dry between trials to eradicate scent markings of the previous animal. The behaviour of the mice was recorded using a camera (JVC G2-MG750) positioned 70cm directly above the open field box. The floor of the square

open field was marked by an internal square of 30 cm length, and four transversing lines from the walls to the internal square (see Figure 2.1).

Each trial was ten minutes in duration. On initiation of the trial mice were placed in the centre of the open field arena and behaviours were observed and recorded for the duration of the trial. Behaviours were scored through post-test offline analysis using the video recordings by the same researcher.

Behaviours assessed included:

- time spent in the central square versus peripheral square,
- degree of ambulation (number of lines crossed by the mouse),
- rearing (number of times the mouse stood completely erect on its hind legs)
- grooming (number of times the mouse scratched its face and fur with its forepaws).

These behaviours are recognised indicators of anxiety, as discussed in chapter 3, which can be modified by anxiolytic pharmacological reagents (Prut & Belzung 2003; Choleris et al. 2001).

2.3.2.2 Novel Object Recognition (NOR) Test

NOR tests are used to test recognition memory in rodents (Antunes & Biala 2012). NOR tests were also performed in the open field arena, 24 hours after the open field test (trial 1). The second trial (trial 2) in the NOR test, to assess whether the animal remembered something it had encountered in trial 1, took place 24 hours later. Exploration of an object was defined as follows: directing the nose to the object at a distance of no more than 2 cm, sniffing the object and/or touching the object with the nose, sitting on the object was also considered as exploratory behaviour. The time spent exploring each object was recorded and analysed using the video footage later.

Initially, a cylindrical multicoloured solid object on the left (height 10cm, diameter 6.5cm) and a yellow square Lego® brick (10.2cm, 6.2cm x 6.2cm, height x width x length) on the right (Figure 2.2) were present in the arena. The objects could not be displaced by a mouse. Twenty four hours later one of the items (the cylinder) was exchanged for a spiny blue rubber ball on a solid base (height 11.9cm, diameter 9.3cm plus blunt spines of 2.7cm). The behaviour of the mice towards this new object was recorded and analysed a later time point. In order to avoid the presence of olfactory trails the objects were always thoroughly cleaned after each mouse.

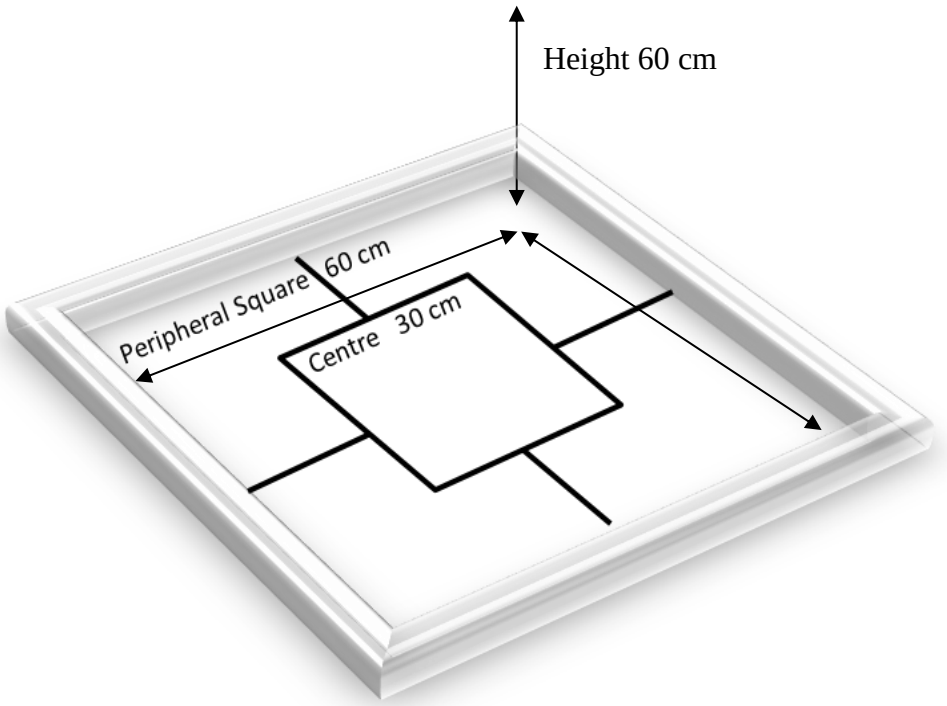
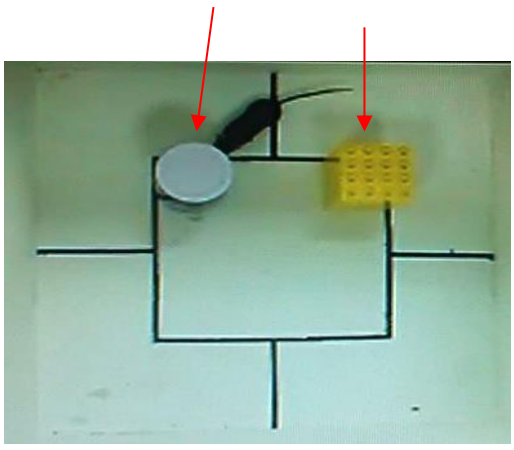


Figure 2.1: A diagram detailing the dimensions of the open field arena

TRIAL 1 - Cylinder and Lego Block



TRIAL 2 -Blue Ball replaces Cylinder

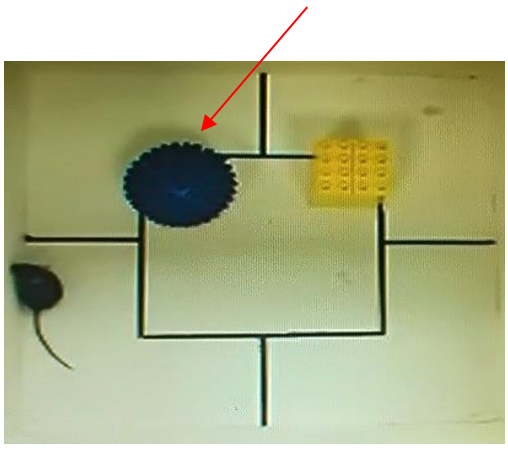


Figure 2.2: Novel Object Recognition Test still images from video recording of trial

The cylinder is replaced in trial 1 with a blue ball for trial two. The yellow Lego block does not change between trials.

2.3.2.3 Tail Suspension Test

This test permits assessment of depressive symptoms in rodents and has been used to test the effectiveness of anti-depressant reagents (Steru et al. 1985). Mice were suspended by the tail, using adhesive Scotch tape to a flat surface. The behaviour of the mice was recorded using a camera which was positioned 70cm in front of the mouse. The duration of the test was 6 minutes long, the final 4 minutes of the test were analysed, giving a habituation time for mice in the test, as per previous protocols (Cryan et al. 2005). The total sum period of immobility (duration of immobility) and latency to first period of immobility are measured for each mouse.

2.4 Collecting and Processing Tissue

Mice were sacrificed by isoflurane anaesthesia (5% in oxygen) and cervical dislocation. Trunk blood was collected following decapitation in eppendorf tubes coated with ethylenediaminetetraacetic acid (EDTA) to prevent coagulation and subsequently centrifuged at 1600g for 10 minutes. The plasma supernatants were removed and snap frozen in liquid nitrogen and stored at -80°C for future Enzyme Linked Immunosorbant Assay (ELISA) analysis.

Brain regions of mice were dissected out and the prefrontal cortex, amygdala, hypothalamus, hippocampus, striatum and midbrain were micro dissected and snap frozen in iso-pentane, a cryo-protectant and stored at -80°C. A midline incision through the abdomen was performed and the diaphragm and colon tissue was removed, snap frozen in liquid nitrogen and stored at -80°C or kept in oxygenated Krebs' physiological saline solution ((Krebs) Table 2.12) for functional studies. The right forelimb and distal colon sections were removed and stored in 4% paraformaldehyde at 4^{o}C for histological examination of tissues.

2.4.1 Histology

2.4.1.1 Skeletal Muscle

Muscle samples were dehydrated (50% ethanol, 70% ethanol, 95% ethanol, 30 minutes each) and then placed in 100% ethanol (60 minutes x3) and the tissue was then cleared in a 1:1 ratio of 100% ethanol to xylene (30 minutes) and xylene (30 minutes and 120 minutes) (Leica TP1020, Histokinet). The tissue was embedded in paraffin (Sakura Tissue-Tek TEC, Histolab Histowax embedding medium) in a pre-programmed Histokinet and cross sections (10μm) were sliced using a microtome (Leica RM2135) and allowed to dry (overnight, 37°C) on gelatin-coated glass slides.

2.4.1.2 Colon

After sacrifice, full colon length from anus to caecum were extracted and measured to the nearest millimetre. Next, excised pieces of colon approximately 1cm from the anus were taken, placed in 4% paraformaldehyde for 24 hours, then transferred to 30% sucrose in order to cryo-protect the tissue and subsequently stored at -80^{o}C until they were cryo-sectioned (CM1850, Leica) at 10μm thickness in preparation or Haematoxylin & Eosin (H&E) staining.

Haematoxylin & Eosin Staining

Slides were equilibrated to room temperature and washed in phosphate buffered saline (PBS) (Table 2.1) for five minutes then stained in Harris Haematoxylin (Table 2.1) for four minutes washed in running water for five minutes then stained in 1% eosin (aqueous) for one minute and washed in water until slide is clear. The slides were then dehydrated in a series of alcohols (70% ethanol, 95% ethanol, 100% ethanol and 100% ethanol), immersed in xylene and cover slipped using a mounting medium (PVA-DAPCO, Sigma Aldrich), air-dried and visualised on a bright-field Olympus Proxis AX70 upright microscope with an Olympus DP50 camera.

Table 2.1: PBS and Harris' Haematoxylin Recipe

Phosphate Buffered Saline	
NaCl	8g
KCl	0.2g
Na_2HPO_4	1.44g
KH_2PO_4	2.44g
up to 500mls dH_20	
Harris' Hematoxylin Recipe	
Aluminium Potassium Sulphate	50g
Hematoxylin	1g
Sodium Iodate	0.2g
Glacial Acetic Acid	20ml
up to 1 litre of dH_20	

2.4.2 Imaging Techniques

2.4.2.1 Skeletal Muscle

Transverse sections were cut through the belly of the muscle and altogether, 28 images per section of H&E stained muscle per mouse were taken. Sections starting at a random point in the muscle and at systemic intervals 1mm away in a cross from this centre point were imaged. Muscle pathology was scored using Image J software (Abràmoff et al. 2004) by analysing both frequency and total area of inflammation as identified by myo-phagocytosis of mononuclear cells (Figure 2.3), the number of central nuclei (central nuclei defined as nuclei located within a fibre) were scored and total number of nuclei were counted (muscle pathology in Figure 3.5).

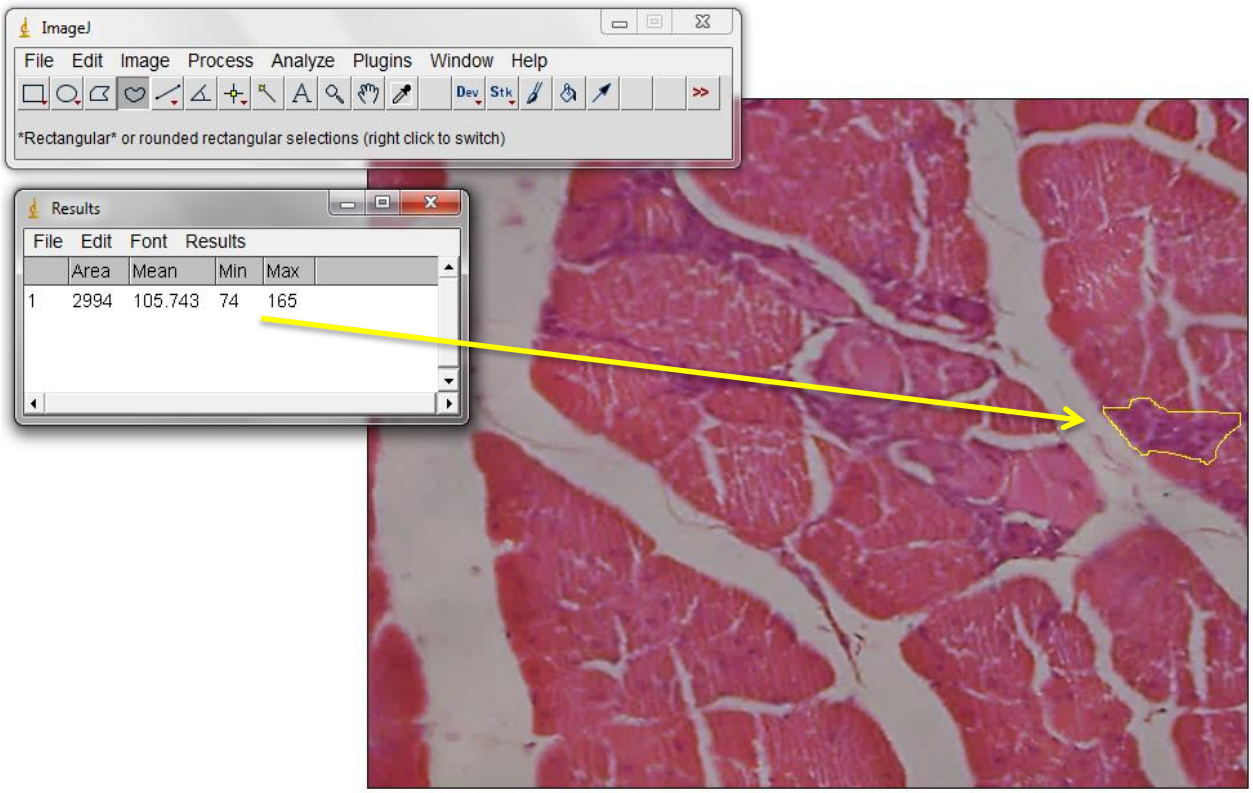


Figure 2.3: Representative image of the technique used to score striated skeletal muscle for myo-phagocytosis

Muscle was scored for inflammation and pathological changes using Image J software. Inflammatory events (as above), muscle fibre area, muscle fibre number, nuclei and central nuclei were counted and measured using Image J.

2.4.2.2 Colon

Colons were cut transversely in 10µm sections, 40µms apart with 5 sections per colon on gelatin coated slides. Following H&E staining images of the sections were taken using an Olympus Proxis AX70 upright bright-field microscope equipped with an Olympus DP50 camera using the x10 objective lens and sections were subsequently analysed for differences in mucosal and muscle thickness (the mean taken from three measurements, Figure 2.4).

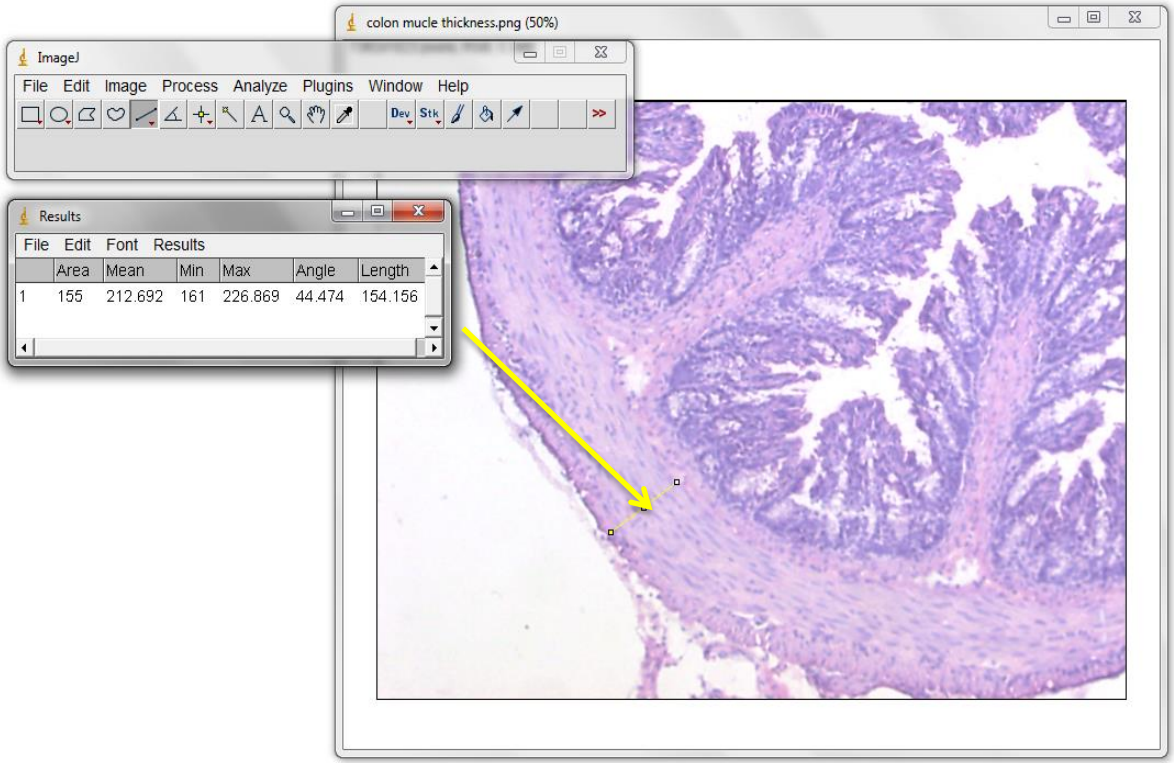


Figure 2.4: Representative image of colon scored for muscle layer thickness
Muscle layer thickness using Image J software. Similarly mucosal thickness was measured and total diameter. Three measurements were taken for each image and averaged.

2.5 Biochemical Analysis

2.5.1 Protein Quantification

To determine protein expression in Extensor Digitorum Longus (EDL) muscle, diaphragm and whole colon, these tissues were prepared for Western blotting by homogenisation in 200µl Lysis buffer (Table 2.2) with added protease inhibitor (2µl, Expedeon). Samples were homogenised mechanically (OMNI GLH, General Laboratory Homogenizer) for 10 seconds and centrifuged (Boeco Germany, U-320R) at 19,000g for 20 minutes at 4^{o}C. Supernatant was collected and diluted 1:100 in deionised water (dH_20) and a Bradford assay was carried out. Bradford protein quantification is a colorimetric assay which measures the shift in absorbance of Commasie Brilliant Blue G-250 (Bradford 1976). The concentration of protein was extrapolated in each sample from a standard curve of protein (Bovine serum albumin (BSA) ranging from 1µg/ml to 100µg/ml, Table 2.3) diluted in deionised water. Absorbance was read at 595nm on a spectrophotometer (Molecular Devices, SpectraMax M3, USA) and the concentration of protein was determined by SoftMax Pro 6 software package.

Table 2.2: Lysis Buffer Recipe

Lysis Buffer	Final Concentration
HEPES	10mM
KCl	10mM
EGTA	0.1mM
EDTA	0.1mM
Triton X-100 (v/v)	0.06%

Table 2.3: Bradford Assay Standard Curve dilutions of Bovine Serum Albumin

BSA Standard Protocol		
From 1mg/ml stock	**dH_20**	**Concentration**
1µl	999µl	1µg
5µl	995µl	5µg
10µl	990µl	10µg
15µl	985µl	15µg
20µl	980µl	20µg
25µl	975µl	25µg
50µl	950µl	50µg
100µl	900µl	100µg

Table 2.4 and 2.5: Running and Transfer Buffer Recipe for Western Blot

Running Buffer	
Tris Base	23mM
Glycine	192mM
SDS	0.01%

Transfer Buffer	
Tris Base	23mM
Glycine	192mM
SDS	0.01%
In 20% Methanol	

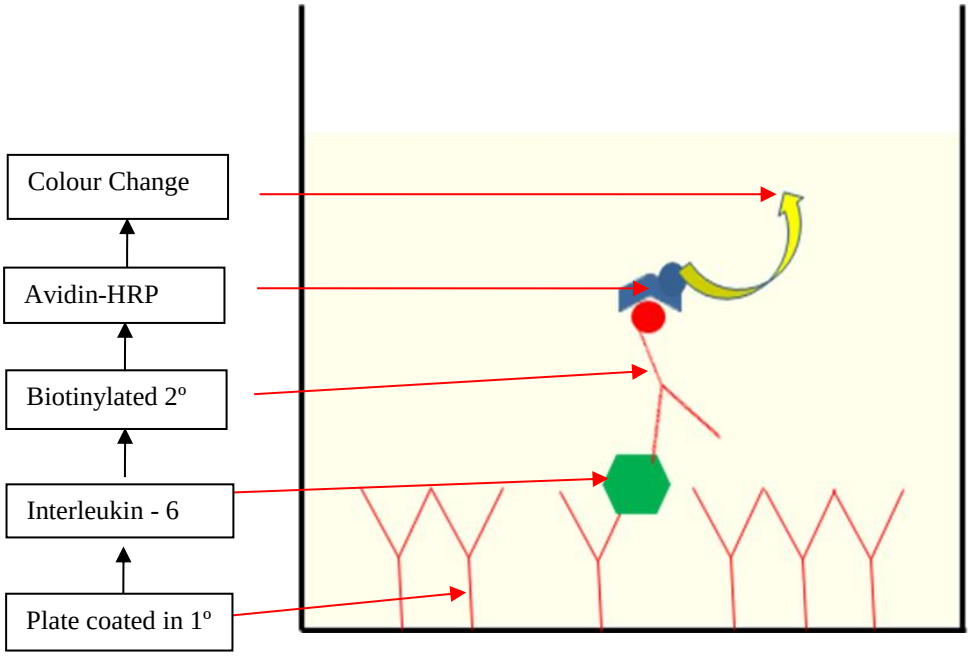
2.5.2 Enzyme Linked Immunosorbent Assay (ELISA)

2.5.2.1 Muscle Homogenate

An ELISA was performed on homogenised right forelimb flexor muscle samples of known total protein concentration after completion of a Bradford protein assay. An ELISA was performed as follows (per manufacturer's instructions, eBioscience).

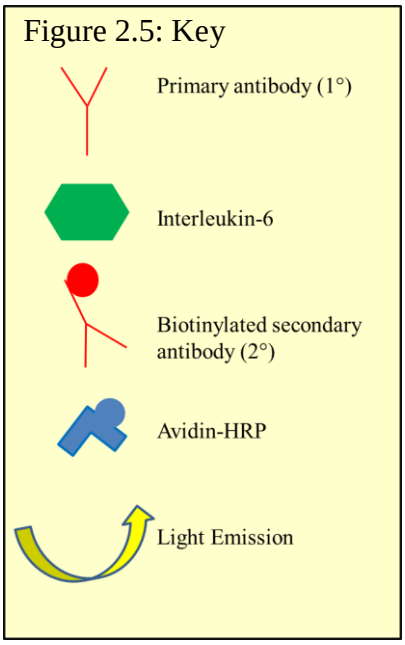
A standard curve was prepared using a serial dilution of standard IL-6 protein supplied with the kit (0 pg/ml, assay diluent as blank, to 500pg/ml), a 96 well plate was pre coated with primary antibody over night at 4°C. It was subsequently washed 5 times with wash buffer (PBS-Tween (0.5%, v/v)) and the wells were blocked for 1 hour with assay diluent. Samples were then added and incubated overnight at 4°C, followed by 5 washes with PBS-Tween and the detection antibody, which was added for 1 hour at room temperature. After 5 washes of PBS-Tween, Avidin-HRP was incubated for 30 minutes, followed by additional washes and the substrate solution, which was added for 5 minutes. The reaction was then stopped with 2M sulphuric acid (H_2SO_4).

The ELISA plate was read at 595nm using a multi well spectrophotometer (Molecular Devices, SpectraMax M3, USA). The standard curve was obtained using GraphPad Prism software and each sample concentration was calculated from the standard curve.



<u>Figure 2.5</u>: Schematic of an Enzyme Linked Immunosorbent Assay in a 96 well plate well

Primary antibody coats the bottom of the well, sample is added including protein of interest which binds to its specific primary antibody, a biotinylated secondary antibody binds to the protein of interest, Avidin-HRP is added, causing a colour change, which is read on a spectrophotometer at 595nm.



2.5.3 Western Blot

Supernatant samples of known protein concentration were prepared for Western blot analysis using sample buffer (Expedeon, Run Blue LDS, Sample buffer). Sodium dodecyl sulfate (SDS) page gels were prepared using a resolving gel (Table 2.7) and a stacking gel (Table 2.8) which were loaded in a western blot upright tank (Pierce, Thermo Scientific) containing running buffer (Table 2.4). Five samples from each group were run on a gel with a molecular weight marker ladder (RunBlue prestained marker, Expedeon) on each gel for 90 minutes at 100 volts. In the same tank, gels were transferred to polyvinylidene fluoride (PVDF) membranes (2μm, Pierce Thermo Scientific) in transfer buffer (Table 2.5) for ninety minutes at 100 volts, 4°C. Membranes were stored in PBS until probed with specific antibodies (Table 2.6).

Membranes were incubated in 5% blocking milk made up in PBS-T (Triton-X (0.05%) for 1 hour at room temperature and incubated with specific antibodies (anti IL-6, anti IL-6 receptors or anti- Glyceraldehyde 3-phosphate dehydrogenase (GAPDH), see Table 2.6) in 2% milk overnight at 4^{o}C. Washes were performed for ten minutes three times with PBS and secondary antibodies conjugated to hydrogen peroxidase conjugated secondary antibody for 1 hour room temperature. The labelled membranes were subsequently exposed to Enhanced Chemiluminescence (ECL) reagent in a 1:1 ratio of solution A and solution B (as per manufacturer's instructions, Aftersham ECL prime Western Blot Detection Reagent, GE Healthcare Life Sciences) incubated and the membrane exposed to X-ray film (CL-Xposure Film, Thermo Scientific), (Figure 2.5).

The ubiquitously expressed protein identified on the same membrane acts as a reference protein and loading control for each run. Protein band densitometry was quantified using Image J software analysis and expression of the protein of interest was express as a ratio of the GAPDH expression per lane, therefore histograms are expressed as mean relative expression of protein of interest (IL-6 or IL6R) as a ratio of total GAPDH in each sample.

See appendix for optimisation images.

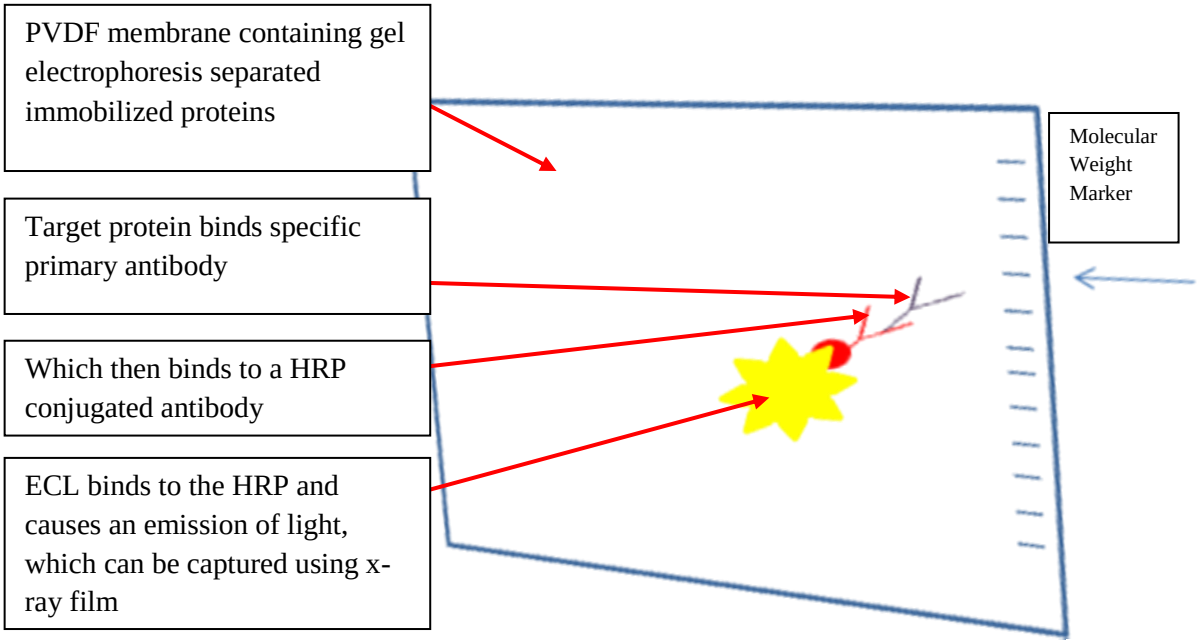


Figure 2.5: Schematic of a PVDF membrane containing immobilised proteins which have been separated by electrophoresis

A molecular marker aids in the determination of the molecular weight of a protein.

A primary antibody specifically binds to the protein of interest, the HRP-conjugated secondary antibody binds to the primary antibody and when ECL is added the light emitted can be detected on x-ray film.

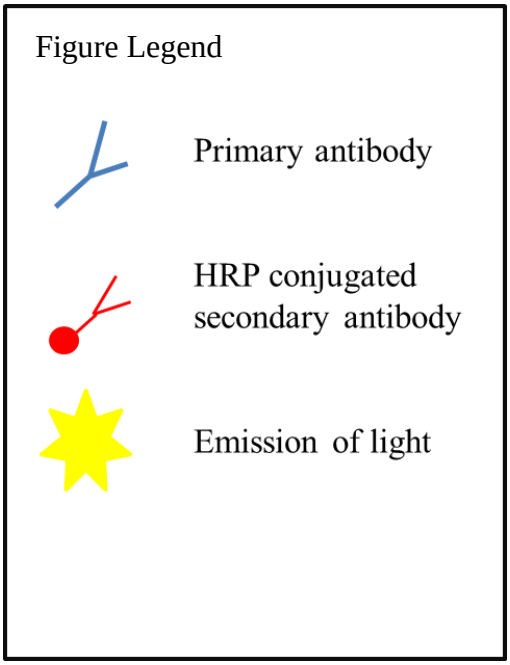


Table 2.6: Table of antibodies used in Western Blot Technique including host animal, dilution and incubation time and temperature and blocking solution.

Blocking solution				
Non-fat skimmed milk (w/v)	5%			
Tween-20 (v/v)	1%			
made in PBS				
Primary Antibodies	Host	Dilution	Duration	Temperature
Anti-IL-6	Rabbit	1 in 500	16 hours	4°C
Anti-IL-6 receptor	Goat	1 in 1000	16 hours	4°C
Anti- GAPDH	Mouse	1 in 20,000	16 hours	4°C
Secondary Antibody				
Anti Rabbit	Goat	1 in 2000	1 hour	Room Temperature
Anti Goat	Rabbit	1 in 5000	1 hour	Room Temperature
Anti Mouse	Goat	1 in 100,000	1 hour	Room Temperature

Table 2.7 and 2.8: **Resolving and Stacking Gel Recipe**

Resolving Gel 12%	
Bis-Acrylamide 30%	3ml
dH_20	2.45ml
SDS	75µl
Tris HCl (1M)	1.9ml
TEMED	4µl
APS	75µl

Stacking Gel 5%	
Bis-Acrylamide 30%	500µl
dH_20	2.05ml
SDS	30µl
Tris HCl (2M)	375µl
TEMED	4µl
APS	100µl

2.6 High Performance Liquid Chromatography (HPLC)

Monoamine detection from brain areas

HPLC is a technique which separates, identifies and quantifies a solute dissolved in a solvent. Standards of the proteins of interest peaks and retention time are used as a reference to quantify specific matching responses and are used to quantify the proteins. Snap frozen dissected brain regions (hypothalamus, prefrontal cortex, hippocampus, amygdala, midbrain, striatum) from WT and *mdx* mice, along with saline- and amitriptyline treated *mdx*mice were weighed and added to HPLC buffer (Table 2.9) in eppendorf tubes. These were kept on ice, and were sonicated (Sonoplus HD 2070, Bandelin) for two seconds. These sonicated samples were centrifuged (Mikro 22 R refrigerated centrifuge) at 19,000g for twenty minutes. 300µl of supernatant were loaded into glass vials and placed in a pre-determined pattern with standards in the first positions, after half the samples and at the last position in the HPLC machine (SCL 10-Avp system controller, LC-10AS pump, SIL-10A auto injector, CTO-10A oven, LECD 6A electrochemical detector, Shimadzu).

The chromatograms were processed using the Class 5-VP software using an equation to quantify the monoamines and metabolites with appropriate standards (Table 2.10). The peak heights of each monoamine in the samples were then entered into an excel spreadsheet where the sample concentrations in ng/g of tissue were calculated (Table 2.11).

Table 2.9: HPLC Buffer Recipe

HPLC buffer	**g/4l**
Citric Acid	84.056
Sodium Dihydrogen Phosphate	55.196
1-Octane sulfonic Acid	1.211
EDTA disodium salt	0.1488
with the addition of	
Methanol	400ml
N Methyl 5 HT	2ng/20µl

Table 2.10: HPLC Internal Standards

Amine	mg/10ml
NA (Noradrenaline, Norepeinephrine, Arterenol bitartrate Hydrate)	18.75
L-Dopa (3,4 Diyhdroxy-L-tryptophan, L-3,4-Dihydroxyphenylalanine)	10
DOPAC (3,4 Dihydroxyphenyl Acetic Acid)	10
DA (Dopamine, Dopamine Hydrochloride, 3-Hydroxytyramine HCL)	12.38
5HIAA (5-Hydroxy Indole-3-Acetic acid)	10
HVA (Homovanillic acid, 4-Hydroxy-3 Methoxy Phenylacetic acid)	10
5-HT (Serotonin, 5-Hydroxytryptamine creatinine Sulfate)	22
Internal Standard, N-Methyl 5-HT (N-Methy-5-Hydroxy-tryptamine Oxalate salt)	14.7

Table 2.11: **Equation and Legend to determine $A_{unk,}$ Amount of Amine in sample (ng/g of tissue)**

$$\frac{(PH_{sample}/PH_{IS,\ sample})}{PH_{\ standard}/PH_{\ IS,\ standard}} x A_{\ stdm}/A_{i\ sm} \times A_{IS\ S} x \frac{1000}{20} x \frac{1000}{W} = A_{\ unk}$$

PH_{sample}	Peak Height of Amine in sample
$PH_{IS,\ sample}$	Peak Height of Internal standard in sample
A_{stdm}	Amount of amine in standard mix (ng/20ml) = 2
A_{ISm}	Amount of Internal std in standard mix (ng/20ml) = 2
A_{ISS}	Amount of Internal Std in sample (ng/20ml) = 2
A_{unk}	Amount of Amine in sample (ng/g of tissue)
$PH_{standard}$	Peak Height of Amine in standard mix
$PH_{IS,Standard}$	Peak Height of Internal standard in standard mix.
W	Weight of tissue (mg)

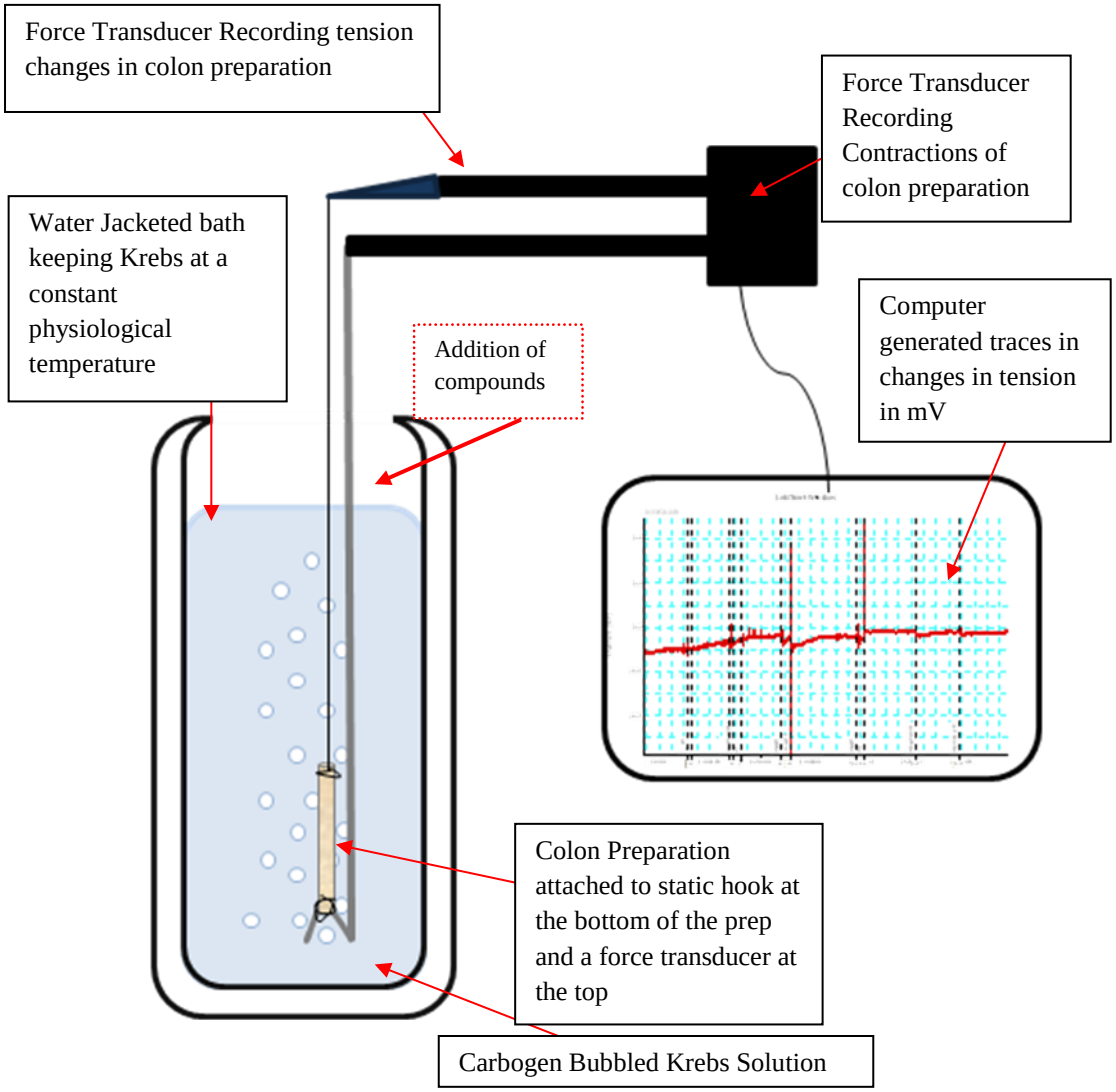
2.7 Organ Baths

2.7.1 Colon Organ Baths

Excised colons, with faecal pellets carefully washed out, were transferred to ice cold Krebs' saline. Organ baths consisted of a vertical 25 ml bath attached to a transducer which recorded isotonic contractions (PowerLab 2/25) and software (Chart 5 for Windows) at 37 ^{o}C. The transducer was calibrated using a one gram weight and tissue equilibrated for 20 minutes (as per Figure 2.6). One centimetre lengths were tied to both ends using cotton thread. Solutions were added to the bath containing the colon and between each addition the muscle and bath was washed with Krebs' except after addition of Tetrodotoxin (TTX). Basal levels were measured as the millivolt (mV) recording just before the addition of any compound and amplitude change recorded as the change in this baseline to peak height in the twenty minute period. The frequency of contractions was also measured.

Table 2.12: Krebs' Physiological Solution

Krebs' Physiological Solution	
Monosodium Phosphate	1.2 mM
Sodium Chloride	117mM
Potassium Chloride	4.8 mM
Magnesium Chloride	12mM
Sodium Bicarbonate	25mM
Calcium Chloride	2.5mM
Glucose	11mM



<u>Figure 2.7:</u> Schematic of the colon organ bath set-up

A water jacketed bath filled with Krebs solution is bubbled with Carbogen (95% O_2/5% CO_2). The colon preparation is tied to a static hook at the bottom and attached to a force transducer at the top with non-elastic thread. This force transducer generated a trace showing contractions in mV.

2.7.2 Diaphragm Organ Baths

A 3mm strip of diaphragm was dissected with central tendon attached and extending to a rib. Cotton thread was tied to the central tendon and hung vertically in a tissue bath (as per Figure 2.9) with aerated Krebs solution at 37 °C, the rib was tied to a hook in order to record isotonic and isometric contractions in this muscle. The muscle strip was equilibrated for 20 minutes.

A dual-mode force transducer (Aurora Scientific Inc.) was used to measure performance, which could hold the force or length, depending on requirements in each test. Electrical stimulation of the diaphragm strips was obtained through the use of two metal electrodes running vertically on either side of the diaphragm strip.

Using ASI Dynamic Muscle Control (v5.300) software, the optimum length (L_O, muscle length producing maximal isometric twitch force in response to supra-maximal stimulation) was determined by incrementally adjusting the micropositioner between intermittent stimulations and tetanic stimulations (100Hz). Once determined, the muscle remained at this length for the full protocol. Next the muscle was allowed a ten minute equilibration period. A protocol as performed as timeline below (Figure 2.8).

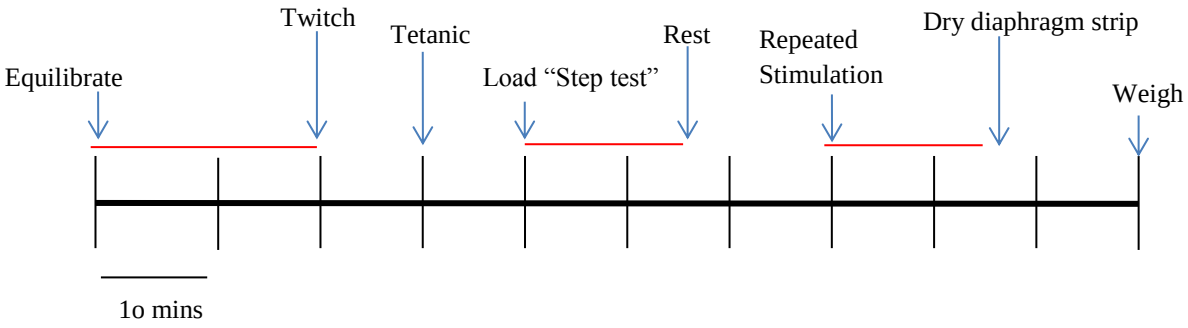


Figure 2.8: Protocol for diaphragm organ bath
Following a 20 minute equilibration time at 37°C, a twitch was elicited at supra maximal stimulation and optimal length was determined. Next tetanic force was measured. The transducer was then used in an isotonic set up, to record muscle shortening at increments of total force for a "step" test. A repeated stimulation at 33% of total force was performed. The muscle strip was then left to dry and was weighed to determine the cross sectional area for analysis.

Holding the force transducer static, force was recorded in milli Newtons. A single isometric twitch force, contraction time, half-relaxation time and performance during repeated stimulation were then determined in response to electrical field stimulation.

First, a single twitch was elicited (supra-maximal voltage, 1 ms duration).

Twitch force, contraction time (time to peak force) and half-relaxation time (time for peak force to decay by 50%) and peak tetanic force were determined post-test using ASI 611A Dynamic Muscle Analysis (v5.100).

Force was normalised to cross sectional area (CSA), density of muscle (1.06kg/L) is a constant.

CSA= Muscle weight (grams)/Optimal length (cm)*density of muscle

Shortening velocity was recorded from the first detectable length change in the strip for duration of 30ms.

Work was calculated as the product of isotonic afterload and the amount of maximal shortening.

Power was calculated as a product of isotonic afterload and shortening velocity.

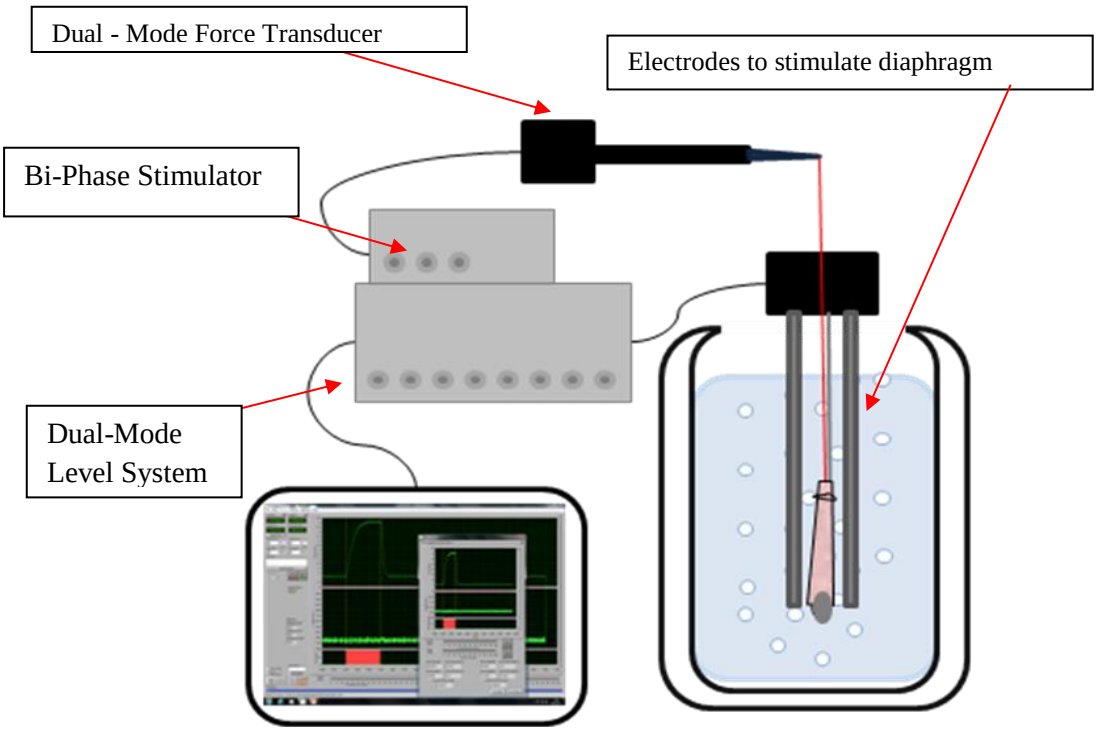


Figure 2.9: Schematic of the diaphragm organ bath set-up
Similar to the colon organ bath, water jacketed bath filled with Krebs solution is bubbled with Carbogen. The diaphragm preparation is tied to a static hook at the bottom and attached to a force transducer at the top with non-elastic thread. A computer generated trace is recorded in milli Newton and millimetre. Different from the colon set-up, two electrodes flank the preparation to stimulate the muscle. The force transducer can remain static to record isometric contraction or set at increments of stiffness to record contractions of the diaphragm strip.

2.8 Statistical Analysis of Data

N numbers for each experimental group were decided using power calculations based on previous studies in our laboratory and studies in the literature. The minimum number of animals were used to garner data that would predict significance at the $p<0.05$ level. Unless stated otherwise, Graph Pad Prism was used to perform statistical analysis. Student's t- test was performed between two groups, one way ANOVA or two-way ANOVA were performed between multiple groups and appropriate post-hoc tests were used to compare between groups. Statistical significance illustrated as *$p<0.05$, **$p<0.01$, ***$p<0.001$, *ns* not significant.

2.9 Reagents

Anti IL-6 receptor antibody (MR16-1) used in the intervention study (Study 2 & 3) was a kind gift from Chugai Pharmaceuticals Ltd., Tokyo, Japan. All other reagents were purchased commercially from Sigma Aldrich, Fischer Scientific or as stated in the text.

Chapter 3: Investigating the potential benefits of amitriptyline in treating inflammation and mood in *mdx* mice

3.1 Introduction

3.1.1 Mood Disorders in Duchenne Muscular Dystrophy

Although largely under-diagnosed, there is some evidence for mood disorders in DMD and in other muscular dystrophy. Patients have a low grade but persistent depression compared to age-matched healthy controls patients (Fitzpatrick et al. 1986). However, understanding the aetiology or cause of these depressive symptoms in DMD has largely been overlooked as the more severe symptoms of DMD take priority such as progressive tissue inflammation and loss of function. Indeed, this is the most prevalent and chronic feature of the disease (Evans et al. 2009), but given the well-reported co-morbidity of depression in other inflammatory diseases, it is perhaps not that surprising that depression is also prevalent in DMD patients (Fitzpatrick et al. 1986; Bothwell et al. 2002; Abresch et al. 1998).

Stress is known to directly contribute to inflammatory diseases, through increased secretion and activation of cytokines and by increasing numbers of leukocytes, natural killer cells and CD8+ T-lymphocytes and decreasing the numbers of B lymphocytes (Maes 2008; Connor & Leonard 1998) In contrast, the increased secretion of glucocorticoids characteristic of chronic stress (from the adrenal glands in response to cortisol is associated with decreased secretion of pro-inflammatory cytokines) and immunosuppression (Herbert and Cohen, 1993; Leonard, 2001; Raison and Miller, 2001). Recent interest in the connection between DMD pathophysiology and stress reveals a connection between sympathetic nervous system dysfunction and stress disorders in patients (Sabharwal 2014). Thus, like in other inflammatory diseases, regulating inflammation in DMD may have additional positive therapeutic effects on mood. Conversely, tackling depression and mood disorders in DMD may have be beneficial in the regulation of inflammation (Du et al. 2013; Venihaki et al. 2001; Gerber & Bale 2012; Vallières & Rivest 1999).

3.1.2 Amitriptyline as a potential pluripotent anti-depressant

Amitriptyline is classified as a tricyclic antidepressant (TCA), with a wide range of pharmacological actions (Inglis et al. 1963), including anti-oxidant (Leduc et al. 2002), anti-inflammatory (Achar et al. 2009) and anti-nociceptive effects (Abdel-Salam et al. 2003), although full pharmacological profile and mode of action of amitriptyline is not completely understood. That said, the anti-depressant effects of amitriptyline are attributed to its affinity for receptor sites for noradrenaline and serotonin, inhibiting noradrenaline- and increasing serotonin (Giuseppe et al. 2007) reuptake at synapses. Along with other TCAs, amitriptyline is commonly used to treat chronic pain disorders including neuropathic and inflammatory pain (Abdel-Salam et al. 2003). Studies have shown that amitriptyline attenuates pain in inflammatory and neuropathic pain in rats, especially when combined with opiates (Tai et al. 2006). Furthermore, in a model of tubule interstitial renal fibrosis and inflammation it decreases inflammation and slows the progression of fibrosis (Achar et al. 2009).

Although TCAs have largely been replaced by newer antidepressants with fewer side-effects, the therapeutic characteristics of amitriptyline may have potential benefits in treating mood disorders and inflammation in DMD. Indeed, TCA's seem to be more effective than the corticosteroid, prednisone in preventing muscle loss in a *C. elegans* model of dystrophin-dependent degeneration (Carre-Pierrat et al. 2011). Moreover, a recent investigation demonstrated that TCAs such as amitriptyline have beneficial effects on muscle function in *mdx mice* (Carre-Pierrat et al. 2011).

3.1.3 Hypothesis

We hypothesise that depression in DMD is contributed to by inflammatory molecules which result in the dysregulation of the HPA axis. Thus, the TCA with anti-inflammatory actions amitriptyline is a promising candidate for treating symptoms in DMD.

3.1.4 Specific Study Aims

- To characterise the behavioural phenotype of the *mdx* mouse model of DMD and investigate the effects of amitriptyline on these behaviours.

- Investigate changes in amine levels in the brain associated with mood disorders following amitriptyline treatment.

- To examine the effects of amitriptyline treatment on skeletal muscle pathology and inflammation in the *mdx* mice.

3.2 Methods

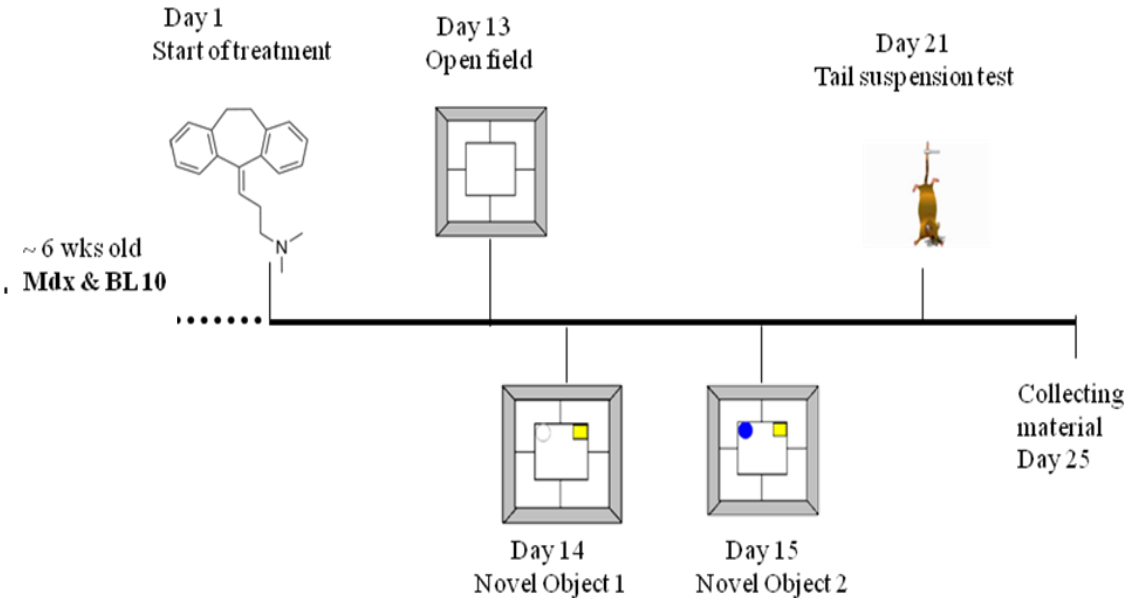
3.2.1 Animals and experimental design

Male C57BL/10ScSn (wild-type (WT) control) and C57BL/10ScSn-*mdx*/J (*mdx, dystrophin deficient*) mice (20g to 25g body weight) were randomly assigned to the following groups: untreated WT versus untreated *mdx* and saline-treated *mdx* versus amitriptyline-treated *mdx mice* (Table 3.1). Mice were administered one subcutaneous injection of amitriptyline (10 mg/kg body weight) or saline (0.9% NaCl) each day for 25 consecutive days.

Table 3.1 Treatment groups and timeline

The timeline illustrates the experimental protocol for comparing treatment with amitriptyline or saline in a number of behavioural tests including the open field arena, the novel object recognition test and the tail suspension test.

Groups	Treatment		
	Untreated	Saline	Amitriptyline
C57/BL/10ScSn WT	10	7	7
C57Bl/10ScSnDmd*mdx*/J(*mdx*)	10	7	7



3.2.2 Techniques

Open Field (chapter section 2.3.2.1)

Novel Object Recognition Test (chapter section 2.3.2.2)

Tail Suspension Test (chapter section 2.3.2.3)

Collecting Tissue and Blood (chapter section 2.3.2.3)

Mice were sacrificed 3 days after the last behavioural test by isofluorane anaesthesia and cervical dislocation. Brains were taken and prefrontal cortex, hypothalamus, striatum, hippocampus, amygdala were dissected out and stored at -80°C until HPLC was performed from WT and *mdx mice* treated with saline or amitriptyline.

Right Extensor Digitorum Longus (EDL) was dissected out and snap frozen for IL-6 quantification. Left EDL was immersed in 4% PFA and processed for histology.

Histology (chapter section 2.4.2.1)

Paraffin embedded skeletal EDL muscles from untreated WT and *mdx* mice and amitriptyline and saline treated *mdx* mice were sectioned and stained with H & E as previously described in the methods section. Pathological markers such as percentage of centralised nuclei and infiltration of inflammatory cells within and between fibres were scored.

Protein Quantification (chapter section 2.5.1)

EDL muscle from WT and *mdx* mice was homogenised and protein was extracted for ELISA (as detailed in section 2.5.2.1) and HPLC (as detailed in section 2.6) analysis.

3.3 Results

Part 1: Assessing *mdx* behaviours and skeletal inflammation

3.3.1 Behavioral phenotype of *mdx* mice

3.3.1.1 Anxiety behaviours

Given rodent's natural tendency to avoid bright open spaces combined with its instinct to explore new environments, the brightly-lit, exposed open field arena is a useful tool to measure anxiety-like behaviours between different strains or following therapeutic interventions in mice. Thus, comparably more time spent in the corners or edges of the arena are indicative of increased anxiety. Offline analysis of the 10 minute trial found that *mdx* mice (81.5±10.06, n=10) spent less time in the centre than WT mice (100.6±6, n=7, $p<0.05$) in the first five minutes of the trial (Figure 3.1iv). Similarly, *mdx* mice (70.2±5.6) spent less time in the centre compared to WT mice (74±6.1, $p<0.05$) in the second five minutes of the trial (Figure 3.1v) and indeed, overall, *mdx* mice spent less time exploring the centre of the arena than WT control animals ($p<0.05$) (Figure 3.1vi). No differences were noted in the incidence of grooming, but differences were found in total time spent grooming (Figure 1i), which can also be indicators of anxiety (Maes et al. 2012).

As loss of dystrophin is associated with loss of muscle function I examined ambulatory activity in the *mdx* mice to ensure that the apparent anxiety-like phenotype was not in fact due to impaired motor function. Thus, in the demarcated open field arena (Figure 2.1, methods chapter) the ambulatory activity of the *mdx* and WT mice was scored as the number of total crossings across each line. No differences in the number of crossings were apparent between the *mdx* (26.5±5, n=10) and WT (42.2±3.1, n=9, $p>0.05$) mice in the first five minutes (Figure 3.1i), the second 5 minutes between *mdx* (37.5±3.1, n=9) and WT (51.4±7.8, n=10, $p>0.05$) (Figure 3.1ii) or indeed, over the combined 10 minutes (Figure 3.1iii, $p>0.05$). A time trial of ambulation was also undertaken in one minute intervals and

no differences were found suggesting that the capacity to move and explore was not hindered in the *mdx mouse* at the time point examined.

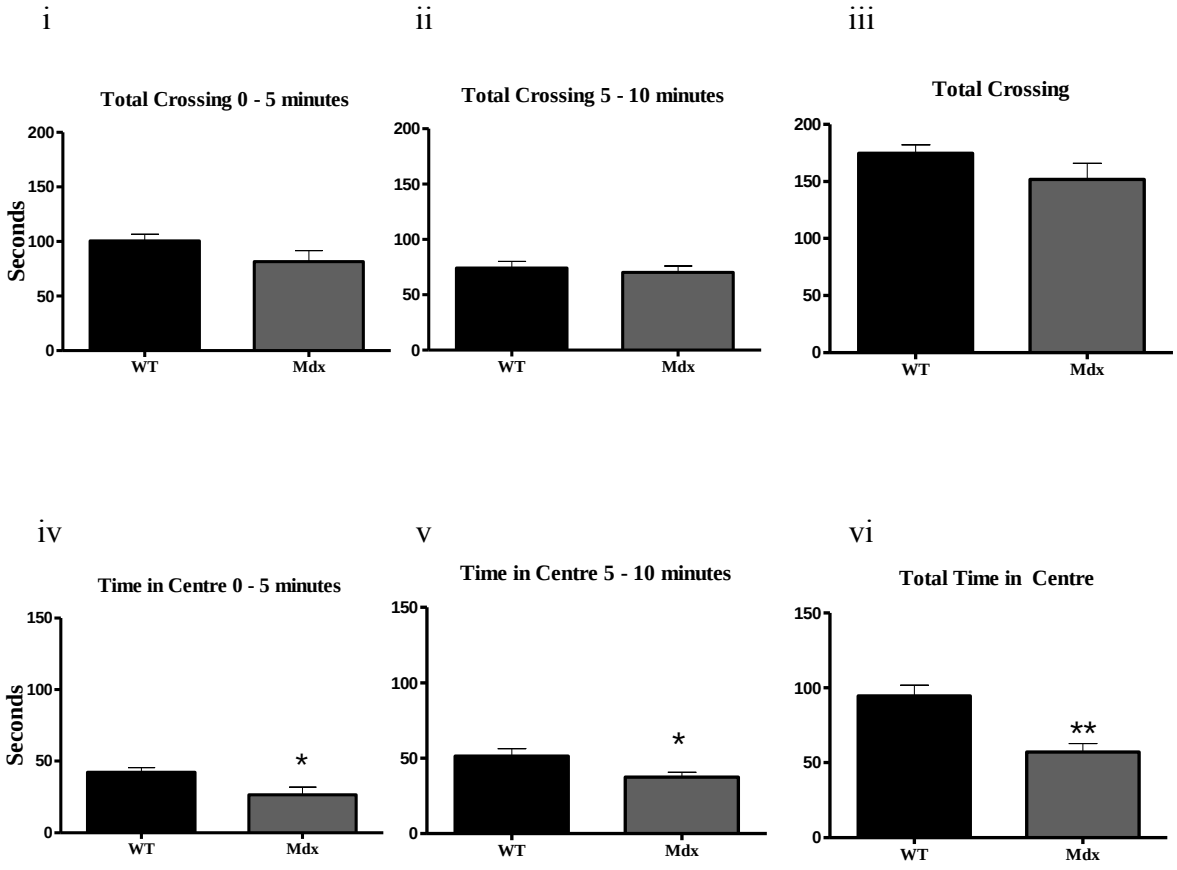
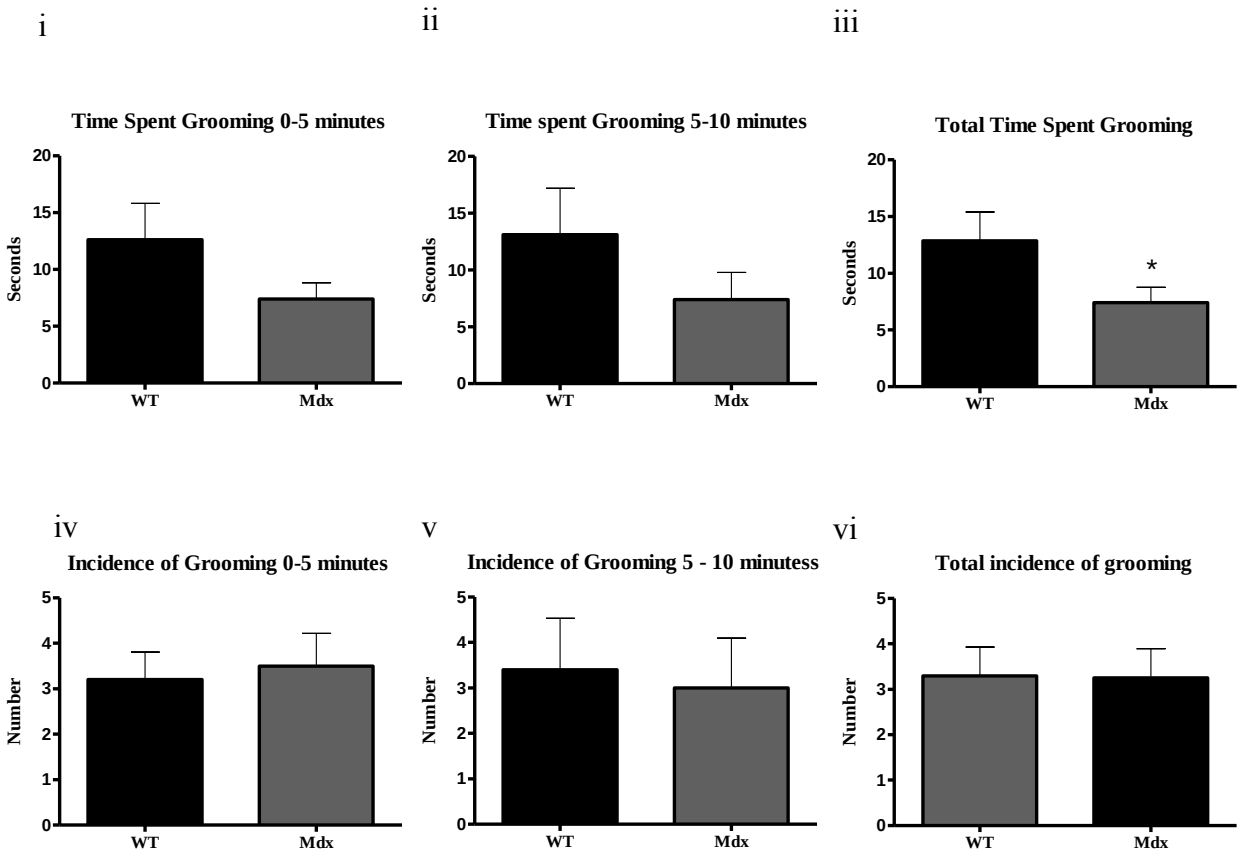


Figure 3.1: Open Field Behavioural Analysis

*Student's t tests results of locomotor activity assessed by time spent transversing lines in the arena in the first 5 minutes (i), second 5 minutes (ii) and total time (iii). Histograms (iv) illustrate the time spent exploring the centre of the arena in the first five minutes and in the second 5 minutes (v) and total time (vi). n=10, *p<0.05, **p<0.01*



<u>Figure 3.2</u>: Open Field Behavioural Analysis

*The histograms illustrate grooming behaviour in the first 5 minutes (i), second 5 minutes (ii) and total time spent grooming (iii) during the open field trial. The incidences of grooming behaviour in the first (iv) and second 5 minutes (v) and total time (vi) of the trial are shown in the histograms. n=10, * p<0.05*

3.3.1.2 *Mdx* mice and WT mice explore a novel object for comparable time in the NOR test

The NOR test is used to assess learning and recognition memory in rodents (Antunes & Biala 2012). The time spent exploring the new object, which was only presented on day 2 in comparison to the object consistently present on day 1 and 2 as a percentage of total exploration of both objects was comparable between *mdx* mice and WT mice (Figure 3.3, n=10, $p>0.05$).

3.3.1.3 *Mdx* mice exhibit depressive like-behaviour

In the tail suspension test, which is an established test to indicate depression-like behaviour in rodents (Porsolt et al. 2001), the time spent immobile in the last 4 minutes of a six minute test was analysed. *Mdx* mice spent more time immobile (154.3±12.2 seconds, n=8) during this inescapable stressor than their WT controls (106.9±11.2 seconds, n=7, $p<0.05$, Figure 3.4i). Moreover, the latency to immobility, or the time it took for the mice to display despair at the inescapable stress, was shorter in *mdx* mice (6.5±3 seconds, n=9) than WT controls (35.6± 5.5 seconds, n=9, $p<0.05$, Figure 3.4ii).

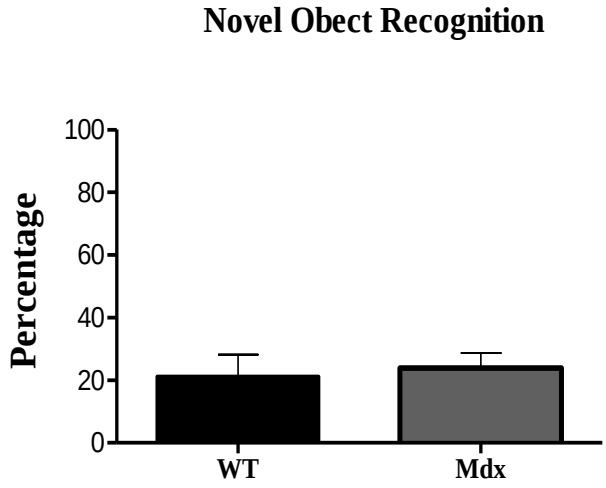


Figure 3.3: Novel Object Recognition Test Analysis
WT *and mdx mice spent the same amount of time exploring a novel object compared to overall time exploring the two objects. n=10, p>0.05*

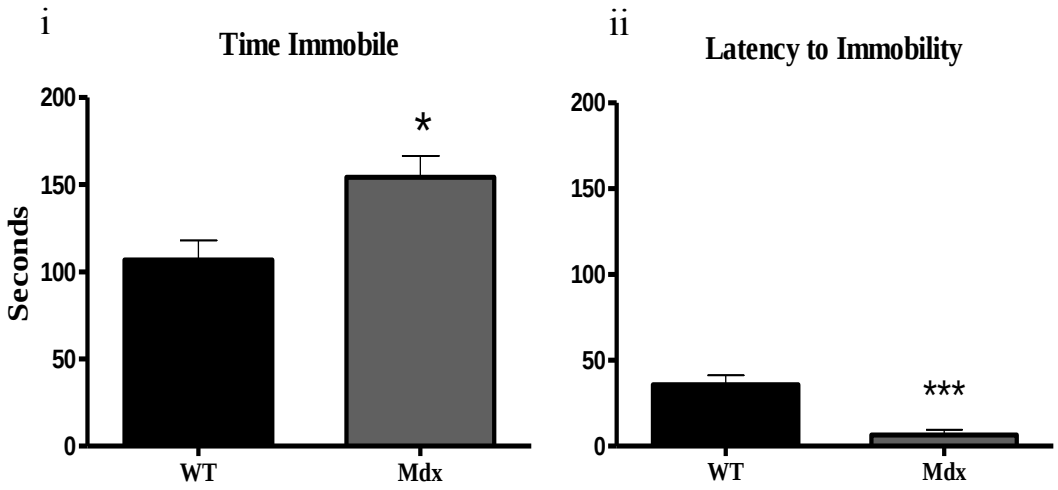
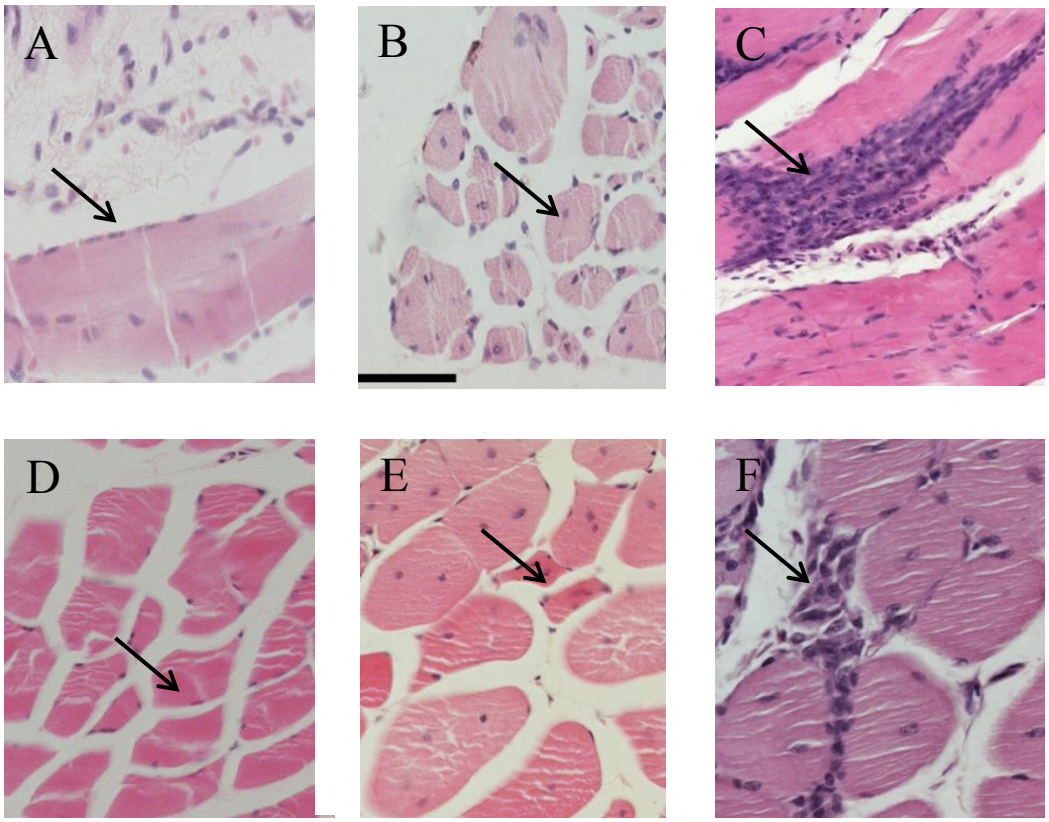


Figure 3.4: Tail Suspension Behavioural Analysis
*The time spent immobile (or despairing at the inescapable stressor) in the last 4 minutes of a tail suspension trial is higher in mdx mice (i) whereas the latency to first period of immobility is shorter in mdx mice (ii). n=10, *p<0.05, ***p<0.001*

3.3.2 *Mdx* striated skeletal muscle exhibit histological signs of regeneration and infiltration of mononuclear cells

Inflammation was scored as the number of fibres with inflammatory events such as the infiltration of phagocytes into the muscle cells, termed myophagocytosis as a percentage of the total number of fibres per image. The area of inflammation as a percentage of the total area of fibres imaged was also analysed. The total area of inflammation in *mdx* mice (8.7±2.1, n=10 per group) was higher than in WT mice (1.1±0.1, n=10, $p<0.001$, Figure 3.5ii). Moreover *mdx* mice (12.9±1, n=10) had a higher number of inflammatory events than their WT controls (5.3±0.4, n=10, $p<0.001$) and the frequency of inflammatory incidents of immune cell infiltration in cross sections of EDL muscle histology (Figure 3.5iii). Centralised nuclei are a marker of regeneration. In EDL muscle in *mdx* mice (54.7±4.3, n=10) more centralised nuclei as a percentage of total nuclei per image were identified as compared to the WT muscle (20.7±3.2, n=10, $p<0.001$, Figure 3.5i).



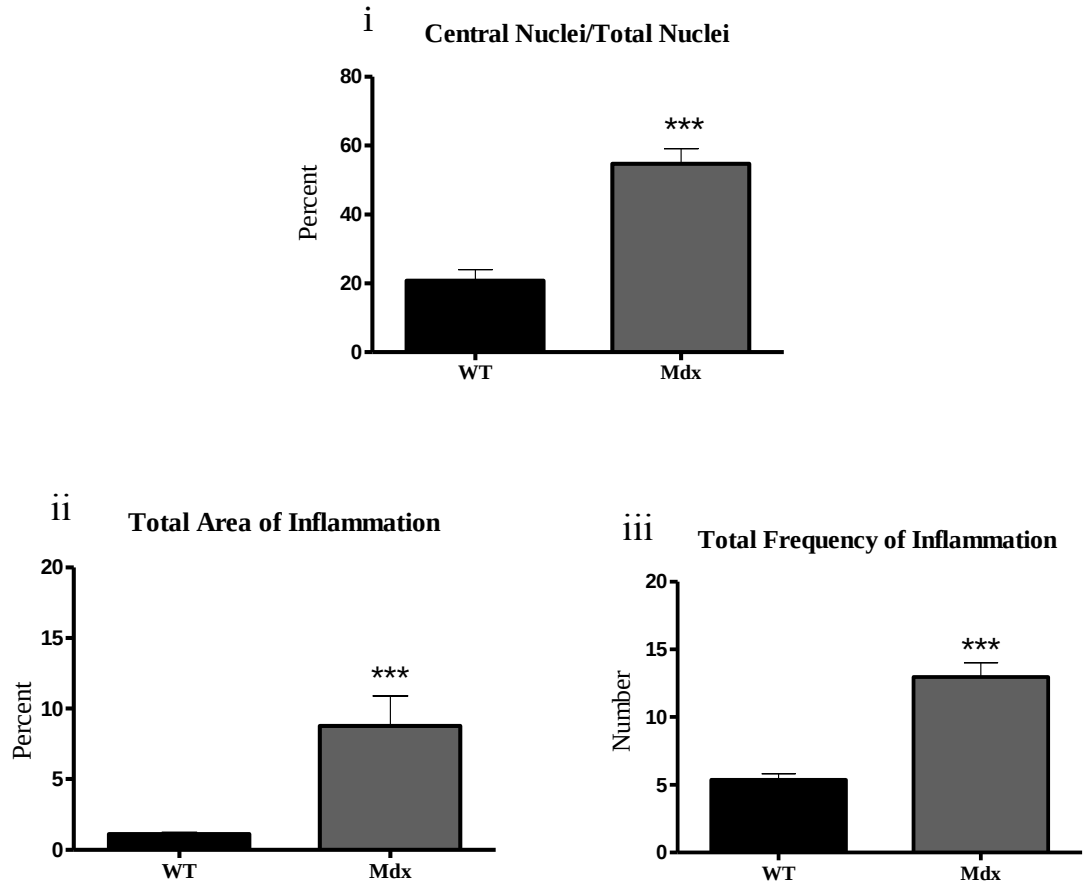
Representative images of* WT *skeletal muscle (A and D) and muscle pathology found in dystrophin deficient mice (B, C, E & F) cut at 10µm and stained with haematoxylin and Eosin (H&E). Scale bar 100µm.

A - C: Sections through H&E stained skeletal muscle.

In **A**, muscle not showing pathology - a high number of peripheral nuclei is seen. In dystrophic muscle: **B**, chains of central nuclei can be seen in both fibres, along with normal peripheral nuclei, and in **C** a fibre undergoing myophagocytosis. Shown with arrows.

D - F: Transverse sections through H&E stained skeletal muscle.

In **D**, muscle not showing pathology – with peripheral nuclei and uniform fibre diameters. In dystrophic muscle, **E** a high number of central nuclei and varying fibre sizes are seen, in **F** fibres are being infiltrated, and there is some fibrosis. Shown with arrows.



<u>Figure 3.5</u>: Pathohistological Analysis of skeletal muscle inflammatory markers

Skeletal tissue from mdx mice have higher percentage of central nuclei than WT *(a) a larger area of inflammation (b) and a higher incidence of inflammation (c) as compared to WT controls. n=10, *** p<0.001*

3.3.3 IL-6 ELISA for Homogenized Muscle

IL-6 is a known pro-inflammatory cytokine released from muscle fibres. Using ELISA analysis of homogenised right forelimb flexor muscle, IL-6 trended towards being increased in *mdx* (34.89±8.125) over WT mice (15.21±1.86, Figure 3.6, $p>0.05$), however, this was not statistically significant.

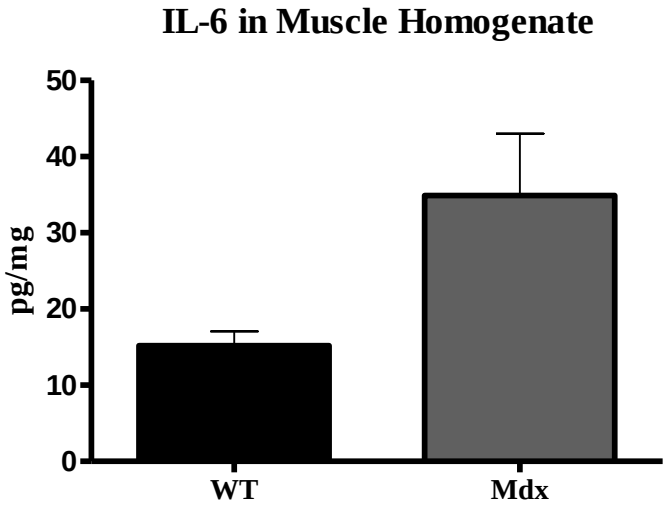


Figure 3.6: ELISA analysis of IL-6 in homogenised skeletal muscle of the forelimb
Mdx mice have double IL-6 levels per milligram of protein than WT *mice; however this is not statistically significant in a student's t test.*

3.4 Part 2

Intervention Study - The effects of amitriptyline on *mdx* behaviour and inflammation

3.4.1: The effects of amitriptyline on *mdx* behaviour and inflammation

By characterising the behavioral profiles of *mdx* mice, I discovered they exhibit depressive and anxiety like behaviours in addition to extensive inflammation in their skeletal muscle. To assess the therapeutic efficacy of amitriptyline on any or all of these symptoms I compared two groups of *mdx* mice, a control group treated with saline and a group treated with amitriptyline.

3.4.1.1 Amitriptyline had anxiolytic effects in *mdx* mice

Mdx mice treated with amitriptyline spent more time in the centre of the open field (114.8±2.5s, n=7, $p<0.05$) than saline-treated *mdx* mice (35.2±6.3s, n=5) in the first five minutes of the trial (Figure 3.7iv) and a comparable amount of time in the second five minutes of the trial (Figure 3.7v, $p>0.05$). Overall, for the total ten minutes, amitriptyline-treated *mdx* mice spent more time exploring the centre of the arena (49.1±4, n=5) as compared to WT controls (57.2±7, n=7, $p<0.05$, Figure 3.6vi). Ambulatory activity of both *mdx* groups was again scored as number of total crossings across each line and no differences were noted between amitriptyline-(64±7.2s , n=6) and saline-treated (67±7.7s, n=7, $p>0.05$) *Mdx* mice in the first five minutes (Figure 3.7i) or between amitriptyline-treated *mdx* mice (49.1±4, n=6) and saline-treated mice (57.2±5.9, n=7, $p>0.05$) the second five minute trial (Figure 3.7b), or indeed, over the total ten minute trial (Figure 3.7iii).

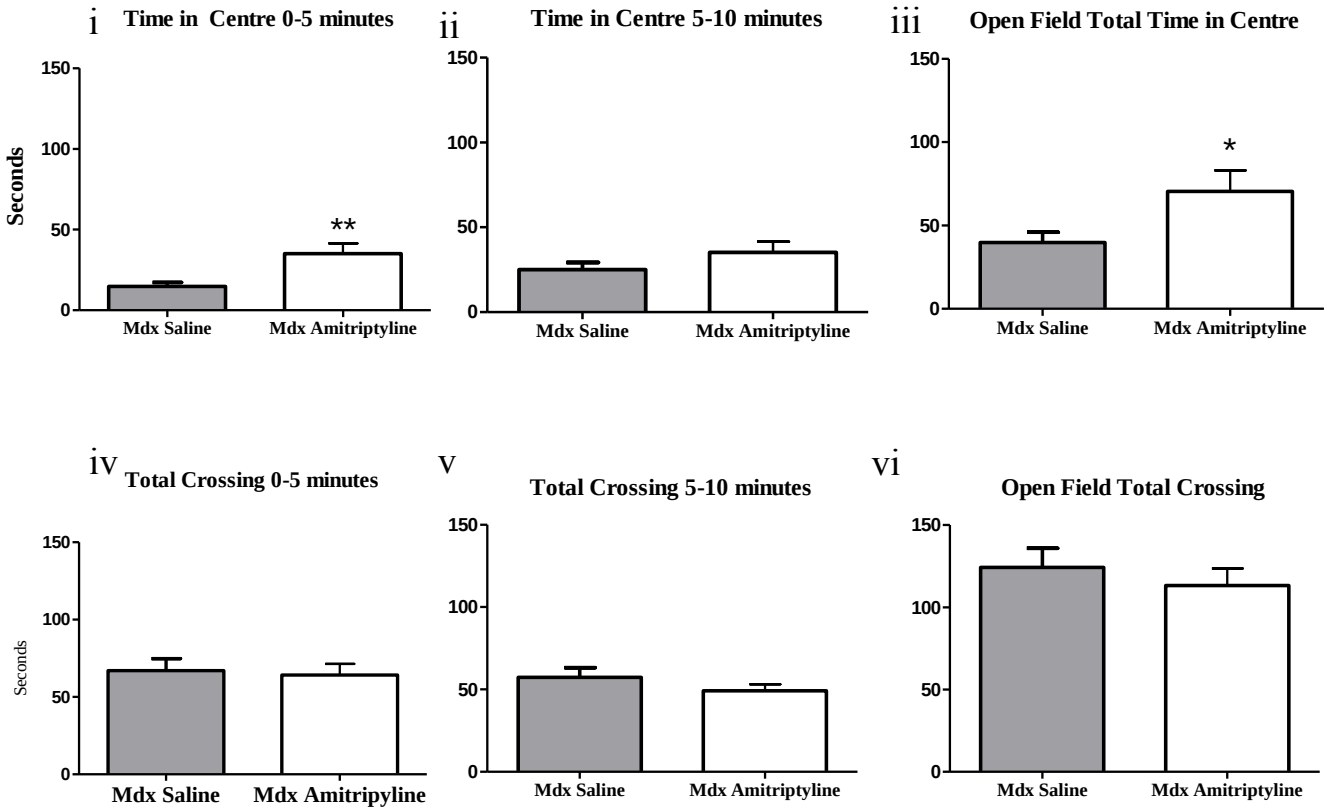


Figure 3.7: Open Field Behavioural Analysis of amitriptyline treated *mdx* mice compared to saline *mdx* controls

*Students t tests results analysing locomotor activity assessed by time spent transvering lines in the arena in the first 5 minutes (i), second 5 minutes (ii) and total time (iii) time spent in the centre of the arena in the first five minutes (iv) and in the second 5 minutes (v) and total time (6) n=7, *p<0.05, **p<0.01*

3.4.1.2 Amitriptyline increases exploration of a novel object in *mdx* mice

While control *mdx* mice did not show any difference in the time spent exploring a new object as compared to the WT mice, treatment with amitriptyline resulted in *mdx* mice spending a longer time exploring the novel object (74.67± 4.8 seconds, n=7) as compared to saline-treated *mdx* controls (50.05±3.5 seconds, n=7, $p<0.01$, (Figure 3.8).

3.4.1.3 Amitriptyline alleviates depressive behaviour in behavioural tests

Amitriptyline-treated *mdx* mice spent less time spent immobile (78.4±13.7 seconds n=7) in the TST as compared to their saline-treated counterparts (89.5±3.7 seconds, n=7, $p<0.05$, Figure 3.9i) indicating an anti-depressant effect of amitriptyline. Moreover, amitriptyline treatment increased the latency to immobility in *mdx* mice (89.5±3.7 seconds, n=7) compared to saline-treated mice (24±5.4 units, n=7, $p<0.05$, Figure 3.9ii).

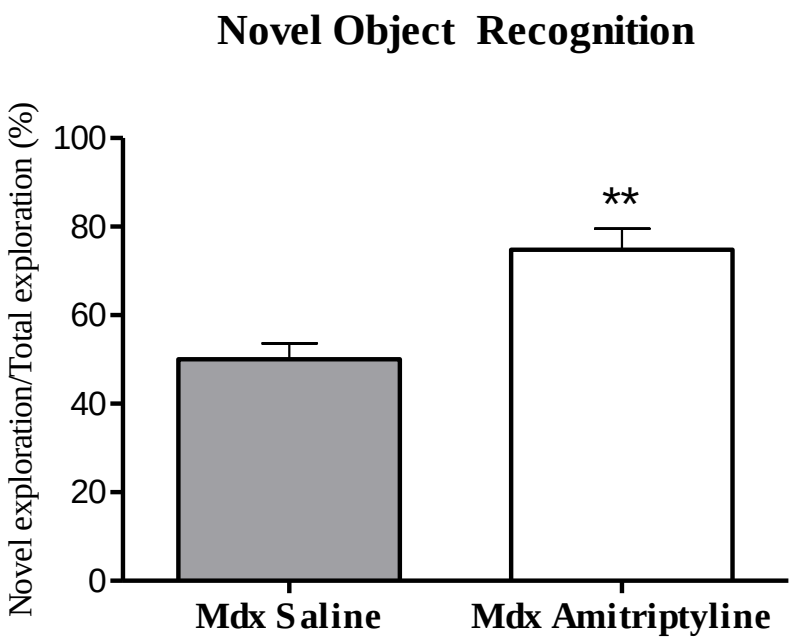


Figure 3.8: Novel Object Recognition Behavioural Analysis of amitriptyline treated *mdx* mice compared to saline *mdx* controls

*Results analysing time spent exploring novel object over total exploration shows amitriptyline increases novel object exploration. n=7, **p<0.01*

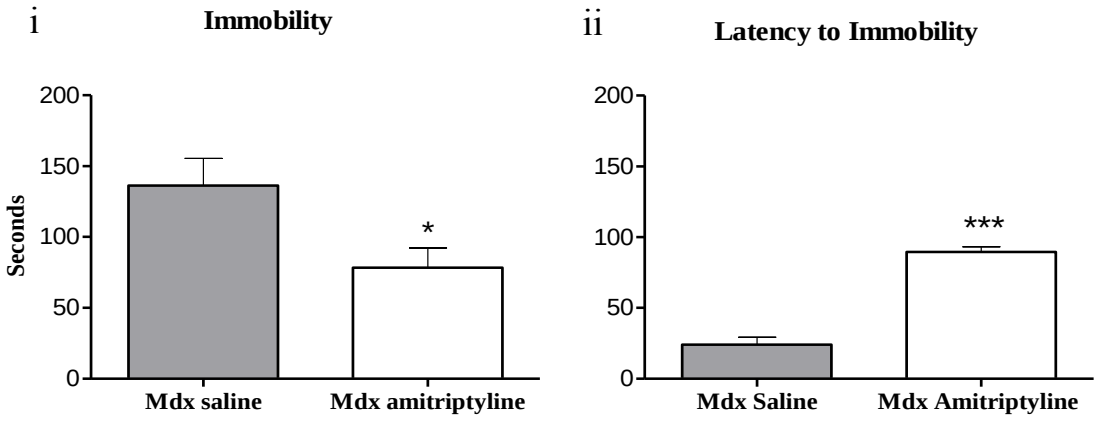


Figure 3.9: Tail Suspension behavioural Analysis of amitriptyline treated *mdx* mice compared to saline controls

*Student's t tests results analysing time immobile in the last 4 minutes of a tail suspension trial (i) and latency to first period of immobility (ii) indicating amitriptyline alleviates depressive symptoms in mdx mice. n=7, *p<0.05, ***p<0.001*

3.4.2 Amitriptyline alters amine levels in several brain regions of *mdx* mice

As monoamines have been attributed an important role in mood disorders such as anxiety and depression, the effects of amitriptyline on monoamine expression in several brain regions associated with mood disorders were determined using HPLC analysis. As detailed in Table 3.2, in the WT mice amitriptyline increased noradrenaline levels ($p<0.01$) in the hippocampus and in the midbrain ($p<0.05$), where alterations in neurotransmitters have been associated with depressive-like behaviour. DOPAC/DA turnover was also increased ($p<0.05$) in the midbrain. Amitriptyline did not change monoamine levels in any other brain regions examined in the WT mouse.

In *mdx* mice, serotonin levels were increased in the amygdala, a region important in processing emotionally-evoked memories following amitriptyline treatment in comparison to saline-treated *mdx* mice ($p<0.05$). Amitriptyline also induced an increase in amygdalar HVA/DA turnover ($p<0.05$). In the hippocampus, amitriptyline increased 5HT ($p<0.05$), 5-HIAA ($p<0.05$) and DOPAC levels ($p<0.05$). Amitriptyline evoked a decrease in HVA ($p<0.05$). In the midbrain, DA ($p<0.05$) and DOPAC ($p<0.05$) were increased following administration of amitriptyline. Furthermore, amitriptyline stimulated an increase in 5-HIAA ($p<0.05$) and 5-HIAA/5HT turnover ($p<0.05$) in this region. Monoamine levels were not altered by treatment with amitriptyline in either the prefrontal cortex or the striatum (Summarised in tables in Figure 3.2 & 3.3, n=3-5 for each brain region).

Table 3.2: HPLC monoamine analysis of areas important in depression and anxiety in WT – *amygdala, hippocampus, hypothalamus, striatum, prefrontal cortex and midbrain in amitriptyline treated* WT *versus saline treated* WT *mice. Data presented as mean ± SEM and n numbers. * p<0.05, **p<0.01 (/ = monoamine below detectable level)*

WT	Amygdala		Hippocampus		Hypothalamus	
Concentration (ng/g)	Saline	Amitriptyline	Saline	Amitriptyline	Saline	Amitriptyline
5HT	287.6±42.21	651.1±200.7	825.4±99.42	1551±388.4	1470±139.2	2987±1204
n=	4	3	5	5	5	5
5HIAA	218.8±98.77	169.7±68.05	1695±1220	916.3±169.4	615.6±121.5	1267±445.1
n=	5	4	5	5	5	5
NA	147.2±81.85	195.5±65.82	438.7±38.02	1124±211**	3287±1068	6316±2240
n=	3	4	5	5	5	5
DA	181.9±48.1	275.8±113	79.07±10.58	106.6±30.62	721.8±302.3	1339±544.2
n=	4	4	5	4		5
DOPAC	/	/	30.28±5.271	52.71±29.97	103.5±26.32	243±67.43
n=			5	5	55	5
HVA	479.9±296.2	141.1±58.07	185.3±20.85	318.5±99..56	201.6±37.46	302.5±108.5
n=	5	4	5	5	5	5
Turnover (ratio)						
5HIAA/5HT	0.4180±0.03306	0.3410±0.02539	0.6262±.04803	0.6363±0.06975	0.3321±0.009421	0.4480±0.04192 *
n=	5	4	4	5	5	5
DOPAC/DA	/	/	0.3959±0.07781	0.2678±0.1003	0.1711±0.01911	0.2190±0.04720
n=			5	5	5	5
HVA/DA	0.9983±0.2396	0.5146±0.1343	2.428±0.3068	2.472±0.8543	0.3657±0.07204	0.2472±0.04222
n=	5	5	5	4	5	5

WT	Striatum		Prefrontal Cortex		Midbrain	
Concentration (ng/g)						
5HT	2880±930.9	2496±1445	691.8±104.7	1388±428.8	2880±930.9	2496±1445
n=	4	4	4	5	5	5
5HIAA	1336±442.6	633.7±58.15	419.7±233.5	344.2±104.1	1336±422.6	633.7±58.15*
n=	4	3	4	5	5	5
NA	1630±1093	1114±882.1	420.7±261.9	677.4±162.3	1630±1093	1114±882.1*
n=	5	4	4	5	5	5
DA	30728±10419	12792±2990	130.1±105.6	94.75±31.21	30728±10419	12792±2990
n=	4	4	4	5	5	5
DOPAC	2570±716.6	1154±70.24	/	/	2570±716.6	1154±70.24
n=	4	3			5	5
HVA	4250±1944	2463±312.9	194.5±124.8	203.8±52.06	4250±1944	2463±312.9
n=	4	3	4	5	5	5
Turnover (ratio)						
5HIAA/5HT	0.4660±0.03060	1.719±1.117*	0.2623±0.01486	0.2530±0.02552	0.6152±0.1011	0.5959±0.06048
n=	4	4	5	5	5	5
DOPAC/DA	0.1202±0.03472	0.1185±0.03976	/	/	0.1565±0.03255	0.2717±0.04065 *
n=	4	4			5	5
HVA/DA	0.09208±0.01344	0.07692±0.003487	2.091±0.1948	2.329±0.3316	0.9911±1.508	1.249±1.820
n=	3	4	4	5	5	5

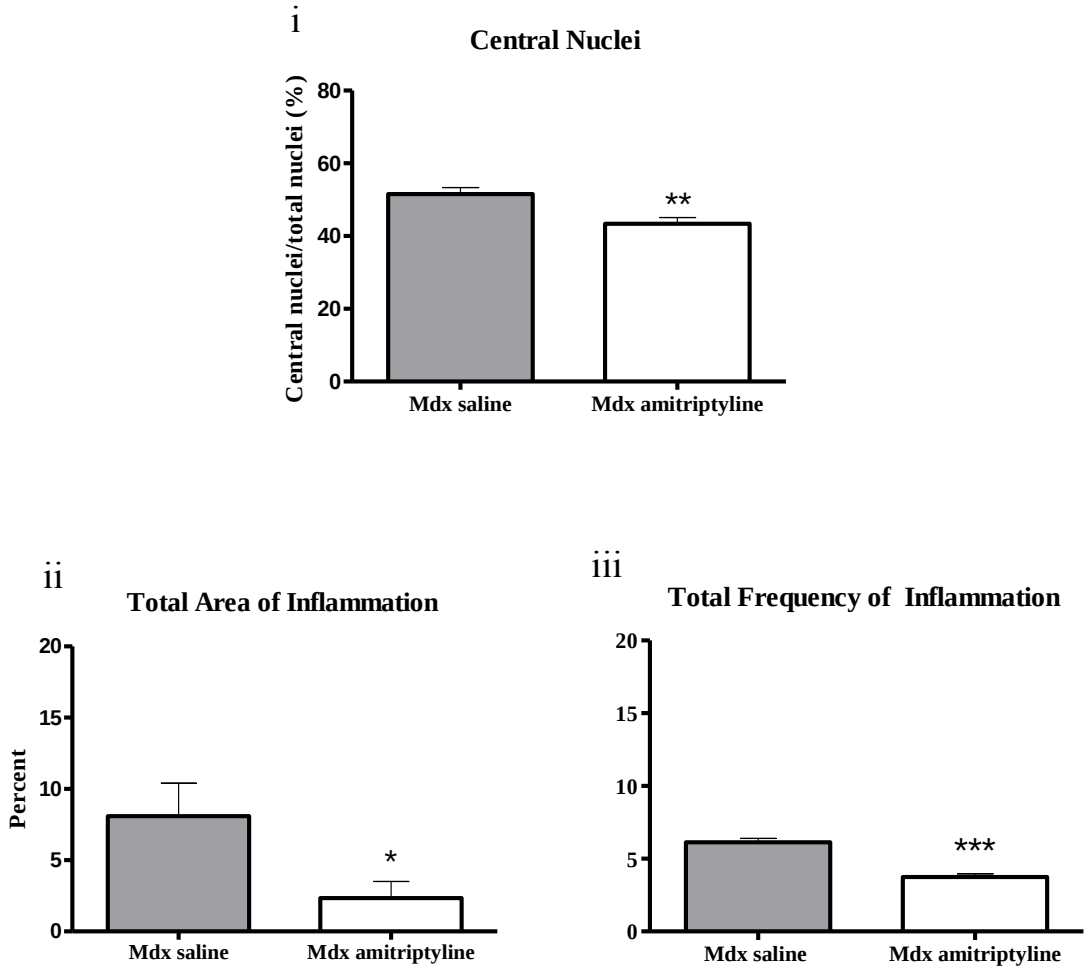
Table 3.3: HPLC monoamine analysis of areas important in depression and anxiety in *mdx*– *amygdala, hippocampus, hypothalamus, striatum, prefrontal cortex and midbrain in amitriptyline treated mdx versus saline treated mdx mice. Data presented as mean ± SEM and n numbers. * p<0.05, **p<0.01 (/ = monoamine below detectable level)*

Mdx	Amygdala		Hippocampus		Hypothalamus	
Concentration (ng/g)	Saline	Amitriptyline	Saline	Amitriptyline	Saline	Amitriptyline
5HT	697.8 ± 149.6	1258 ± 179*	674 ± 98.38	993.9 ± 71.6 *	923.5 ± 199.6	534.7 ± 76.96
n=	5	5	4	6	7	6
5HIAA	1322 ± 506.9	1159 ± 161.4	647.0 ± 59.33	804 ± 30.13 *	1008 ± 107.2	588.6 ± 119.1
n=	7	7	4	6	7	5
NA	944.2 ± 293.3	624.6 ± 152.4	562.3 ± 66.04	716.3 ± 54.18 *	3235 ± 340.8	2183 ± 330.7
n=	7	7	5	7	7	6
DA	848 ± 274.7	563 ± 118.8	63.27 ± 9.457	81.19 ± 10.00	857.9 ± 99.57	514.3 ± 100.7 *
n=	6	6	5	7	7	6
DOPAC	/	/	31.54 ± 9.814	58.28 ± 6.3 *	267 ± 24.75	182.4 ± 43.39
n=			5	6	7	6
HVA	1122 ± 391.7	989.9 ± 315.8	65.7 ± 9.407	75.53 ± 12.86	307.4 ± 33.02	162.4 ± 31.3 *
n=	6	7	5	7	7	6
Turnover (ratio)						
5HIAA/5HT	0.9186 ± 0.1212	1.25 ± 0.1189	0.7987 ± 0.04804	0.8582 ± 0.02933	1.248 ± 0.1609	1.235 ± 0.2216
n=	7	6	6	6	7	7
DOPAC/DA	0.6947 ± 0.3182	0.8629 ± 0.1405	0.5468 ± 0.1041	0.6944 ± 0.1284	0.32 ± 0.02265	0.4187 ± 0.08239
n=	6	7	6	7	7	7
HVA/DA	0.4519 ± 0.1236	1.140 ± 0.2065 *	1.141 ± 0.1081	0.9845 ± 0.1506	0.4457 ± 0.1203	0.3643 ± 0.02848
n=	5	7	6	7	7	7

Mdx	Striatum		Prefrontal Cortex		Midbrain	
Concentration (ng/g)	Saline	Amitriptyline	Saline	Amitriptyline	Saline	Amitriptyline
5HT	861.4 ± 51.51	921.1±83.55	761.2 ± 149.9	658.7 ± 195.3	963.8 ± 103.9	1133 ± 118.3
n=	6	7	7	7	5	5
5HIAA	644.8 ± 70.91	614.7±52.54	602.6 ± 135.7	551.5 ± 129.1	849.7 ± 38.62	1206 ± 62.36 **
n=	6	7	7	7	5	5
NA	485.1 ± 74.54	512.3±58.24	717.3 ± 167.5	764.7 ± 195.3	1254 ± 87.85	1452 ± 152.2
n=	5	7	7	7	5	5
DA	8404 ± 1004	9405±292.2	169.4 ± 90.49	78.36 ± 22.08	188 ± 16.28	262.3 ± 21.68 *
n=	6	7	7	7	6	5
DOPAC	2431 ± 243.2	1988±188.4	123.2 ± 36.21	91.06 ± 26.33	48.17 ± 2.278	87.84 ± 15.44 *
n=	5	7	7	7	5	6
HVA	1239 ± 148.5	1261±82.95	116.6 ± 34.53	83.43 ± 23.21	110.9 ± 23.23	127.5 ± 12.02
n=	6	6	7	7	6	5
Turnover (ratio)						
5HIAA/5HT	0.7440 ± 0.06626	0.6718±0.026654	0.7823 ± 0.07461	0.9447 ± 0.07448	0.8499 ± 0.04140	1.068 ± 0.06264
n=	6	7	7	7	5	6
DOPAC/DA	0.2655 ± 0.03939	0.2099±0.01515	1.165 ± 0.2509	1.138 ± 0.08269	0.3081 ± 0.03440	0.3691 ± 0.03975
n=	6	7	7	7	6	6
HVA/DA	0.1476 ± 0.005821	0.1297±0.005685	0.9985 ± 0.231	1.137 ± 0.1040	0.5849 ± 0.1030	0.4080 ± 0.08664
n=	6	7	7	7	6	6

3.4.3 Amitriptyline reduces histopathological changes in *mdx* mice

Amitriptyline-treated *mdx* mice had a significant decrease in the number of centralised nuclei in cross-sections of EDL muscle (43.3±1.7%, n=7), compared to WT mice (51.4±1.8%, n=7, $p<0.01$, Figure 3.10i). Amitriptyline-treated *mdx* mice also displayed a decrease in the total area of inflamed muscle (2.3±1.1μm^2, n=7) as compared to saline-treated mice (8±2.3μm^2, n=7, $p<0.05$, Figure 3.10ii). The number of discrete individual areas of inflammation were also decreased in amitriptyline treated *mdx* mice (3.7±0.2 μm^2, n=7) as compared to saline treatment (6.1±0.2 μm^2, n=7, $p<0.001$, Figure 3.10iii).



<u>Figure 3.10:</u> Pathohistological Analysis Tail Suspension behavioural Analysis of amitriptyline treated *mdx* mice compared to saline *mdx* controls

*mdx mice treated with amitriptyline have less central nuclei than saline treated mdx mice (i) a reduced area of inflammation (ii) and a less incidence of inflammation (iii) n=7, * $p<0.05$, ** $p<0.01$ *** $p<0.001$*

3.4.4 Amitriptyline lowers IL-6 levels in plasma of treated *mdx* mice

Amitriptyline treatment of plasma from *mdx* mice indicated that amitriptyline reduces circulating IL-6 levels in *mdx* mice (Figure 3.11, n=7, $p<0.05$).

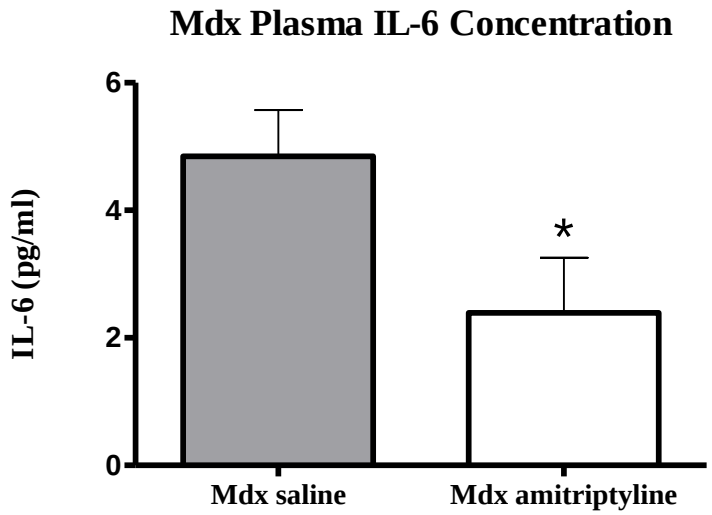


Figure 3.1: ELISA analysis of IL-6 in plasma Analysis of amitriptyline treated *mdx* mice compared to saline *mdx* controls

*Student's t test reveal mdx mice treated with amitriptyline have significantly less IL-6 than saline treated mdx mice. n=7, * p<0.05*

3.5 Discussion

3.5.1 The behavioural profile of *mdx* mice

Consistent with the human condition where the prevalence of anxiety disorders and depression is increased (Rubinsztein et al. 1998; Roccella et al. 2003) our behavioural studies on dystrophin deficient *mdx* mice identified altered behavioural profiles.

5.5.1.1 Anxiety in *mdx* mice

The open field behavioural test is comprehensively described in the literature (Walsh & Cummins 1976; Prut & Belzung 2003), and in our test this brightly-lit exposed arena revealed that as compared to untreated WT mice, untreated *mdx* mice show signs of anxiety indicated by the avoidance of the brightly lit middle area, despite their innate exploratory drive. The anxiety-like behaviours in the open field are supported by a study carried out in other behavioural tests in *mdx* mice; the light-dark box which similarly identified anxious traits in dystrophin deficient mice (Vaillend & Ungerer 1999). However, other behavioural assessments such as the elevated plus maze, did not detect any signs of anxiety in these animals (Sekiguchi et al. 2009) at this age.

One concern with this type of behavioural test is whether deficiencies in motor function would reduce exploration of the open field. Indeed, when studying behaviours which are dependent on locomotion in this model, it is imperative that the age of the mice is considered. For this reason 8-10 week old *mdx* mice were studied as they have high skeletal muscle regenerative capacity at this age, reducing the risk of motor deficits as a source of false results (Porter et al. 2002). As previously established *mdx* mice do not show motor deficiencies until 6 months of age (Pastoret & Sebille 1995) and have previously been used in behavioural testing. This is consistent with rotarod experiments at this age (Spurney et al. 2009) (~12 weeks old) where no deficits were seen.

Indeed, when overall movement during the course of the trial were compared between *mdx* and WT mice, no differences were detected which reassured us that the reduction in exploration and implied increase in anxiety, was not simply due impaired ambulation. Nonetheless, one study states that during the dark phase *mdx*

mice exhibit less spontaneous locomotor activity than WT controls at this age (Nakae et al. 2012) although this spontaneous dark activity is dissimilar to our trial.

5.5.1.2 Alleviating anxiety in *mdx* mice

Amitriptyline treatment increased exploration of the middle of the arena when compared to saline controls, indicating an anti-anxiety effect of amitriptyline, similar to previous studies which described such an effect (Liu et al. 2007) in mice, to my knowledge this is the first report of alleviation of anxiety in *mdx* mice in the open field with treatment of amitriptyline. Dissimilar to our findings, amitriptyline did not have an anxiolytic affect in mice in the plus maze, but similar to our study it did not alter the ambulatory behaviour in mice. In our study *mdx* mice exhibited similar locomotor activity in the trial when compared to the saline *mdx* group.

5.5.1.3 Depressive symptoms in the *mdx* mouse

Clinical depression is common in DMD patients (Bushby et al. 2010) although this has often been attributed as a consequence of the severity and seriousness of the disease, and a psychological cause rather than a pathophysiological one (Roccella et al. 2003). However, the TST revealed that *mdx* mice also exhibit depressive-like behaviours, showing increased despair in the face of an inescapable stress when compared to WT mice, thus indicating that the pathology associated with dystrophin deficiency may underlie the increased susceptibility of DMD sufferers to depression. Moreover, the reduced time for *mdx* mice to show this despair in their inescapable stress of the TST and their increased immobility indicates that these mice are pre-disposed to depression-like behaviour.

Again, caution is needed when using dystrophic animals in behavioural tests, indeed I did not find locomotor deficits, but the TST was chosen over the forced swim test because, although both tests are established behavioural tests of depressive like behaviour (Castagné et al. 2010), the TST requires less physical effort from muscle groups which would be affected first in the animals.

5.5.1.4 Amitriptyline as an anti-depressant in *mdx* mice

Amitriptyline is an antidepressant known to alleviate depressive symptoms in people suffering from major depression, this was established more than 50 years ago (Inglis et al. 1963), and amitriptyline, however replaced with more specific drugs is still prescribed in cases of depression today (Leucht et al. 2012). Amitriptyline is efficacious in reversing despair depressive behaviours in TST in mice (Caldarone et al. 2003; Steru et al. 1985). Moreover when I tested the efficacy of amitriptyline, this depressive index was reversed in *mdx* mice compared to saline controls, further indicating the potential beneficial effects of this anti-depressant for improving the quality of life of DMD patients.

A classic hypothesis of the pathogenesis of depression implicates the dysregulation of monoamines in subcortical brain regions underpins the development of major depression (Hirschfeld 2000) and as a consequence of this fact, treating depressed patients with compounds which regulate the levels of monoamines in the brain have been efficacious in treating depression (Anderson 2000). There is clear cognitive defects in a cohort of DMD patients(Anderson et al. 2002) and defects in the central nervous system due to dystrophin deficiency may lead to changes in brain areas important in the pathogenesis of depression (Lidov et al. 1993).

3.5.2 Altered expression of monoamines in *mdx* brain

I found through monoamine analysis in the brain reveals *mdx* mice respond differently to amitriptyline treatment than WT mice, increased levels of monoamines involved in the aetiology of depression in *mdx* mice may indicate that amitriptyline works through the modulation of monoamines in DMD, as it does in other causes of depression.

As previously discussed, given the behavioural results identified depressive and anxiety-like behaviours in the *mdx* mice and consistent with its reported actions (Steru et al. 1985) and chronic administration of amitriptyline normalized these phenotypes. Amitriptyline acts as a serotonin noradrenaline reuptake inhibitor (SNRI) but with higher efficacy for the 5HT receptor (Giuseppe et al. 2007), and depression is now more often treated with selective-serotonin reuptake inhibitors (SSRIs), however this is due to fewer side-effects rather than improved efficacy

(Barbui & Hotopf 2001) and as mentioned amitriptyline is still occasionally prescribed for treatment-resistant depression (Broquet 1999; Leucht et al. 2012).

To investigate the underlying chemical changes in brain regions associated with these mood changes, levels of brain monoamines were analysed in WT and *mdx* mice treated with saline or amitriptyline. In WT mice, amitriptyline treatment resulted in increased levels of NA in the hippocampus. DOPAC/DA turnover in the midbrain and 5HIAA/5HT turnover in both the striatum and the hypothalamus were increased following amitriptyline treatment. However, amitriptyline caused decreases in midbrain levels of 5HIAA and NA in the WT mouse. In the *mdx mouse* a greater number of changes in monoamine expression were observed and the pattern of change was different to the WT mouse.

As 5HT is the major neurotransmitter involved in depression, evidence of both receptor dysfunction, monoamine turnover rate changes 5HT/HIAA and levels are implicated in the disease (Cowen 2008) and consistent with the crucial role of 5HT in mood disorders (Naughton et al. 2000), the actions of amitriptyline resulted in increased concentrations of 5HT in two regions of the limbic system, the amygdala and the hippocampus and elevations of 5HIAA in the hippocampus of *mdx* but not WT mice. Neural circuitry in both these regions have been linked with anxiety (Rosen & Schulkin 1998) and depressive-like behaviour (Luethi et al. 2008). 5HT/5HIAA turnover and 5HIAA concentrations were also elevated in the midbrain, a region which relays serotonergic signals to the hippocampus and is associated with depressive-like behaviour.

Amitriptyline is thought to have some effect on NA uptake (Giuseppe et al. 2007) and NA levels were increased in the hippocampus of both strains. Moreover, glucosteroids receptors are modulated in the hippocampus by both monoamine levels and by amitriptyline in cultured hippocampal primary cells (Lai et al. 2003), and as discussed the HPA axis which is activated in depression and stress may therefore reap benefits from amitriptyline normalised the monoamine expression and thus the glucosteroids effects in the hippocampus. Interestingly, NA levels were decreased in the midbrain of WT mice following treatment.

Concentrations of DA and DOPAC were unchanged in WT brains but amitriptyline-treated *mdx* mice displayed increased expression of DA and DOPAC in the midbrain, increased concentrations of DOPAC in the hippocampus and increased HVA/DA turnover in the amygdala. Interestingly, the hypothalamus of the *mdx* mice was the only region with decreased levels of DA and the DA metabolite, HVA. When comparing the WT and *mdx* mice, the greatest divergence appears to be in changes in the dopamine system following amitriptyline. 5HT and DA have extensive interaction (Damsa et al. 2004) and amitriptyline has been shown to increase DA receptor expression in the striatum of rats (Huzarska et al. 2006), however the precise mechanism of amitriptyline-induced changes in the DA system in dystrophin-deficient *mdx* mice requires further investigation.

As absence of dystrophin has also been linked to increased prevalence of cognitive defects in DMD patients (Anderson et al. 2002) such as lowered IQ and memory deficits (Roccella et al. 2003). However, our studies examining object recognition memory in the novel object recognition test, revealed no memory defects in the *mdx* mouse. However, it has been previously reported that *mdx* mice exhibit impairments in long term memory consolidation (Anderson et al. 2002) and passive avoidance learning and retention (Muntoni et al. 1991). In relation to changes in monoamine levels, 5HT-dependent mechanisms are thought to contribute to hippocampal and amygdalar learning (Meneses et al. 1997), and therefore amitriptyline-induced enhancement of object discrimination memory in *mdx* mice may have occurred through modulation of 5HT in these areas. This is further supported by data that show a beneficial effect of central 5-HT2A receptor antagonism on cognition (Altman & Normile 1988).

To summarise, it is apparent that amitriptyline is an accepted and effective antidepressant whose full mechanisms of actions are not fully elucidated (Leucht et al. 2012), it is known however to work through the modulation and normalisation of monoamine levels in the brain (Cowen 2008; Lai et al. 2003) and indeed it has changed monoamine levels in the areas studied, brain areas which are implicated in depression. Moreover, amitriptyline may also be modulating cytokine levels, as it can work as an anti-inflammatory in animal models of disease (Hajhashemi et al.

2010; Leduc et al. 2002), and as discussed raised cytokine profiles in disease can be a cause of depression in a subset of patients.

3.5.3 Histopathological changes in *mdx* skeletal muscle

While treatment of mood disorders in DMD is clearly important for patient wellbeing, the overwhelming and most debilitating symptoms of this disorder are the inflammation and subsequent loss of function in skeletal muscle leading to severe disability and ultimately a premature death. Thus, assessment of the effects of amitriptyline on inflammation in skeletal limb muscle was carried out.

An increase of myophagocytosis, the infiltration of phagocytic white blood cells into the muscle (both number of discrete areas and total area of inflammation) was seen in *mdx* mice EDL muscles when compared to WT mice, which is consistent with previous reports (Gordon et al. 2012). Moreover, *mdx* mice have a higher percentage of central nuclei in myofibres. This signifies regeneration of skeletal muscle, which is an early indicator of dystrophic muscle, whereas, normal skeletal muscle has around 3% central nuclei (Seidman 1983) some cases of *mdx* mice in this study had up to 50% central nuclei. Consistent with other studies (Payne et al. 2006), in control *mdx* mice I observed inflammation indicative of regenerating myofibres in the *extensor digitorum longus* muscle tissue. The inflammation was in the form of immune cell infiltration.

Our study has found that amitriptyline treatment results in a reduction of centralised nuclei and reduced levels of inflammation in the *mdx* muscle, with reduction of the total area of inflammation and the number of inflammatory events following treatment. The underlying mechanisms contributing to the anti-inflammatory effects of amitriptyline have not yet been fully reported but can reduce inflammation in (Hajhashemi et al. 2010) and reduce an immune response, implicating amitriptyline in depression as having the ability to normalise cytokine expression such as IL-6 (Kubera et al. 2000).

Accumulating evidence from studies in rodents indicates that TCAs, including the drug amitriptyline, have anti-inflammatory effects on various organ systems(Abdel-Salam et al. 2003) which is in part due to the modulation of chemokines such as

TGFβ1, IL-6 or TNF (Tai et al. 2006; Xia et al. 1996). TCAs are also known to reduce macrophage infiltration, however full explanation of the mechanism of action will require further research (Achar et al. 2009). However, structurally similar TCAs such as fluoxetine induce an anti-inflammatory response due to its ability to interact with opioid receptors (Hajhashemi et al. 2010), therefore further investigation will be required to elucidate this mechanisms involved.

3.5.4 Interleukin-6 - a key modulator of inflammation in DMD?

I have demonstrated that the pro-inflammatory cytokine, IL-6 is elevated in the muscle of *mdx* mice however, the variation did not allow the test to reach significance. I analysed plasma levels of IL-6 in treated *mdx* mice and compared this to saline treated *mdx* mice, IL-6 plasma levels were reduced following therapeutic intervention with amitriptyline.

As muscle inflammation is reduced by amitriptyline the release of IL-6 from skeletal muscle into plasma would also likely to be reduced and in this way IL-6 may be an important marker of inflammatory levels in skeletal muscle.

However, amitriptyline may also be having a direct effect on IL-6 levels by reducing release of the pro-inflammatory cytokine from the immune cells (Xia et al. 1996) and thereby reducing the pro-inflammatory effects of this immune mediator. Moreover, the effect may be a centrally controlled phenomenon – in the HPA axis, namely the hippocampus, by modulation of monoamines or glucosteroid receptors (Kubera et al. 2000).

Since IL-6 is regarded as a marker of depressive symptoms in chronic inflammatory disorders like rheumatoid arthritis (Yusof & Emery 2013) and indeed a biomarker of depression manifesting in patients with lung cancer (Du et al. 2013) – diseases which has a high depression/inflammation co-morbidity, I hypothesised this may be a causative mediator in patients, and indeed in *mdx* mice. I did find an increase in IL-6 in *mdx* mice, consistent with other studies (Huynh et al. 2013; Kostek et al. 2012). This result did not show statistical significance at ($p>0.05$) although its mean pg/mg of tissue is almost double the amount of interleukin-6, this lack of power may be due to the nature of the tissue and the protocol used.

Homogenized muscle is a heterogeneous tissue containing blood vessels, adipocytes, and other material which could possibly be a source of IL-6.

Therefore, it was decided to analysis IL-6 in blood plasma of drug treated animals to investigate if levels of IL-6 circulating changed, amitriptyline can reduce IL-6 levels from monocytes and can modulate various cytokines which interact with IL-6 (Xia et al. 1996). Indeed, IL-6 levels are reduced in the circulation following amitriptyline treatment. Taken with the data provided on the behavioural and histological benefits in *mdx* mice with the treatment of amitriptyline, we infer that IL-6 reduction in the *mdx* circulation is a clear benefit to the progression of disease in dystrophin deficiency.

3.6 Conclusions

Given its anti-depressant as well as anxiolytic and anti-inflammatory effects in the dystrophin-deficient *mdx* mouse, amitriptyline offers a potential therapeutic strategy which may have great benefits to some DMD patients. However, as Amitriptyline can have detrimental side effects, such as cardiac arrhythmias, cautious prescribing of this drug which is already on the market and has been used for many years in people for a range of diseases is advisable. This potential new use for an old drug could improve the quality of life for DMD sufferers without the delay imposed by clinical trials.

Chapter 4: The role of IL-6 and Urocortin 2 in dysfunction of the diaphragm in the *mdx* mouse

4.1 Introduction

4.1.1 Dytrophin deficiency in the diaphragm

Diaphragm dysfunction is a severe and detrimental symptom of dystrophin deficiency in patients with DMD; as repeated contraction and load bearing on striated muscle determines the severity of the pathological signature of each muscle, it is not surprising that the diaphragm undergoes degeneration of function in this disease. Patients suffer diurnal hypercapnia due to a loss of respiratory skeletal muscle tone, a reduction in vital capacity and sleep apnoeas (Simonds et al. 1998). Patients benefit from artificial ventilation as the condition continues into their teenage years (Finsterer 2006) which undoubtedly aids survival for patients (Vittorino et al. 1994) in the second decade of life. Cardiopulmonary failure dominates the pathology in the late stages of the disease and this pulmonary insufficiency is the leading cause of premature death in up to 90% of patients (Mosqueira et al. 2013; Beck et al. 2006).

It is difficult to fully elucidate diaphragm pathology in patients of the disease through pulmonary function testing, however there is evidence of reduced force generation capabilities and the muscle undergoes rapid progressive weakening, muscle fibre loss and fibrosis (Beck et al. 2006) evident by a thickened appearance in patients as early as ten years of age (De Bruin et al. 1997).

4.1.2 Diaphragm dysfunction in the *mdx* mouse

Animal models of DMD are useful to explore the mechanisms of disease progression in dystrophin deficient diaphragms. Diaphragm dysfunction in *mdx* mice diverges from the human disease in all skeletal muscle due to the high regenerative capacity of *mdx* skeletal muscle (Anderson et al. 1988), except for the diaphragm. Dystrophin deficient diaphragm muscle undergoes inflammation, the primary pathology of the disease and becomes fibrotic with collagen replacing functional fibres which have undergone regeneration until exhaustion (Turgeman et al. 2008), and loss of force production in the muscle (Bates et al. 2013). Different from limb skeletal muscle, functional changes are evident from an early age. This feature of the *mdx* model of DMD provides an important tool to test the efficacy of therapeutic strategies, more so because the phenotype is mild in the limb skeletal muscle.

Striated muscle contractile function has previously been studied in *mdx* mice, especially under isometric conditions (generating force without length change). Twitch peak force production (one contraction) is reduced. Moreover, tetanic maximal force (force produced from a summation of stimuli, resulting in a full tetanus contraction) was also reduced, indicating dysfunction in the diaphragm at a young age. Moreover, twitch time to peak (speed of coupling) or 50% peak force decay time (uncoupling) are found to be unchanged compared to WT; these results ascertained from single fibre functional measurements illustrate that at three months of age, cross bridge kinetics or cycling rate are unaffected in *mdx* mice (Gosselin & Williams 2006).

Although little is known about the isotonic kinetics (eccentric and concentric dynamic movements, muscle capable of shortening against a load) in *mdx* mice, power production has been investigated in stretched diaphragm lengths i.e., at lengths greater than optimal length, where power is reported to be reduced (Stevens & Faulkner 2000). Intervention studies utilise these differences between *mdx* mice and WT controls to test the efficacy of palliative treatments (Gosselin & Williams 2006; Gregorevic et al. 2002; Nakae et al. 2012).

4.1.3 Investigating Potential Therapies

4.1.3.1 CRFR agonists

CRFR2 agonists have previously proven beneficial in treating muscle dysfunction in *mdx* mice. Their effectiveness is attributed to an ability to increase muscle mass, modulate proteolysis and activate signalling pathways, specifically anabolic pathways (Hall et al. 2007). CRFR2 is a modulator of muscle hypertrophy and atrophy (Hinkle et al. 2003), and can reduce nerve damage, corticosteroid induced atrophy and immobilisation (disuse) loss of muscle mass (Hinkle et al. 2003). It is reported in the latter study that intervention with non-selective CRF receptor agonists can cause muscle loss (Hinkle et al. 2004), therefore an endogenous CRFR2 selective agonist, Urocortin 2 is an attractive candidate for a therapeutic target in *mdx* mice, as opposed to a CRFR1 agonist, which works conversely to the beneficial CRFR2 agonist, these studies have begun to elucidate the role of CRFR2 in skeletal muscle function in health and disease.

4.1.3.2 Interleukin-6 and skeletal muscle damage

IL-6 levels are raised in patients with DMD (Messina et al. 2011) and also in *mdx* mice (Gordon et al. 2012; Hunt et al. 2011; Klingler et al. 2012). It is long known that IL-6 plays a significant role in muscle regeneration after exercise and damage (Pedersen & Febbraio 2008), with an up regulation of STAT 3 signalling in muscle stem cells following lengthening induced damage (McKay et al. 2009) and in inflammation in skeletal muscle (Kostek et al. 2012). Blocking IL-6 signalling however, leads to a pro-inflammatory state in *mdx* mice although there was an 11% increase in hind limb strength (Kostek et al. 2012). Although limb strength can potentially be improved, no functional tests on diaphragm performance in the presence of an IL-6 signalling blocker have been reported. Of note, diaphragm isometric function has been rescued in *mdx* mice treated with an NFκB blocker (Peterson et al. 2011), which may implicate a role for IL-6 signalling (Libermann & Baltimore 1990) because as discussed, IL-6 can activate this signalling pathway (Huang et al. 2009). Although generally associated with inflammation, IL-6 may also act as an anti-inflammatory cytokine, signalling through its classic signalling pathway (Rose-John 2012), but it also modifies fibrosis throughout body tissues (Meléndez et al. 2010); attenuates fibrosis in liver cells (Nasir et al. 2013) and can reduce collagen deposits in the skin of multiple sclerosis (MS) patients (Shima et al. 2010). Moreover, it was suggested as a therapy for attenuating collagen damage in rheumatoid arthritis (Alonzi et al. 1998) and indeed, forms the basis of 'Tocilizumab' human anti interleukin-6 antibody treatment.

4.1.3.3 Co-treatment

Following the interaction reported between the CRF family of proteins and IL-6 in other tissues (Kageyama et al. 2006; Ando et al. 1998; O' Malley et al. 2011; Tsatsanis et al. 2007; Huang et al. 2009; O' Malley et al. 2013), in the context of inflammation in cardiac myocytes (Huang et al. 2009) and GI dysfunction in IBD (O' Malley et al. 2013), I speculated that this interaction may also play a role in diaphragm skeletal muscle dysfunction in *mdx*.

4.1.4 Hypothesis

We hypothesise that blocking IL-6 signalling and stimulating the CRFR2 receptor using exogenous Urocortin 2 will ameliorate diaphragm dysfunction in dystrophin deficient *mdx* mice.

4.1.5 Specific Study Aims

- To characterise *mdx* diaphragm compared to WT controls under isometric and isotonic conditions ex vivo.

- To examine IL-6 and IL-6 receptor levels in *mdx* compared to WT mice.

- To test the therapeutic efficacy of anti IL-6 receptor ± Urocortin 2 treatment *in vivo* on *mdx* diaphragm function.

4.2 Methods

4.2.1 Animals and study protocol

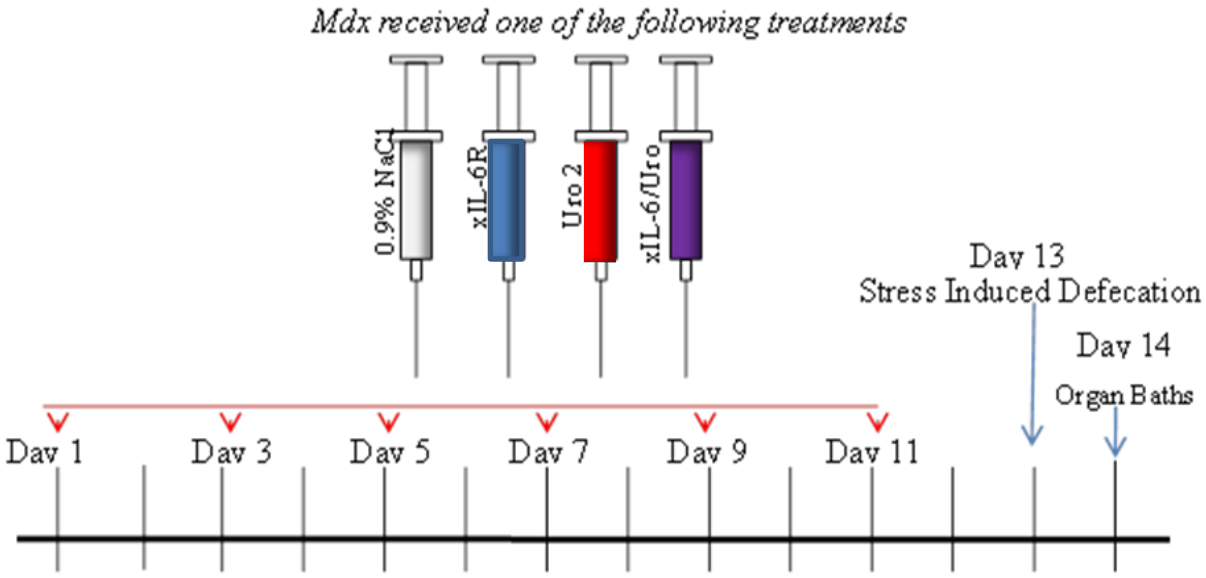
Male C57BL/10ScSn (wild-type control) and C57BL/10ScSn-*Mdx*/J (*mdx*, dystrophic) mice (12 weeks old at time of functional test, 29g±2g body weight) were assigned at random to untreated or treated groups detailed in table 4.1. Treated mice were administered monoclonal anti IL-6 receptor antibodies (0.3mg/kg) or the CRFR2 agonist, Urocortin 2 (30µg/kg) or both by subcutaneous injection (6 subcutaneous injections, saline vehicle) for 2 weeks. Controls were treated with saline (0.9% NaCl (w/v)).

Table 4.1: Experimental groups & details of intervention protocol

Intervention study treatments are colour coded. Saline treated mdx mice are represented in grey, Anti IL-6 receptor antibody (anti IL-6R) in red, Urocortin 2 in blue and a co-treatment of anti IL-6R and Urocortin 2 in purple throughout the thesis.

Six injections of the selected treatment (as indicated by the first six arrows) were given from day 1 to day 11. Stress induced defecation was performed on day 13and animals were sacrificed for tissue on day 14.

Groups	Untreated	Intervention Treatment			
		Saline	Anti IL-6R	Urocortin 2	Anti-IL-6R + Urocortin 2
Mdx	8	8	8	6	8
WT	8				



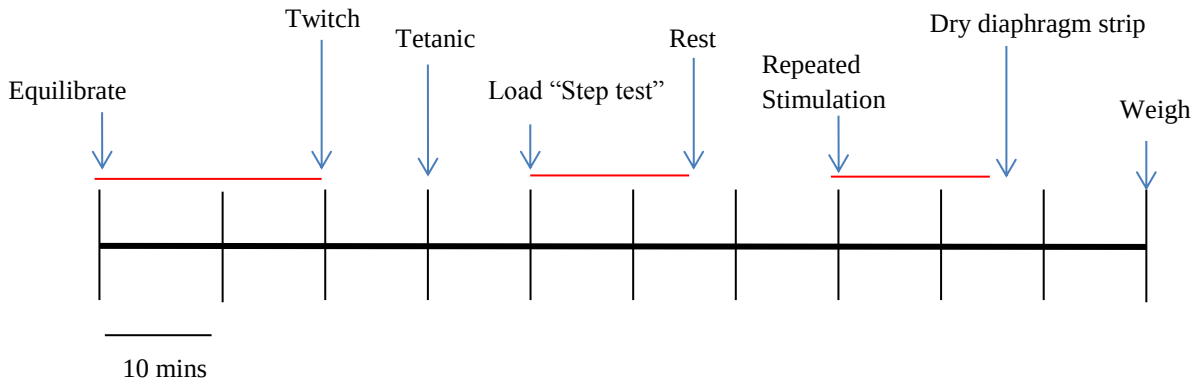
4.2.2 Techniques:

Organ bath (Section 2.7.2)

Diaphragm strip preparation

Isometric Protocol

Isotonic protocol



Protocol described above, Figure 2.7.

Molecular Techniques: Western blotting (section 2.5.3)

Diaphragms were homogenised in lysis buffer (Table 2.2) and western blotting used to quantify expression of IL-6 and IL-6Rs in diaphragm muscle from *mdx* mice which had undergone each of the experimental interventions.

4.3 Results part one: Diaphragm function in WT and *mdx* mice

4.3.1 Diaphragm function in WT and *mdx* mice

4.3.1.1 *Mdx* diaphragms have reduced maximal twitch and tetanic forces

The length at which peak specific force is acquired by each muscle strip did not differ between strains, and the cross sectional area (CSA, cm^2) was also similar between strains (see Table 4.2).

Mdx diaphragms have reduced specific twitch force (force normalised to cross sectional area (CSA)) compared to WT mice (Figure 4.1, $p<0.05$, student's t test). However, time to peak (TTP) and the time for the peak force to decay by 50% (½ RT) were not statistically different between the strains (Figure 4.1, $p>0.05$).

Mdx diaphragms had reduced specific peak forces compared to WT mice (Figure 4.2, $p<0.05$).

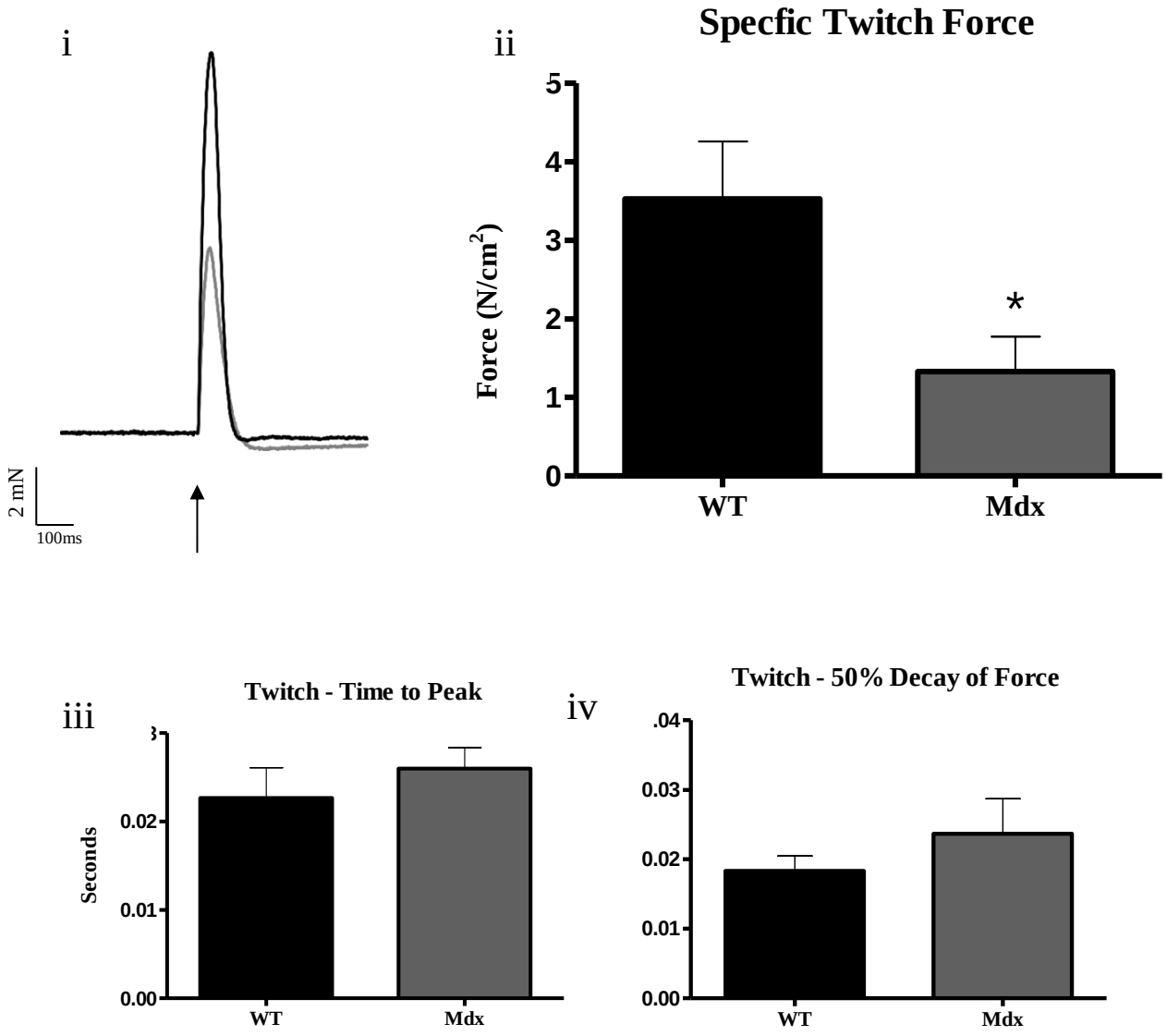
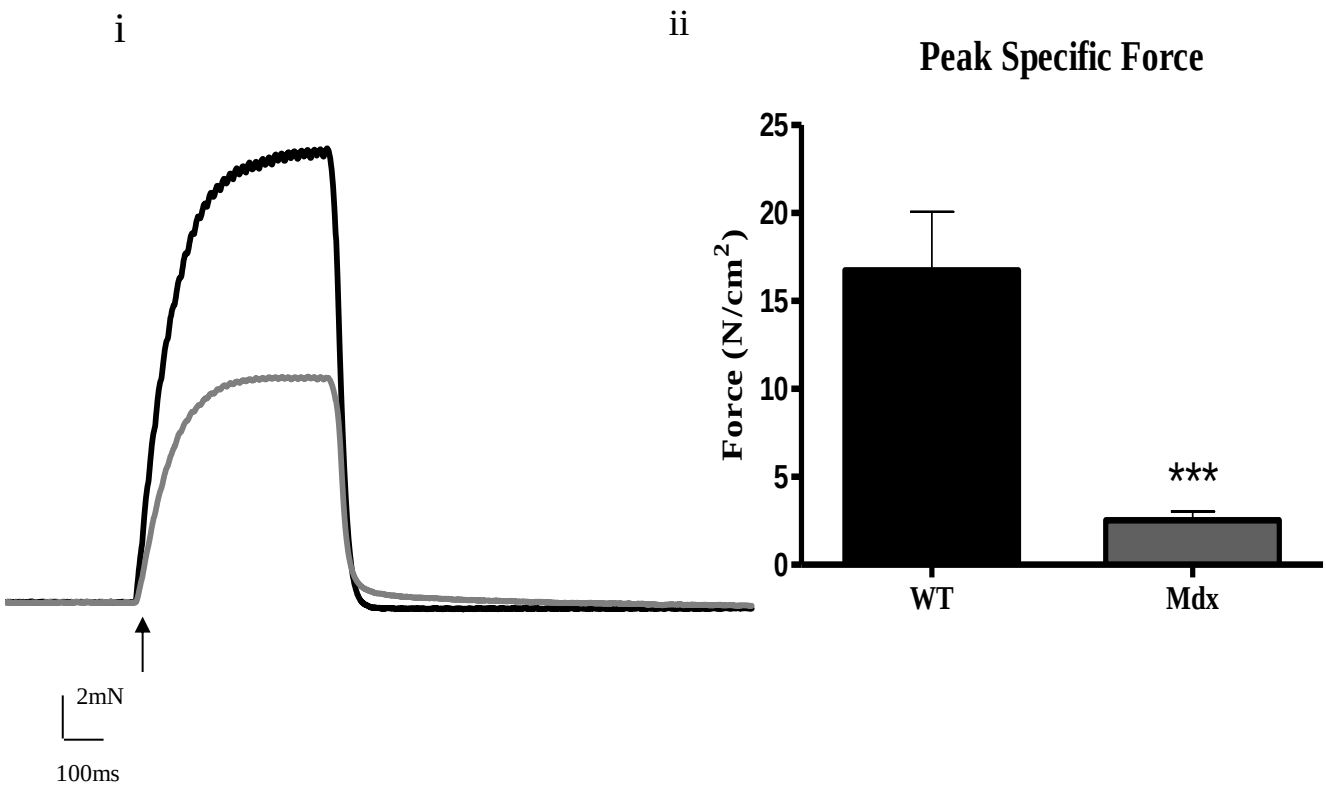


Figure 4.1: Twitch Kinetics of WT and *mdx* mice diaphragm

i A representative original trace of twitch force comparing WT *(black line) to mdx (grey line) diaphragm. The arrow represents a single supra maximal stimulation (1ms). ii Specific twitch force; analysis of maximal twitch force recorded at optimal length comparing* WT *and mdx diaphragm. iii Twitch contraction time to peak in seconds; iv Twitch contraction with 50% decay of force. n=7 for all groups, * p<0.05*



<u>Figure 4.2:</u> Peak Specific Force of WT and *mdx* mice diaphragm

i A representative original trace of peak tetanic force comparing WT *(black line) to mdx (grey line). The arrow represents supra maximal stimulation at 100Hz lasting 300ms. ii Specific tetanic force of maximal tetanic force recorded at optimal length in* WT *and mdx diaphragm strips. n=7, *** p<0.05*

Table 4.2: Diaphragm preparation properties and isometric kinetic values WT and *mdx* mice

Neither optimal length (cm) nor cross sectional area (CSA, cm^2) differed between WT and mdx mice. Isometric kinetic values calculated from raw force measurements and normalised to CSA were also comparable between strains. Expressed as mean ± S.E.M.

	Units	Group	
		WT	*Mdx*
Optimal Length	mm	9 ± 0.07071	9.3 ± 1.3000
CSA	cm^2	0.005185 ± 0.001189	0.0375 ± 0.01837
Peak Twitch Force	N/cm^2	3.528 ± 0.7327	1.31 ± 1.4441
Time To Peak	s	0.02267 ± .003432	0.026 ± 0.00237
½ Relaxation Time	s	0.01833 ± 0.002116	0.0236 ± 0.005009
Peak Tetanic Force	N/cm^2	16.74 ± 3.329	2.53 ± 0.4994

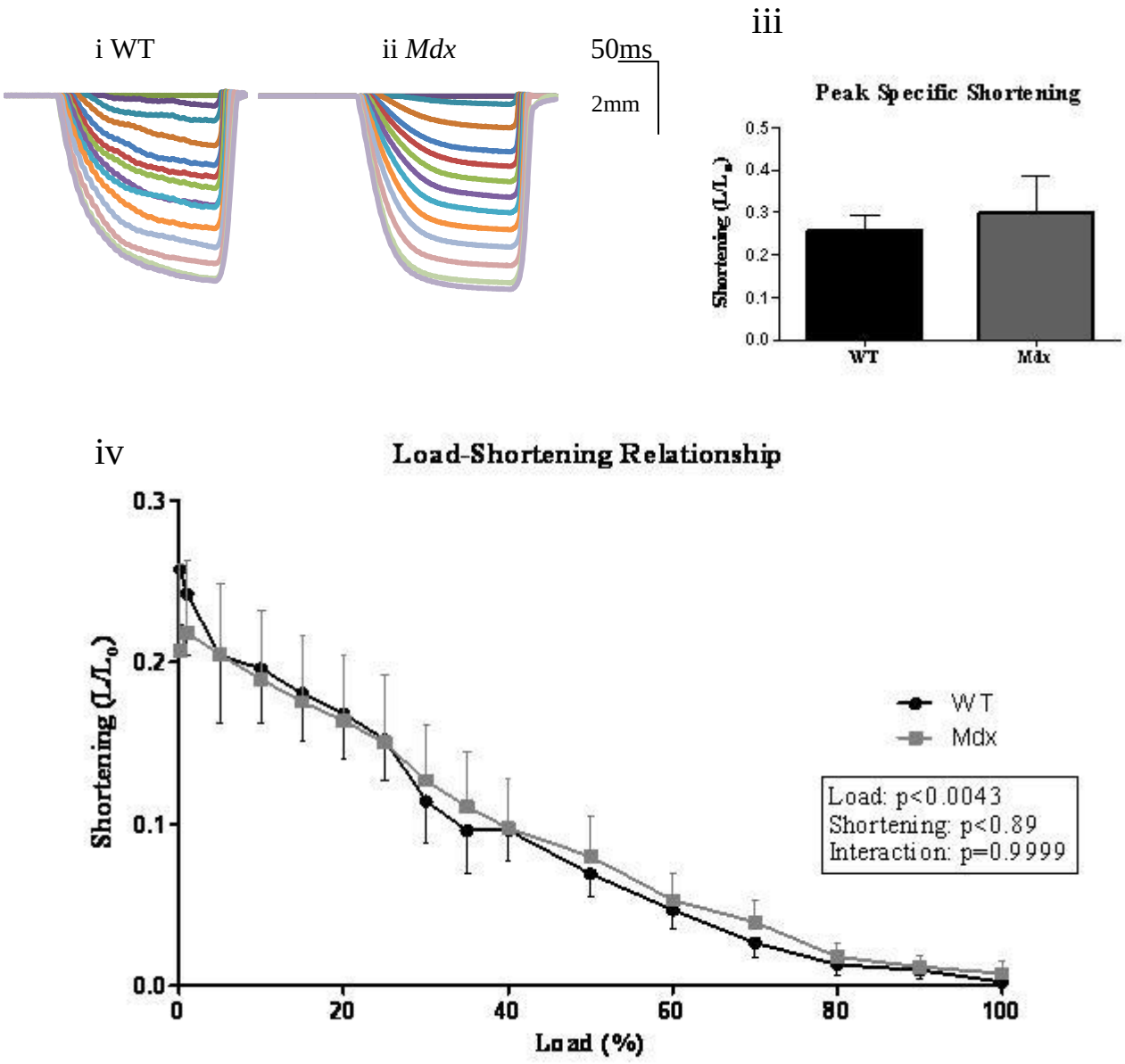
4.3.1.2 *Mdx* diaphragms produce significantly less work than WT mice

Load- Shortening Relationship

Mdx diaphragm strips shorten in response to electrical stimulus to a similar extent in WT and *mdx* diaphragm strips (Figure 5.3iv, n=7, $p>0.05$) when normalised to optimal length. Peak specific shortening did not differ between strains (n=7, $p>0.05$, Figure 4.3iii).

Load - Work Relationship

Work production (force x distance shortened) was significantly lower in *mdx* mice compared to WT controls (Figure 4.4, n=7). Both load ($p<0.0004$) and work ($p<0.0001$) differed significantly, and a significant interaction was observed ($p<0.0065$, Two-way ANOVA).



<u>Figure 4.3:</u> Load-Shortening Relationship in WT and *mdx* diaphragm

i Representative original traces of muscle shortening in a WT *and (ii) mdx diaphragm in response to stimulation at different loads. iii Peak specific shortening, measured as a ratio of shortening/optimal length (L/Lo) in* WT *and mdx diaphragms. (p>0.05, n=7 for both groups) iv Load/shortening relationship, measured as a ratio of shortening/optimal length (L/Lo) as a function of load. Two way ANOVA (genotype x load), revealed a significant effect of load on muscle shortening (*p<0.05), but no difference between* WT *and mdx diaphragms; there was no interaction.*

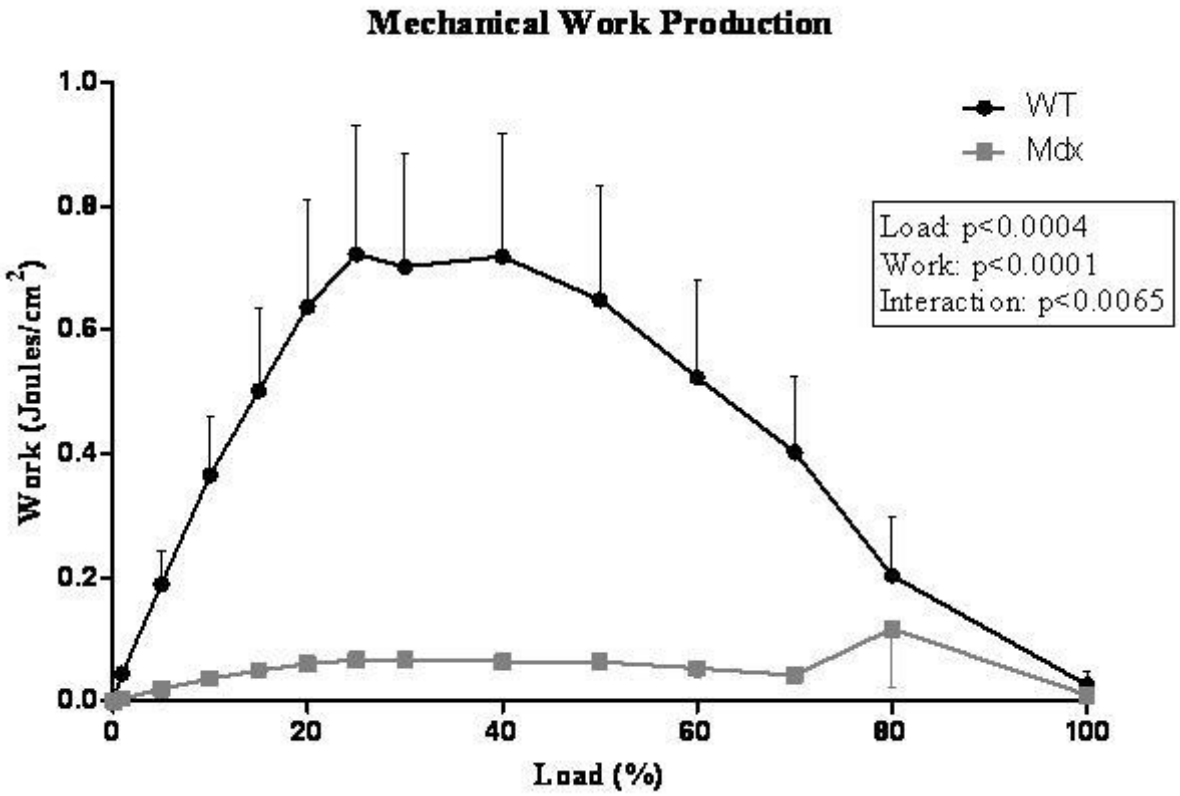


Figure 4.4: Mechanical Work Production in WT and *mdx* diaphragm
Work-Load relationship, expressed as Joules per cm^2 as a function of load. Two way ANOVA (genotype x load), revealed a significant difference in muscle work between WT *and mdx diaphragms; there was a significant effect of load and a significant interaction. n=7 for both groups.*

4.3.1.3 There is no difference between *mdx* and WT shortening velocity over a series of loads and peak shortening velocities are not changed

Peak shortening velocity was compared and no significant difference was detected between diaphragm muscle from *mdx* and WT mice (Fig 4.5 i, $p>0.05$).

Shortening velocity was equivalent in *mdx* and WT diaphragms ($P>0.05$), two-way ANOVA; Figure 4.5 ii). There was a significant effect of load on shortening velocity ($p<0.0001$); there was no significant interaction ($p>0.05$).

4.3.1.4 *Mdx* diaphragms produce less power compared to *WT* controls

Peak power was compared using a Student's t test. *Mdx* diaphragms produce significantly less power than WT diaphragms (Figure 4.6 i, $p<0.01$).

Two-way ANOVA (genotype x load) of the Load-Power relationship, measured as the (shortening velocity x specific force as a function of load), revealed that *mdx* diaphragms generated significantly lower power (Figure 4.6 ii, $p<0.0001$) compared to WT. There was a significant effect of load on muscle power ($p<0.0001$), and a significant interaction ($p<0.0001$).

ii

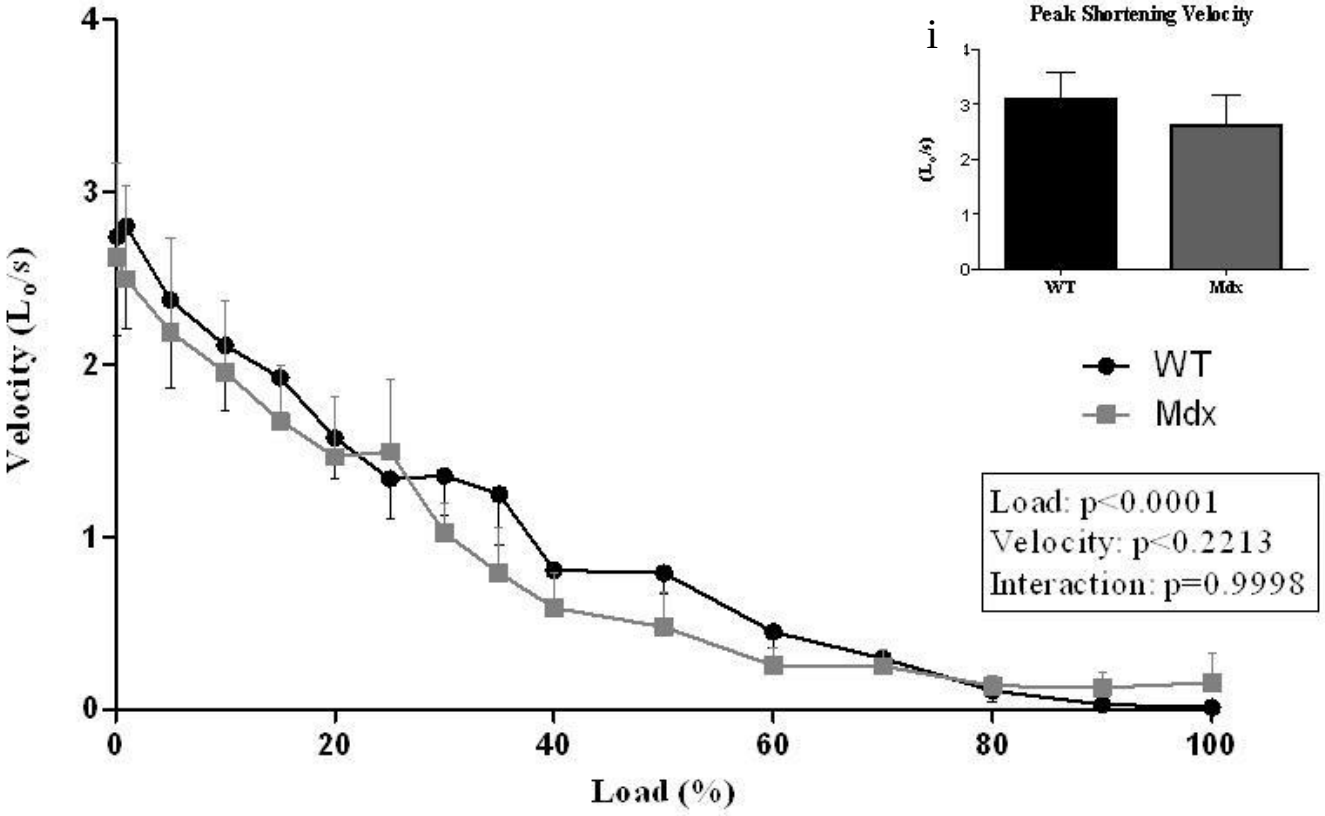


Figure 4.5: Load-Shortening Velocity relationship in WT and *mdx* diaphragm
i Peak velocity of shortening (Lo/s) is equivalent in WT *and mdx diaphragm strips(P>0.05). ii - Two way ANOVA (genotype x load) revealed no significant difference in shortening velocity between* WT *and mdx. There was a significant effect of load on velocity of muscle shortening but no interaction. n=7 for both groups.*

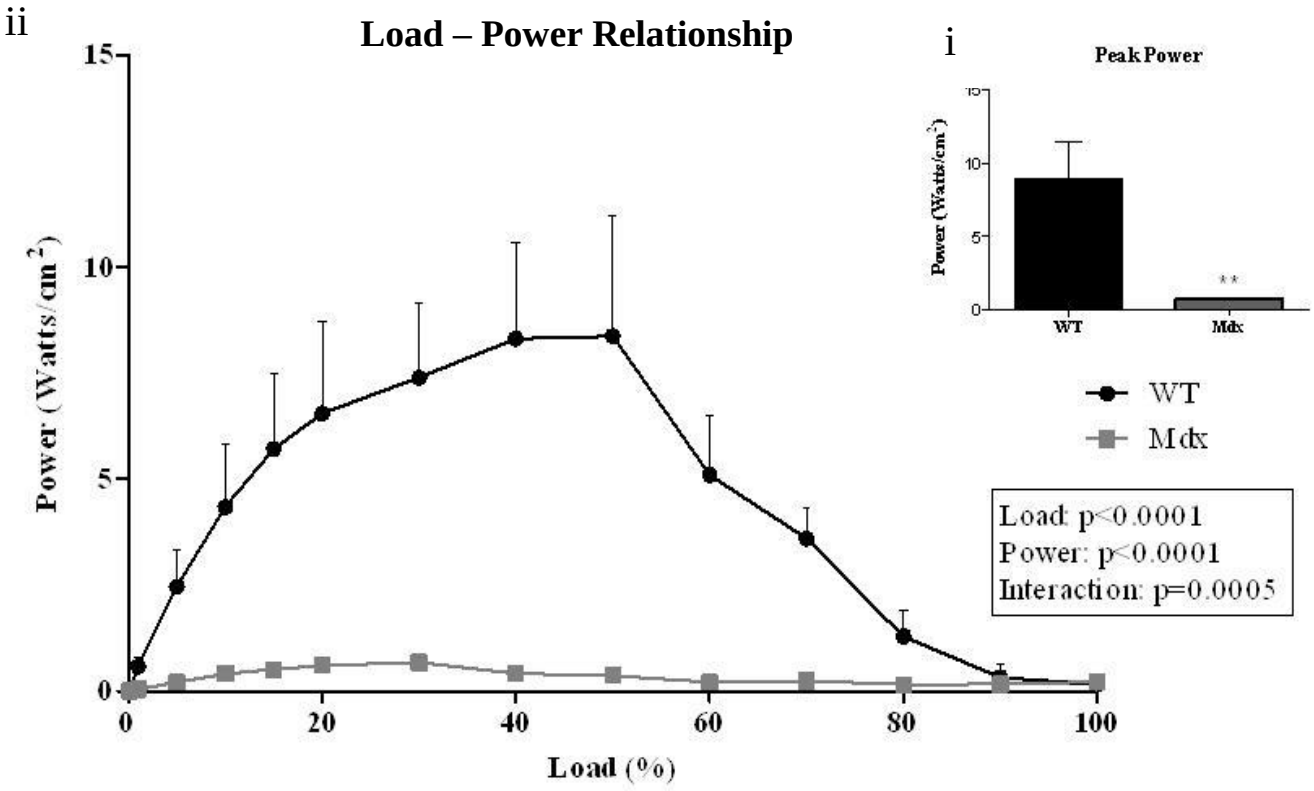


Figure 4.6: Load - Power relationship in WT and *mdx* diaphragm

i Power production (Watts per cm^2).–is lower in mdx diaphragm compared to WT *(P<0.01). ii - Two way ANOVA (genotype x load) revealed a significant difference in power between mdx and* WT *diaphragms. There was a significant effect of load and a significant interaction; **p<0.01, n=7 for both groups.*

4.3.2 Repeated Stimulation

4.3.2.1 *Mdx* diaphragms shorten more than WT diaphragms in isotonic muscle fatigue test

Shortening – Time Relationship

Two-way ANOVA (muscle shortening x time) revealed that *mdx* diaphragms shorten more than WT diaphragms ($p<0.05$) during repeated muscle stimulation. There was a significant effect of time (repeated stimulation) on muscle shortening (Figure 4.7, $p<0.05$). There was no significant interaction.

4.3.2.2 *Mdx* diaphragms have lower shortening velocity during repeated muscle stimulation

Two-way ANOVA analysis of velocity decay over time revealed that shortening velocity was significantly different in *mdx* diaphragms compared to WT. There was a significant effect of time (repeated muscle stimulation) on muscle shortening (Figure 4.8, $n=7$, $p<0.05$). There was no significant interaction.

4.3.2.3 *Mdx* mice produce lower power in muscle fatigue test

Power – Time Relationship

Two-way ANOVA of power decay over time during repeated muscle stimulation revealed that power was different in *mdx* and WT diaphragms ($p<0.0001$). As expected, time (repeated stimulation) was a significant factor ($p<0.0001$). There was a significant interaction (Figure 4.9, $n=7$, $p<0.001$).

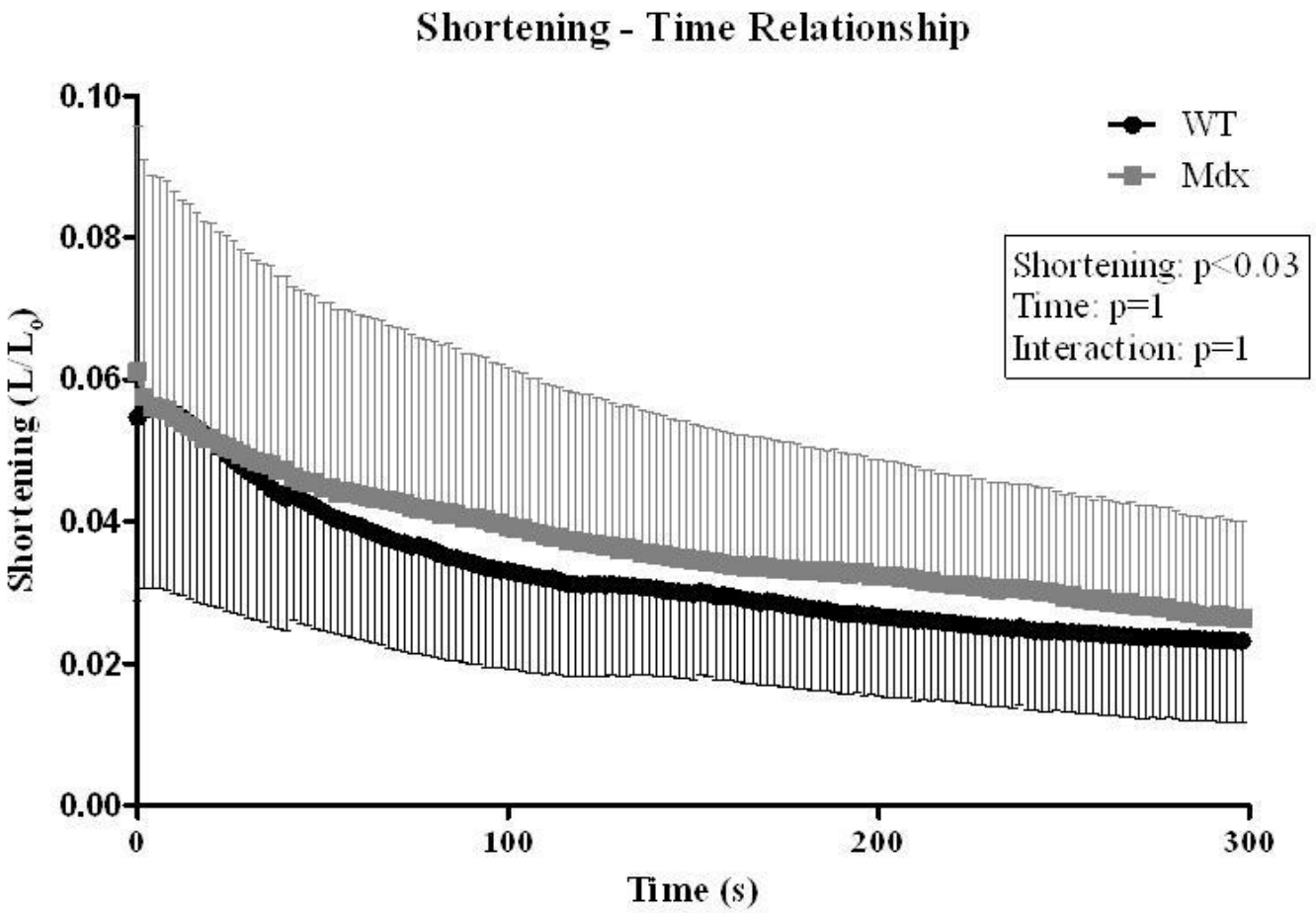


Figure 4.7: Shortening-Time relationship in WT and *mdx* diaphragms during repeated muscle stimulation

The graph illustrates the shortening of muscle strips following repeated stimulation. Two way ANOVA comparing shortening from WT *and mdx revealed a significant difference between* WT *and mdx (* p<0.05), No time difference or interaction was observed. n=7 in both groups.*

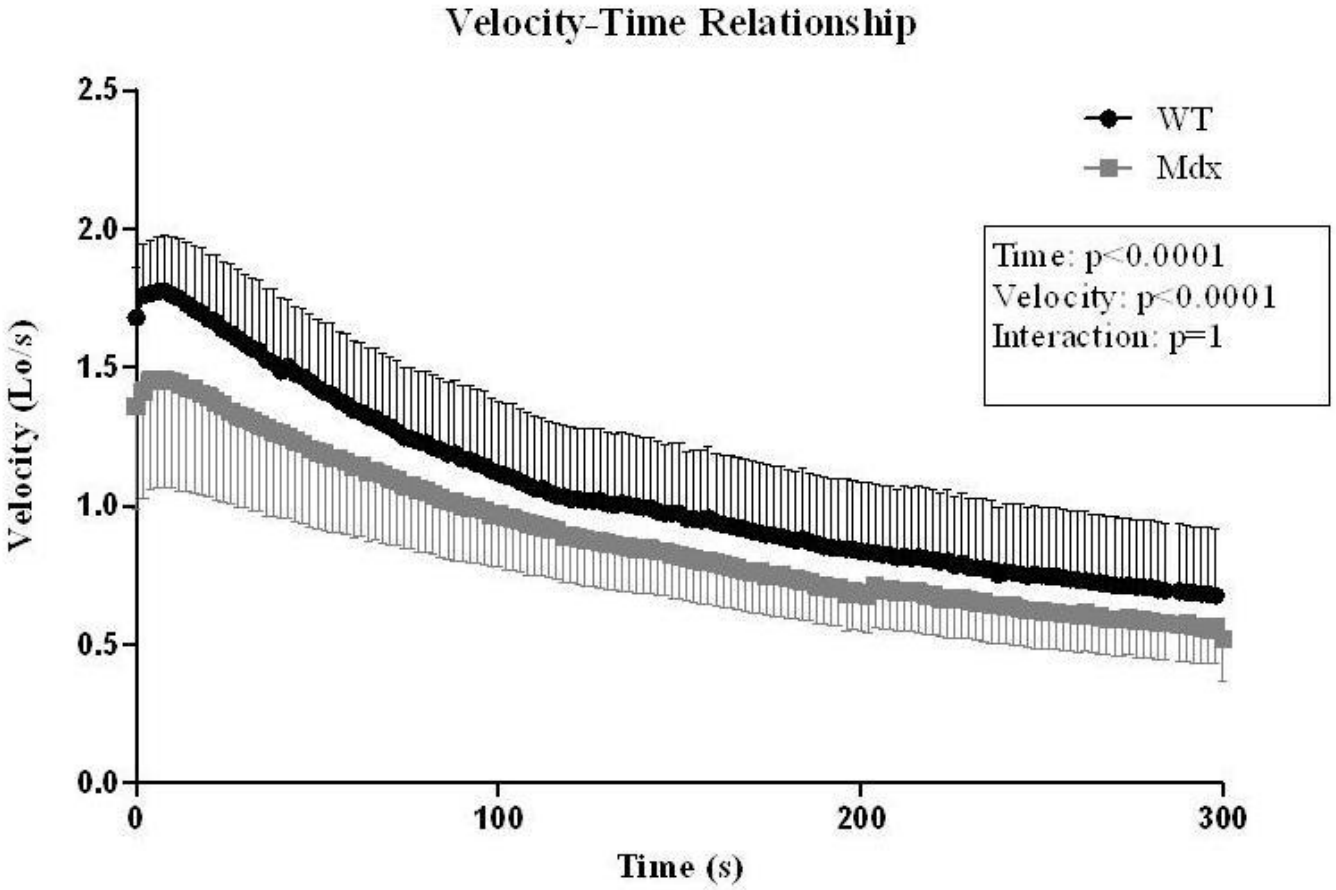


Figure 4.8: Velocity-Time relationship comparing WT and *mdx* diaphragm during repeated muscle stimulation

The graph illustrates velocity during repeated stimulation. Two way ANOVA comparing shortening velocity in WT *and mdx revealed differences in time and velocity between* WT *and mdx diaphragms (p<0.0001). There was no significant interaction. n=7 in each group.*

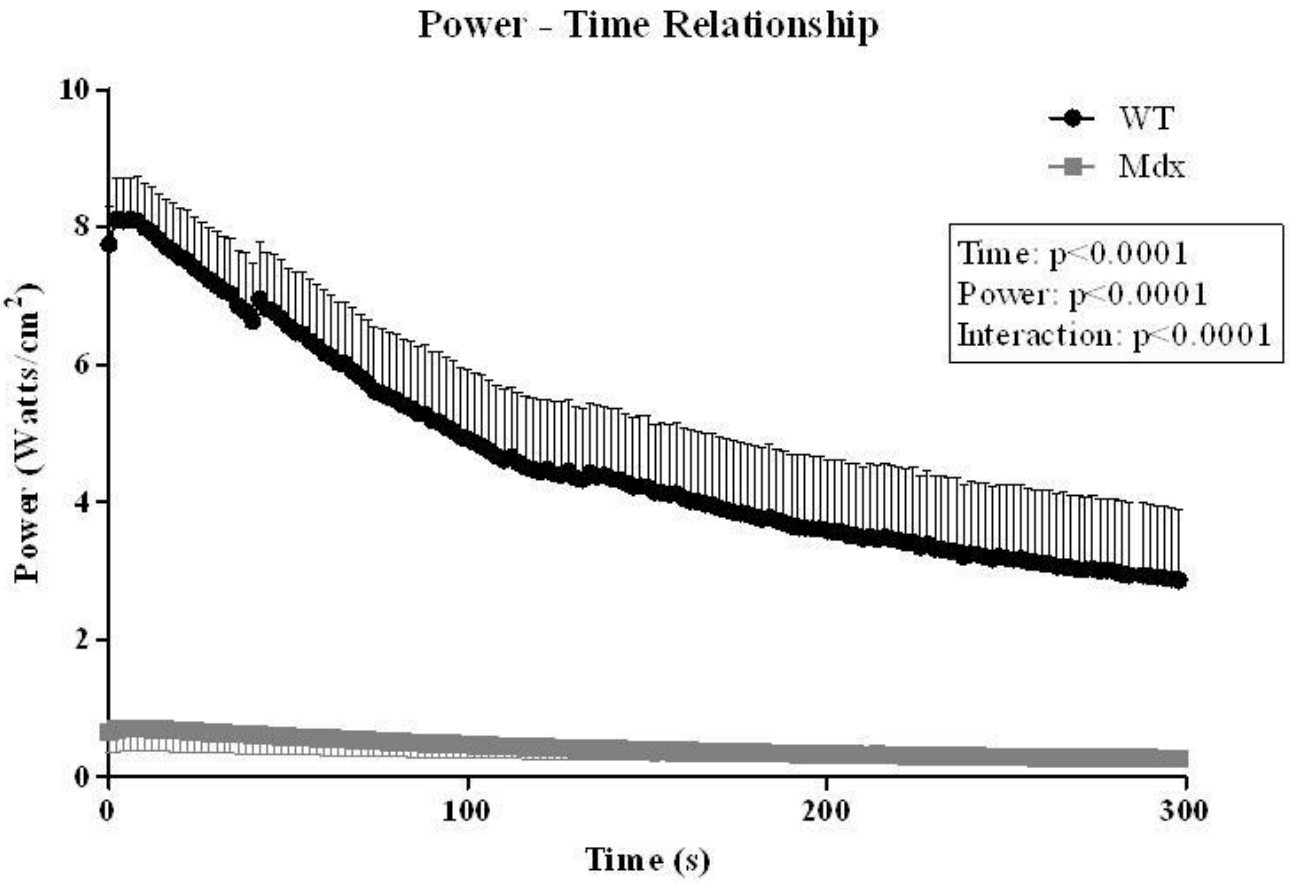


Figure 4.9:. **Power-Time relationship comparing WT and *mdx* diaphragms during repeated muscle stimulation**

The graph illustrates power production during repeated stimulation. Two way ANOVA comparing power in WT *and mdx diaphragms revealed differences in time and power Interaction between the factors (time x power) was also significant. n=7 in each group.*

Part Two: Effect of monoclonal IL-6R antibodies and/or a CRFR 2 agonist (Urocortin 2) on *mdx* diaphragm muscle function

4.4.1 Diaphragm Function with intervention studies compared to saline treated *mdx* mice

4.4.1.1 Anti IL-6R and/or Urocortin 2 increase twitch specific force in *mdx* diaphragm muscle

Mdx diaphragms have reduced twitch force compared to WT controls. Treatment with anti IL-6R did not modify this ($p>0.05$, n=8). However, Urocortin 2 did cause recovery of twitch specific force compared to saline treated *mdx* mice (Figure 4.10ii, $p=0.056$, n=6-8). The beneficial effects of Urocortin 2 were moderated by co-treatment with anti-IL-6R ($p=0.06$, n=6-8, figure 4.10 (i). Half relaxation time (iii) and time to peak (iv) were not changed by treatment.

4.4.1.2 *Mdx* mice treated with anti IL-6R in the presence of Urocortin 2 have higher maximal tetanic force

Similarly, *mdx* diaphragms have reduced specific tetanic force when compared to WT controls but anti IL-6R treatment with Urocortin 2 recovered this function (Figure 4.11ii, n=6-8, $p<0.05$, one way ANOVA). No significant effect was noted for anti IL-6 receptor blockade or Urocortin 2 treatment alone ($p>0.05$, Figure 4.11ii, n=6-8).

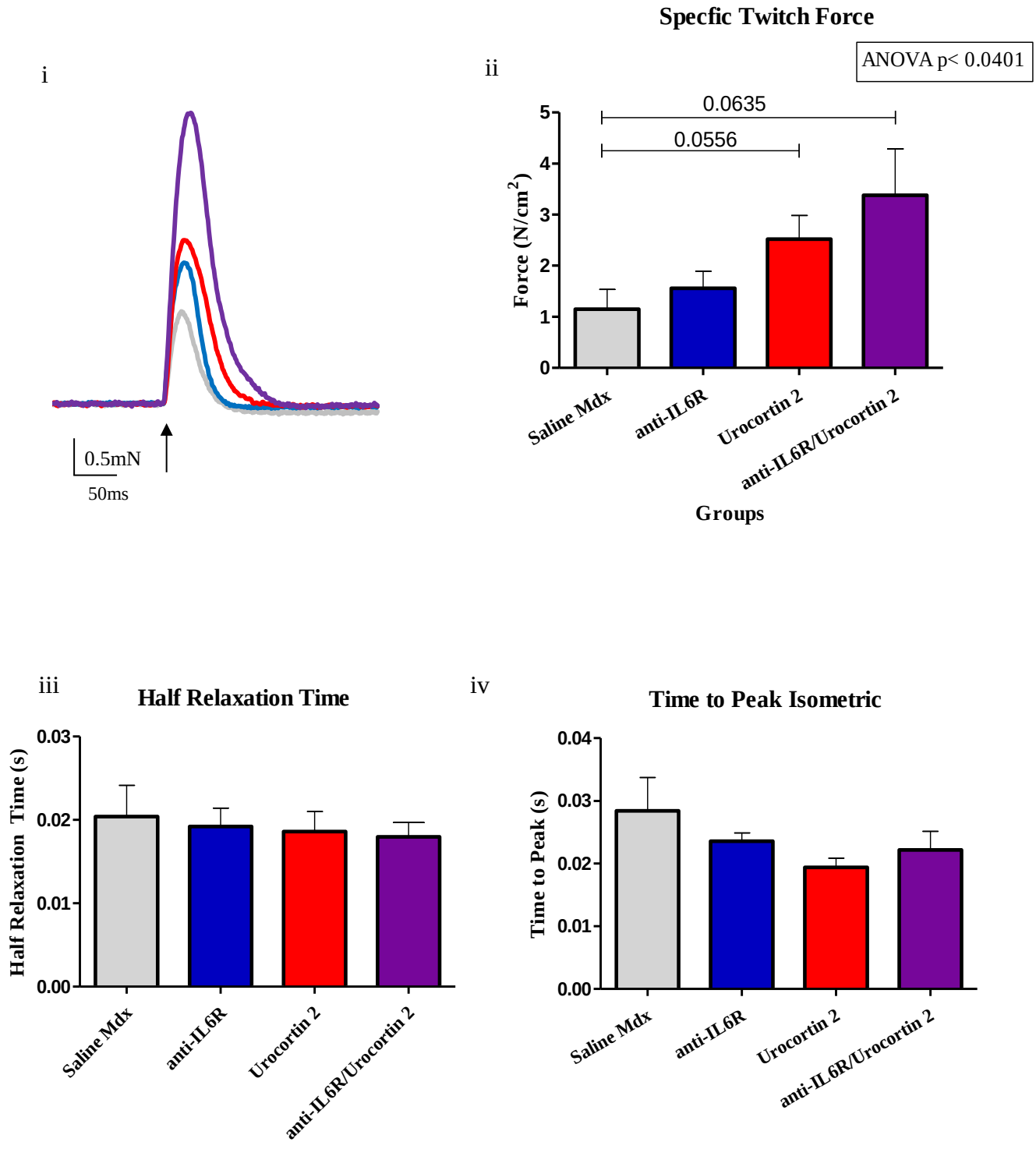
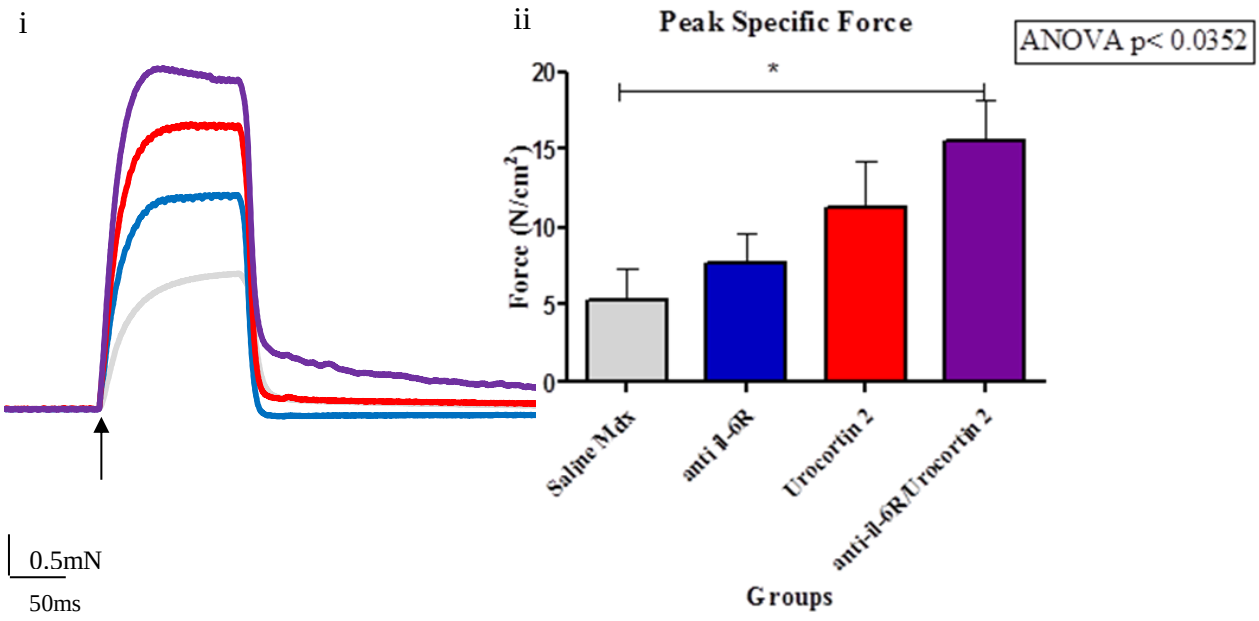


Figure 4.10: Twitch Kinetics in *mdx* diaphragm with and without drug interventions
i Representative original traces of twitch force comparing mdx mice treated with saline (grey line), anti IL-6 receptor antibody (anti IL-6R, blue line), Urocortin 2 (red line) and a co- treatment of anti-IL-6R and Urocortin 2 (purple line). ii The histogram shows specific twitch force values in treated mdx mice. Only Urocortin 2 significantly recovered the maximal twitch force recorded at the optimal length (n=6). iii The twitch relaxation (50% decay of force in seconds)was unchanged by treatments. iv The twitch contraction (time to peak in seconds) was unchanged by any treatment. n=6-8.



<u>Figure 4.11:</u> Specific Peak Force in *mdx* diaphragms with or without drug interventions

*i Representative original traces of tetanic force comparing mdx mice treated with saline (grey line), anti IL-6 receptor antibody (anti IL-6R, blue line), Urocortin 2 (red line) and a co- treatment of anti-IL-6 and Urocortin 2 (purple line). ii The peak specific force revealed a significant effect of anti IL-6R + Urocortin 2 co-treatment. One way ANOVA analysis revealed a treatment difference * $p<0.05$, $n= 6-8$.*

Table 4.3: Diaphragm preparation properties and isometric kinetic values for saline and treated *mdx* mice

Neither optimal length nor CSA differed between treatment groups or vehicle (saline) treated mdx mice. Isometric kinetic values calculated from raw force measurements normalised to CSA. Represented as mean ± S.E.M

	Units	Intervention Treatment			
		Saline	Anti-IL-6R	Urocortin 2	Anti-IL-6R + Urocortin 2
Optimal Length	mm	8.938 ±0.6972	7.833 ±0.7817	9.8±0.5831	8.833 ±0.4944
CSA	cm^2	0.003966 ±0.0007183	0.006247 ±0.0008684	0.003600 ±0.0005559	0.004770 ±0.0008181
Peak Twitch Force	N/cm^2	1.146 ±0.3899	1.556 ±0.3330	2.524 ±0.4632	3.379 ±0.9091
Time To Peak	s	0.02842 ±0.005294	0.0236 ±0.001288	0.0194 ±0.001435	0.0222 ±0.002948
½ Relaxation Time	s	0.02042 ±0.003747	0.0192±0.0022	0.01863 ±0.002375	0.0180 ±0.001688
Peak Tetanic Force	N/cm^2	5.341±1.957	7.692 ±1.843	11.26 ±3.032	15.54 ±2.677

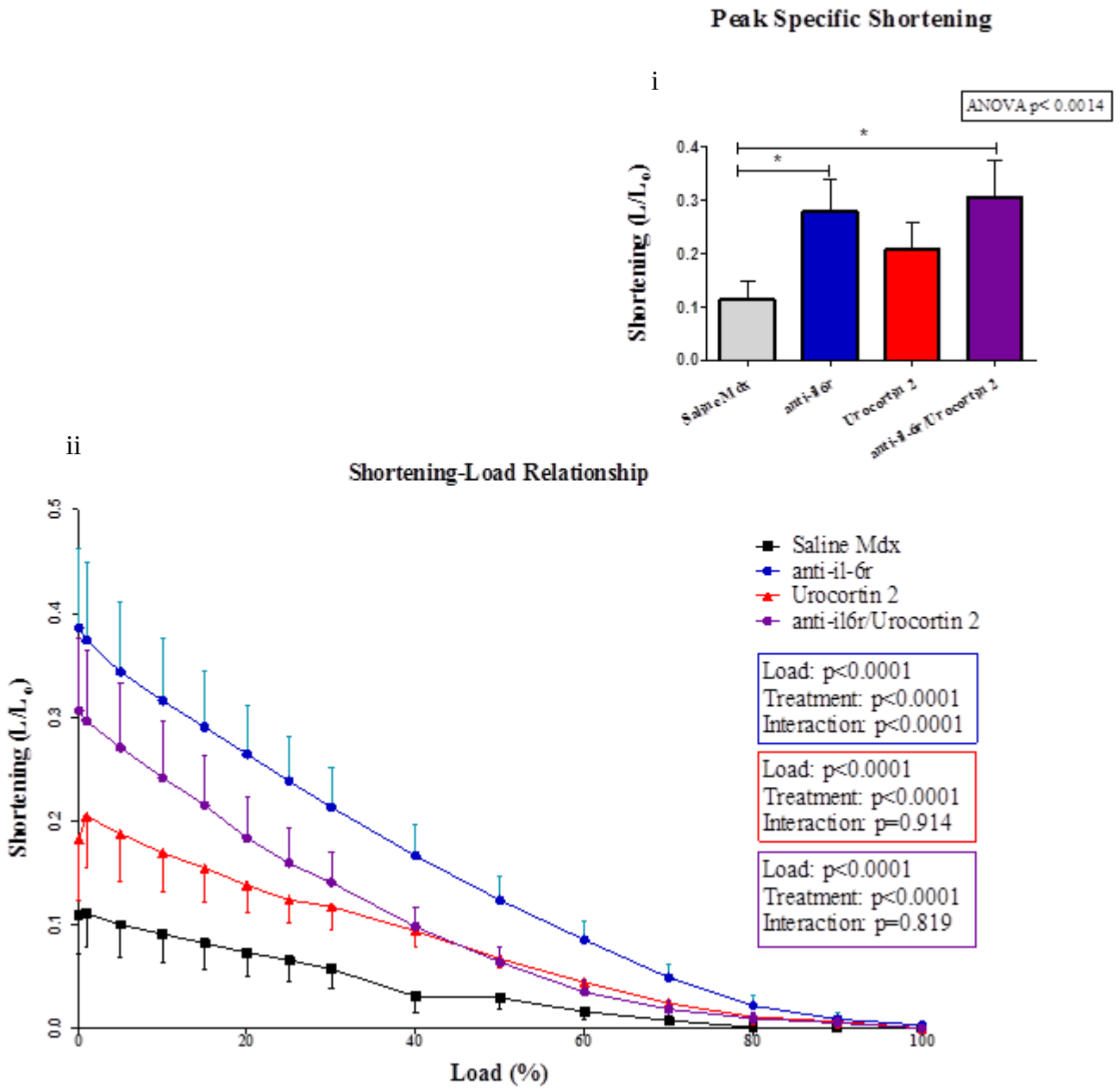
4.4.1.3 Blocking IL-6 signalling increases specific shortening and increases the length of shortening over the load continuum in the presence or absence of Urocortin 2

In *mdx* mice treated with anti IL-6R in the presence or absence of Urocortin 2, or treated with Urocortin 2 alone, the diaphragms shorten significantly more than diaphragms from saline treated *mdx* mice (Figure 4.12, n=6-8, $p<0.0001$, two way ANOVA). As expected, load is a significant factor ($p<0.0001$) and there was a significant interaction between anti IL-6R treatment (treatment x load) compared to saline treated animals ($p<0.0001$).

4.4.1.4 Blocking IL-6 signalling increases work production over the load continuum in the presence or absence of Urocortin 2, as does Urocortin 2 treatment alone

Load - Work Relationship

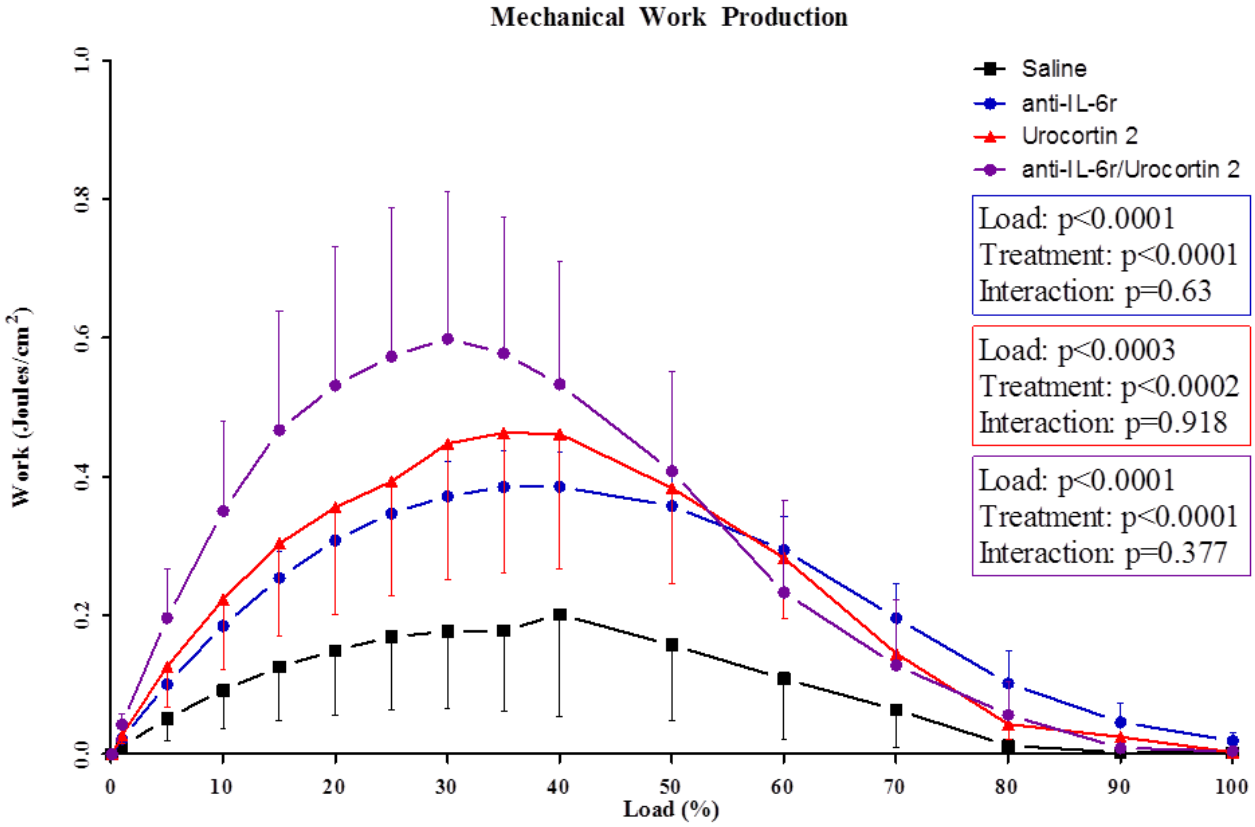
Work production was increased in all groups compared to saline controls. (Figure 4.13, $p<0.001$ n=6-8). Load was a significant factor for each treatment ($p<0.0001$) but there was no significant interaction (treatment x load) ($p>0.05$).



<u>Figure 4.12:</u> Load-Shortening Relationship in *mdx* diaphragms with and without interventions

Comparing mdx mice administered saline (black), anti IL-6 receptor antibody (anti IL-6R, blue), Urocortin 2 (red) and a co- treatment of anti-IL-6R and Urocortin 2 (purple).

*i The graph shows the load/shortening relationship, measured as a ratio of shortening/optimal length (L/Lo). Peak specific shortening (L/Lo) increased following anti IL-6R and co treatment of anti IL-6R + Urocortin 2 ii Two way ANOVA revealed a significant difference between all three interventions when compared to saline; there was a significant interaction also in the anti-IL-6 R treatment group.*p<0.05, n=6-8.*



<u>Figure 4.13:</u> Mechanical Work Production in *mdx* diaphragms with and without interventions

The work - shortening relationship (Joules per cm^2) in diaphragm muscle from mdx mice administered saline (black), anti IL-6 receptor antibody (anti IL-6R, blue), Urocortin 2 (red) or a co- treatment of anti-IL-6R and Urocortin 2 (purple) is graphed above. Two way ANOVA revealed a significant difference between all three interventions when compared to saline; there was no significant interaction, n=6-8.

4.4.1.5 Blocking IL-6 signalling increases peak velocity production and IL-6R and Urocortin 2 co-treatment increases muscle shortening velocity

There was no significant difference in the peak velocity of muscle shortening in diaphragms taken from *mdx* mice from any treatment group with the exception of anti-IL-6R which stimulated an increase in the velocity ($p<0.05$, n=6-8, Figure 4.14i).

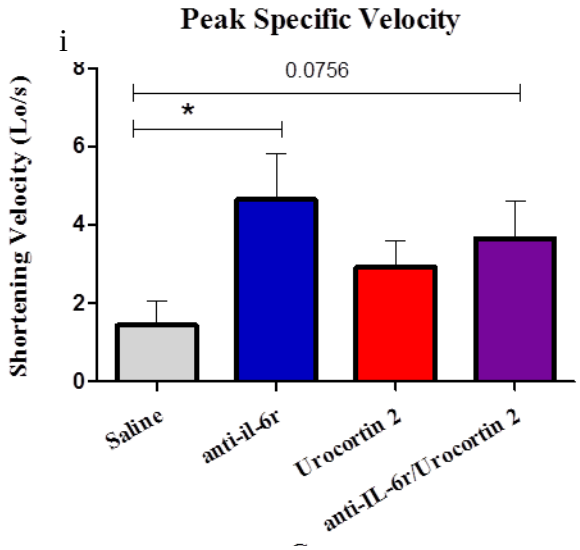
Mdx mice treated with anti IL-6R had significantly higher diaphragm shortening velocity (Figure 4.14ii, n=6-8, $p<0.0001$, two-way ANOVA) as did treatment with Urocortin 2 alone ($p<0.0227$), compared to saline treated *mdx* mice. Load was a significant factor ($p<0.0001$).There was no significant interaction.

4.4.1.6 Power production was increased by anti IL-6R and Urocortin 2

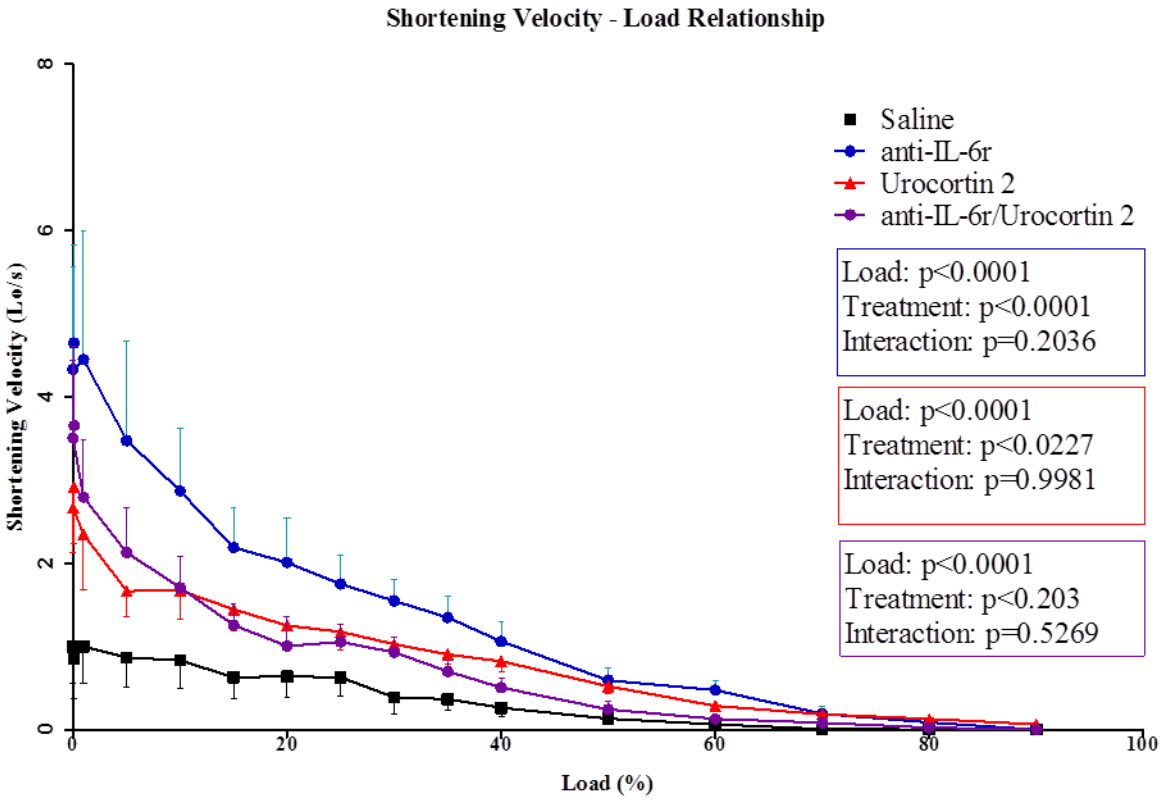
Peak diaphragm power was not different between saline and treated *mdx* mice ($p>0.05$, Figure 4.15i, n=6-8).

The Load-Power relationship was measured as the velocity x specific load. Two way ANOVA revealed that all treatments increased diaphragm power production; anti IL-6R alone (Figure 4.15ii, n=7, $p<0.001$) and in the presence of Urocortin 2 ($p<0.001$), and Urocortin 2 treatment alone ($p<0.01$) compared to saline treated *mdx* mice. Load was a significant factor ($p<0.0001$) but there was no interaction between power and load ($p>0.05$).

i

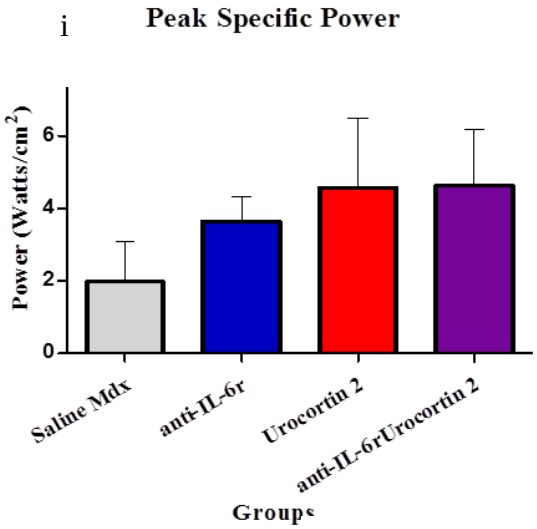


ii



<u>Figure 4.14</u>: Load/Velocity Relationship in *mdx* diaphragms with or without intervention

*The velocity of shortening (ratio of shortening/optimal length (L/Lo) over 300 milliseconds (ms) expressed as (Lo/s)) of mdx mice administered saline (black), anti IL-6 receptor antibody (anti IL-6R, blue), Urocortin 2 (red) and a co-treatment of anti-IL-6R + Urocortin 2 (purple) is graphed above. i The peak shortening velocity is increased with anti IL-6R treatment. ii. Anti IL-6R treatment increases shortening velocity, as does treatment with Urocortin 2, (two way ANOVA). Load is a significant factor, but no interaction is seen in any treatment. * $p<0.05$, n= 5-8.*



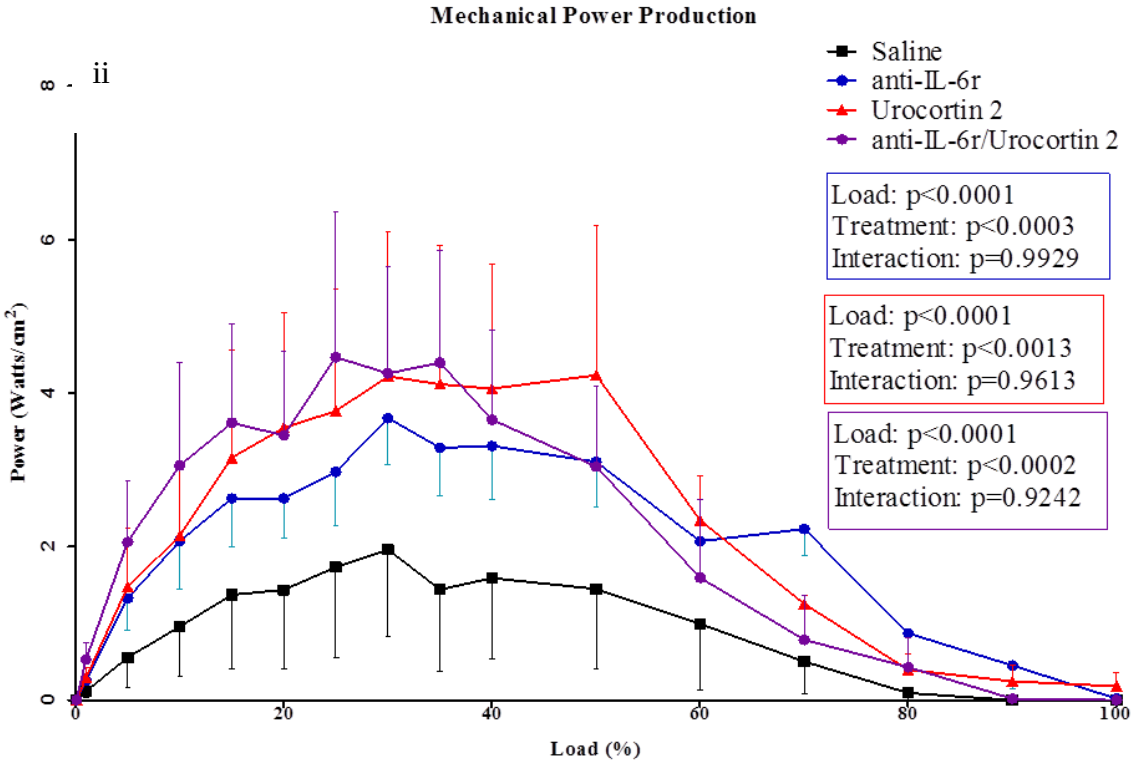


Figure 4.15: Mechanical Power Production in *mdx* diaphragms with or without intervention

Power production (Watts per cm^2) in mdx mice treated with saline (black line), anti IL-6 receptor antibody (anti IL-6R, blue line), Urocortin 2 (red line) and a co-treatment of both (purple line) is graphed above. i Peak Power was not changed by any treatment (p>0.05, one way ANOVA, n=7). ii Treatment with anti IL-6R in the presence or absence of Urocortin 2 increased power production over the load continuum, as did treatment with Urocortin 2 alone (Two way ANOVA, p<0.001, n=6-8) and a load effect in all intervention treatments. No interaction was observed between treatments, n=6-8.

4.4.2 Repeated Muscle Stimulation

4.4.2.1 Anti IL-6R and Urocortin 2 treatment increase shortening in a repeated stimulation protocol

Over a load continuum, shortening is significantly increased in *mdx* diaphragm muscle treated with anti IL-6R, urocortin 2 or both. In a repeated stimulation protocol, two-way ANOVA revealed that in all treated *mdx* mice the diaphragm shortens (L/L_o) significantly more than saline treated mice. L/L_o was reduced to a greater extent with repeated stimulation in treated muscle compared to saline-treated controls, time (repeated stimulation) was a significant factor (Figure 4.16, $p<0.0001$ n=6-8).

4.4.2.2 Blocking IL-6 signalling in *mdx* mice significantly causes a higher velocity during repeated muscle stimulation compared to saline and other treatments

Two-way ANOVA of shortening velocity decay over time, revealed a significant effect of anti IL-6R treatment ($p<0.0001$). There was no significant difference in Urocortin 2 treated mice compared to control and shortening velocity was reduced in anti IL-6R treated mice in the presence of Urocortin 2 ($p<0.0001$, Figure 4.17, n=6-8). Time (repeated stimulation) was a significant factor and there was a significant interaction (velocity x time) in anti IL-6R treated *mdx* mice. (Figure 4.17, $p<0.0001$, n=6-8).

4.4.2.3 IL-6R and Urocortin 2, significantly conserves power production in *mdx* mice

Two-way ANOVA of power decay over time revealed that diaphragm power was significantly higher in all treated diaphragms compared to saline treated control *mdx* mice. Time was a significant factor (Figure 4.18, n=6-8, $p<0.0001$) but there were no significant interactions ($p>0.05$).

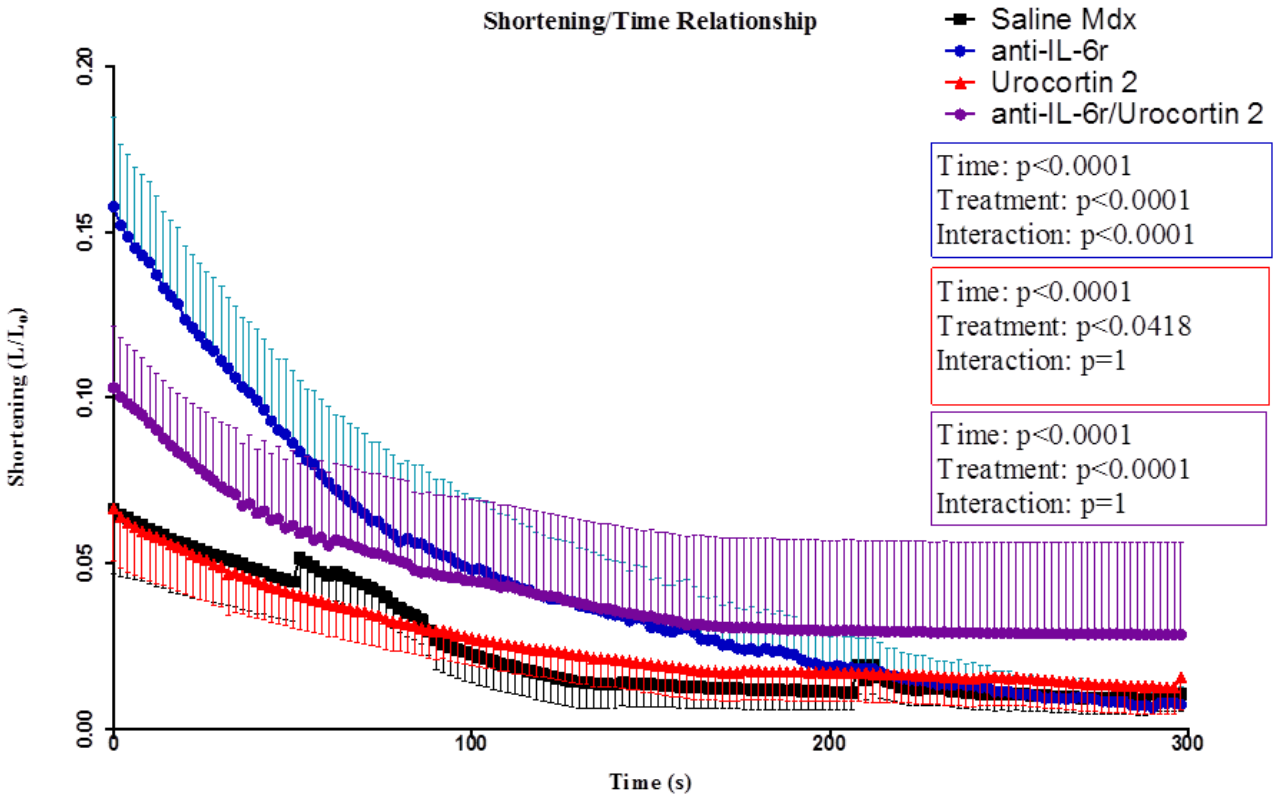


Figure 4.16: Muscle Shortening-Time relationship in *mdx* diaphragms with or without intervention

The graph illustrates muscle shortening (shortening/optimal length (L/Lo)) in dx mice treated with saline (black line), anti IL-6 receptor antibody (anti IL-6R, blue line), Urocortin 2 (red line) and a co-treatment of both (purple line). In a repeated stimulation protocol diaphragm strips are stimulated at 33% specific force. Time is a significant factor for all treatments over the repeated stimulation protocol. Treatment with anti-IL-6R in the absence or presence of Urocortin 2 increases shortening over the repeated stimulation ($p<0.0001$) more so than Urocortin treatment alone ($p<0.0418$).There is an interaction observed with anti-IL-6R treatment ($p<0.0001$) (Two way ANOVA, n=6-8).

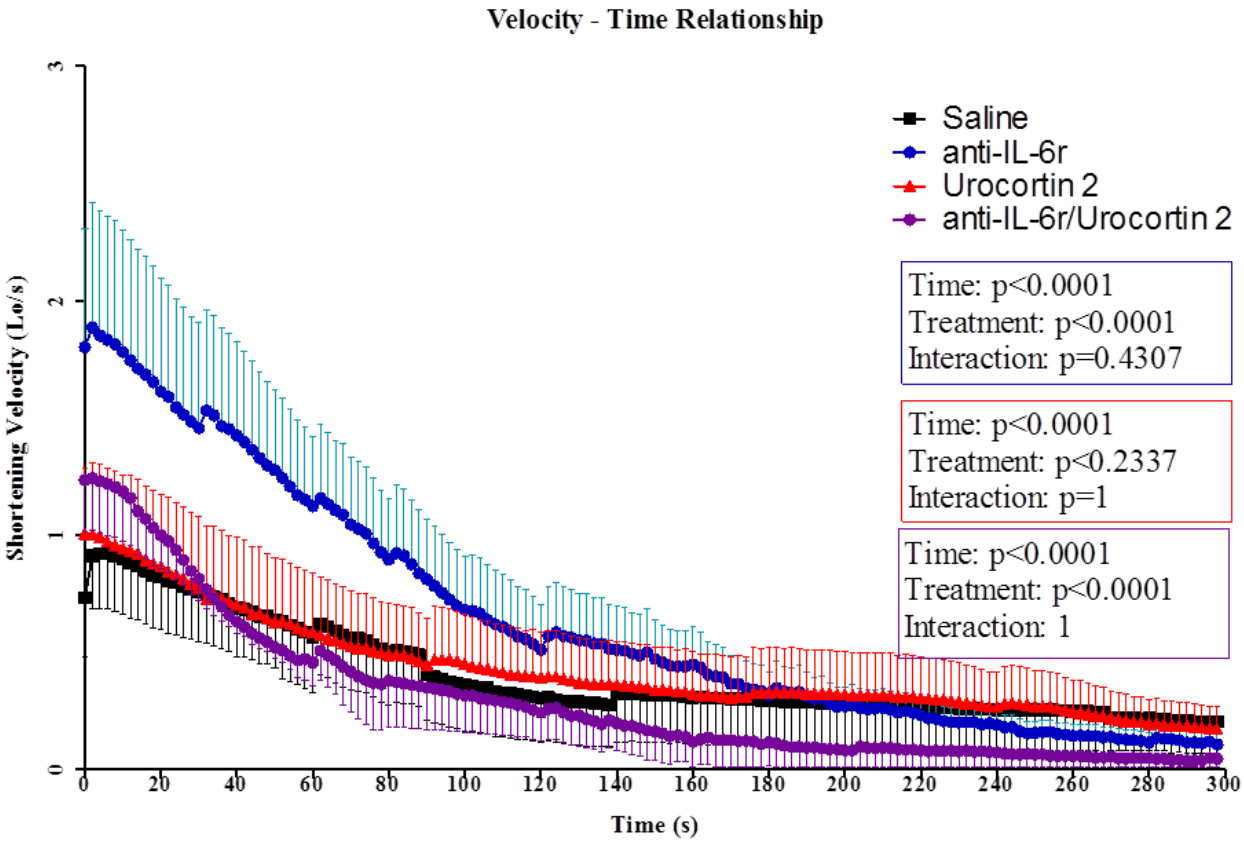
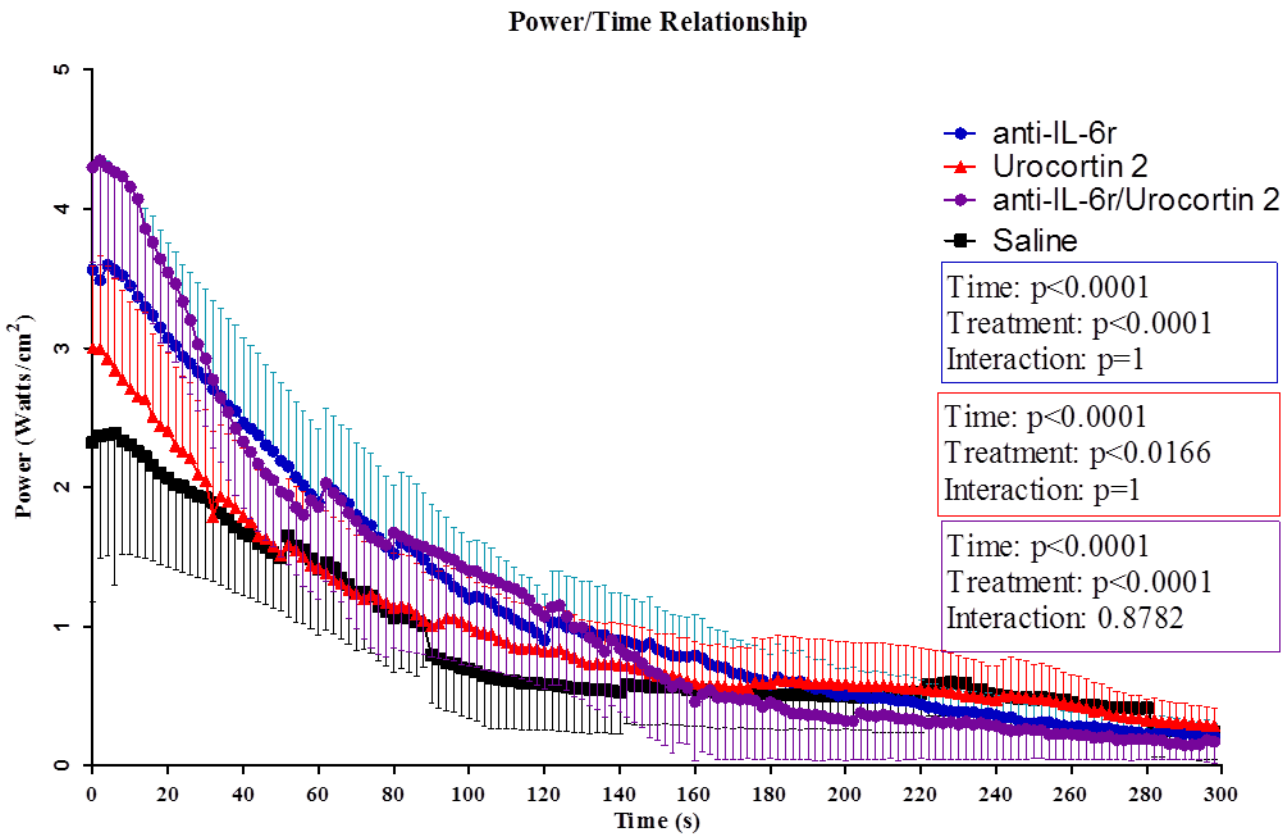


Figure 4.17: Velocity-Time relationship in treated *mdx* diaphragms with or without intervention

The graphs shows velocity (shortening/optimal length per second over 300 milliseconds Lo/L)) in mdx mice treated with saline (black line), anti IL-6 receptor antibody (anti IL-6R, blue line), Urocortin 2 (red line) and a co-treatment of both (purple line). In a repeated stimulation fatigue protocol, diaphragm strips are stimulated at 33% specific force. Time is a significant factor for all treatments over the repeated stimulation protocol ($p<0.0001$). Treatment is a significant in anti IL-6R treated mice in the absence and presence of Urocortin 2 ($p<0.0001$), but not Urocortin 2 treatment alone ($p<0.2337$). There is no interaction observed. (Two way ANOVA, n=5-8).

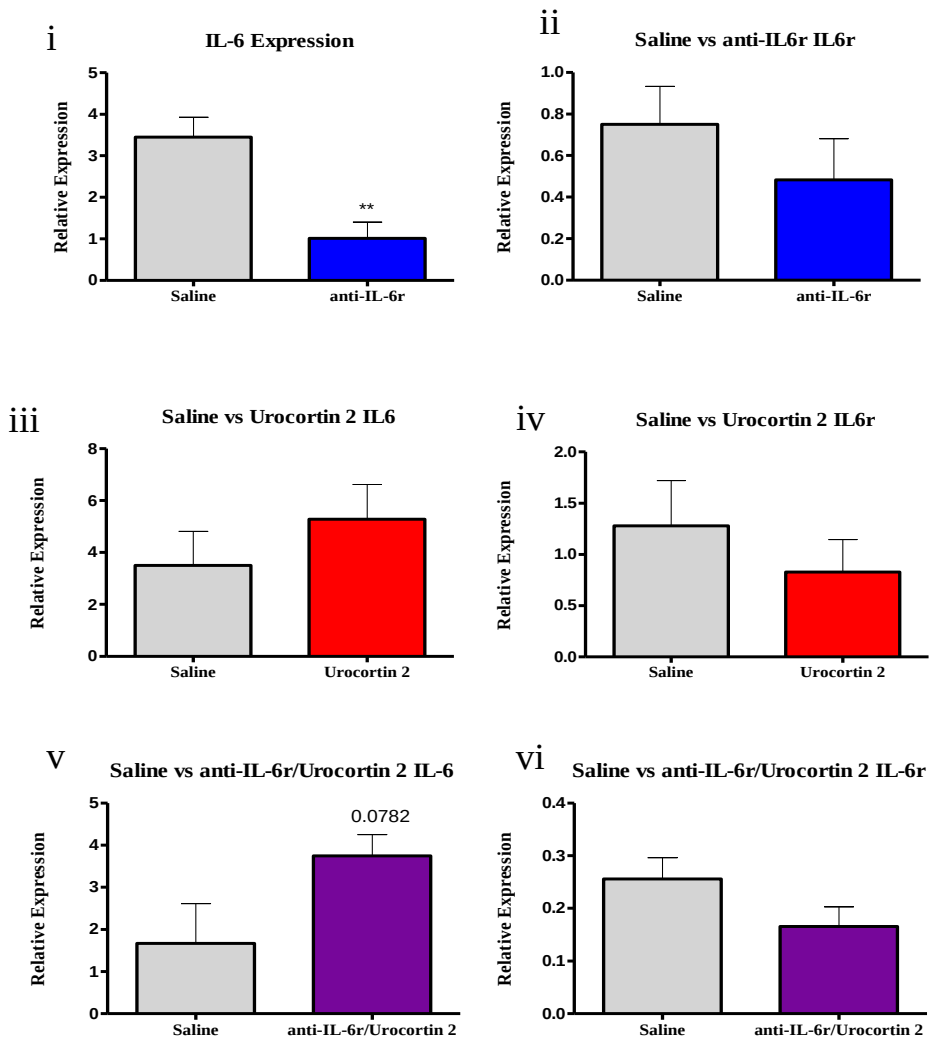


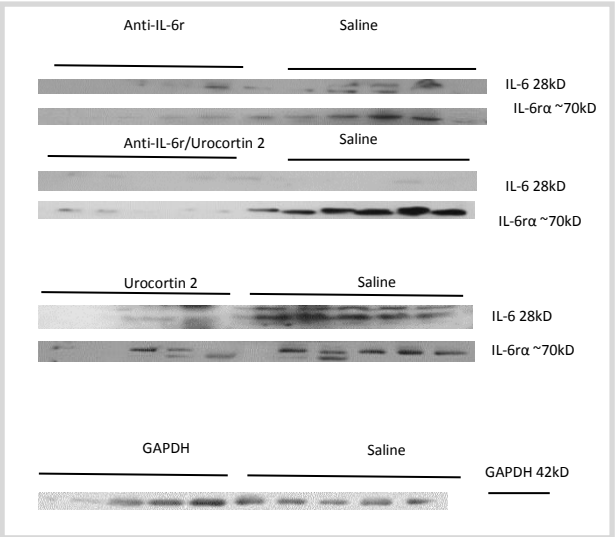
<u>Figure 4.18:</u> Power-Time relationship comparisons in *mdx* diaphragms with or without intervention

The graphs shows power (Watts per cm^2. in mdx mice treated with saline (black line), anti IL-6 receptor antibody (anti IL-6R, blue line), Urocortin 2 (red line) and a co-treatment of both (purple line). In a repeated stimulation fatigue protocol diaphragm strips are stimulated at 33% specific force. Time is a significant factor for all treatments over the repeated stimulation protocol ($p<0.0001$). Treatment is a significant in anti IL-6R treated mice in the absence and presence of Urocortin 2 ($p<0.0001$), and with Urocortin 2 treatment alone ($p<0.0166$). There is no interaction observed. (Two way ANOVA, n=5-8).

4.4.3 Blocking IL-6 signalling in *mdx* mice significantly lowers IL-6 protein in diaphragm muscle

Mdx mice treated with anti IL-6R have significantly less IL-6 protein in diaphragm homogenates than saline treated mice (Fig 4.19i, $p<0.01$, $n=5$). However, IL-6 receptor expression itself was unchanged. IL-6 protein was not reduced significantly in Urocortin 2 treated mice or in the co-treatment group (Urocortin 2 + anti IL-6R). IL-6 receptor expression was also unaffected in the latter two groups ($p>0.05$, $n=5$).





<u>Figure 4.19:</u> Western Blot Densitometry analysis of IL-6 and IL-6 receptor expression in *mdx* diaphragms

*i The graphs and representative blots illustrate the change in expression of IL-6 protein (n=5, p<0.01) and ii IL-6R (p>0.05) following treatment with anti IL-6 receptor antibodies (IL-6R). iii The graphs and representative blots illustrate the change in expression of IL-6 protein (p>0.05) and iv IL-6R (p>0.05) following treatment with Urocortin 2. v The graphs and representative blots illustrate the change in expression of IL-6 protein (p<0.01) and vi IL-6R (p>0.05) following co-treatment ** p<0.01, n=5.*

4.5 Discussion
Key findings:

Mdx versus WT mice

- *Mdx* mouse diaphragm exhibits a reduction in twitch force generation compared to age matched WT mice.
- *Mdx* mouse diaphragm exhibits a reduction in peak tetanic force compared to WT mice.
- *Mdx* mouse diaphragm exhibits a reduction in mechanical work production compared to WT mice.
- *Mdx* mouse diaphragm exhibits a reduction in power production compared to WT mice.
- *Mdx* mouse diaphragm is less resistant to fatigue than WT mice.

Intervention Studies

- Urocortin 2 alone or with anti IL-6R produces a higher twitch force compared to saline treated *mdx* mice.
- Co-treatment of anti IL-6R and Urocortin 2 produces a significantly higher peak force compared to saline treated *mdx* mice.
- Anti IL-6R alone and in conjunction with Urocortin 2 induces an increase in shortening of diaphragm strips compared to saline treated *mdx* mice. Anti IL-6R also increases the velocity of shortening.
- All intervention treatments increase mechanical work production, with co-treatment producing the largest increase.
- All intervention treatments increase diaphragm power production.
- All intervention treatments have moderate effects on fatigue, especially earlier in the trial.
- IL-6 protein levels are reduced significantly in *mdx* diaphragms when treated with anti IL-6R compared to saline treated mice.

Muscle force generation and isometric fatigability of skeletal muscle comparing WT and *mdx* muscle is somewhat explored in the vast *mdx* literature; however isotonic protocols exploring *mdx* diaphragm shortening kinetics, work and power are rarely investigated, although isotonic properties are perhaps more physiologically relevant in DMD. Isotonic, or muscle contraction that induces a length change in muscle cause micro lesions in muscle fibres, which then initiate a cascade of events which are detrimental to fibre health and function (Vilquin et al. 1998; Yang et al. 1998).

As the diaphragm is the most affected skeletal muscle in the *mdx* murine model of DMD, it is often utilised to explore dystrophin deficiency and test the efficacy of potential palliative treatments (Coirault et al. 2002; Tinsley et al. 1998; Mizunoya et al. 2011; Hara et al. 2011), as I do in this study.

The focus of this project was to test both isometric and isotonic muscle contractions in untreated *mdx* mice and explore these properties following pharmacological intervention *in vivo* with a specific rat anti mouse IL-6 receptor antibody (MR16-1), the CRFR2 agonist, Urocortin 2 or a combination of both agents together in *mdx* mice.

Because the pathology associated with dystrophin deficiency causes an inflammatory environment (Deconinck & Dan 2007; Porter et al. 2002; Manzur et al. 2007), and a loss of regenerative capacity of muscle fibre causes increased connective tissue (Klingler et al. 2012; Wehling-Henricks et al. 2008; Abdel-Salam et al. 2009) and weaker branched muscle (Lovering et al. 2009); I hypothesised that blocking a key pro-inflammatory cytokine, IL-6 which is involved in skeletal muscle metabolism and inflammation would improve function of the muscle (Pedersen & Febbraio 2008; Jonsdottir et al. 2000; Nishimoto & Kishimoto 2004; Desreumaux 2000; Daisuke et al. 2014).

Recently, a group have demonstrated that this antibody does not only reduce inflammation through the modulation of gene transcription in immune response cells, such as infiltrating macrophages – which I reproduced in study one (chapter 3) in *mdx* muscle, but can also promote muscle regeneration in injured muscle (Fujita et al. 2014). Counter-intuitively, blocking IL-6 receptor signalling using the same monoclonal antibody resulted in an increase in inflammation in limb skeletal muscle, although, the study did identify increased function of this limb. Additionally, this study is a chronic 5 week administration study of the antibody, indicating that

perhaps a long term blocking of IL-6 is detrimental due to its pleotropic anti- or pro-inflammatory effects depending on cell type and environment. Controlling IL-6 levels acutely in dystrophic muscle may be a more effective treatment (Kostek et al. 2012).

Similarly, studies relevant to this project which focus on stimulating the CRFR2 receptor have shown beneficial effects in *mdx* muscle. CRFR2 agonists can act as stimulators of anabolic signalling pathways, which can promote hypertrophy and reduce muscle necrosis. Studies have used both a synthetic analogue PG-873637 (Hinkle et al. 2007; Hall et al. 2007) and a non-selective CRFR agonist, sauvagine (Hall et al. 2007) to explore this hypothesis in *mdx* muscle as a potential therapeutic strategy. Remarkably, PG-873637 treatment is comparable to corticosteroid treatment (Hinkle et al. 2003). As steroid treatment is a somewhat affective palliative care in cohorts of patients, suggesting CRFR2 agonism may be of therapeutic benefit for patients with DMD, especially as long term steroid use can have detrimental side effects, or can "wear off" (Manzur et al. 2007).

What has not been extensively studied however is the connection between IL-6 and CRFR2 agonists in skeletal muscle function and pathology in *mdx* mice. There is a well-documented interaction between the stress hormone system (CRF and the Urocortin family) and IL-6 in the enteric nervous system (Taché et al. 1993), in immune cells and in both smooth (Kageyama et al. 2006) and striated muscle of the cardiac system (Huang et al. 2009) in rodents. Our findings suggest that this crosstalk between the stress and immune systems also occur in diaphragm muscle.

4.5.1 Isometric contractile properties of *mdx* muscle

Consistent with the literature (Gregorevic et al. 2002; Hinkle et al. 2007), specific twitch force reveals that WT mice can produce significantly higher forces in diaphragm muscle strips than *mdx* mice at the age studied (12 weeks). *Mdx mouse* diaphragm does not exceed 25% twitch force compared to WT control diaphragm. Similarly, peak specific force is significantly lower in *mdx* compared to WT controls consistent with other studies (Gregorevic et al. 2002; Hinkle et al. 2007; Bates et al. 2013; Faulkner et al. 2008). Force generation is relative to the number of functional cross bridge connections made during skeletal muscle contraction (Attal et al. 2000; Lecarpentier et al. 1998) and in *mdx* diaphragm at this age, this dysfunction is most likely due to loss of functional muscle fibres (Lovering et al. 2009; Williams et al. 1993) and an increase in connective tissue (Turgeman et al. 2008; Gosselin & Williams 2006), caused by the loss of dystrophin mechanical support (Batchelor & Winder 2006; Petrof et al. 1993).

Whilst exploring the force generation capacity of diaphragm muscle, muscle kinetics can be extrapolated. In practice, the most useful parameters examined in *mdx* mice are time to peak (TTP) and time for the force to decay by half (½ RT). Changes in these kinetic parameters between mouse strains may indicate a change in fibre type and/or a change in calcium handling in myocytes. At this age, *mdx* mice start to exhibit changes in fibre type compared to WT mice, however the changes may not affect isometric twitch force kinetics (Gregorevic et al. 2002) as these changes in type 11x and type 11a fibres are known to generate a similar force (Geiger et al. 2000). However, it is generally accepted that fibre change does not start until mice are 16 weeks of age in dystrophic muscle (Guido et al. 2010), however I did not find changes. As *mdx* mice age it is apparent that the velocity of the acto-myosin interaction slows (Coirault et al. 2002) due not only to contractile apparatus changes but to altered sarcoplasmic reticulum (SR) calcium handling (Kargacin & Kargacin 1996). However, in our study I found the TTP of a twitch contraction was not different between the strains nor was the 1/2 RT of the relaxation, which suggests no alterations in the actomyosin apparatus at 12 weeks of age.

Perhaps a limitation to this study is the calculation of force from the raw isometric output, force is calculated by utilising the CSA, assuming muscle density to be constant. In *mdx* muscle at three months, muscle weight may include split or necrotic muscle fibres evident with the histopathological studies of the diaphragm at this age (Claflin & Brooks 2008; Arakia et al. 1997). Thus, the determination of specific force (force normalised to CSA) may have exaggerated the muscle deficit. However, it is important to note than when absolute force measurements were compared (force in mN), *mdx* diaphragm was weaker than WT control, moreover optimal length does not differ between WT and *mdx* diaphragm muscle strip preparations nor does CSA.

4.5.2 Effect of intervention on *mdx* isometric contractile properties

When specific twitch force was compared across treatments, anti IL-6R and Urocortin 2 or a combination of the two agents bore interesting results. Differences between treatments and a partial additive effect were noted in twitch force. Anti IL-6R therapy rescued the loss of muscle force noted in *mdx* muscle tissue. Urocortin 2 and anti IL-6R in combination with Urocortin 2 showed a trend towards an increase in specific tetanic forces, although this did not reach statistical significance. This appears to be due to a higher variability in *mdx* tissue contraction.

These results suggest that blocking IL-6 signalling systemically can make the diaphragm produce a higher force than saline treated mice, and therefore a more capable, functional muscle. This may be due to a reduction in the inflammatory environment at a crucial time (10–12 weeks of age in the mice) and indeed molecular analysis results show a lower level of IL-6 protein in the receptor antibody treated group. This is likely beneficial to muscle contraction and may be indicative of a physiologically healthier muscle.

Activation of the CRFR2 as previously described can reduce atrophy in skeletal muscle. In one study, a reduction in atrophy is reported in both immobilization and in non-immobilization models of skeletal muscle atrophy in the EDL (Hinkle et al. 2003). It was also reported that activation of the CRFR2 can increase maximum tetanic force, which is similar to the tetanic force increase

observed in this project. Interestingly, in their study CSA was increased, illustrating that CRFR2 agonists can increase muscle mass (Hall et al. 2007). In the present study, CSA of muscle fibres was not directly examined; rather muscle bundles of equivalent size were mounted for functional analysis. It is suggested that the increase in muscle force may be due to CRFR2 agonists' ability to lower the catabolic muscle response induced by the pro-anxiolytic CRFR1 receptor activity in the HPA axis (Hinkle et al. 2003). CK levels in serum were reduced in treated *mdx* mice, and using Urocortin 2 as a CRFR2 agonist also results in the reduction of CK levels (Reutenauer-Patte et al. 2012), indicating a less "leaky" or damaged muscle fibre profile within skeletal muscle.

Co-treatment did not elicit a complete additive effect on force production; however it is established in other tissues that an interaction exists between IL-6 and CRF, namely in the nervous system (Vallières & Rivest 1999), in striated cardiomyocytes (Huang et al. 2009), aortic smooth muscle (Kageyama et al. 2006) and colonic enteric neurons (O' Malley et al. 2013) and a potential interaction in respiratory skeletal muscle could prove beneficial for dystrophic diaphragm of DMD patients given that studies have found anti-inflammatory treatments and CRFR2 agonism to be beneficial.

It is worth noting however, that CRFR2 agonism may also play a role in promoting a pro-inflammatory environment through NFκB dependent induction of pro inflammatory IL-8 (Moss et al. 2007). In colonic smooth muscle it also has a role in apoptosis in macrophages (Tsatsanis et al. 2005) through CRFR2 agonism acting as a paracrine anti-inflammatory signal, suggesting a self-modulating anti-inflammatory role between CRF and its ligands.

Investigating IL-6 levels in Urocortin 2 treated mice compared to saline treated mice, did not show a significant reduction in IL-6 or its receptor, suggesting the mechanisms through which it exerts its beneficial effects is more complex than simply an anti-inflammatory modulation of the pathological environment. It is likely however, that a reduction in IL-6 signalling results in a reduction in inflammatory induced pathology (Fujita et al. 2014). Urocortin 2 is likely promoting hypertrophy and slowing apoptosis of macrophages as well as slowing muscle atrophy through activation of CRFR2.

The interaction is likely to be complex and is beyond the scope of the current project – it is evident however that Urocortin 2 in this study did not alter IL-6 levels, or receptor expression in the diaphragm muscle of *mdx* muscle compared to saline treated animals.

4.5.3 Isotonic contractile shortening of *mdx* muscle compared to WT controls

Exploring shortening over a load continuum revealed that at 12 weeks of age, *mdx* diaphragm strips "shorten" to the same extent (relative to resting optimal length) as WT diaphragms. The slope of the load relationship is similar between strains.

These data suggest that at this age there is no difference in the actin-myosin contractile properties of the *mdx* fibres or more specifically, cross bridges kinetics and calcium handling in the SR (Claflin & Brooks 2008; Attal et al. 2000) contrary to studies reporting that dystrophic fibres undergo hyper-contractility (Claflin & Brooks 2008). However, the apparent discord between these results may be due to the study of skeletal limb muscles compared to diaphragm muscle of this study.

Possibly, a limitation in the study is that optimal length was recorded only to the nearest millimetre. This may increase the margin of error in the ratio of shortening to optimal length.

4.5.4 Effect of interventions on *mdx* isotonic contractile shortening properties

Perhaps an unexpected result is the difference between treatments in the data for muscle shortening. Even though the optimal length of treated diaphragm strips were similar, anti IL-6R treatment alters muscle shortening which suggests IL-6 has a role in calcium handling and indeed it has been noted that chronic levels of IL-6 can interact with SR normal function and decrease contractility in cardiac muscle. Additionally, IL-6 can stimulate rises in intracellular calcium in enteric neurons (O'Malley et al, 2011), skeletal muscle from *mdx* mice exhibit elevated levels of both IL-6 and intracellular calcium (Allen et al. 2010) but it is unknown if IL-6

stimulates *mdx* diaphragm myocytes (Yu et al. 2005). Treatment with Urocortin 2 had no significant effect.

4.5.5 Isotonic mechanical work production of *mdx* muscle compared to WT controls

Characterising mechanical work production in *mdx* diaphragm using an isotonic protocol is not commonly performed. Examining the contractile properties, including myosin isoforms (Petrof et al. 1993) and isometric force production is more common but has its limitations. It is not abstract to conclude that the differences in work production are due to the cross bridge numbers and function as opposed to actomyosin dynamic changes, as our isotonic results showing a large reduction in force generation capabilities and the lack of difference in shortening profile in the *mdx mouse* compared to the WT in our study. Work production has been examined previously in *mdx* mice diaphragm; this work however, was oscillatory stretch work using an isometric protocol, and the authors also found in support of our study that *mdx* diaphragm is capable of generating less mechanical work than WT mice (Stevens & Faulkner 2000).

Our study examined mechanical work produced over a continuum of loads, WT mice produced a bell shaped curve, with peak work at 30-40% of load, consistent with the literature (Attal et al. 2000) relating to specific muscle thermodynamics and cross bridge kinetics (Rall 1985). Work production in *mdx* mice was significantly lowered, and although shortening is similar between strains, force production is significantly reduced which accounting for the decline in mechanical work production (*work = force x shortening*).

4.5.6. Effect of intervention on work production

Mechanical work production was significantly improved by addition of the intervention treatments. Anti-IL-6R treatment improves work production as does Urocortin 2 treatment. This recovery is a result of a combination of a higher distance of muscle shortening and higher forces in the treatment groups. Urocortin 2 appears to shift the bell curve to the left, making peak specific mechanical work most

efficient at a lower percentage load. This indicates a change in the dynamic capabilities of the muscle. Addition of anti IL-6 receptor antibody in the presence of Urocortin 2 improves work production to the greatest extent, showing an additive effect. Interestingly, it also shifts the bell curve to the left, with peak work being at a lower percentage load than the other treatments or compared to saline controls, indicating that co-treatment is the most effective treatment in improving the pathophysiology in muscle dynamic contractile properties in *mdx* muscle.

4.5.7 Isotonic shortening velocity and power production in *mdx* mice compared to WT controls and the change in shortening velocity following treatments

Velocity of shortening

Assessment of shortening velocity, which is measured during the isotonic contraction protocol over incremental loads, reveals no difference between *mdx* and WT animals in this study. Shortening velocity, similar to isometric kinetics (TTP and 1/2 RT) is not affected in *mdx* mice at l2 weeks, it has been previously seen that actin-myosin coupling is changed in *in vitro* motility assays (Coirault et al. 2002). This suggests, as has previously been noted, that *in vivo* muscle actin-myosin coupling and detachment kinetics are not significantly different, but force generation is substantially lowered.

Addition of anti IL-6R and Urocortin 2 alone or in combination increases the shortening velocity. Anti IL-6R increases the shortening velocity significantly and more than either Urocortin 2 alone or anti IL-6R and Urocortin 2 combined. Urocortin 2 alone or in co-treatment with anti IL-6R appeared to reduce velocity compared to anti IL-6R treatment alone, potentially due to its effect of increasing shortening.

Muscle Power Production

Although an important physiological muscle parameter, power production to contract and produce mechanical work is little examined in *mdx* mice, it was previously thought that power production was not decreased steadily, but it has been found to be 33% lowered in a study investigating limb muscle (Lynch et al. 2001), (*force x*

velocity), consistent with our study where diaphragm power production is substantially decreased in *mdx* mice compared to WT controls. Due to a significant lowering of force and a slight lowering of velocity in *mdx* animals, the resulting power is depressed and there is essentially no power-load relationship such as that observed in the WT animals.

Peak power does not differ between the treatments when compared to saline treated *mdx* mice – with maximal power production at 30% load. However, analysis of the power-load relationship shows a significant increase in power in the anti-IL-6R treatment group compared to control. It has been reported that compounds which modulate atrophy can increase power production in *mdx* mice (Lynch et al. 2001), which may explain the benefits Urocortin 2 is having in power production. Co treatment with anti IL-6R have similar treatment effects greater than anti IL-6R treatment alone on power production.

4.5.8 Repeated stimulation in *mdx* muscle – Isotonic Fatigue Protocol

The diaphragm muscle is constantly contracting and relaxing to enable breathing; as such its fibre composition reflects its need to resist fatigue. As discussed in the context of force generation, fibre types at this age in *mdx* muscle do not exhibit a change in resistance (Guido et al. 2010) to fatigue. Fatigue has been studied in isometric preparations in *mdx* mice (Gregorevic et al. 2002) and in other skeletal muscles, which investigates the loss of specific force in response to repeated stimulation (Olivier et al. 2006). Isotonic fatigue however explores the capacity of muscle to perform work and generate power in response to repeated stimulation.

Muscle shortening over 300 ms is significantly higher in *mdx* mice, compared to WT mice. The isotonic protocol is performed at 33% load (maximum specific force), and this was standardised for both groups. However it should be noted, at this load *mdx* muscle shortens to a greater extent than WT mice, therefore the protocol may have favoured *mdx* preparations. Nonetheless, *mdx* mice are similarly resistant to fatigue in the repeated protocol compared to WT animals, the slope of the shortening is equivalent to the WT animals, even though there is no time or interaction effect on either genotype.

Urocortin 2 alone did not affect isotonic fatigue, but anti IL-6R treatment had interesting effects. Even though there is a steeper slope of reduction in contraction, shortening starts from higher peak shortening compared to the other treatments, perhaps indicating a less stable modulation of calcium handling and cycling (Hortemo et al. 2013) within a myofibre in the absence of IL-6 and moreover IL-6 has interactions of myosin light chain 2, which is dephosphorylated in repeated contraction protocols (Hortemo et al. 2013).

Of most interest, co-treatment caused the muscle to be more fatigue tolerant than anti IL-6R alone and the latter 200 seconds of the test shows a significantly higher conservation of degree of shortening or loss of sustained shortening length and at the end of the test has a significantly higher capacity to shorten than saline treated or either treatment alone. This leads us to conclude that perhaps co treatment is best at conserving physiological ability of *mdx* diaphragm muscle to resist fatigue.

4.5.9 Effect of repeated stimulation on velocity and power production

Velocity of shortening

Shortening velocity was altered in *mdx* mice compared to WT mice in the repeated stimulation protocol; revealing that WT mice are more resistant to fatigue induced reduction in velocity of shortening than *mdx* mice, the decline in shortening velocity with repeated stimulation in this specific protocol is greater in *mdx* diaphragms and although in skeletal muscle dystrophin deficiency does not seem to have effects in excitation contraction coupling compared to normal mice (Hollingworth et al. 1990), velocity is susceptible to fatigability in diaphragm muscle of *mdx* mice.

Treatment with anti IL-6R reveals a higher peak shortening velocity than the other treatments resulting in a steeper slope and therefore a rundown of force conservation in *mdx* muscle, similar to its shortening profile. Urocortin 2 treatment produces a profile very different from anti IL-6R treatment, it has sustained shortening but a reduction in velocity, revealing slower but a more resistant profile to fatigue, perhaps due to the mechanisms discussed as per the shortening – time relationship. Urocortin 2 did not produce a conservation of velocity compared to the other treatments, and

its profile is similar to that of saline treated *mdx* mice, indicating no therapeutic effect of Urocortin 2 on velocity maintenance.

Power-time relationship

There is a dramatic difference between the strains in power. WT mice show a progressive rundown in power with repeated muscle stimulation; *mdx* mice in comparison have very low initial power and show a further reduction over time.

Power rundown in the repeated muscle stimulation protocol once again benefits from the treatment of anti IL-6R and Urocortin 2 treatment. Whereas all treatments lead to improved power compared to saline *mdx* mice, it would appear that co- treatment with both anti IL-6R and Urocortin 2 results in higher initial power and better maintenance of power during the fatigue trial.

4.6 Conclusions

Mdx diaphragm muscle contractile properties are significantly different from WT mice at 12 weeks of age. From the literature we know this dysfunction worsens with age in *mdx* mice, comparable to the human DMD condition. Force production is the most obvious physiological dysfunction and this affects mechanical work and power production in *mdx* diaphragms, similarly patients exhibit a reduction in force production and a thickened hypertrophic muscle.

Taking an anti-inflammatory approach to therapy for ameliorating the progression of the disease, I treated *mdx* mice with MR16-1, an antibody which binds to and neutralises IL-6Rs, thereby blocking IL-6 signalling and this had a beneficial effect, increasing diaphragm force production. Moreover, treating *mdx* mice with a CRFR2 agonist, Urocortin 2 also rescued force production in *mdx* mice.

Interestingly, there is some interaction of these compounds in the *mdx* muscle, as a partial additive effect was observed in several key parameters of the study. Because the two treatments appear to improve muscle physiology in different ways, for instance, anti IL-6R increases shortening and restores work, velocity and power whereas Urocortin 2 increases force, work and power, co-treatment of *mdx* with both agents produced the most beneficial effect in diaphragm contractile properties. This study has identified two key targets for potential new therapeutic strategies in the treatment of DMD.

Chapter 5: The role of IL-6 and CRF in gastrointestinal dysfunction in the *mdx* mouse

5.1 Introduction

5.1.1 GI function is altered in patients with DMD

GI function is compromised in patients with DMD, many patients exhibit gastrointestinal hypomotility (Barohn et al. 1988), pseudo obstruction (Leon et al. 1986) and constipation which has been attributed to lack of mobility of the patient and weakened abdominal walls (O Borrelli et al. 2005), which aids the intestines in the movement of its contents. However, an additional consideration is the absence of dystrophin in smooth muscle in DMD patients (Hoffman et al. 1987; Byers et al. 1991). Indeed histological examination of post mortem smooth muscle from DMD patients reveals fibrosis and pathological features such as oedema and muscle wall fragility (Dinan et al. 2003) indicating pathological changes also occur in this tissue in the absence of dystrophin. Consistent with the human clinical presentation, adult (12-18 months) dystrophin-deficient *mdx* mice have altered GI smooth muscle dysfunction, with evidence of slowed transit times in the colon, reduced faecal output but normal gastric emptying *in vivo* (Mulè et al. 2010). Changes in electrical impulses controlling spontaneous contractions in the colon were also revealed in a study of younger (16 weeks) *mdx* mice (Tameyasu et al. 2004). However, of the mechanistic changes in GI smooth muscle underlying dysfunction is not well understood.

5.1.2 Interleukin-6 and GI function

IL-6 is a pro-inflammatory cytokine, which is released from a variety of tissues including skeletal muscle (Plomgaard et al. 2005). It is released in response to changes in metabolism of exercised muscle and also due to local inflammation (Pedersen & Febbraio 2008). However, it is also secreted by immune cells, neurons (März et al. 1998) and epithelial cells (Ding et al. 2000). As circulating IL-6 levels are elevated in DMD (Rufo et al. 2011; Messina et al. 2011) and membrane-bound IL-6 receptors are expressed on smooth muscle cells (O' Malley, Dinan, et al. 2011a), enteric neurons (O' Malley, Liston, et al. 2013) and the mucosal cells in the GI tract (Atreya & Neurath 2005) in addition to the added sensitivity endowed by the soluble version of this receptor, this cytokine may contribute to GI dysfunction in

DMD. Indeed, IL-6 has been shown to play a role in other inflammatory GI disorders such as IBS (Barbara et al. 2006), colitis (Gustot et al. 2005), Crohns disease and in colon cancer (Atreya & Neurath 2005).

In the case of IBS, elevated IL-6 levels have been proposed as a biomarker of the disease (Clarke et al. 2009) but it has also been shown to have functional effects on GI secretion and contractility. The role of IL-6 in GI dysfunction in DMD is unknown. However, blocking IL-6 signalling with an IL-6 receptor antibody, MR16-1 surprisingly resulted in raised levels of inflammatory markers but was found to be beneficial in increasing forelimb strength in *mdx* mice. This was contrary to the hypothesis proposed in the study that blocking IL-6 signalling would reduce muscle damage, as opposed to a broad dampening of the immune response (Kostek et al. 2012), which has been reported to be detrimental to muscle repair (Summan et al. 2006; Chazaud et al. 2003). As discussed in chapter 4, recently, the elucidation of the mechanism by which MR16-1, and therefore IL-6 signalling blocking works has revealed that in skeletal muscle it reduces STAT3 phosphorylation and accelerated muscle regeneration (Fujita et al. 2014). However, no studies have examined the effect of blocking IL-6 signalling in bowel function in *mdx* mice.

5.1.3 The role of the stress hormone - CRF in GI dysfunction in the *mdx* mouse

Stress is a detrimental factor in many diseases, as is the case with both psychological (Bonaz & Bernstein 2013) and immune stressors in IBS. Moreover, there is high comorbidity between this functional bowel syndrome and mood disorders such as anxiety and depression (Walker et al. 2011; Fitzgerald et al. 2008). In chapter 3, I discussed the prevalence of mood disorders in DMD and have provided evidence of depression- and anxiety-like behaviours in the dystrophin-deficient *mdx* mouse. Mood disorders can be exacerbated by stress, which is initiated by secretion of corticotrophin-releasing factor (CRF) from the paraventricular nucleus of the hypothalamus which subsequently stimulates the HPA axis (Bale & Vale 2004).

CRF binds to two receptors, CRFR1 and CRFR2. CRF receptors are also expressed in the GI tract where CRFR1 appears to have a stimulatory effect on colonic motility and contributes to visceral hypersensitivity in rodents inducing

functional GI changes including an increase in gastric motility, transit time and defecation (Martínez et al. 2002) and visceral hypersensitivity (Nijsen et al. 2005; Mart et al. 2004) whereas activation of CRFR2 inhibits motility in the gut, delaying gastric emptying and can reduce sensitivity to induced visceral pain in rodents (Nijsen et al. 2005; Martínez et al. 2002) and also has anti-inflammatory effects (Tsatsanis et al. 2005).

The related protein Urocortin 2 has a higher affinity for CRFR2 which are commonly expressed in the peripheral system; in macrophages (Tsatsanis et al. 2005) and in the GI tract (O'Malley, Dinan, et al. 2010). Two studies examined the effects of CRFR2 antagonism in skeletal muscle in *mdx* mice where it was found have anti-inflammatory effects, improved diaphragm function and reduced mRNA levels of pro-inflammatory genes concluding that the effects of the CRFR2 antagonism in the diaphragm is due to a pluripotent effect on the muscle (Reutenauer-Patte et al. 2012), and increase in muscle weight and decrease in non-specific marker of disease serum CK levels (Hall et al. 2007). To date, CRFR2 agonists have not been tested on smooth muscle function in *mdx* mice

5.1.4 Interaction between IL-6 and the CRF family of proteins

Crosstalk between IL-6 and CRF may be important in the exacerbation of GI symptoms in DMD as has been proposed in other GI disorders such as IBS (O' Malley et al. 2013). IL-6 can activate the HPA axis, using a CRF dependent (Vallières & Rivest 1999) or independent pathway (Bethin et al. 2000). Moreover, IL-6 can stimulate the CRF pathway, namely ACTH which through the release of corticosteroids from the adrenal gland, in turn suppresses IL-6 (Venihaki et al. 2001) plasma levels, which implicates the CRF stress response in modulating the immune response. Besides in the central nervous system, crosstalk is apparent between IL-6 and the CRF related proteins in various tissues, as discussed Urocortin 2 can induce IL-6 gene transcription in rodent aortic smooth (Kageyama et al. 2006) and modulates IL-6 levels in stromal cells (Zoumakis et al. 2000). Moreover, CRF antagonism increases IL-6 levels in plasma in psychological stress models (Ando et

al. 1998) and IL-6 is necessary for the CRF-stimulated stress response and can regulate its own mRNA levels (Vallières & Rivest 1999).

5.1.5 Hypothesis

IL-6 and CRF-mediated signalling mechanisms have been linked to GI dysfunction in other disorders such as IBS. Therefore, we hypothesised that modulating IL-6 and CRF signalling would improve GI function in *mdx* mice.

5.1.6 Specific Chapter Aims

- To investigate whether loss of dystrophin causes morphological or functional changes in the GI tract of *mdx* mice
- To assess the effectiveness of blocking IL-6Rs and/or activating CRFR2 in alleviating GI dysfunction in the *mdx* mouse

5.2 Methods

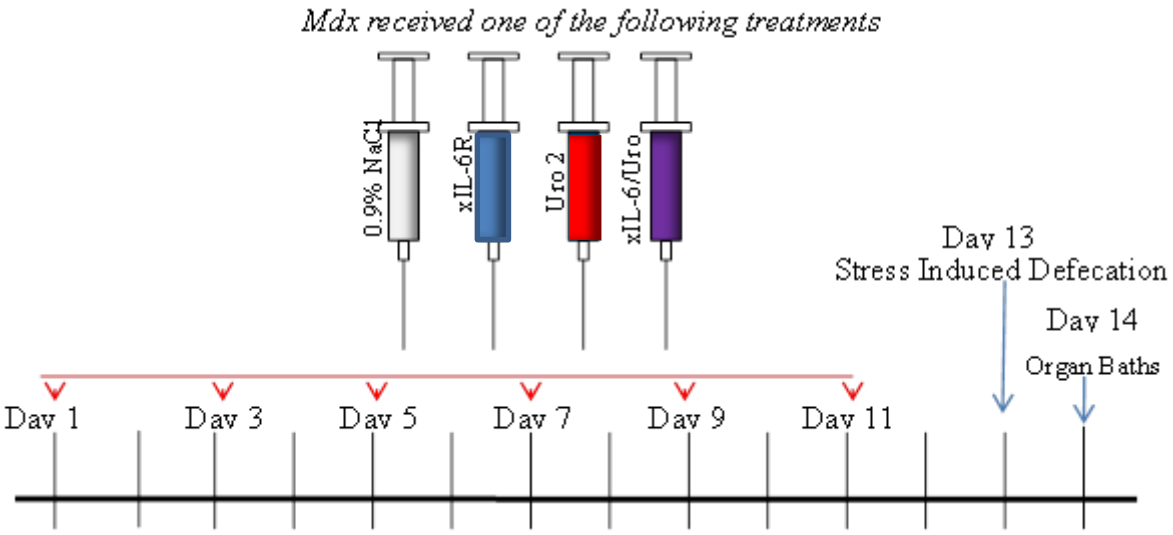
5.2.1 Animals and Experimental Design

Baseline values were compared between two groups of untreated 10 week old WT and *mdx* mice (n=12 mice per group). In the intervention study, *mdx* mice were randomly assigned to one of four experimental groups (see Table 5.1, n=5-8 mice per group). *Mdx* mice were subcutaneously injected with saline (0.9% NaCl), rat anti mouse IL-6 receptor monoclonal antibody (0.2mg/kg body weight, MR16-1 provided from Chugai Pharmaceutical Co., Ltd, Tokyo, Japan), the CRFR2 agonist, Urocortin 2 (30µg/kg body weight) or both. The study of 6 injections lasted 2 weeks and as detailed protocol is displayed in Figure 5.1.; mice were randomly assigned to a group and received the dose in no more than 100µl of vehicle (saline), then underwent a stress induced defecation study on day 13 and were sacrificed for functional studies on day 14.

Table 5.1: Experimental groups and N numbers & a timeline of injection and in vivo experimentation

Intervention Study treatment are colour coded. Saline treated mdx mice are represented in grey, Anti IL-6 receptor antibody in red, Urocortin 2 in blue and a co-treatment of Anti IL-6 receptor antibody and Urocortin 2 in purple throughout the thesis. Six injections of randomly assigned treatment were given from Day 1 to Day 11, Stress Induced Defecation was performed on Day 13 and animals were sacrificed for organ baths on Day 14

Groups	Untreated	Intervention Treatment			
		Saline	Anti IL-6R	Urocortin 2	Anti-IL-6R + Urocortin 2
Mdx	8	8	8	6	8
WT	8				



5.2.2 Techniques

Stress Induced Defecation (as described in chapter 2.3.1)

Collecting Tissue and Blood (as described in chapter 2.4)

Colons were excised, measured for length and stored in carbogen-bubbled ice-cold Krebs saline buffer for organ bath functional testing.

Distal colon was frozen to -80^{o}C for protein analysis.

One centimetre of colon from WT and *mdx* mice were transferred to 4 % PFA fixative for histological processing.

Organ Baths (as described in chapter 2.7.1)

Protein Quantification (chapter 2.5.1)

Distal colon were homogenised in 200µl lysis buffer and stored at -80oC for Western Blot analysis

Western Blot (chapter 2.5.3)

Protein quantification of IL-6 and IL-6Rs were determined using Western blot techniques in whole distal colon tissues from *mdx* mice which had undergone each of the experimental interventions

Histology (chapter 2.4.1)

Sections of distal colon were fixed, frozen, cryostat sectioned in the transverse plane and mounted on glass slides in preparation for H& E staining and subsequent analysis of smooth muscle histology measuring colonic layer thickness.

5.3 Results

Part One: Characterisation of distal colon physiology in *mdx* and WT mice

5.3.1 Mdx faecal wet weight or water content does not differ from WT controls

To investigate potential pathophysiology in *mdx* colons resulting from loss of dystrophin, mice at 12 weeks of age were compared to age matched WT mice. *In vivo* stress-induced defecation was assessed and faecal boli weight and water content examined, rate of defecation was recorded over a ninety minute period. The wet weight of expelled pellets was similar between *mdx* and WT mice (Figure 5.1ii, n=12, $p>0.05$). Moreover, the water content did not differ between *mdx* and WT mice either (Figure 5.1i, $p>0.05$) indicating that the consistency of the faecal matter wasn't different in *mdx* mice.

Nonetheless, in the first 15 minutes of the trial *mdx* mice (n=12) excreted fewer boli than WT mice (Figure 5.2i, n=2, $p<0.05$) and in the second 15 minute increment *mdx* mice excreted fewer boli than WT mice (Figure 5.2i, n=12, $p<0.05$). The 15 minutes from 45 to 90 minutes had similar excretory patterns (Figure 5.2i, $p>0.05$). When examined cumulatively, over 90 minutes, *mdx* mice excreted fewer boli than WT mice (Figure 5.2ii, n=12, $p<0.05$) suggesting that faecal transit, which is regulated by smooth muscle contractile activity, is slower in *mdx* mice.

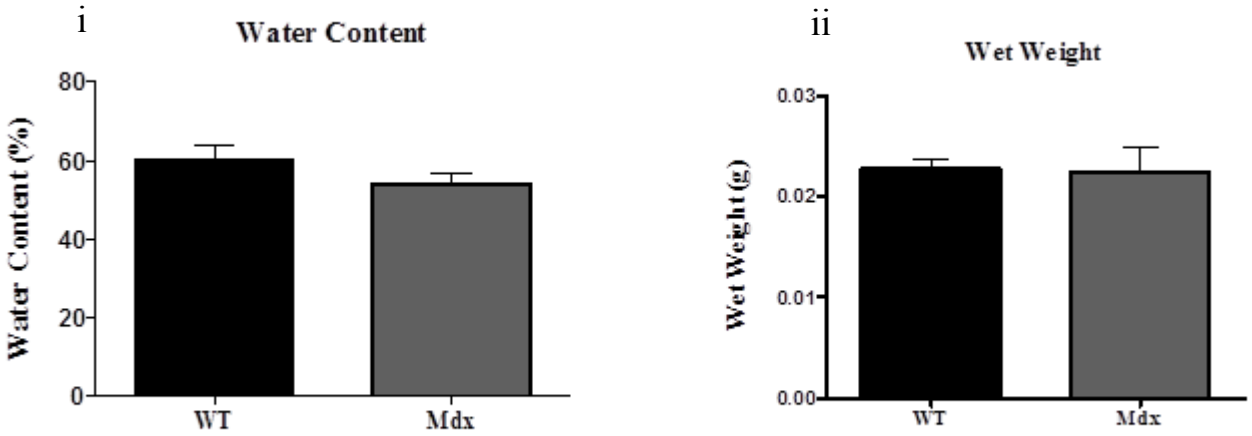
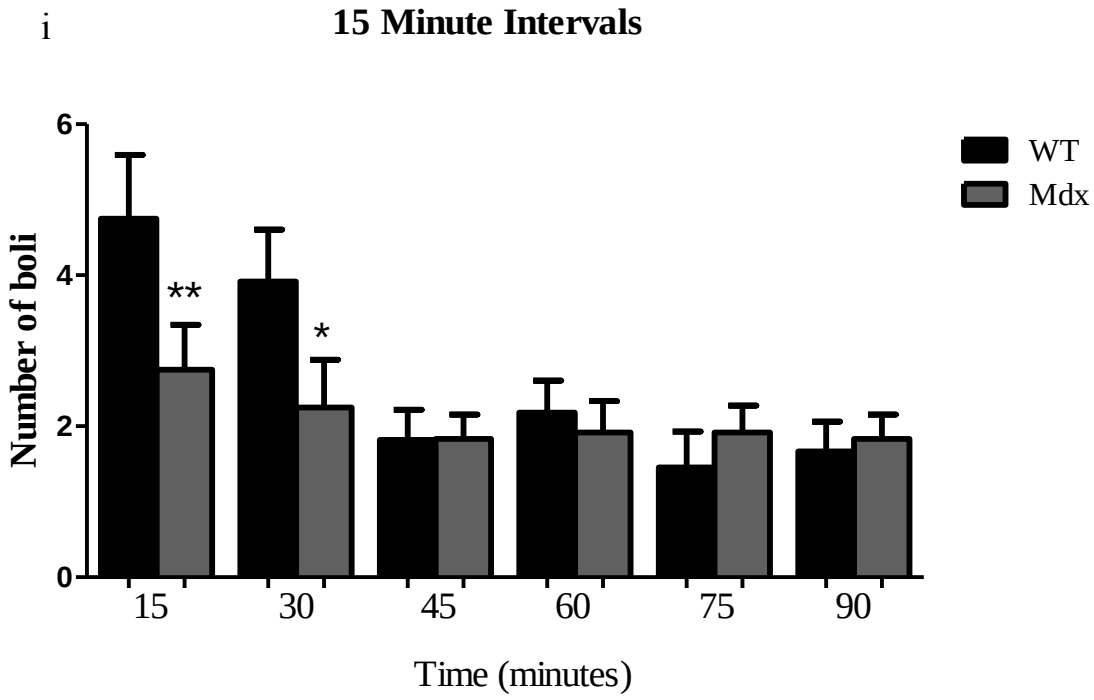
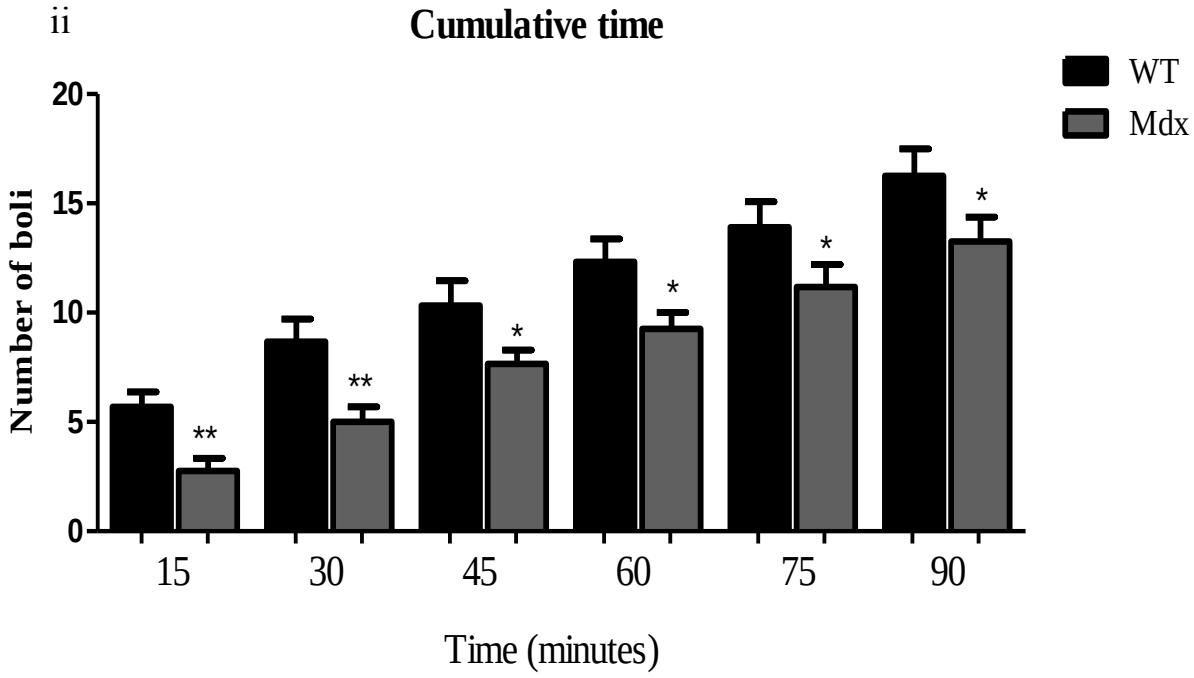


Figure 5.1: Analysis of faecal weight and water content between WT and *mdx* mice
i Water content, as a percentage of total faecal pellet weight, does not differ between the strains nor does the ii wet weight of faecal boli excreted. n=12, p>0.05

i



ii



<u>Figure 5.2:</u> Analysis of faecal boli excreted between *mdx* and WT mice

The number of faecal boli excreted by mdx mice in the first and second 15 minute intervals was lower than the WT *control. No difference in excretory rate was noted in other time intervals (i). The cumulative number of faecal boli excreted was consistently higher in the* WT *mice over the 90 minute trial (ii). n=12, * p<0.05, ** p<0.01*

5.3.2 Alterations in *mdx* colonic morphology

5.3.2.1 Colon length is shorter in *mdx* mice compared to WT mice

I looked at the colon as it is involved in motility in the distal GI tract (Sarna 2010) and symptoms such as motility and stool differences are apparent in DMD patients (Bushby et al. 2010) and patients with inflammatory bowel diseases (Ohama et al. 2007; Atreya & Neurath 2005). I found that total colon length was shorter in *mdx* mice compared to WT mice (Figure 5.3iii, $n=12$, $p<0.05$) and this was due to a shortening of the distal colon in *mdx* mice (Figure 5.3ii, $p<0.05$) as no change was observed in proximal colon length (Figure 5.3i, $p>0.05$).

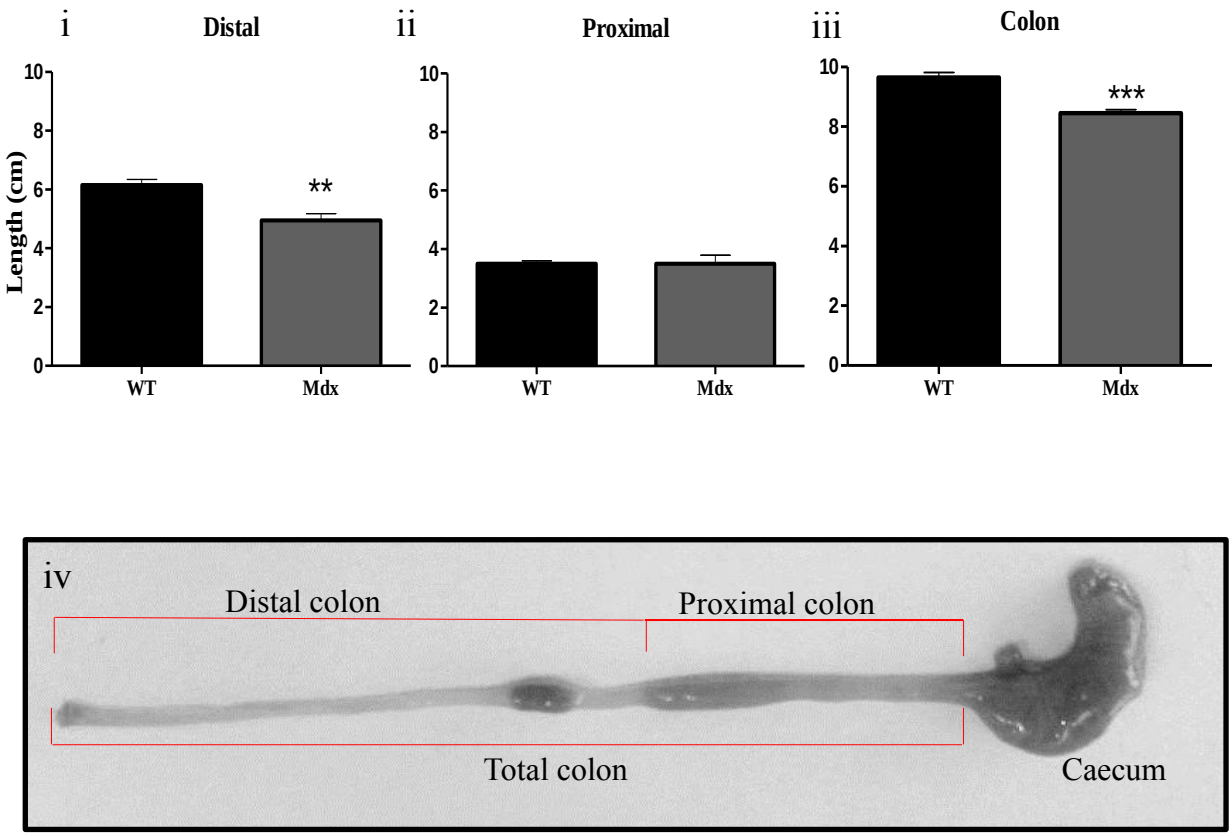
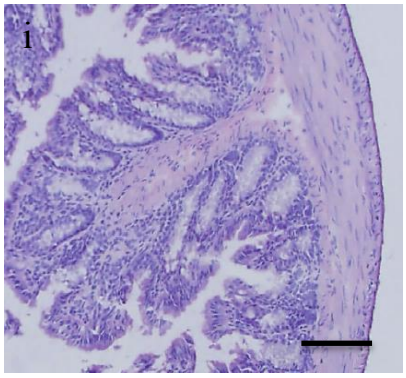


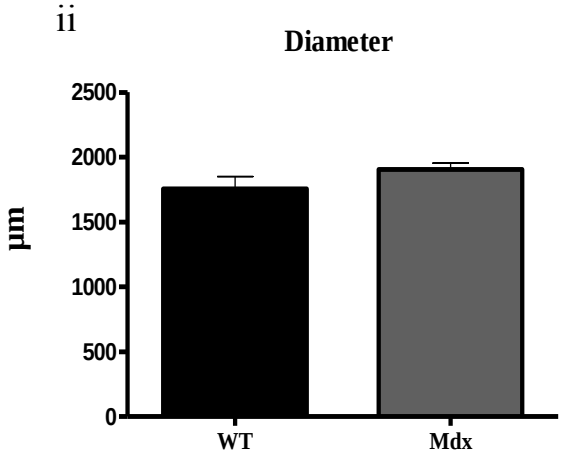
Figure 5.3: Colon Morphology in *mdx* and WT mice

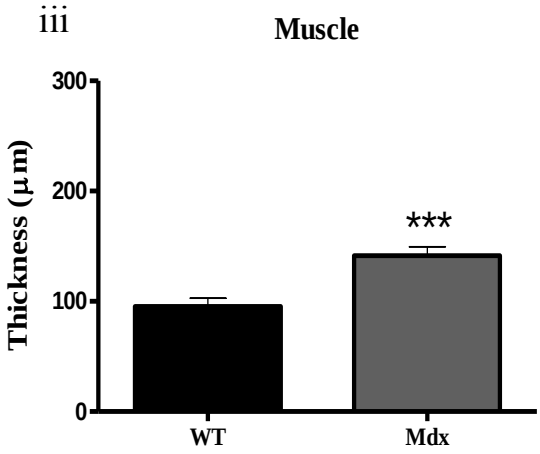
*(i) The length (in centimetres) of the distal colon is shorter in mdx mice than WT controls whereas the length of the (ii) proximal colon (as indicated in the image (iv) was comparable between strains. (iii) The total colonic length was shorter in the mdx mice. (iv) A representative image of an mdx mouse gastrointestinal tract from the caecum to the rectum indicating the regions of the proximal and distal colon assessed. n=7, ** p<0.01, ***p<0.001*

5.3.2.2 *Mdx* muscle wall thickness is thickened when compared to WT colon wall thickness

The thickness of muscle and mucosal layers in H&E-stained cross sections of distal colon indicated that the distal colonic muscle layer in *mdx* mice was thickened compared to WT controls (Figure 5.4iii, n=4, $p<0.001$), which may be indicative of muscle contraction or hypertrophy caused by loss of dystrophin. No strain differences were found in the thickness of mucosal layers in this region (Figure 5.4iv, $p>0.05$) and both strain had comparable colonic diameters (Figure 5.4ii, $p>0.05$).







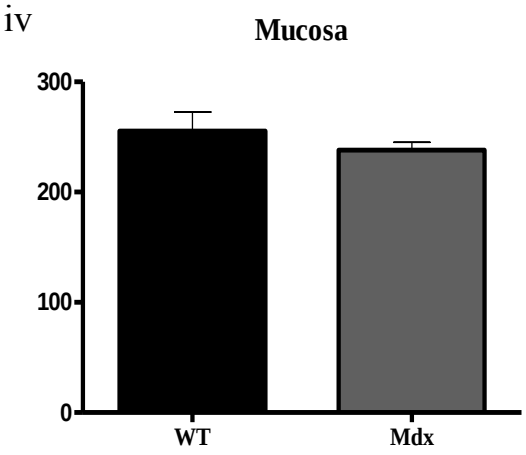


Figure 5.4: Histological analysis of colon layer thickness

i The representative image of H&E stained colon (magnification x10) with scale bar 100µm.(ii) No difference in colonic diameter was apparent but (iii) the muscle layer was thicker in mdx mice. (iv Mucosal thickness was similar in WT *and mdx mice. n=7, *** p<0.001*

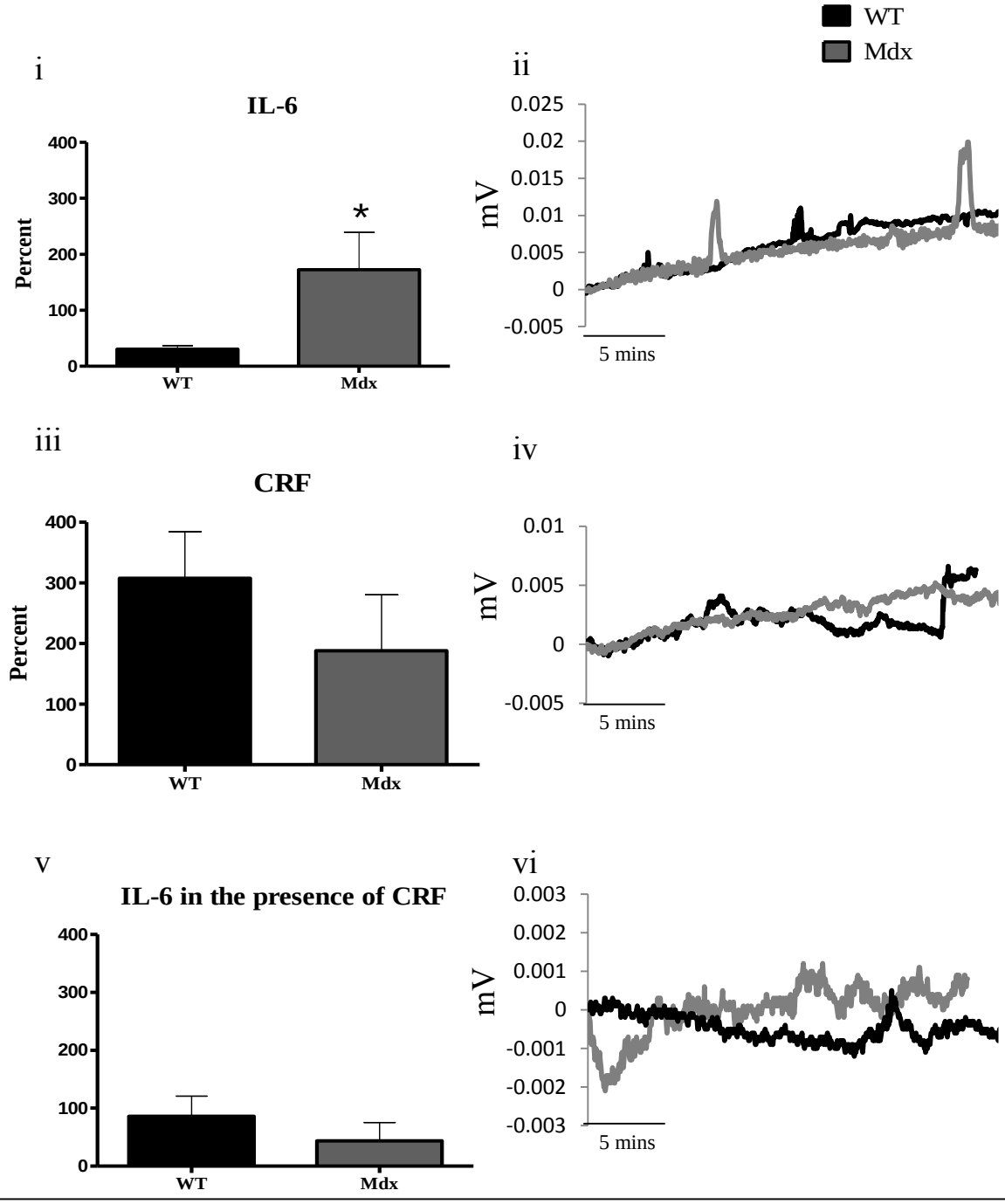
5.3.3 Functional differences in *mdx* colon contractility

Given that *mdx* colons are shorter than their WT counterparts and stress-induced faecal transit times are slower, dystrophin appears to contribute to normal GI smooth muscle function. Further functional studies were carried out in organ baths to determine the contractile activity in the *mdx* mouse. The amplitude of the contraction evoked in whole colonic sections from untreated *mdx* mice and WT mice, (n=5 per group) were assessed by normalising contractions evoked by IL-6 or CRF (200nM, 20 minute duration) to a maximal response evoked, Carbachol (CCh, 100nM), which is a acetylcholine agonist, and causes contractions in smooth muscle tissue. Amplitude of contraction that is the change in mV from baseline to peak of largest contraction

There was no difference in response to CCh in WT or *mdx* mice. *Mdx* mice was greater in exogenous recombinant IL-6 addition evoked colonic contractions in both WT and *mdx* tissues, however the amplitude of contractions in *mdx* was greater (Figure 5.5i, n=5, $p<0.05$) was added to the distal colon preparation.

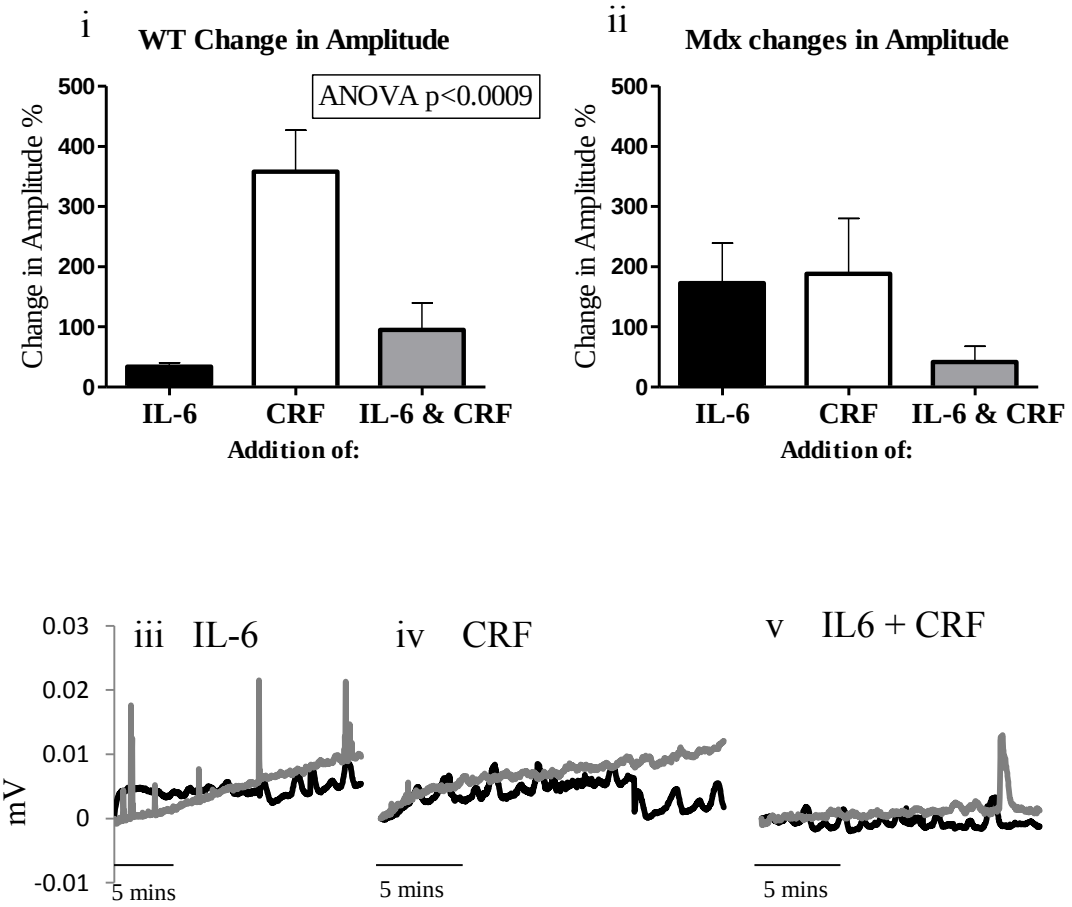
Addition of CRF evoked large contractile responses in both WT and *mdx* colons but there were no significant difference between the strains (Figure 5.5iii and iv). When both IL-6 & CRF were added together and regardless of whether this addition was carried out at the start or the end of the experiment, reduced contractile activity was noted in both strains (Figure 5.5iii).

In WT mice, the presence of IL-6 appeared to suppress the contractile activity evoked by CRF (Figure 5.6i, $p<0.0009$,) whereas in *mdx* mice, the tissue appears equally sensitive to IL-6 and CRF with a reduced response when both are present does not (Figure 5.6ii, $p>0.05$). Two way ANOVA (Not shown) (strain x reagent) reveals no strain difference, but the effect of IL-6 and CRF were different ($p<0.0031$) and there was an interaction between the two factors ($p<0.0409$).



<u>Figure 5.5</u>: Amplitude change induced by addition of IL-*6 or CRF* to *in vitro* colon preparations in untreated *mdx* and WT mice in an organ bath

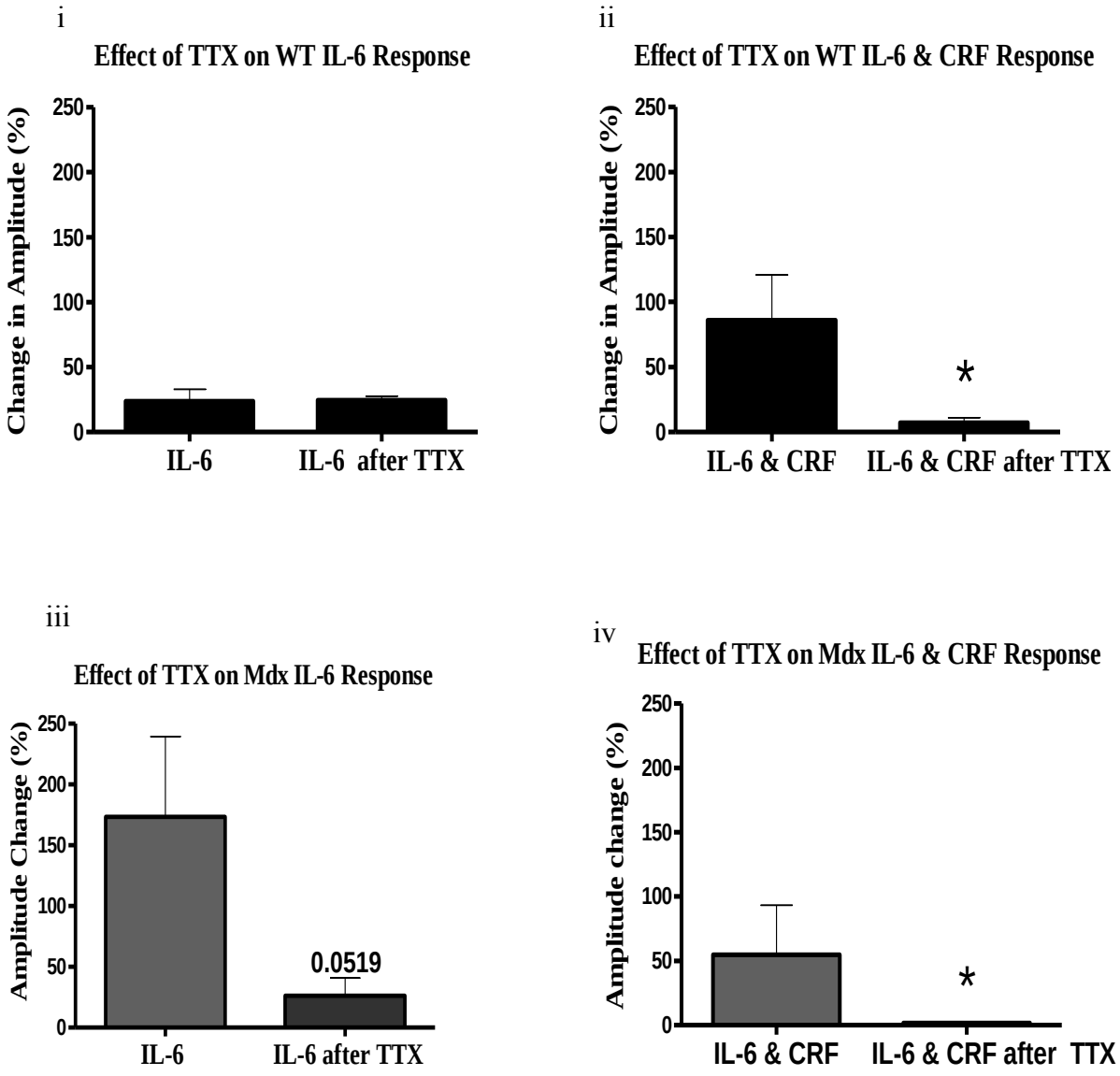
WT *and mdx colon preparations produced amplitude change in mV with the addition of recombinant IL-6, CRF or IL-6 in the presence of CRF. This reaction was normalised to the maximum amplitude change induced by Carbacol. ii, iv & vi A representative raw data trace comparing* WT *and mdx mice treated with IL-6 (ii), CRF (iv) or IL-6+CRF (vi) over a twenty minute period. Black traces represent* WT *mice colons, grey traces represent the mdx mice colons. IL-6 produced a significant increase in amplitude change (i) in mdx mice (ii) compared to* WT *mice. CRF had comparable reactions in* WT *and mdx mice (iii & iv,) and IL-6 in the presence of CRF had a similar and reduced reaction in* WT *versus mdx mice (v & vi). n=5, *p<0.05*



<u>Figure 5.6:</u> Amplitude change induced by addition of IL-6 and CRF or both, to in vitro colon preparations in untreated *mdx* and WT mice in an organ bath
One way ANOVA shows a difference between compounds to the compounds added (i). mdx colon had similar reactions to each compound added (ii) A representative raw data trace comparing WT *and mdx mice treated with IL-6 (iii), CRF (iv) or IL-6+CRF (v) over a twenty minute period. Black traces represent* WT *mice colons. Grey traces represent the mdx mice colons.*

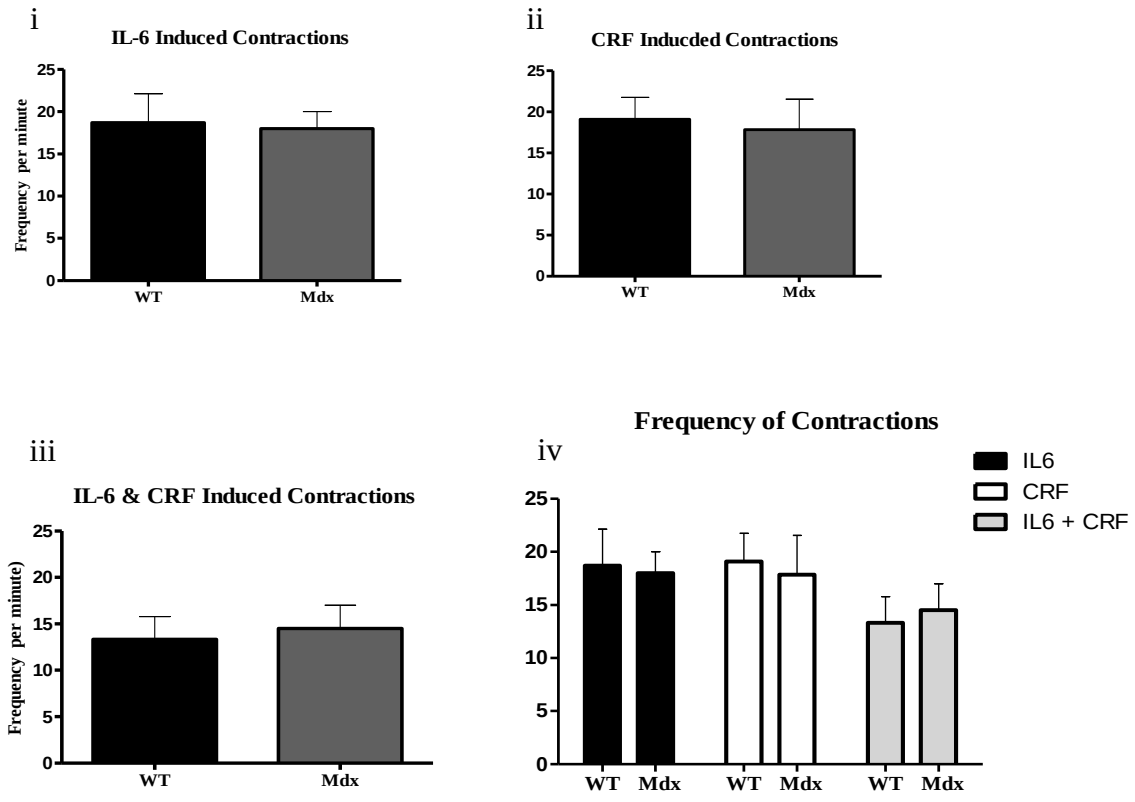
To assess the component of the contraction which was neurally-mediated, the tissue was pre-incubated with the Na^+ channel blocker, tetrodotoxin (TTX, 100nM, duration of incubation). In WT mice the presence of TTX did not alter the IL-6-evoked contraction (Figure 5.7i, n=5, $p>0.05$) but reduced the amplitude of the IL-6 & CRF-evoked contraction (Figure 5.5ii, n=5, $p<0.05$). Interestingly, in *mdx* mice, both IL-6- (Figure 5.7iii, $p\leq0.05$) and IL-6 + CRF-evoked (Figure 5.7iv, n=5, $p<0.05$) contractions were sensitive to TTX indicating the importance of myenteric neuronal activity to these effects in this dystrophin-deficient strain.

The frequency (number of contractions per minute over the 20 minute period) evoked by each factor was analysed. Addition of IL-6 caused comparable contraction frequency between WT and *mdx* mice (Figure 5.8i, n=3-6, $p>0.05$), as did CRF details (figure 5.8ii n=5, $p>0.05$) and IL-6 & CRF (Figure 5.8iii n=5, $p>0.05$). When a two way ANOVA was performed (strain x reagent), no strain difference, effect of reagent or interaction between the factors was observed figure (Figure 5.8iv, n=5, $p>0.05$).



<u>Figure 5.7:</u> Effect of amplitude change on reaction to TTX blocked colonic contractibility in excised colon preparations in an organ bath

*There was no reduction in amplitude change in WT tissues in response to IL-6 (i) and a reduction in the amplitude of contraction in response to IL-6 and CRF (ii). in mdx tissues TTX causes inhibition of the responses to both IL-6 (iii) and IL-6 + CRF (iv). (n=3-6 colons per group) * $p<0.05$*



<u>Figure 5.8:</u> Frequency of Contractions evoked by IL-6 and CRF or both excised colon preparations in an organ bath

The number of contractions did not differ between WT and mdx mice in addition of IL-6 (i), CRF (ii) or IL-6 + CRF (iii) after comparing them using a student's t test. When a two way ANOVA (iv) was performed, addition of neither compound, nor stain was significant, and no interaction was found. (n=3-6) p> 0.05

5.3.4 Summary of results Part 1

Consistent with deficiencies in smooth muscle caused by loss of dystrophin, our studies found that *mdx* mice exhibited a number of changes in GI function as compared to WT controls. *mdx* mice excrete fewer boli compared to WT mice in the first 30 of a stress induced defecation protocol This indicates that *mdx* mice have functional changes in their lower GI tract resulting in slowed transit times and this significant effect is reflected in the cumulative result, where overall *mdx* mice excrete fewer faecal boli than similarly stressed WT mice. This is comparable to slowed GI transit in human DMD sufferers (Barohn et al. 1988).

Consistent with this, gross morphological examination of the colon showed a shorter overall length and this stemmed from the distal colon. Histological examination of the colon showed a thickened wall, and this is conjunction with the shortening of the colon may indicate contraction of the gut in *mdx* mice. Alternatively, the thickened muscle layer may represent muscle cell hyperplasia. In contrast, there was no evidence of alterations in the thickness of the mucosal layer and analysis of the faecal water content suggests no abnormality in stool consistency which would indicate changes in absorpto-secretory function.

Thus, loss of dystrophin appears to be specific to problems associated with smooth muscle function although unlike the characteristic inflammation in *mdx* skeletal muscle, histopathological analysis did not reveal obvious inflammatory infiltrate or fibrosis in colonic smooth muscle.

To assess the functional consequences of these pathophysiological changes in *mdx* colonic smooth muscle, organ bath experiments assessed contractile activity in WT and *mdx* colons. When challenged with IL-6 than WT tissues and TTX blocks this effect demonstrating the neuronal component to this response. It appears that IL-6 evokes contractions in WT colonic muscle through direct activation of smooth muscle, whereas loss of dystrophin and the associated smooth muscle dysfunction in *mdx* mice leads to contractile activity that is much more dependent on neural activity, probably mediated by the myenteric plexus. Thus, IL-6 likely binds to receptors on myenteric neurons subsequently activates contraction of GI smooth muscle cells in *mdx* colons. CRF stimulated large contractions in both WT and *mdx* strains and interestingly, this response was dampened when both IL-6 & CRF were

present, indicating potential crosstalk between these two factors which may be important in regulating GI activity. Moreover, this activity was sensitive to TTX indicating the importance of neural regulation of GI contractility and this may give a clue as to the neuronal site of interaction between IL-6 and CRF.

Part Two: Effect of blocking IL-6R signalling in the absence or presence of a CRFR2 agonist on *mdx* mouse colonic pathophysiology

The second part of this study compares the pharmacological intervention of anti IL-6 receptor antibody and Urocortin 2 or a combination of both on the histological and physiological readouts carried out on the control WT and *mdx* mice.

5.4.1 Faecal output in *mdx* mice was not changed by intervention treatments

The wet weight of expelled pellets was compared between four groups of *mdx* mice, those treated with a saline vehicle, a group which received anti IL-6R antibodies, a group treated with Urocortin 2 and a group which received both anti IL-6R and Urocortin 2. None of the treatments evoked any changes (Figure 5.9i, $p>0.05$,) in student's t test compared to saline, or in a one way ANOVA comparing all treatments. Similarly no differences in water content were found between any treatment group and saline (Figure 5.9ii, $p>0.05$).

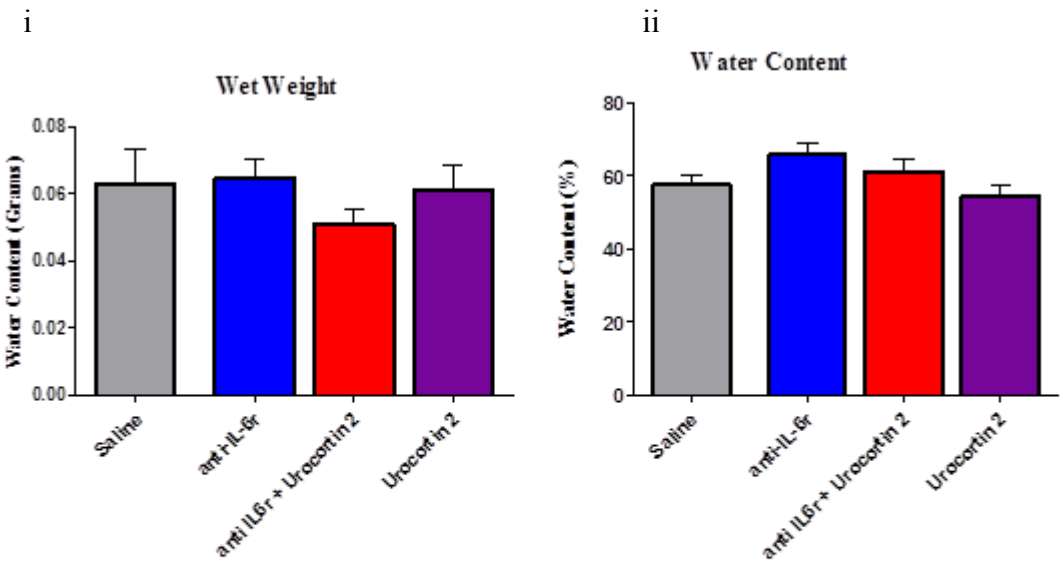


Figure 5.9: Faecal water content with or without intervention

Wet weight (i) and water content (ii) does not differ between saline and each treatment group. n=5-8, p>0.05

5.4.2 The effects of interventions on colonic motility in *mdx* mice

To assess the efficacy of the interventions, each intervention was compared to saline-treated *mdx* controls in the same stress induced defecation protocol as before. Pellets excreted by *mdx* mice were counted in 15 minute intervals and cumulatively over the 90 minute open field trial and compared between saline and anti IL-6R (Figure 5.10i & ii, n=8), Urocortin 2 (Figure5.11i & ii), n=5-8), and anti IL-6R/Urocortin 2 treatments (Figure 5.12i & ii, n=8).

5.4.2.1 Saline vs. anti IL-6R Treatment

Treatment with anti IL-6R increased faecal output in the first 15 minutes and the third fifteen minute intervals of the 90 minute trial (Figure 5.10i, $p<0.05$), and caused a significant increase every 15 minutes of the cumulative trial (Figure 5.10ii, $p<0.05$).

5.4.2.2 Saline vs. Urocortin 2 Treatment

Treatment with Urocortin 2 shows no significant difference between saline treated animals except in the 45-60 minute interval (Figure 5.11i, $p<0.05$), and no significant changes cumulatively (Figure 5.11ii, $p>0.05$).

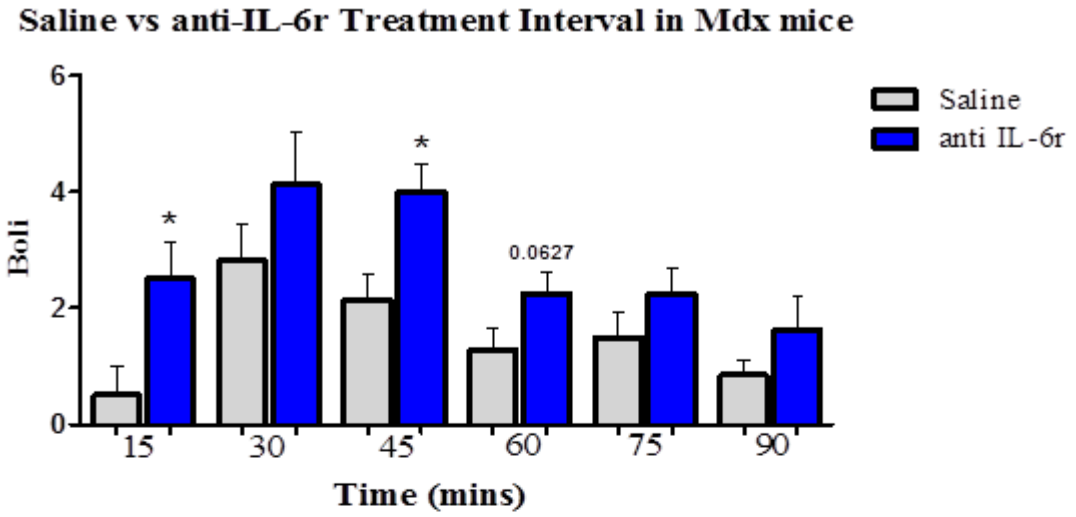
5.4.2.3 Saline vs. anti IL-6R/Urocortin 2 Treatment

Treatment with anti IL-6R/Urocortin 2 increased faecal output in the third fifteen minute intervals of the 90 minute trial (Figure 5.12i, $p<0.05$), but not significantly in the cumulative trial (Figure 5.12ii, $p>0.05$).

5.4.2.4 Comparing treatments

No significant interaction is seen between treatments and time, but in the interval 2 way ANOVA (Figure 5.13i, n=5-8) there is a time difference and in the cumulative two way ANOVA (Figure 5.13ii, n=5-8) both time and treatment differed significantly.

i



ii

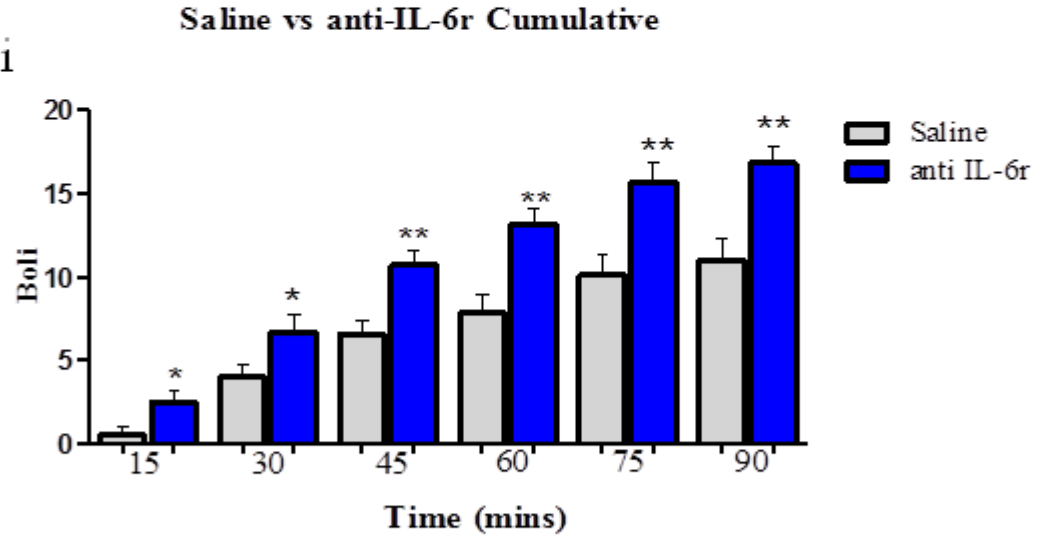
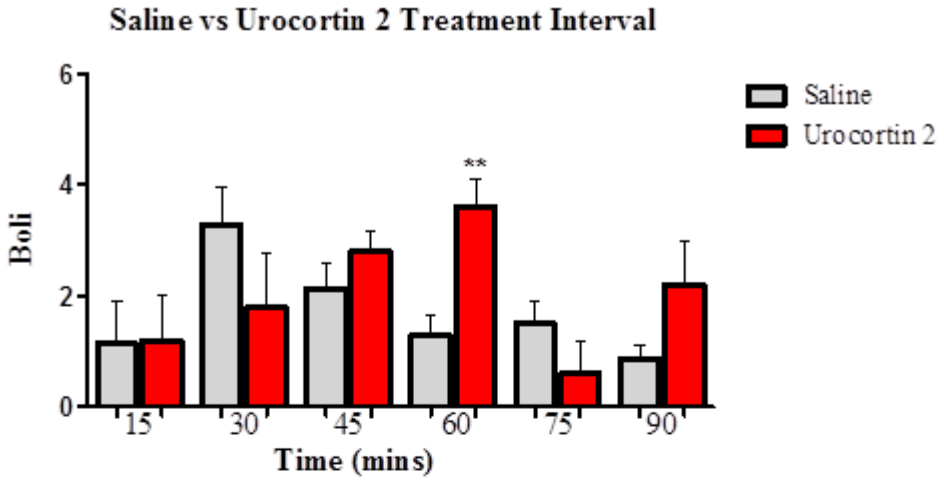


Figure 5.10: Analysis of faecal boli excreted

*Saline treated versus anti-IL-6R treated mice (n=8) in 15 minute intervals (i) or cumulatively over 90 minutes trial (ii). n=8, * $p<0.05$, ** $p<0.005$*

i



ii

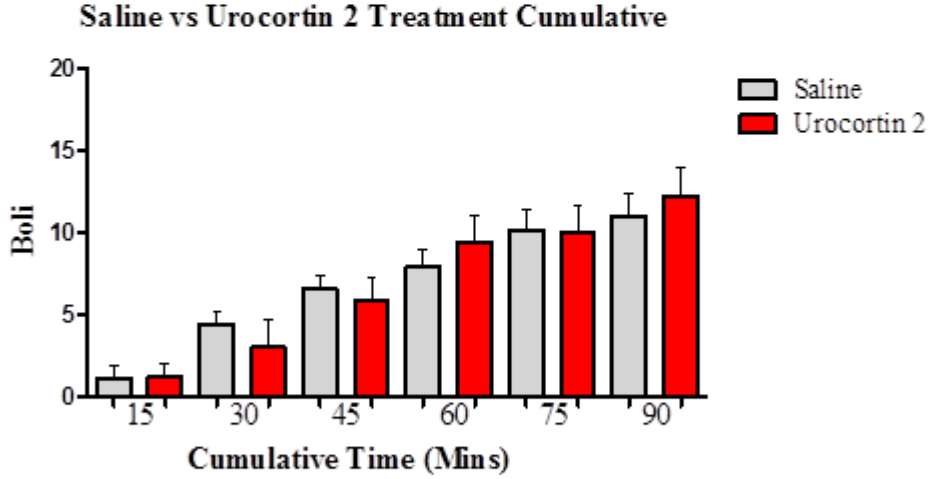
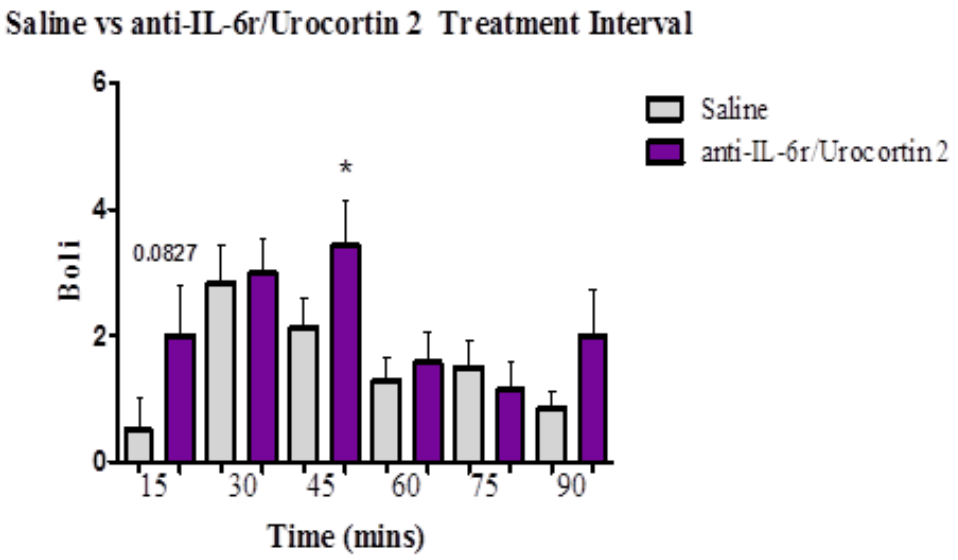


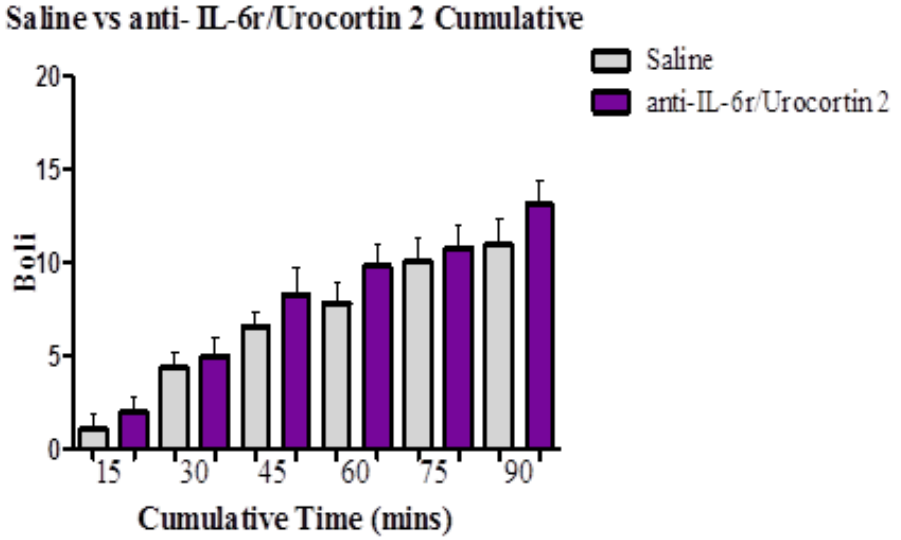
Figure 5.11: Analysis of faecal treatment times after treatment with Urocortin 2

*Saline treated versus Urocortin 2 treated mice in 15 minute intervals (i) or cumulatively over 90 minutes trial (ii). n=6-8, ** $p<0.005$*

i

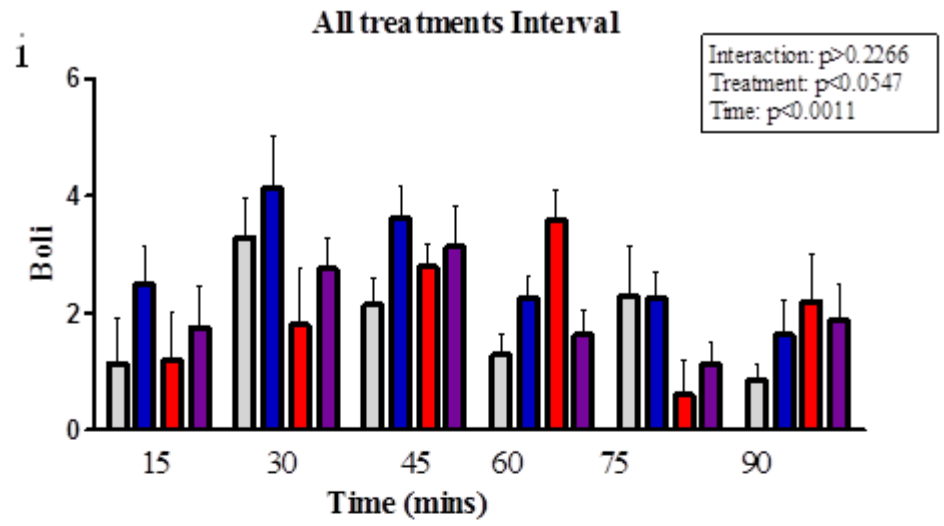


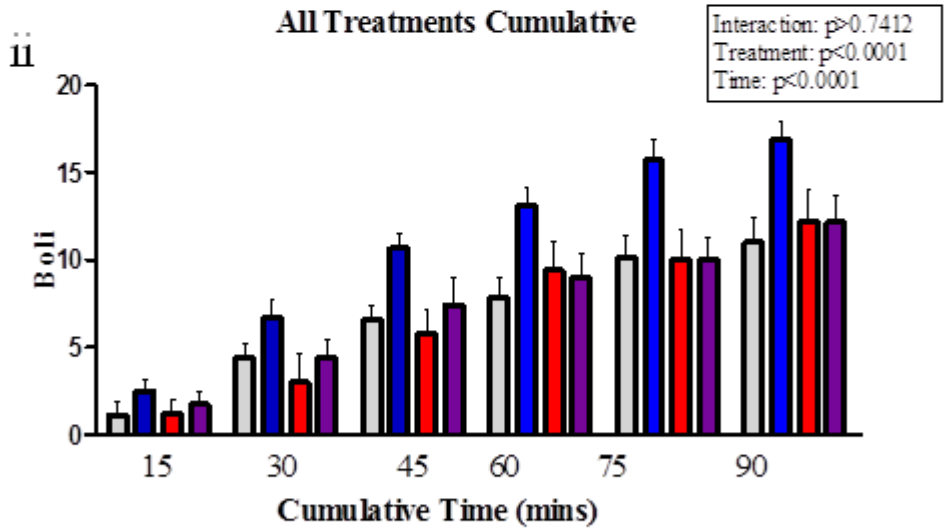
ii



<u>Figure 5.12:</u> Analysis of faecal transit times after treatment with anti IL-6R and Urocortin 2

Saline treated versus anti IL-6R/Urocortin 2 treated mice in 15 minute intervals (i) or cumulatively over 90 minutes trial (ii). (n=8) p<0.05*





<u>Figure 5.13</u>: Faecal output comparing all treatments

Comparing treatments in interval (i) and cumulative (ii) faecal output, no interaction is seen but a time effect is seen in 15 minute intervals (i) and both treatment and time are significantly different in the cumulative score of the protocol (ii). (n=5-8) p>0.05

5.4.3 *Mdx* colonic length following interventions

5.4.3.1 Saline vs. anti IL-6R

Total colonic length was decreased in *mdx* mice as compared to WT colons however, following treatment with anti IL-6R antibodies colons were longer than saline-treated comparators (Figure 5.14i, n=8, $p<0.05$) and this was due to changes in the distal colon (Figure 5.14iii, n=8, $p<0.05$).

5.4.3.2 Saline vs. Urocortin 2

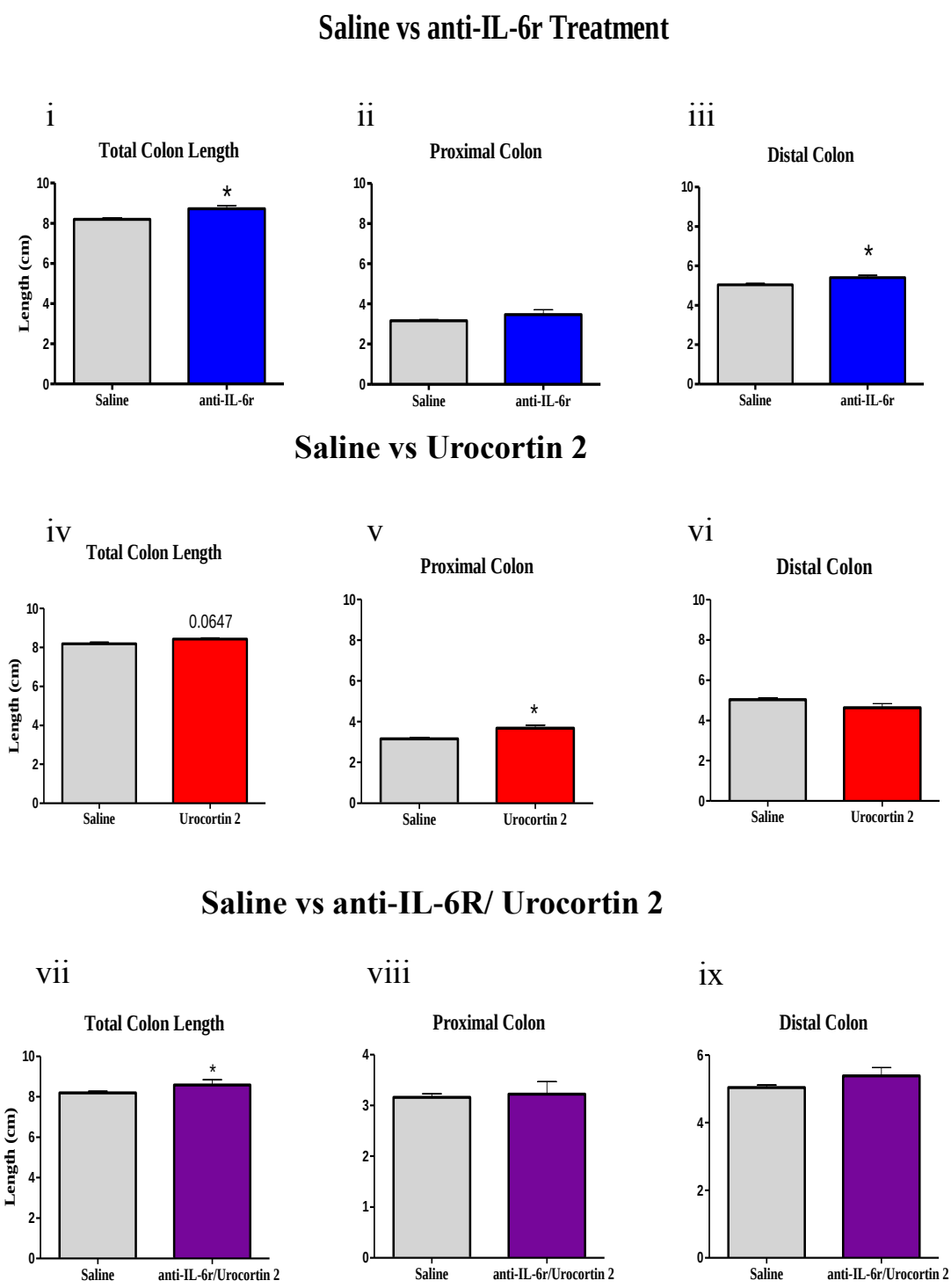
Treatment with Urocortin 2 (n=5-8) also resulted in slightly longer colons (Figure 5.14iv, n=5-8, $p=0.0647$) which was significant in the proximal colon (Figure 5.14v, n=5-8, $p<0.05$) but not the distal colon (Figure 5.14vi, $p>0.05$).

5.4.3.3 Saline vs. anti IL-6R/Urocortin 2

Combined treatment with anti IL-6R/Urocortin 2 resulted in significantly longer total colon length in *mdx* mice (Figure 5.14vii, n=5-8, $p<0.05$) but no significant change in either the proximal or distal regions, indicating both proximal and distal length was moderately increased (Figure 5.14viii & ix, n=5).

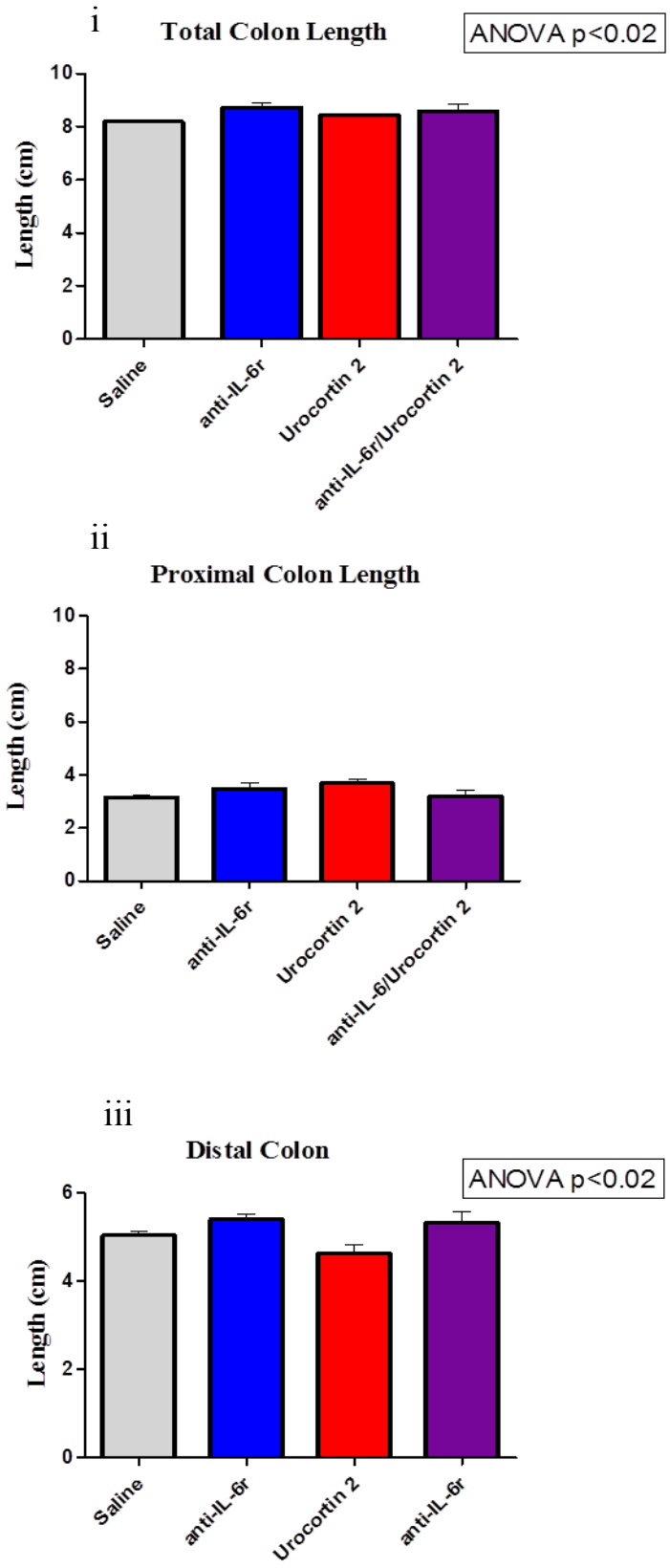
5.4.3.4 Treatment effect

One way AVONA revealed that treatment had an overall effect in total colon length (Figure 5.15i, n=5-8, $p<0.05$), proximal colon lengths did not differ significantly (Figure 5.15ii) and there was a significant increase in distal colon length (Figure 5.15iii, n=5-8, $p<0.05$).



<u>Figure 5.14:</u> Colon length measured with or without drug intervention

*Treatment with anti-IL-6R increased total colon length (i) and distal colon length (iii), treatment with Urocortin 2 increases total colon length (iv) and proximal colon length (v).Treatment combining anti-IL-6R and Urocortin 2 increased colon length (vii) but neither proximal or distal. (n=5-8) * p>0.05,*



<u>Figure 5.15:</u> Colon length measured with or without interventions

*There is a significant difference in treatment in the total colon length amongst the groups (i) and distal colon length (iii), but no difference between proximal colon lengths (ii) In a one way ANOVA. n=5-8,*p<0.05*

5.4.4 Interventions change the amplitude of contraction in *mdx* mice

5.4.4.1 *Mdx* mice treated with anti IL-6R

In *mdx* mice administered anti IL-6R antibodies the amplitude of the IL-6-evoked contraction was reduced when compared to saline treated *mdx* mice (Figure 5.16i and trace i, n=8, $p<0.05$). Not surprisingly, blocking IL-6 signalling did not change CRF-evoked contractions (Figure 5.16ii and *trace ii*, n=8, $p>0.05$) nor did it have any effect on contractions evoked by IL-6 & CRF (Fig 5.16iii and *trace iii*, n=8, $p>0.05$). One way ANOVA analysis of anti IL-6R (Figure 5.17i) showed no difference,

5.4.4.2 *Mdx* mice treated with Urocortin 2

IL-6 evoked smaller contractions in *mdx* mice treated with the CRFR2 agonist, Urocortin 2 as compared to *mdx* mice who received saline (Figure 5.16 iv and *trace iv*, n=5, $p<0.05$). There was no difference in the amplitude of the contraction evoked by CRF between Urocortin 2 and saline-treated *mdx* groups, but a significant reduction in the amplitude of the IL-6 & CRF-evoked contraction was noted in Urocortin 2-treated *mdx* mice (Figure 5.16 vi and *trace vi*, n=5, $p>0.05$). One way ANOVA analysis of Urocortin 2 treated mice shows a difference in amplitude change to the addition of IL-6 and CRF (Figures 5.17ii, $p=0.09$).

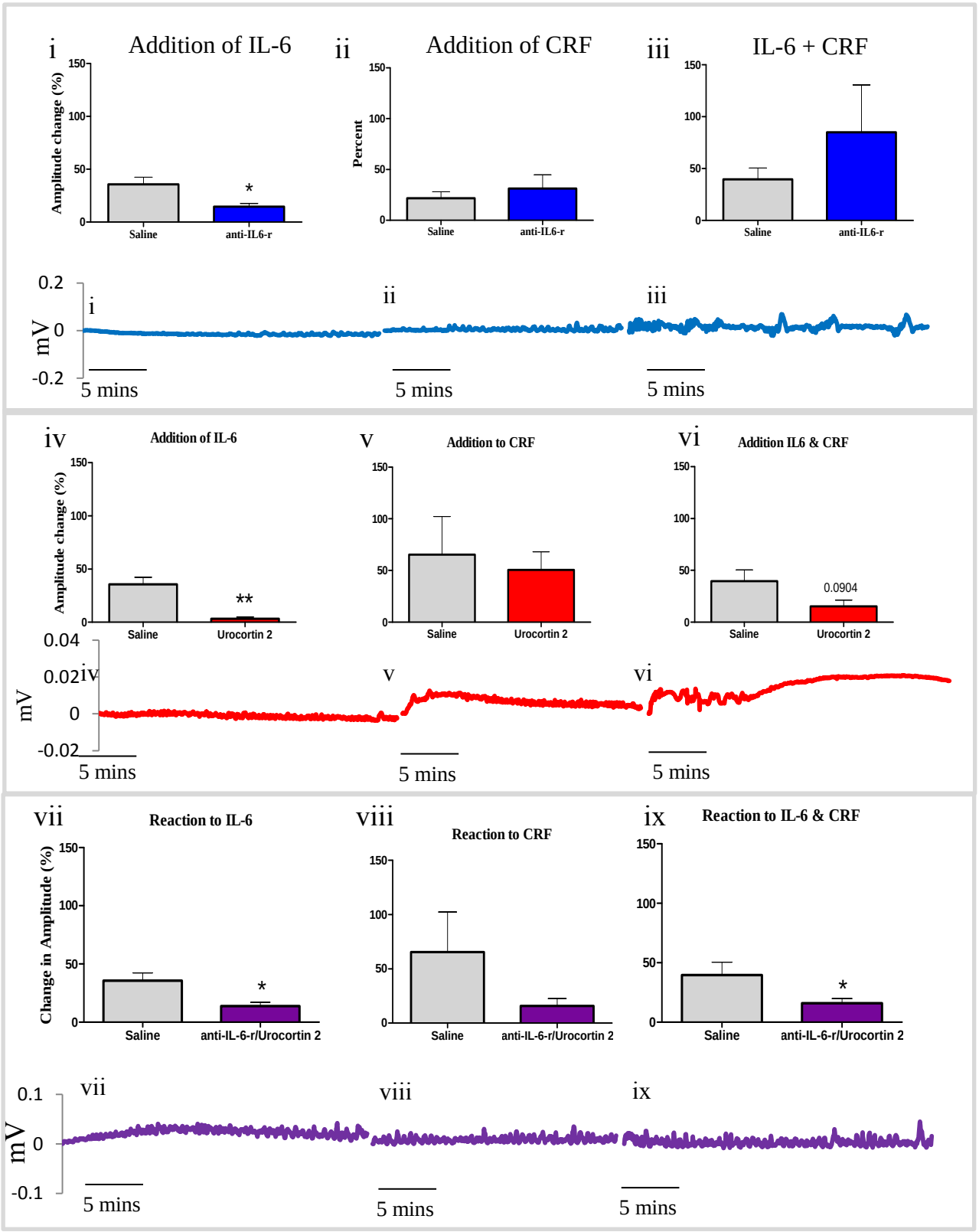
5.4.4.3 *Mdx* mice treated with anti IL-6R and Urocortin 2

Mdx mice treated with combined Urocortin 2 and anti IL-6R had a significant reduction in the contractile response evoked by IL-6 compared to saline-treated mice (Figure 5.16vi and *trace vi*, n=8, $p<0.05$), there was no difference in responses evoked by CRF between groups, but a significant reduction in the amplitude of the contraction evoked by IL-6 & CRF was noted in *mdx* mice treated with anti IL-6R and Urocortin 2 (Figure 5.16ix and *trace ix*, n=8, $p<0.05$). Treatment with anti IL-

6R/Urocortin2 shows no differences between compounds when analysed using one-way ANOVA (Figure 5.17iii, n=8, $p>0.05$).

5.4.4.4 Comparing treatments

Two way ANOVA analysis (not shown, n=5-8) reveals no treatment effects, but there was a difference between the interventions and a significant interaction effect.



<u>Figure 5.16:</u> Treated *mdx* mice compared to saline in the addition of compounds; IL-6, CRF or IL-6+CRF

*Saline vs anti-IL-6-r shows a reduction in amplitude change to the addition of IL-6 (i), and no changes with the addition of CRF (ii) or IL-6 & CRF (iii). Saline vs Urocortin 2 shows a reduction in amplitude change to the addition of IL-6 (iv), and no changes with the addition of CRF (v) or IL-6 & CRF (vi). Saline vs anti-IL-6R Urocortin 2 shows a reduction in amplitude change to the addition of IL-6 (vii), and no changes with the addition of CRF (viii) or IL-6 & CRF (ix). Labelled traces labelled corresponding to histogram it represents, 20 minute raw data (mV) (n-5-8) * $p<0.05$, ** $p<0.005$*

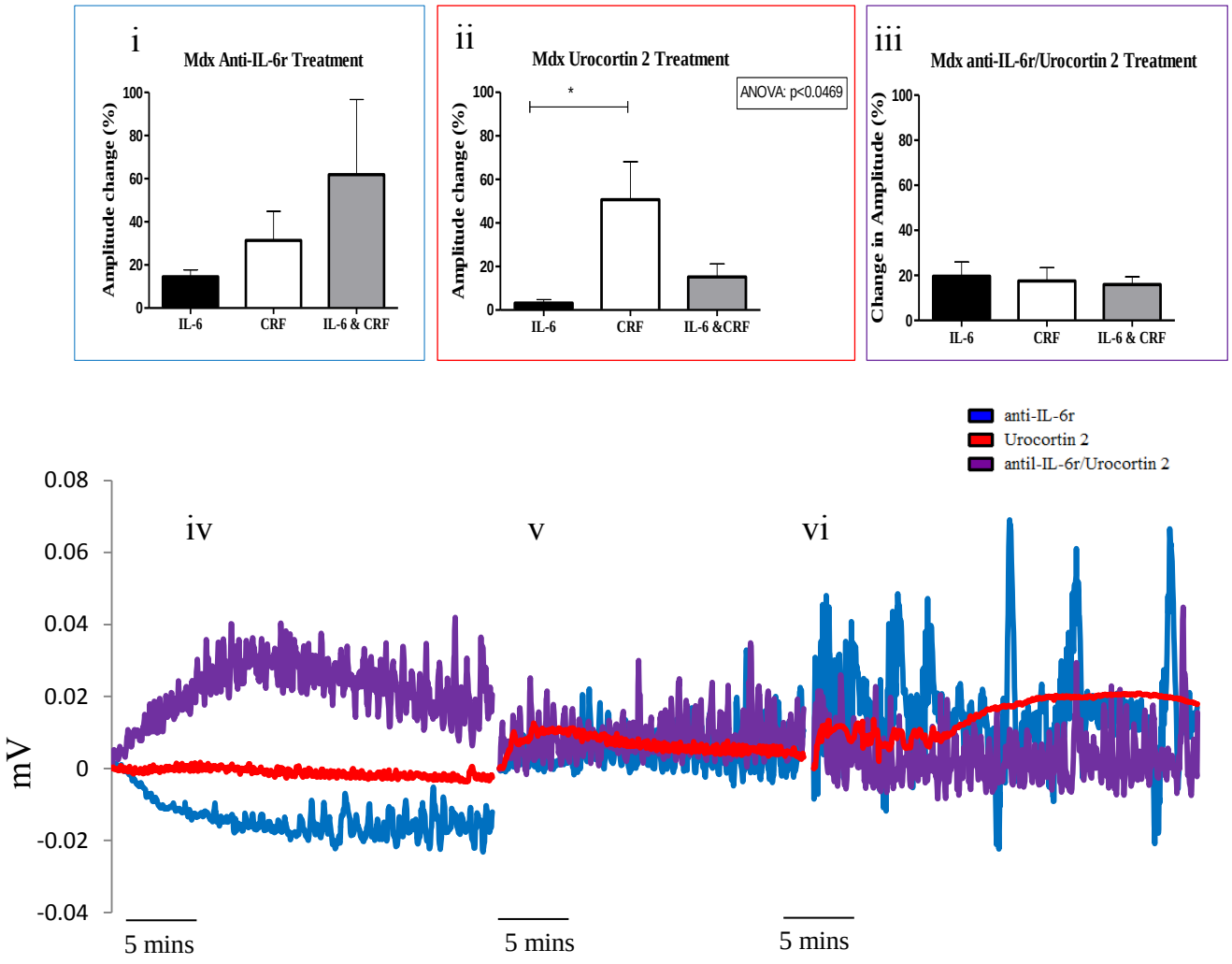


Figure 5.17: Contractile properties of *mdx* treated mice with the addition of IL-6, CRF or both in an organ bath

*One way ANOVA analysis of treated mdx anti-IL-6R treated mice in the addition of compounds; IL-6, CRF or IL-6& CRF. Saline vs anti-IL-6-R (i) shows no significant differences between treatments. Urocortin 2 treated mice shows a difference in amplitude change to the addition of IL-6 and CRF (ii) Treatment with anti-IL-6R/Urocortin 2 shows no differences between compounds (iii), (n=5-8) * p<0.05*
Representative traces (twenty minute trace, mV) show the differences between anti IL-6 treated mdx mice (red line), Urocortin 2 treated mice (blue line) and co- treatment of anti IL-6 and Urocortin 2 (purple line). Addition of IL-6 to these treatments is shown in (iv), addition of CRF is shown in (v) and addition of IL-6 in the presence of CRF in (vi).

5.4.5 Intervention studies change the frequency of contractions in *mdx* mice when compared to saline *mdx* mice

5.4.5.1 Addition of IL-6

Comparing contraction rates between treatments reveals treatment differences in a one way ANOVA. Addition of IL-6 (Figure 5.18i, n=8) shows significant differences between treatments namely between anti IL-6R vs Urocortin 2 ($p<0.05$) treated animals, anti-IL6r vs anti IL-6R/Urocortin animals ($p<0.001$) and saline vs Urocortin 2 treated animals ($p<0.001$), saline vs anti IL-6R/Urocortin 2 ($p<0.001$).

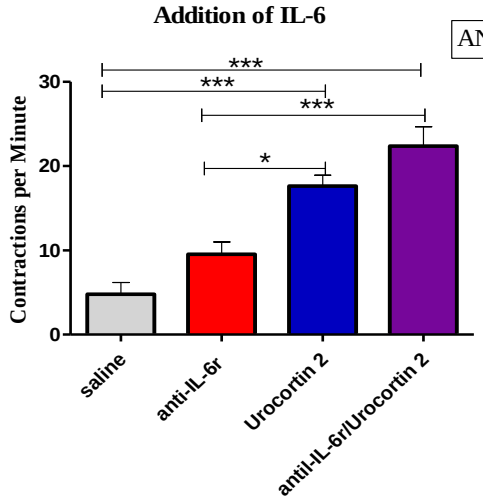
5.4.5.2 Addition of CRF

Addition of CRF (Figure 5.18ii) shows a significant increase in contraction rate in saline vs anti-IL-6 treated mice ($p<0.05$), saline vs Urocortin 2 treated mice ($p<0.05$), saline vs anti IL-6R/Urocortin 2 treated mice ($p<0.001$), anti-IL-6 vs anti IL-6R/Urocortin 2 ($p<0.01$) and Urocortin 2 vs anti IL-6R/Urocortin treated mice ($p<0.05$).

5.4.5.3 Addition of IL-6 + CRF

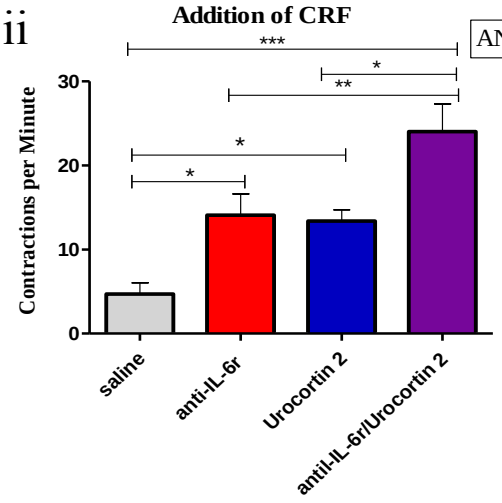
In mice treated with Urocortin 2, addition of IL6 & CRF (Figure 5.18iii) increased the colonic contraction rate as compared to saline-treated control mice vs. Urocortin 2 treated mice ($p<0.05$), saline vs anti IL-6R/Urocortin 2 treated mice ($p<0.001$) and anti IL-6R vs anti IL-6R/Urocortin 2 treated mice ($p<0.01$).

i



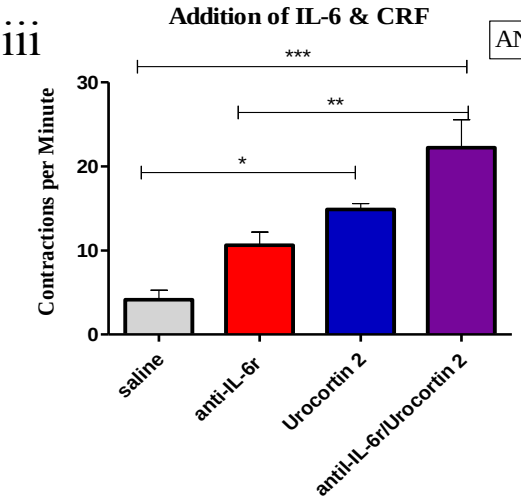
Addition of IL-6 (i) shows significant differences in the frequency of contractions between treatments namely between anti-IL-6R vs Urocortin 2 treated animals, anti-IL6r vs anti-IL-6R/Urocortin animals and saline vs Urocortin 2 treated animals, saline vs anti-IL-6R/Urocortin 2.

ii



Addition of CRF (ii) shows a significant change in contraction frequency in saline vs anti-IL-6 treated mice, saline vs Urocortin 2 treated mice, anti-IL-6R, saline vs anti-IL-6R/Urocortin 2 treated mice and Urocortin 2 vs anti-IL-6R/Urocortin treated mice.

iii



Addition of IL-6 & CRF showed a significant increase in the frequency of contractions comparing saline vs Urocortin 2 treated mice, saline vs anti-IL-6R/Urocortin 2 treated mice and anti-IL-6R vs anti-IL-6R/Urocortin 2 treated mice (iii).

<u>Figure 5.18:</u> Frequency of Contraction per minute of *mdx* mouse colon preparations in an organ bath

*Addition of compounds compared between treatments as contraction per minute with the addition of compounds. (n=5-8) * p<0.05 **p<0.001 ***p<0.001*

5.4.6 Intervention studies change levels of IL-6 and IL-6 receptor in the colon of treated mice compared to saline controls

5.4.6.1 *Mdx* mice treated with anti IL-6 receptor antibody

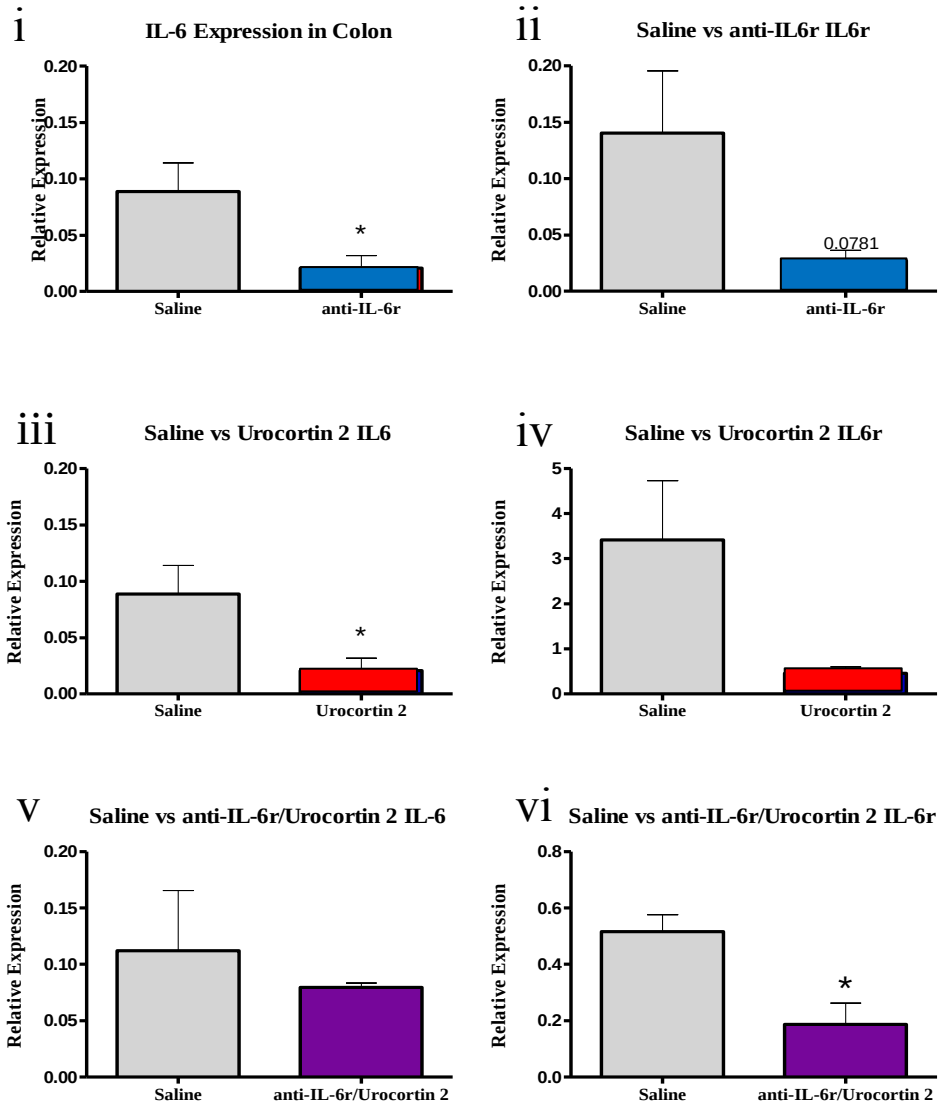
Using western blot techniques, I determined that anti IL-6R treatment significantly reduces IL-6 levels (Figure 5.19i, n=5, $p<0.05$) in the whole distal colon compared to saline treated animals when IL-6 is expressed as a ratio of the housekeeper protein, GAPDH expression. Expression of IL-6 receptors in the colon was also reduced, although it did not quite reach significance (Figure 5.19ii, n=5, $p=0.07$).

5.4.6.2 *Mdx* mice treated with Urocortin 2

Treatment with Urocortin 2 also significantly decreases IL-6 levels (Figure 5.19iii, n=5, $p<0.05$) but not IL-6R levels (Figure 5.19iv, $p>0.05$).

5.4.6.3 *Mdx* mice treated with anti IL-6 receptor antibody and Urocortin 2

Co-treatment of mice with anti-IL-6 receptor/Urocortin 2 significantly decreases IL-6 receptor expression (Figure 5.19v, n=5, $p<0.05$) but not IL-6 levels (Figure 5.19vi, n=5, $p>0.05$).



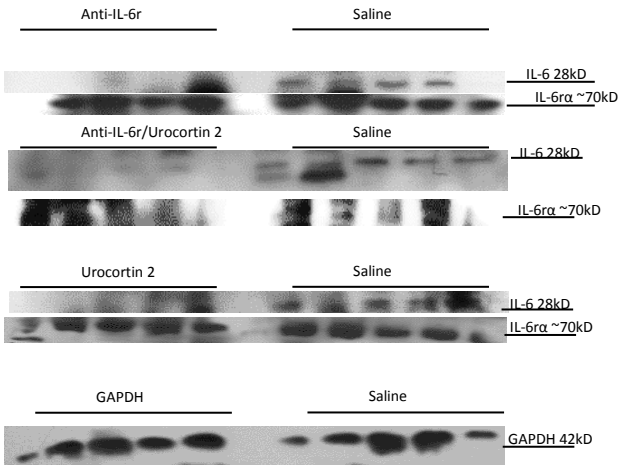


Figure 5.19: *Western Blot densitometry analysis. IL-6 and IL-6r were analysed as a ratio to GAPDH. In anti-IL-6 treated mice IL-6 expression was reduced in colons (i) similarly IL-6R was reduced but not to a significant level (p=0.781). In anti-IL-6R/Urocortin 2 mice IL-6 levels were unchanged (iii) but IL-6R expression was reduced. In Urocortin 2 treated mice IL-6 expression was reduced significantly (v) and IL-6r was reduced but not significantly. (n=5) *p<0.05*
[vii] represents western blots for IL-6 and IL-6R in the treatments.

5.5 Discussion

Main findings of the study:

Mdx and WT mice

- *Mdx* mice display altered defecation patterns.
- *Mdx* mice have shorter colons, more so in the distal colon.
- *Mdx* Distal colonic muscle walls are thickened.
- The amplitude of contractions evoked in the excised colons of *mdx* mice in response to exogenous IL-6 was larger than WT controls.
- Exogenous contractions evoked by IL-6 were ameliorated by TTX addition in *mdx* mice but not WT mice, implicating the enteric neurons as a source of IL-6 induced contractions.

Intervention Studies

- Defecation rate improved with anti-IL-6 receptor antibodies, Urocortin 2 treatment also increased total faecal output but this was somewhat delayed.
- Colon length is increased by anti IL-6R treatment, more so in distal colon, by Urocortin 2 treatment in the proximal colon and in total length.
- Contractile activity evoked by IL-6 in distal colon preparations from *mdx* had less IL-6-evoked activity in mice treated with anti IL-6R, with Urocortin 2 and in mice treated with both anti IL-6R and Urocortin 2.
- Frequency of contractions evoked by IL-6 compared to saline-treated *mdx* mice were similar in anti-IL6r treated animals higher in Urocortin 2-treated mice and higher between co treatment or either treatment alone.

- CRF-evoked contractile activity was not changed in colons taken from mice treated with anti IL-6R, Urocortin 2 or both; however the frequency of contractions was increased in mice treated Urocortin 2 almost doubled in mice treated with both factors.
- Colonic expression of the IL-6 receptor was reduced in anti IL-6R treated animals, it was also reduced in Urocortin 2 treated animals and co treated animals.
- Levels of IL-6 were reduced in anti IL-6R and Urocortin 2 animals, but not significantly reduced in co treated animals.

The focus in this study was *mdx* dystrophin deficit colon and distal colon in particular, indicated as the portion of the GI tract most affected by a chronic inflammatory environments (Atreya & Neurath 2005; Bonaz & Bernstein 2013; Ohama et al. 2007), and more so because it is apparent there is an inflammatory response in DMD patients in the GI tract (Korman et al. 1991; Dinan et al. 2003), mouse colon expresses dystrophin in a variety of cells, namely myenteric neurons (Vannucchi et al. 2001), interstitial cells of cajal and muscularis externa (Vannucchi et al. 2002). *Mdx* mice do not express dystrophin in the colon (Vannucchi et al. 2001) in the non-disease states and I aimed to investigate whether dystrophin deficiency in colon contributes to GI dysfunction and the role IL-6 and Urocortin 2 play in this physiology.

Cytokines such as IL-6 are overexpressed in DMD and *mdx* mice (Kumar & Boriek 2003; Fujita et al. 2014; Pan et al. 2008; Miles et al. 2011) and may contribute to colonic changes. IL-6 can activate the enteric neurons (O' Malley et al. 2013) and has a role in facilitating contractions in rat model of depression (Zhang et al. 2013) and along with IL-1 are seen to be neuromodulators in the gut, causing excitation by also suppressing cholinergic inhibition presynaptically (Kelles et al. 2000) in enteric neurons therefore it is apparent IL-6 plays a key role in the physiology of the gut.

It is not known however, how IL-6 induced changes are implicated in dystrophin deficient gut or whether patients could benefit from an anti- IL6 treatment in GI symptoms of the disease. As patients share symptoms with other gut diseases it is intuitive to hypothesis these may share mechanisms which produce undesirable symptoms in the gut. Neutralisation of IL-6 in IBD has been seen to be efficacious in ameliorating inflammation (Wang et al. 2013), inflammation causes changes in motility due to changes in cytokine profile, changes in excitatory neurotransmitter receptor expression, disturbances in normal physiological action of calcium channels to name a few (Ohama et al. 2007). Moreover, as increased cytokines including IL-6 (and TNF) are implicated in disease that exhibit slowed colonic motility, it is likely reducing IL-6 reduces this deficit (Ang et al. 2012).

CRFR2 receptors can inhibit gastric emptying (Martinez et al. 2004; Martínez et al. 2002) but in distal colon does not seem to have an effect on contraction (Martínez et al. 2002) but in stress models can interact with localised

with CRFR1 receptors and an suppress stress induced contractions (Gourcerol et al. 2011). An interaction between IL-6 and CRF, whereby immune activation and stress are proposed to exacerbate symptoms in IBS animal models (O' Malley et al. 2013) and may similarly affect one another in the smooth muscle dysfunction and pathogenesis of the gut in DMD.

Urocortin 2 exerts anti-inflammatory events through a number of cascades and this may be due to distribution of receptor types in different tissues. In the colon, Urocortin 2 binds with high affinity to the CRFR2 receptor, which has been shown to have anti-inflammatory effect by regulating the pro-inflammatory profile of the gut (Chang et al. 2007). CRF and the Urocortins can supress secretion of several components of the inflammatory response including TNF-α from mice primary macrophages (Tsatsanis et al. 2007) and moreover activation of the CRFR2 subtype can induce macrophage apoptosis thereby modulating inflammation (Tsatsanis et al. 2005). PG 873637, a CRFR2 agonist has been found to be beneficial in *mdx* mice, albeit in skeletal muscle where its effects have been through increasing muscle hypertrophy (measured by weight of the muscle of both skeletal and cardiac muscle) (Hinkle et al. 2007) and a functionally healthier diaphragm muscle. In the functional study of the diaphragm the CRFR2 agonist improved force generation, this improvement is associated with a range of gene changes implicating anti-inflammatory and anti-fibrotic effects in the muscle (Hinkle et al. 2007) .

5.5.1 Faecal output changes in *mdx* mice

The faecal transit times in WT and *mdx* mice were compared. Indicative of colonic health, I monitored the faecal output from mice when placed in a brightly lit stressful environment. Stress induced defecation is a well-established rodent behavioural test (O'Malley et al. 2010; O' Malley et al. 2011b). In our protocol, I recorded output in 15 minute intervals to examine time increments and to create a time line of faecal pellet output, but also to enable accurate calculation of water content through a desiccation protocol (Julio-Pieper et al. 2010). I also used a cumulative timeline of these 15 minute intervals to give insight on the number of boli excreted through the trial. As I discovered in Study 1 that *mdx* exhibit depressive and anxiety like

behaviours I would hypothesise a higher rate of defecation, induced from stress sensitivity in the colon.

However I deduced from the reduced number of boli in the early interval faecal output times, in *mdx* mice compared to WT mice, as the literature reveals no evidence of increased sensitivity to stress in the WT mice I used, I concluded that colonic transport is slowed. This has been reported previously in small intestine transit time of *mdx* mice, although stomach gastric emptying times was not been affected (Mulè et al. 2010) – indicating the lower GI dysfunction is responsible for the altered output.

In patients with DMD, orocaecal transit time has been previously studied in the 1990's, and no differences were reported from controls or compared to other neuromuscular diseases. However there are some limitations in this study; with previous histopathological evidence of GI smooth muscle fibrosis and inflammation in post mortem tissue (Barohn et al. 1988) and symptoms (Gottrand 1991) indicating functional changes, no differences were found in orocaecal transit time. However, these results should be treated with caution, as ingestion of liquid which passed through the pylorus was measured rather than a bolus of chyme (Korman et al. 1991). Optimisation of the technique was used in a study and they reported a reduction in gastric emptying time in patients with DMD, through a radio-linked oatmeal meal (Barohn et al. 1988), reducing the slip-through effect of liquid which may have masked the slowed transit in earlier experiments.

5.5.2 Faecal output changes in *mdx* mice and a role for IL-6 signalling and Urocortin 2 in transit time

In our studies, when *mdx* mice are treated with an anti-IL-6 receptor antibody for 2 weeks, colonic transit time is faster than saline treated animal, an effect than may be beneficial for DMD patients, by normalising transit time. This normalisation is indicative of a beneficial effect of blocking IL-6 signalling in the colon, This action may be explained by blocking the pro-inflammatory effect of blocking IL-6 signalling, a recent study utilising the MR16-1 antibody I used in my studies, have shown that blocking IL-6 signalling can reduce gene expression in macrophages in

damaged muscle tissue (Fujita et al. 2014). Moreover as increased cytokines including IL-6 (and TNF) are implicated in disease that exhibit slowed colonic motility, it is likely reducing IL-6 reduces this deficit (Ang et al. 2012), it may be due to the direct neutralisation of IL-6 receptors as IL-6 can elicit contractions through the neurons in the myenteric plexus (Zhang et al. 2013) in disease states. Both IL-6 protein and IL-6 receptor expression was reduced in mice treated with MR16-1 treatment, blocking IL-6 signalling.

CRF and the Urocortins can supress secretion of several components of the inflammatory response including TNF-α from mice primary macrophages (Tsatsanis et al. 2007) and moreover activation of the CRFR2 subtype can induce macrophage apoptosis thereby modulating inflammation (Tsatsanis et al. 2005). PG 873637, a CRFR2 agonist has been found to be beneficial in *mdx* mice, albeit in skeletal muscle where its effects have been through increasing muscle hypertrophy (measured by weight of the muscle of both skeletal and cardiac muscle) (Hinkle et al. 2007) and a functionally healthier diaphragm muscle. In the functional study of the diaphragm the CRFR2 agonist improved force generation, this improvement is associated with a range of gene changes implicating anti-inflammatory and anti-fibrotic effects in the muscle (Hinkle et al. 2007) .It is clear that Urocortin 2 exerts anti-inflammatory events through a number of cascades and this may be due to distribution of receptor types in different tissues. In the colon, Urocortin 2 binds more strongly to the CRFR2 receptor, which has been shown to have anti-inflammatory effect by regulating the pro-inflammatory profile of the gut (Chang et al. 2007), and I found in animals treated with Urocortin 2, expression of IL-6 was reduced in colonic tissue. An interaction between IL-6 and CRF, whereby immune activation and stress are proposed to exacerbate symptoms in IBS animal models (O' Malley et al. 2013) and may similarly affect one another in the smooth muscle dysfunction and pathogenesis of the gut in DMD, interestingly when Urocortin 2 was co-treated with anti-IL-6 receptor antibody it reduced IL-6 receptor levels, but not the protein, beyond the scope of these functional tests however, it is indicative of a complex interaction of IL-6 and Urocortin 2 in the gut.

5.5.3 Faecal composition is not changed in *mdx* mice

The other main function of the colon is water and ion absorption and secretion; I found that the water content of *mdx* faecal boli was similar between WT and *mdx* mice. Water content, which is an indicator of the faecal form – ranging from watery unformed stools associated with diarrhoea to hard dry pellets observed in constipation, was not different between the WT mouse and the *mdx* strain as the pellet formation appeared normal and was no difference in wet of dry weight either. Although symptoms indicating a change in water and ion transport such as constipation and diarrhoea have been reported in DMD patients (Gottrand 1991), our studies do not find any evidence of altered stool formation in *mdx* mice in these measured parameters.

Indeed, changes in gut barrier permeability which is important as a defence against inflammatory initiation from agents in the tract (Arrieta et al. 2006) has not been observed in smooth muscle of patients or *mdx* mice, and while aquaporin's are expressed in the gut, in both neurons (Thi et al. 2008) and colonic epithelial cells (Tonghui & Verkman 1999) no evidence of dysregulated protein has been found in *mdx* mice. However, it has been implicated in skeletal muscle of patients (Frigeri et al. 2002) where its expression is reduced, this reduction is thought to be due to its association with the DAPC proteins (Frigeri et al. 2002).

It is likely however that the divergence in *mdx* and human disease may contribute to the lack of pathology of this type. Symptoms such as constipation are attributed to immobility of patients or weakened abdominal wall skeletal muscle controlling motility of the GI tract (Gottrand 1991) as opposed to aberrant absorption or secretion. The consistency of the faecal pellets was not affected by any of the interventions.

5.5.4 Morphological changes in *mdx* mice

To investigate further I examined excised colon length in WT and *mdx* mice. Simply calculating colon length to the nearest millimetre yielded some interesting results. *Mdx* colon length is reduced compared to WT mice. Although, this seems counter intuitive when you take into consideration that transit time is also reduced, it may actually explain the dysregulated propulsion through the colon.

I hypothesised this shortening may be due to changes in contraction mechanics or due to an inflammatory and fibrotic environment. Evidence exists that

shortened colon length is due to inflammation in animal models with inflammatory disease, such as colitis, and is used a disease marker (Kwon et al. 2008) and indeed in patients with DMD, GI fibrosis and inflammatory events have been seen post-mortem (Barohn et al. 1988).

However in other regions of the GI tract a reduction in thickness of smooth muscle walls are reported in patients (Dinan et al. 2003), however this apparently is organ specific as diaphragm thickening has also been reported (De Bruin et al. 1997) .

Thickened muscular walls in distal sections of colon are consistent with increased contraction of the circular muscle layer which may contribute to the shortened colon. Indeed contracture (a contracted state which is a pathological sustained contraction) in skeletal muscle is common in patients with DMD (Allen & Whitehead 2011) and seen in *mdx* muscle (Claflin & Brooks 2008).

I hypothesised this may be the case in smooth muscle. However, no inflammatory infiltrate which dominates in skeletal muscle pathology (Arakia et al. 1997) was apparent in the colonic cross-sections at this age, despite the raised cytokine profile at this age (Porter et al. 2002) and GI dysfunction our study has elucidated.

5.5.4.1 Morphological changes in *mdx* mice by blocking IL-6 signalling and CRFR2 agonism

Thus, the capacity of anti IL-6 receptor antibody treatment to cause elongation of the *mdx* colons is unlikely to be caused by blocking the pro-inflammatory effect. However, it may be due to modulation of myenteric neurons which regulate smooth muscle function, specifically circular muscle contraction (Natale et al. 2003; O' Malley et al. 2013) Alternatively, the thickening of the smooth muscle layer may indicate muscular hypertrophy as seen in cardiac tissue (Meléndez et al. 2010), thus IL-6 may be associated with this pathology.

Treatment with Urocortin 2 also results in a lengthening effect in the colon, especially so in the proximal colon. This is different to anti IL-6R treatment, which is not entirely surprising, although CRFR2 promotes anti-inflammatory mechanisms; it does so differently to blocking IL-6 signalling. It has been seen to reduce to inflammation through the induction of apoptosis of pro-inflammatory macrophages

(Tsatsanis et al. 2005). However, in the absence of evident inflammation, Urocortin 2 may be having a direct effect on muscle mass as has been seen in other muscle types (Hinkle et al. 2003; Hinkle et al. 2003; Hall et al. 2007) or indeed, stimulating changes through actions on the myenteric neurons (Maillot et al. 2002; Chang et al. 2007; O'Malley et al. 2010).

It is clear that CRFR2 agonism has beneficial effects in *mdx* mice skeletal muscle, increasing muscle mass (Hall et al. 2007) Co-treatment of anti-IL-6 and Urocortin 2 does indeed increase colon length, but not specifically in the proximal or distal colon, the lengthening occurs in both portions presumably.

5.5.5 Colonic contractile changes in *mdx* to exogenous stimuli

5.5.5.1 Colonic reactivity to IL-6, CRF or a combination of both

As mentioned mouse colon expresses dystrophin in a variety of cells, namely myenteric neurons (Vannucchi et al. 2001), interstitial cells of cajal and muscularis externa (Vannucchi et al. 2002). *mdx* mice do not express dystrophin in the colon (Vannucchi et al. 2001).

The loss of dystrophin affects the electrical activity in cells, resting membrane potentials in smooth muscle cells increased to -36mV in *mdx* cells compared to -50mV in normal conditions. This is somewhat attributed to the derangement in NOS which is associated with the DAPC (Serio et al. 2001), but the cause not fully elucidated. Furthermore, loss of normal GI pressure, propulsion and fluid ejection is indicative of a nervous system dysfunction due to dystrophin deficiency from the normally expressing neurons of the enteric nervous system (Mancinellia et al. 1995).

To complement the transit time and propulsion *in vivo* study which indicated that there were changes to *mdx* smooth muscle function I excised distal colon sections and recorded electrical changes using an organ bath which measured contractile tension in the muscle. Moreover, I used exogenous IL-6 to ascertain if it had a role in the contraction of *mdx* smooth muscle, I also used CRF, and a

combination of both to investigate if there is crosstalk between the two in the control of contractions in *mdx* mice, as seen in other inflammatory disease models.

Our studies found that whole colon preparations of *mdx* mice react differently to WT controls when distal segments of colon are stimulated with IL-6 or CRF, or a combination of both. IL-6 causes an amplitude change in *mdx* mice far greater than that in WT mice, and the contraction had characteristics consistent with an increased and sustained tension. This change in amplitude, bigger contractions than WT colon preparation includes circular and longitudinal muscle and the enteric nervous system however, so elucidating the particular cause of contraction is difficult to ascertain using only this technique.

However, as previously mentioned *mdx* colons are particularly sensitive to stimuli as their cells are easier to depolarise due to the change in the resting potential (Serio et al. 2001). IL-6 is known to interact with myenteric neurons of the colon and can excite myenteric neurons in rodents (O' Malley et al. 2011; O' Malley et al. 2013). IL-6 can cause excitation of enteric neurons consequently causes contractions(O' Malley et al. 2013), however myogenic contractions are reported in patients with IBDs caused by IL-6, and indeed IL-6 can be secreted by human smooth muscle cells in culture (Salinthone et al. 2004). Thus, IL-6 appears to have a role in normal colonic morphology and function and loss of dystrophin seems to interfere with this.

5.5.5.2. Neuronally mediated contractions are evoked by IL-6 in *mdx* mice

Inhibition of voltage gated sodium channels with TTX indicated the importance of neural activity to IL-6 evoked contractions in *mdx* mice but not the WT controls (Bartoo et al. 2005; Holmberg et al. 2007). It has previously been reported in proximal colon segments pre-incubated with TTX produce a higher amplitude of spontaneous contractions which is comparable to WT proximal colons, however this is attributed to circular muscle layer and recorded as changes in intraluminal pressure (Mulé et al. 1999), and no spontaneous basal tone contractions were recorded after addition of TTX in our experiments this distal in the colon. Moreover it has been shown that IL-6R are located, not only in smooth muscle cells but also in the myenteric plexus of the colon in rodents and this is where the stimulatory effect is

propagated in animals which have raised systemic inflammatory cytokine profiles (Zhang et al. 2013).

5.5.5.3 Treatment with anti IL-6 receptor and CRFR2 agonism using Urocortin 2 effects on colonic reactivity to IL-6, CRF or a combination of both

In *mdx* mice where IL-6 signalling is inhibited through the immuno-neutralisation of IL-6 receptors, predictably the amplitude of the colonic contraction evoked by IL-6 was normalised and was thus similar to the response in WT mice. Interestingly however, when IL-6 and CRF were used to stimulate colons from these mice, there is an increase in the amplitude of the colonic contraction, although it doesn't quite reach significance, which may indicate an additive effect of CRFR2 activation. Indeed, co-localisation of CRF receptors and IL-6 receptors is known to exist in neurons in the hypothalamus (González-Hernández et al. 2006) and in the propia lamina, in the mucosae and enteric neurons of rat colon sections (O' Malley et al. 2013; O' Malley et al. 2011).

Interaction between these receptors has not been researched in smooth muscle; however it is clear that the lack of dystrophin changes sensitivity of colonic smooth muscle to IL-6 and Urocortin 2, which has implications for diseases that are exacerbated by inflammation and stress as is the case in DMD.

Similarly, and in support of the hypothesis that there is crosstalk in the colon between IL-6 and CRFR2, is the fact that IL-6-evoked colonic contractions were also reduced in colons taken from *mdx* mice treated with Urocortin 2.

Moreover, the contraction evoked by IL-6 and CRF was also reduced in Urocortin 2 treated mice, but no change was observed when CRF was added by itself.

However comparing the addition of IL-6 and CRF in Urocortin 2 treated mice shows a significantly higher contraction amplitude change to CRF compared to either IL-6 alone or a combination of IL-6 and CRF and binding to CRFR2 can decrease the compounding amplitude and increase of the amplitude of contractions to IL-6, but increases the frequency of smaller contractions.

The additive effect of a CRFR2 agonist and IL-6R neutralising antibodies was noted in a reduction in amplitude change to IL-6, and a reduction in amplitude to IL-6 and CRF, and when contractions were counted in the 20 minute period the compound was incubated with the colon I saw an increase in contraction frequency, which is additive for both IL-6 and CRF.

The effects of Urocortin 2 may be due to its beneficial effect on muscle health. Evidence exists that colons in IBS patients (Dinan et al. 2003) exhibit inflammation, and share symptoms of inflammatory colonic disease, however I did not see obvious infiltration in colons, it may be reducing the inflammatory environment (la Fleur et al. 2005; Tsatsanis et al. 2005; Moss et al. 2007). This positive effect on colon may reducing the contracture trace profile (the loss of full relation and a "stepping up" of contractions) of the smooth muscle contractions and therefore allowing more frequent but smaller, less sustained contractions .

Similarly for CRF incubations, which almost doubles contractions for IL-6 and CRF, incubated together, suggesting if there isn't a straight forward interaction between the two. In several systems, eg gut-brain axis, a complex interaction has been hypothesised previously (O' Malley et al. 2013) in IBD's. The result suggests that this co-incubation, in the colon preparations have an additive effect in regard to contraction frequency and reduction in amplitude. Evidence from previous results, including the different changes in lengthening (anti IL-6 receptor antibody lengthening the distal colon, and Urocortin 2 lengthening the proximal colon, and a combination treatment lengthening not one segment in particular) indicates they may work through very diverging mechanisms.

Not surprising perhaps is the significant decrease in IL-6 levels and IL-6 receptor levels in the colons treated with anti-IL-6 receptor antibody at this dose/duration.

This indeed validates the treatment, and reveals that blockage of the receptor by the antibody can reduce the IL-6 expression in colon, a reduction in IL-6 levels and in particular the reduction in active IL-6 receptor may underlie the changes in amplitude and frequency of contractions. This may be mediated through the myenteric neurons in inflammatory environments in rodent colons (Zhang et al. 2013). Interestingly, mice treated with Urocortin 2 also had a reduction in IL-6 levels in colonic tissue, but not IL-6R expression. As discussed this may be due to the

overall anti-inflammatory effect of CRFR2 agonism, and the emerging apparent interaction between the family of CRF proteins and IL-6. It is interesting to see a significant reduction in IL-6 levels in the mice treated with Urocortin 2, IL-6 is released from neurons (März et al. 1998), smooth muscle (Kageyama et al. 2006) inflammatory cells and in contracting muscle (Erta et al. 2012), so it is difficult to fully explain the reduction in IL-6 level here. It may be indicative of a healthier state of the organ i.e. less inflammation, as the CRF system can regulate IL-6 during inflammation (Venihaki et al. 2001) or signalling interaction between the CRF system and IL-6, which is already begun to be elucidated in other tissues (Ando et al. 1998; Tsatsanis et al. 2007).

In contrast, combination treatment did not significantly reduce IL-6 levels but did decrease IL-6R expression. Evidence of a complex interaction is obvious, however when a co-treatment of anti IL-6 receptor antibody with Urocortin 2, as when administered separately they reduce IL-6 levels but together do not decrease amplitude levels.

However, anti IL-6 receptor antibody did still block IL-6 receptor signalling in the presence of Urocortin 2, it is likely however, this is happening on a local tissue level (Kageyama et al. 2006) and that systemic IL-6 and Urocortin 2 are interacting in a manner which is both modulating IL-6 levels itself, and through the central HPA axis (Vallières & Rivest 1999), perhaps by modulating CRFR1 corticosteroid catabolic effects on either skeletal muscle (and thus this damaged muscle releasing circulating IL-6)(Hinkle et al. 2004), or a more direct, but as of yet unknown, effect on colonic smooth muscle cells.

5.5.6 Conclusions

This study investigated the GI consequence of dystrophin deficiency by comparing colonic function and morphology in *mdx* and WT mice. As symptoms in patients suffering from DMD include vomiting, constipation and DMD colons exhibit fibrosis and inflammation in their GI tract, it is speculated that dystrophin deficiency causes IBD type pathology in mice. In inflammatory diseases blocking IL-6 signalling can reduce some GI pathological features, and is a readily available treatment, tolerated well in patients with Crohns disease (Ito 2005; Daisuke et al.

2014) in this study I have showed in vivo pathological differences in *mdx* mice compared to WT mice, such as slowed GI motility, thickened muscle walls, and shortened colon length.

Blocking IL-6 signalling using the MIR16-1 monoclonal anti IL-6R Ab (Tamura 1993) increased transit time, but did not change the composition of the faecal pellets, it also reduced the IL-6 induced contractions, which are likely to be regulated by myenteric neurons, in which is in contrast to the WT mice which appear to be mediated through direct effects on the muscle cells.

Urocortin 2 has less beneficial effects than anti IL-6R, in colonic motility but still elicited some effects. although CRFR2 agonists have been beneficial in *mdx* skeletal muscle (Hinkle et al. 2007) and I see here, that systemic injection of Urocortin 2, acts to benefit smooth muscle.

Stimulating colonic preparations however did reveal an additive effect of the drugs on contraction frequency and a similar pattern of amplitude change to the recombinant exogenous IL-6 and CRF additions demonstrating a likely crosstalk between these two factors in this tissue.

These studies provide evidence of the potential benefits of therapeutic interventions targeting IL-6 receptor signalling and/or the effects of the stress hormone, CRF. Largely, left untreated due to the debilitating effects of deterioration of other bodily systems, improving gut function in DMD offers an important potential improvement in the quality of life of patients.

Chapter 6: Summary and Conclusions

6.1 Summary of Results

In chapter 3, I utilised the *mdx* mouse model of DMD, to investigate behavioural changes associated with dystrophin deficiency (Anderson et al. 2004) or possibly chronic inflammation and its crosstalk with the stress system (Varghese et al. 2006; Camacho 2013; Gerber & Bale 2012). Our studies identified behavioural profiles consistent with increased anxiety and depression. I subsequently assessed the effects of amitriptyline, a TCA, on the altered behaviours and on chronic skeletal muscle inflammation, which is characteristic of the *mdx* mouse.

Predictably, amitriptyline had anti-depressant-like effects but it also improved the anxiety exhibited by the *mdx* mice in the open field test. Indeed, monoamine analysis in several brain regions revealed that *mdx* mice respond differently to amitriptyline treatment than WT mice, indicating that amitriptyline works through the modulation of central monoamines.

However, the full mechanisms by which amitriptyline works in *mdx* pathology is not yet completely understood. In addition to the mood altering effects of amitriptyline, inflammatory cell infiltrate in skeletal muscle sections was decreased following treatment and number of myofibres with centralised nuclei, which are indicative of regenerating fibres was reduced. In dystrophic muscle, regeneration is a precursor to loss of function. Because of the central role of inflammation in DMD, I investigated changes in the pro-inflammatory cytokine, IL-6 which is involved in inflammation, but also stress and depression. Amitriptyline reduced circulating IL-6 levels.

In the subsequent studies the direct roles of IL-6 and the stress factor, CRF in DMD pathophysiology were investigated. I first examined diaphragm function which, in the *mdx* mouse model most closely recapitulates human DMD (De Bruin et al. 1997; Grounds et al. 2008). Monoclonal antibodies against the IL-6 receptor and the Urocortin 2, the CRF receptor 2 agonist, which has beneficial peripheral effects on *mdx* muscle (Hall et al. 2007; Hinkle et al. 2007) were investigated. I also included a group which was treated with both of these factors as crosstalk between IL-6 and CRF proteins (Ando et al. 1998; Kageyama et al. 2006; Kageyama & Suda 2003; M.

Huang et al. 2009) suggested that they may have beneficial effects if administered together.

Our studies determined that isometric force generating conditions, *mdx* mouse diaphragm exhibits a reduction in twitch force generation and Urocortin 2 or co-treatment of anti IL-6R rescued this to some extent. Moreover, co-treatment produced a significantly higher peak force compared to saline treated *mdx* mice. Interestingly, anti IL-6R alone and with Urocortin 2 induced an increase in shortening of diaphragm strips. Anti IL-6R also increased velocity of shortening of *mdx* diaphragm, through as of yet an unknown mechanism.

In an isotonic setup, where muscle shortening as a percentage of its maximal specific force load is recorded, *mdx* mouse diaphragm exhibits a reduction in mechanical work production. All intervention treatments increased mechanical work production, with co-treatment of anti IL-6R and urocortin 2 produced the largest increase. *Mdx mouse* diaphragm exhibits a reduction in power production compared to WT mice. All intervention treatments increase diaphragm power production, which is important because of the continuous contraction and relaxation of the diaphragm muscle. The fatigue ability of this muscle was also assessed and *mdx mouse* diaphragm was found to be less resistant to fatigue. However, this was improved moderately by all intervention treatments.

In chapter 5, I utilised the same cohort of treated *mdx* mice to investigate the colonic deficits which have been reported in DMD patients (O Borrelli et al. 2005; Korman et al. 1991) and has also been observed in *mdx* mice (Tameyasu et al. 2004; Vannucchi et al. 2004; Mulé et al. 1999). Consistent with deficiencies in smooth muscle caused by loss of dystrophin, our studies found that *mdx* mice exhibited a number of changes in GI function as compared to WT controls. *Mdx* mice exhibited slowed transit times and excrete fewer faecal boli than similarly stressed WT mice. This is comparable to slowed GI transit in human DMD sufferers (Barohn et al. 1988). Moreover, colon lengths were shorter and the muscle wall appeared thickened which may indicate aberrant smooth muscle contraction or muscle cell hypertrophy. Thus, loss of dystrophin appears to be specific to problems associated with smooth muscle function although unlike the characteristic inflammation in *mdx* skeletal

muscle, histopathological analysis did not reveal obvious inflammatory infiltrate or fibrosis in colonic smooth muscle.

To assess the functional consequences of these pathophysiological changes colonic contractile activity in response to IL-6, CRF or both were assessed in WT and *mdx* tissues. Although control responses evoked by the cholinergic agonist Carbachol were comparable, *mdx* colons were more sensitive to the stimulatory effects of IL-6 which is neurally-mediated probably through activity of the myenteric plexus. This contrasts with the stimulatory effects IL-6 in WT colons which do not have a neural component, thus, loss of dystrophin and the associated smooth muscle dysfunction appears to lead to a compensatory mechanism which relies on neural activity. CRF stimulated large contractions in both WT and *mdx* strains and interestingly, this response was dampened when both IL-6 & CRF were applied together, indicating potential crosstalk between these two factors which may be important in regulating GI activity when the stress system and the inflammatory response are both chronically activated which is likely to be the case in DMD.

To investigate the potential of therapeutically targeting IL-6Rs and/or CRFRs in *mdx.* GI function, colonic tissue from mice treated with IL-6R, Urocortin 2 or both was assessed. Indeed, the treatments did have functional effects with anti IL-6RR increasing transit time, colonic length and resulting in a reduction in the amplitude of IL-6-evoked contractions although the frequency of contractions was unaffected. The amplitude of CRF- and IL-6 & CRF- evoked contractions was unchanged by anti IL-6R treatment but the frequency of the contractions was increased by both.

Urocortin 2 treatment was also associated with increased faecal transit times, although this was noted later in the trial and to a lesser extent. No change in colonic length was evident but the amplitude of IL-6-evoked contractions was reduced in these mice even though the frequency of contractions was unaffected. The amplitude of CRF- and IL-6 & CRF-evoked contractions was not altered by Urocortin 2 treatment but again, the frequency of the contractions was increased by both stimulants.

mdx mice which received both anti IL-6R and Urocortin 2 did not show the same increase in faecal transit as those mice treated with IL-6R alone, indicating that Urocortin 2 may have a moderating influence on this readout. However, colonic length was increased in comparison to saline-treated *mdx* mice and the amplitude of

IL-6-evoked contractions was reduced. The amplitudes of CRF-evoked contractions were unchanged but contractile activity evoked by IL-6 & CRF was decreased. Moreover, the frequencies of contractions evoked by IL-6, CRF and IL-6 & CRF were all increased significantly.

IL-6 is a marker of inflammation and also indicative of structural damage in contracting muscles (Jonsdottir et al. 2000; Pedersen & Febbraio 2008), however, I have also demonstrated that IL-6 has functional effects in terms of colonic contractility. CRF, the key stress hormone released by the hypothalamus, can also evoke colonic contractions and I have provided evidence that crosstalk between these factors, which may occur when both inflammatory and stress systems are chronically activated, can modulate both colonic tissue structure and function. In terms of normal GI function, targeting IL-6Rs and CRFR2 in *mdx* mice has proven to be beneficial.

6.2 Limitations

Perhaps the first limitation in this study was the *mdx* mouse model. Although a genetic mimic of DMD, the pathological signature of dystrophin deficiency deviates from the human disease, therefore in extrapolating the implications of the experimental data, leaves questions as to whether these are transferable to the human disease.

In the first study, I was unable to quantify IL-6 levels to a satisfactory level in skeletal muscle which exhibited evidence of inflammation. In the studies that followed I aimed to rectify this by quantifying IL-6 levels in the muscle using Western blots. Nonetheless, I did determine that circulating IL-6 levels were reduced following treatment with amitriptyline.

In study two, I detected novel protective effects of anti IL-6-R and/or Urocortin 2, however, further research will be required to elucidate the underlying mechanisms which regulate these effects. Moreover, it is noteworthy to mention that studies have found absolute measurements of power in *mdx* mice were normal compared to WT until it was normalised to fibre numbers in the preparation, indicating the weight of muscle can conceal true ability of the muscle to produce force. As our results were

calculated using CSA, this may mask more specific results. CSA assumes that the weight of the muscle preparation is composed of muscle fibres and in the calculation of CSA muscle density is considered a constant. This limitation could be overcome by using single fibre preparations; regrettably, this was unavailable for the current study in our laboratory.

6.3 Future Studies

It would be interesting to examine isotonic capabilities of IL-6 and Urocortin treated mice in single fibre preparations. Moreover, although not available for this study, histological analysis of the diaphragm muscle for signs of inflammation and changes in cell type during treatment would go to further elucidate the mechanisms by which anti IL-6Rs are having their effects. Understanding the complex interactions between IL-6R and CRFR signalling at a cellular level both in WT and *mdx* skeletal and smooth muscle and in associated neural cells will require alternative experimental techniques such as calcium imaging or electrophysiology

6.4 Implications

The results of our study on Amitriptyline, a drug already on the market for the treatment of depression, stress, pain and inflammatory diseases, suggests a potential new use for this old drug in. However, caution is to be used when prescribing tri cyclic antidepressants and it is important it is on a patient to patient basis as it has been implicated in cardiac toxicity and DMD patients have weakened heart muscle.

In study 2 and 3, I demonstrated that blocking IL-6 signalling can benefit both diaphragm and GI function. Monoclonal antibodies against IL-6 receptors are already prescribed for use in rheumatoid arthritis, but we have identified a new disease in which this therapy may be effective, perhaps when co-administered with a CRFR2 agonist.

Chapter 7: Bibliography

Aartsma-Rus, A. et al., 2006. Entries in the Leiden Duchenne muscular dystrophy mutation database: An overview of mutation types and paradoxical cases that confirm the reading-frame rule. *Muscle & Nerve*, 34(2), pp.135–144.

Abdel-Salam, E., Abdel-Meguid, I. & Korraa, S.S., 2009. Markers of degeneration and regeneration in Duchenne muscular dystrophy. *Acta Myologica*, 28(3), pp.94–100.

Abdel-Salam, O.M.., Nofal, S.M. & El-Shenawy, S.M., 2003. Evaluation of the anti-inflammatory and anti-nociceptive effects of different antidepressants in the rat. *Pharmacological Research*, 48(2), pp.157–165.

Abràmoff, M.D., Magalhães, P.J. & Ram, S.J., 2004. Image Processing with Image J. *Biophotonics International*, July 6.

Abresch, R., Seyden, N. & Wineinger, M., 1998. Quality of life. Issues for persons with neuromuscular diseases. *Phys Med Rehabil Clin N Am*, Feb(9(1)), pp.233–48.

Achar, E. et al., 2009. Amitriptyline attenuates interstitial inflammation and ameliorates the progression of renal fibrosis. *Kidney International*, 75(6), pp.596–604.

Acharyya, S. et al., 2007. Interplay of IKK / NF- κ B signaling in macrophages and myofibers promotes muscle degeneration in Duchenne muscular dystrophy. *The Journal of clinical investigation*, 117(4), pp.889–901.

Allen, D.G. et al., 2010. Calcium and the damage pathways in muscular dystrophy. *Canadian journal of physiology and pharmacology*, 88(2), pp.83–91.

Allen, D.G. & Whitehead, N.P., 2011. Duchenne muscular dystrophy--what causes the increased membrane permeability in skeletal muscle? *The international journal of biochemistry & cell biology*, 43(3), pp.290–4.

Alonzi, T. et al., 1998. Interleukin 6 Is Required for the Development of Collagen-induced Arthritis. *The Journal of Experimental Medicine*, 187(4), pp.461–468.

Altman, H. & Normile, H., 1988. What is the nature of the role of the serotonergic nervous system in learning and memory: prospects for development of an effective treatment strategy for senile dementia. *Neurobiology Aging*, Sep-dec(9 (5-6)), pp.627–38.

Anderson, I., 2000. Selective serotonin reuptake inhibitors versus tricyclic antidepressants: a meta-analysis of efficacy and tolerability. *Journal of affective disorders*, 58(1), pp.19–36.

Anderson, J., Bressler, B. & Ovalle, W., 1988. Functional regeneration in the hindlimb skeletal muscle of the mdx mouse. *J Muscle Res Cell Motil*, Dec(9(6)), pp.499–515.

Anderson, J., Weber, M. & Vargas, C., 2000. Deflazacort increases laminin expression and myogenic repair, and induces early persistant functional gain in mdx mouse muscular dystrophy. *Cell Transplant*, Jul-Aug(9(4)), pp.551–64.

Anderson, J.L. et al., 2002. Brain function in Duchenne muscular dystrophy. *Brain : a journal of neurology*, 125(Pt 1), pp.4–13.

Anderson, J.L., Head, S.I. & Morley, J.W., 2004. Long-term depression is reduced in cerebellar Purkinje cells of dystrophin-deficient mdx mice. *Brain Research*, 1019, pp.289–292.

Ando, T. et al., 1998. Peripheral corticotropin-releasing factor mediates the elevation of plasma IL-6 by immobilization stress in rats. *The American journal of physiology*, 275(5 Pt 2), pp.R1461–7.

Andreetta, F. et al., 2003. Immunomodulation of TGF-beta1 in mdx mouse inhibits connective tissue proliferation in diaphragm but increases inflammatory response: Implications for antifibrotic therapy. *Journal of Neuroimmunology*, 15(5), p.II.

Ang, L., Xiong, J. & Chen, Z., 2012. IL-6, TNF-α, and iNOS is associated with decreased colonic contraction in rats with multiple organ dysfunction syndrome. *Journal of Surgical Research*, 178(2), pp.51–57.

Angelini, C. & Tasca, E., 2012. Fatigue in muscular dystrophies. *Neuromuscular disorders : NMD*, 22 Suppl 3, pp.S214–20.

Anon, 2012. Newborn screening for Duchenne muscular dystrophy gains support. *American Journal of Medical Genetics Part A*, December 1(12), pp.viii–ix.

Antoni, F.A., 1986. Hypothalamic Control of Adrenocorticotropin Secretion: Advances since the Discovery of 41-Residue Corticotropin-Releasing Factor. *Endocrine Reviews*, Novembe(7), pp.351–378.

Antunes, M. & Biala, G., 2012. The novel object recognition memory: neurobiology, test procedure, and its modifications. *Cognitive processing*, 13(2), pp.93–110.

Arakia, E. et al., 1997. Targeted disruption of exon 52 in the mouse dystrophin gene induced muscle degeneration similar to that observed in Duchenne muscular dystrophy. *Biochemical and biophysical research communications*, 238(2), pp.492–7.

Arechavala-Gomeza, V. et al., 2010. Revertant fibres and dystrophin traces in Duchenne muscular dystrophy: implication for clinical trials. *Neuromuscular disorders : NMD*, 20(5), pp.295–301.

Arrieta, M.C., Bistritz, L. & Meddings, J.B., 2006. Alterations in intestinal permeability. *Gut*, 55(10), pp.1512–20.

Ashton, E. et al., 2008. Simultaneous mutation scanning for gross deletions, duplications and point mutations in the DMD gene. *Eur J Hum Genet*, January(16(1)), pp.53–61.

Atreya, R. & Neurath, M.F., 2005. Involvement of IL-6 in the Pathogenesis of Inflammatory Bowel Disease and Colon Cancer. *Clinical Reviews in Allergy and Immunology*, 28, pp.187–195.

Attal, P. et al., 2000. Isotonic mechanics of a pharyngeal dilator muscle and diaphragm in the rat before and after fatigue. *Eur Resir J*, 15, pp.308–313.

Baccari, M. et al., 2007. Reversal by relaxin of altered ileal spontaneous contractions in dystrophic (mdx) mice through a nitric oxide-mediated mechanism. *American Journal of Physiology - Regulatory, Integrative and Comparative Physiology*, 293, pp.R662–R668.

Baldwin, Jr., A.S., 2001. The transcription factor NF-κB and human disease. *J Clin Invest*, 107(1), pp.3–6.

Bale, T.L. & Vale, W.W., 2004. CRF and CRF receptors: role in stress responsivity and other behaviors. *Annual review of pharmacology and toxicology*, 44, pp.525–57.

Baltgalvis, K.A. et al., 2009. The effects of prednisolone on skeletal muscle contractility in mdx mice. *Muscle Nerve*, 40(3), pp.443–454.

Bamberger, C.M. & Bamberger, A.M., 2000. The peripheral CRH/urocortin system. *Annals of the New York Academy of Sciences*, 917, pp.290–6.

Barbara, G. et al., 2006. Functional gastrointestinal disorders and mast cells implications for therapy - Barbara. *Neurogastroenterology & Motility*, 18(1), pp.6–17.

Barbui, C. & Hotopf, M., 2001. Forty years of antidepressant drug trials. *Acta Pychiatrica Scaninavia*, 104(2), pp.92–95.

Barohn, R., Amato, A. & Griggs, R., 1998. Overview of distal myopathies: from the clinical to the molecular. *Neuromuscular disorders : NMD*, 8(5), pp.309–16.

Barohn, R.J. et al., 1988. Gastric hypomotility in Duchenne's muscular dystrophy. *New England Journal of Medicine*, 319, pp.15–18.

Bartoo, A.C., Sprunger, L.K. & Schneider, D.A., 2005. Expression and distribution of TTX-sensitive sodium channel alpha subunits in the enteric nervous system. *The Journal of comparative neurology*, 486(2), pp.117–31.

Batchelor, C.L. & Winder, S.J., 2006. Sparks, signals and shock absorbers: how dystrophin loss causes muscular dystrophy. *Trends in cell biology*, 16(4), pp.198–205.

Bates, G. et al., 2013. Molecular, cellular, and muscle strip mechanics of the mdx mouse diaphragm. *American journal of physiology. Cell physiology*, 304(9), pp.C873–80.

Baydur, A. et al., 1990. Decline in Respiratory Function and Experience with Long-Term Assisted Ventilation in Advanced Duchenne's Muscular Dystophy. *Chest*, Apr(97(4)), pp.884–9.

Beck, J. et al., 2006. Diaphragmatic function in advanced Duchenne muscular dystrophy. *Neuromuscul Disord*, 16, pp.161–167.

Bethin, K., Vogt, S. & Muglia, L., 2000. Interleukin-6 is an essential, corticotropin-releasing hormone-independent stimulator of the adrenal axis during immune system activation. *Proceedings of the National Academy of Sciences of the United States of America*, 97(16), pp.9317–22.

Bia, B. et al., 1999. Decreased myocardial nNOS, increased iNOS and abnormal ECGs in mouse models of Duchenne muscular dystrophy. *Journal of molecular and cellular cardiology*, 31(10), pp.1857–62.

Blake, D., Tinsley, J. & Davies, K., 1996. Utrophin: a structural and functional comparison to dystrophin. *Brain Pathology*, Jan(6(1)), pp.37–47.

Bob, P. et al., 2010. Depression, traumatic stress and interleukin-6. *Journal of affective disorders*, 120(1-3), pp.231–4.

Boland, B. et al., 1995. Site-dependent pathological differences in smooth muscles and skeletal muscles of the adult mdx mouse. *Muscle Nerve*, June(18(6)), pp.649–57.

Boland, B.J. et al., 1996. Skeletal, cardiac, and smooth muscle failure in Duchenne muscular dystrophy. *Pediatric Neurology*, 14(1), pp.7–12.

Bonaz, B.L. & Bernstein, C.N., 2013. Brain-gut interactions in inflammatory bowel disease. *Gastroenterology*, 144(1), pp.36–49.

Borrelli, O. et al., 2005. Evolution of gastric electrical features and gastric emptying in children with Duchenne and Becker muscular dystrophy. *Am J Gastroenterol*, MArch(100 (3)), pp.695–702.

Borrelli, O. et al., 2005. Evolution of Gastric Electrical Features and Gastric Emptying in Children with Duchenne and Becker Muscular DystrophyGastric Motor Abnormalities in Children with Muscular Dystrophy. *The American Journal of Gastroenterology*, (100), pp.695–702.

Bothwell, J.E. et al., 2002. Duchenne Muscular Dystrophy--Parental Perceptions. *Clinical Pediatrics*, 41(2), pp.105–109.

Bradford, M.M., 1976. A rapid and sensitive method for the quantitation of microgram quantities of protein utilizing the principle of protein-dye binding. *Analytical biochemistry*, 72, pp.248–54.

Broquet, K.E., 1999. Status of Treatment of Depression. *Southern Medical Journal*, 92(9), pp.845–857.

De Bruin, P. et al., 1997. Diaphragm thickness and inspiratory strength in patients with Duchenne muscular dystrophy. *Thorax*, 52, pp.472–475.

Bulfield, G., 1984. X chromosome-linked muscular dystrophy. *Proc Natl Acad Sci USA*, 81(February), pp.1189–1192.

Bushby, K. et al., 2010. Diagnosis and management of Duchenne muscular dystrophy, part 1: diagnosis, and pharmacological and psychosocial management. *Lancet neurology*, 9(1), pp.77–93.

Byers, T., Lidov, W.H.G. & Kunkel, L.M., 1993. An alternative dystrophin transcript specific to peripheral nerve. *Nature Genetics*, 4, pp.77–81.

Byers, T.J., Kunkel, L.M. & Watkinst, S.C., 1991. The Subcellular Distribution of Dystrophin in Mouse Skeletal, Cardiac, and Smooth Muscle. *The Journal of cell biology*, 115(2), pp.411–421.

Caldarone, B. et al., 2003. Sex differences in response to oral amitriptyline in three animal models of depression in C57BL/6J mice. *Psychopharmacology*, 170(1), pp.94–101.

Camacho, A., 2013. Is anxious-depression an inflammatory state? *Medical hypotheses*.

Carlson, C.G., Samadi, A. & Siegel, A., 2005. Chronic treatment with agents that stabilize cytosolic IkappaB-alpha enhances survival and improves resting membrane potential in MDX muscle fibers subjected to chronic passive stretch. *Neurobiology of disease*, 20(3), pp.719–30.

Carre-Pierrat, M. et al., 2011. Pre-clinical study of 21 approved drugs in the mdx mouse. *Neuromuscular disorders : NMD*, 21(5), pp.313–27.

Castagné, V. et al., 2010. Rodent models of depression: forced swim and tail suspension behavioral despair tests in rats and mice. *Curr Protoc Pharmacol*, Jun(Chapter 5), p.Unit 5.8.

Di Certo, M.G. et al., 2010. The artificial gene Jazz, a transcriptional regulator of utrophin, corrects the dystrophic pathology in mdx mice. *Human molecular genetics*, 19(5), pp.752–60.

Chahbouni, M., Escames, G., et al., 2010. Melatonin treatment normalizes plasma pro-inflammatory cytokines and nitrosative/oxidative stress in patients suffering from Duchenne muscular dystrophy. *J Pineal Res*, Apr(48(3)), pp.282–9.

Chamberlain, J. et al., 1997. Interactions between dystrophin and the sarcolemma membrane. *Soc Gen Physiol Ser*, 52, pp.19–29.

Chang, J. et al., 2007. Urocortin 2 expression in the rat gastrointestinal tract under basal conditions and in chemical colitis. *Peptides*, July(28(7), pp.1453–60.

Chazaud, B. et al., 2003. Satellite cells attract monocytes and use macrophages as a support to escape apoptosis and enhance muscle growth. *The Journal of cell biology*, 163(5), pp.1133–43.

Chen, R. et al., 1993. Expression cloning of a human corticotropin-releasing-factor receptor. *Proceedings of the National Academy of Sciences of the United States of America*, 90(19), pp.8967–71.

Chesnokova, V. & Melmed, S., 2002. Minireview : Neuro-Immuno-Endocrine Modulation of the Hypothalamic-Pituitary-Adrenal (HPA) axis by gp130 signallingmolecules. *Endocrinology*, 143(5), pp.1571–1574.

Choleris, E. et al., 2001. A detailed ethological analysis of the mouse open field test: effects of diazepam, chlordiazepoxide and an extremely low frequency pulsed magnetic field. *Neuroscience and biobehavioral reviews*, 25(3), pp.235–60.

Chrousos, G.P., 1995. The hypothalamic-pituitary-adrenal axis and mune-mediated inflammation. *The New England journal of medicine*, 332(20), pp.1351–1362.

Claflin, D.R. & Brooks, S. V, 2008. Direct observation of failing fibers in muscles of dystrophic mice provides mechanistic insight into muscular dystrophy. *American journal of physiology. Cell physiology*, 294(2), pp.C651–8.

Clarke, G. et al., 2009. Irritable bowel syndrome: towards biomarker identification. *Trends in molecular medicine*, 15(10), pp.478–89.

Coirault, C. et al., 2002. Velocity of Actomyosin Sliding in Vitro Is Reduced in Dystrophic Mouse Diaphragm. *American Journal of respiratory and critical care medicine*, 165, pp.250–253.

Compton, A. et al., 2005. The syntrophin-dystrobrevin subcomplex in human neuromuscular disorders. *J Neuropathol Exp Neurol*, Apr(64(4)), pp.350–61.

Connor, T.J. & Leonard, B.E., 1998. Depression, Stress and Immunological Activation The Role of Cytokines in Depressive Disorders. *Life Sciences*, 62(7), pp.583–606.

Coste, S., Murray, S. & Stenzel-Poore, M., 2001. Animal models of CRH excess and CRH receptor deficiency display altered adaptations to stress. *Peptides*, 22(5), pp.733–41.

Coulton, G. et al., 1988. The mdx mouse skeletal muscle myopathy: II. Contractile properties. *Neuropathology and …*, Jul-Aug(14(4)), pp.299–314.

Cowen, P.J., 2008. Serotonin and depression: pathophysiological mechanism or marketing myth? *Trends in pharmacological sciences*, 29(9), pp.433–6.

Cozzoli, A. et al., 2011. Evaluation of potential synergistic action of a combined treatment with alpha-methyl-prednisolone and taurine on the mdx mouse model of Duchenne muscular dystrophy. *Neuropathology and applied neurobiology*, 37(3), pp.243–56.

Croisier, J.L. et al., 1999. Effects of training on exercise-induced muscle damage and interleukin 6 production. *Muscle and Nerve*, 22(2), pp.208–212.

Cros, D. et al., 1989. Muscle hypertrophy in Duchenne muscular dystrophy. *Journal of Neurology*, 236(1), pp.43–47.

Cryan, J.F., Mombereau, C. & Vassout, A., 2005. The tail suspension test as a model for assessing antidepressant activity: review of pharmacological and genetic studies in mice. *Neuroscience and biobehavioral reviews*, 29(4-5), pp.571–625.

Daisuke, K. et al., 2014. *IL-6 and Inflammatory Diseases*,

Damsa, C. et al., 2004. "Dopamine-dependent" side effects of selective serotonin reuptake inhibitors: a clinical review. *J Clin Psychiatry*, Aug(65(8)), pp.1064–8.

Dangain, J. & Vrbova, G., 1984. Muscle development in mdx mutant mice. *Muscle Nerve*, Nov-Dec(7(9)), pp.700–704.

Davies, K.E. & Nowak, K.J., 2006. Molecular mechanisms of muscular dystrophies: old and new players. *Nature reviews. Molecular cell biology*, 7(10), pp.762–73.

Deconinck, A.E. et al., 1997. Utrophin-dystrophin-deficient mice as a model for Duchenne muscular dystrophy. *Cell*, 90(4), pp.717–27.

Deconinck, N. & Dan, B., 2007. Pathophysiology of duchenne muscular dystrophy: current hypotheses. *Pediatric neurology*, 36(1), pp.1–7.

Deleo, F.R., 2013. Attractive shedding. *Blood*, 110, pp.1711–1712.

Deng, B., Glanzman, D. & Tidball, J.G., 2009. Nitric oxide generated by muscle corrects defects in hippocampal neurogenesis and neural differentiation caused by muscular dystrophy. *The Journal of physiology*, 587(Pt 8), pp.1769–78.

Desreumaux, P., 2000. Specific targeting of IL-6 signalling pathway: a new way to treat IBD? *Gut*, 47(4), pp.465–466.

Van Deutekom, J.C. et al., 2007. Local dystrophin restoration with antisense oligonucleotide PRO051. *The New England journal of medicine*, 357(26), pp.2677–86.

Dinan, D. et al., 2003. Gastric Wall Weakening Resulting in Separate Perforations in a Patient with Duchenne ' s Muscular Dystrophy. *American Journal of Roentgenology*, 181(September), pp.807–808.

Ding, S.Z., Cho, C.H. & Lam, S.K., 2000. Regulation of interleukin 6 production in a human gastric epithelial cell line MKN-28. *Cytokine*, 12(7), pp.1129–35.

Dowlati, Y. et al., 2010. A meta-analysis of cytokines in major depression. *Biological psychiatry*, 67(5), pp.446–57.

Du, Y. et al., 2013. Sputum Interleukin-6, Tumor necrosis factor-α and Salivary Cortisol as New Biomarkers of Depression in Lung Cancer Patients. *Progress in neuro-psychopharmacology & biological psychiatry*.

Dubowitz, V., 1976. Screening for Duchenne muscular dystrophy. *Archives of disease in childhood*, 51(249).

Duclos, F. et al., 1998. Beta-sarcoglycan: genomic analysis and identification of a novel missense mutation in the LGMD2E Amish isolate. *Neuromuscular disorders : NMD*, 8(1), pp.30–8.

Dunn, A. & Berridge, C., 1990. Physiological and behavioral responses to corticotropin-releasing factor administration: is CRF a mediator of anxiety or stress responses? *Brain Res Rev*, May-Aug(15(2)), pp.71–100.

Dunn, A.J., Swiergiel, A.H. & de Beaurepaire, R., 2005. Cytokines as mediators of depression: what can we learn from animal studies? *Neuroscience and biobehavioral reviews*, 29(4-5), pp.891–909.

Den Dunnen, J.T. & Beggs, A.H., 2006. Multiplex PCR for Identifying DMD Gene Deletions. *Current Protocols in Human Genetics*, 49(9)(1-9), p.3.22.

Ebihara, S. et al., 2000. Differential effects of dystrophin and utrophin gene transfer in immunocompetent muscular dystrophy (mdx) mice. *Physiol Genomics*, Sep 8(3(3)), pp.133–44.

Emery, A.E.H. & Muntoni, F., 2003. *Duchenne Muscular Dystrophy*,

Engel, W.K. & Hawley, R.J., 1977. Focal lesions of muscle in peripheral vascular disease. *Journal of Neurology*, 215(3), pp.161–168.

Ennen, J.P., Verma, M. & Asakura, A., 2013. Vascular-targeted therapies for Duchenne muscular dystrophy. *Skeletal Muscle*, 3(9), pp.1–12.

Van Erp, C., Irwin, N.G. & Hoey, A.J., 2006. Long-term administration of pirfenidone improves cardiac function in mdx mice. *Muscle & nerve*, 34(3), pp.327–34.

Erta, M., Quintana, A. & Hidalgo, J., 2012. Interleukin-6, a major cytokine in the central nervous system. *International journal of biological sciences*, 8(9), pp.1254–66.

Ervasti, J.M., 2007. Dystrophin, its interactions with other proteins, and implications for muscular dystrophy. *Biochimica et biophysica acta*, 1772(2), pp.108–17.

Ervasti, J.M., 2004. Structure and Function of the Dystrophin-Glycoprotein Complex. In *Molecular Mechanisms of Muscular Dystrophies*. p. Chapter 1.

Ervasti, J.M. & Campbell, K.P., 1991. Membrane organization of the dystrophin-glycoprotein complex. *Cell*, 66(6), pp.1121–1131.

Essex, C. & Roper, H., 2001. Late diagnosis of Duchenne ' s muscular dystrophy presenting as global developmental delay. *BMJ*, 323(July), pp.6–7.

Evans, N.P. et al., 2009. Dysregulated intracellular signaling and inflammatory gene expression during initial disease onset in Duchenne muscular dystrophy. *American journal of physical medicine & rehabilitation*, 88(6), pp.502–22.

Evans, N.P. et al., 2010. Immune mediated mechanisms potentially regulate the diseasecourse of Duchenne muscular dystrophy and provide targets for therapeutic interventin. *American Academy of Physical Medicine and Rehabilitation*, 1(8), pp.755–768.

Fall, A.M. et al., 2006. Induction of revertant fibres in the mdx mouse using antisense oligonucleotides. *Genetic vaccines and therapy*, 4(Dmd), p.3.

Faulkner, J.A. et al., 2008. Diaphragm muscle strip preparation for evaluation of gene therapies in mdx mice. *Clinical and experimental pharmacology & physiology*, 35(7), pp.725–9.

Felder, E. et al., 2005. Structural details of rat extraocular muscles and three-dimensional reconstruction of the rat inferior rectus muscle and muscle-pulley interface. *Vision research*, 45(15), pp.1945–55.

Feng, S. et al., 2013. Study on Duchenne muscular dystrophy gene mutation and prenatal diagnosis. *Zhonghua Yi Xue Yi Chuan Xue Za Zhi*, Feb(30(1)), pp.36–9.

Finsterer, J., 2006. Cardiopulmonary Support in Duchenne Muscular Dystrophy. *Lung*, (184), pp.205–215.

Fitzgerald, P. et al., 2008. Tryptophan catabolism in females with irritale boel syndrome:relationhip to interferon-gamma severity of symptoms and psyciatric co-morbidity. *Neurogastoenterol Motil*, Dec(20 (12)), pp.1291–7.

Fitzpatrick, C., Barry, C. & Garvey, C., 1986. Psychiatric disorder among boys with Duchenne muscular dystrophy. *Dev Med Child Neurol*, Oct(28(5)), pp.589–95.

Fletcher, S. et al., 2006. Dystrophin expression in the mdx mouse after localised and systemic administration of a morpholino antisense oligonucleotide. *The journal of gene medicine*, 8(2), pp.207–16.

La Fleur, S.E. et al., 2005. Role of peripheral corticotropin-releasing factor and urocortin II in intestinal inflammation and motility in terminal ileum. *Proceedings of the National Academy of Sciences of the United States of America*, 102(21), pp.7647–52.

Fong, P. et al., 1990. Increased activity of calcium leak channels in myotubes of Duchenne human and mdx mouse origin. *Science1*, November2(250(4981)), pp.673–6.

Francisco, L. et al., 2010. Depressive symptoms in rheumatoid arthritis patients. *Revista Brasileira de Psiquiatria*, 32(3), pp.257–263.

Frigeri, A. et al., 2002. Altered aquaporin-4 expression in human muscular dystrophies: a common feature? *FASEB journal*, 16(9), pp.1120–2.

Frommberger, U. et al., 1997. Interleukin-6-(IL-6) plasm. *Eur Arch Psychiatry Clin Neurosci*, (247(4)), pp.228–33.

Fujita, R. et al., 2014. Anti-interleukin-6 receptor antibody (MR16-1) promotes muscle regeneration via modulation of gene expressions in infiltrated macrophages. *Biochimica et biophysica acta*, Jan 15(S0304-4165(14)00016-6), pp.1–11.

Gehrig, S.M. et al., 2008. Insulin-like growth factor-I analogue protects muscles of dystrophic mdx mice from contraction-mediated damage. *Experimental physiology*, 93(11), pp.1190–8.

Geiger, P.C. et al., 2000. Maximum specific force depends on myosin heavy chain content in rat diaphragm muscle fibers. *J Appl Physiol*, 89, pp.695–703.

Gerber, A.R. & Bale, T.L., 2012. Antiinflammatory treatment ameliorates HPA stress axis dysfunction in a mouse model of stress sensitivity. *Endocrinology*, 153(10), pp.4830–7.

Gilbert, R.É.N. et al., 1999. Adenovirus-mediated utrophin gene transfer mitigates the dystrophic phenotype of mdx mouse muscles. *Human gene therapy*, 10(8), pp.1299–310.

Giuseppe, G., Barbui, C. & Hotopf, M., 2007. Amitriptyline for depression. *Cochrane Database of Systematic Reviews*, (3).

Glaser, R. & Kiecolt-glaser, J.K., 2005. Stress-induced immune dysfunction:implications for health. *Nature Reviews.Immunology*, 5(March), pp.243–25q.

Godfrey, C. et al., 2011. Dystroglycanopathies: coming into focus. *Current opinion in genetics & development*, 21(3), pp.278–85.

Goemans, N.M. et al., 2011. Systemic Administration of PRO051 in Duchenne's Muscular Dystrophy. *The New England journal of medicine*, March 25, pp.1–10.

González-Hernández, T. et al., 2006. Interleukin-6 and nitric oxide synthase expression in the vasopressin and corticotrophin-releasing factor systems of the rat hypothalamus. *The journal of histochemistry and cytochemistry : official journal of the Histochemistry Society*, 54(4), pp.427–41.

Gordon, B.S., Delgado Díaz, D.C. & Kostek, M.C., 2012. Resveratrol decreases inflammation and increases utrophin gene expression in the mdx mouse model of duchenne muscular dystrophy. *Clinical nutrition (Edinburgh, Scotland)*, pp.1–8.

Gosselin, L.E. & Williams, J.E., 2006. Pentoxifylline fails to attenuate fibrosis in dystrophic (mdx) diaphragm muscle. *Muscle & nerve*, 33(6), pp.820–3.

Gottrand, F., 1991. Archives of Disease in Childhood. *Archives of disease in childhood*.

Gourcerol, G. et al., 2011. Activation of corticotropin-releasing factor receptor 2 mediates the colonic motor coping response to acute stress in rodents. *Gastroenterology*, 140(5), pp.1586–96.e6.

Goyenvalle, A. et al., 2004. Rescue of dystrophic muscle through U7 snRNA-mediated exon skipping. *Science (New York, N.Y.)*, 306(5702), pp.1796–9.

Grange, R.W., 2011. Green tea extract decreases muscle pathology and NF-κB immunostaining in regenerating muscle fibers of mdx mice. *Clin Nutr*, 29(3), pp.391–398.

Gregorevic, P. et al., 2002. Improved contractile function of the mdx dystrophic mouse diaphragm muscle after insulin-like growth factor-I administration. *The American journal of pathology*, 161(6), pp.2263–72.

Gregorevic, P. et al., 2006. rAAV6-microdystrophin preserves muscle function and extends lifespan in severely dystrophic mice. *Nature medicine*, 12(7), pp.787–9.

Grounds, M.D. et al., 2008. Towards developing standard operating procedures for pre- clinical testing in the mdx mouse model of Duchenne muscular dystrophy. *Neurobiol Dis*, 31(1), pp.1–19.

Guido, A.N. et al., 2010. Fiber type composition of the sternomastoid and diaphragm muscles of dystrophin-deficient mdx mice. *Anatomical record (Hoboken, N.J. : 2007)*, 293(10), pp.1722–8.

Gumerson, J.D. & Michele, D.E., 2011. The dystrophin-glycoprotein complex in the prevention of muscle damage. *Journal of biomedicine & biotechnology*, 2011, pp.1–13.

Gustot, T. et al., 2005. Profile of soluble cytokine receptors in Crohn's disease. *Gut*, 54(4), pp.488–95.

Hajhashemi, V. et al., 2010. The role of central mechanisms in the anti-inflammatory effect of amitriptyline on carrageenan-induced paw edema in rats. *Clinics (São Paulo, Brazil)*, 65(11), pp.1183–7.

Hall, J.E. et al., 2007. Effects of a CRF2R agonist and exercise on mdx and wildtype skeletal muscle. *Muscle & nerve*, 36(3), pp.336–41.

Hara, H. et al., 2011. Aquaporin 4 Expression in the mdx Mouse Diaphragm. *Acta histochemica et cytochemica*, 44(4), pp.175–82.

Hinkle, R. et al., 2003. Urocortin II treatment reduces skeletal muscle mass and function loss during atrophy and increases nonatrophying skeletal muscle mass and function. *Endocrinology*, 144(11), pp.4939–46.

Hinkle, R.T. et al., 2003. Activation of the CRF 2 receptor modulates skeletal muscle mass under physiological and pathological conditions. *Am J Physiol Endocrinol Metab*, 285, pp.889–898.

Hinkle, R.T. et al., 2007. Corticortophin releasing factor 2 receptor agonist treatment significantly slows disease progression in mdx mice. *BMC medicine*, 5, p.18.

Hinkle, R.T. et al., 2004. Corticotropin releasing factor 2 receptor agonists reduce the denervation-induced loss of rat skeletal muscle mass and force and increase non-atrophying skeletal muscle mass and force. *Journal of muscle research and cell motility*, 25(7), pp.539–47.

Hirano, T. et al., 1989. A multifunctional cytokine (IL-6/BSF-2) and its receptor. *Int Arch Allergy Appl Immunol*, 88(1-2), pp.29–33.

Hirschfeld, R., 2000. History and evolution of the monoamine hypotheis of depression. *J Clin Psychiatryhiatry*, 61(Suppl 6), pp.4–6.

Hoffman, E., Brown, R. & Kunkel, L., 1987. Dystrophin: the protein product of the Duchenne muscular dystrophy locus. *Cell*, 51(6), pp.919–28.

Hoffman, E.P. et al., 1990. Somatic reversion/suppression of the mouse mdx phenotype in vivo. *Journal of the Neurological Sciences*, Oct(99(1)), pp.9–25.

Hoffman, E.P., Brown Jr., R.H. & Kunkel, L.M., 2003. Dystrophin: The protein product of the duchenne muscular dystrophy locus. *Cell*, 15(5), p.II.

Hollingworth, S., Marshall, M.W. & Robson, E., 1990. Excitation contraction coupling in normal and mdx mice. *Muscle & nerve*, 13(1), pp.16–20.

Holmberg, A., Olsson, C. & Hennig, G.W., 2007. TTX-sensitive and TTX-insensitive control of spontaneous gut motility in the developing zebrafish (Danio rerio) larvae. *The Journal of experimental biology*, 210(Pt 6), pp.1084–91.

Hortemo, K.H. et al., 2013. Multiple causes of fatigue during shortening contractions in rat slow twitch skeletal muscle. *PloS one*, 8(8), p.e71700.

Hu, X.Y., Ray, P.N. & Worton, R.G., 1991. Mechanisms of tandem duplication in the Duchenne muscular dystrophy gene include both homologous and nonhomologous intrachromosomal recombination. *The EMBO journal*, 10(9), pp.2471–7.

Huang, M. et al., 2009. Urocortin induces interleukin-6 release from rat cardiomyocytes through p38 MAP kinase , ERK and NF-kB activation. *Journal of Molecular Endochrinology*, 42, pp.397–405.

Huang, P. et al., 2009. Imatinib attenuates skeletal muscle dystrophy in mdx mice. *FASEB journal : official publication of the Federation of American Societies for Experimental Biology*, 23(8), pp.2539–48.

Hunt, L.C. et al., 2011. Alterations in the expression of leukemia inhibitory factor following exercise: comparisons between wild-type and mdx muscles. *PLoS currents*, 3, p.RRN1277.

Huynh, T. et al., 2013. Selective modulation through the glucocorticoid receptor ameliorates muscle pathology in mdx mice. *The Journal of pathology*, 231(2), pp.223–35.

Huzarska, M., Zieliński, M. & Herman, Z.S., 2006. Repeated treatment with antidepressants enhances dopamine D1 receptor gene expression in the rat brain. *European journal of pharmacology*, 532(3), pp.208–13.

Inglis, J., Jones, R.P. & Sloane, R.B., 1963. A psychiatric and psychological study of amitriptyline (Elavil) as an antidepressant. *Canadian Medical Association journal*, 88, pp.797–802.

Ito, H., 2005. Treatment of Crohn's disease ith anti-IL-6 receptor antibody. *Gastroenterology*, 40(Supplement XVI), pp.32–34.

Ito, K. et al., 2006. Smooth muscle-specific dystrophin expression improves aberrant vasoregulation in mdx mice. *Human Molecular Genetic*, 15(14), pp.5–7.

Itto, A. Ben et al., 2013. Evolution of Molecular Diagnosis of Duchenne Muscular Dystrophy. *J Mol Neurosci*, 50, pp.314–316.

Jacobs, B., van Praag, H. & Gage, F., 2000. Adult brain neurogenesis and psychiatry a no. *Mol Psychiatry*, May(5(3)), pp.262–9.

Jin, R.C. & Loscalzo, J., 2010. Vascular Nitric Oxide: Formation and Function. *Journal of blood medicine*, 2010(1), pp.147–162.

Jonsdottir, I.H. et al., 2000. Muscle contractions induce interleukin-6 mRNA production in rat skeletal muscles. *The Journal of physiology*, 528 Pt 1, pp.157–63.

Julio-Pieper, M. et al., 2010. A novel role for the metabotropic glutamate receptor-7: modulation of faecal water content and colonic electrolyte transport in the mouse. *British journal of pharmacology*, 160(2), pp.367–75.

Kageyama, K. et al., 2006. Urocortin induces interleukin-6 gene expression via cyclooxygenase-2 activity in aortic smooth muscle cells. *Endocrinology*, 147(9), pp.4454–62.

Kageyama, K. & Suda, T., 2003. Urocortin-Related Peptides Increase Interleukin-6 Output via Cyclic Adenoine 5'-Monophosphate-Dependant Pathways in A7r5 Aortic Smooth Muscle Cells. *Endocrinology*, 144(6), pp.2234–2241.

Kameya, S. et al., 1997. Dp260 disrupted mice revealed prolonged implicit time of the b-wave in ERG and loss of accumulation of beta-dystroglycan in the outer plexiform layer of the retina. *Human molecular genetics*, 6(13), pp.2195–203.

Kanagawa, M. & Toda, T., 2008. Fukutin and Fukuyama Congenital Muscular Dystrophy. *Experimental Glycoscience*, pp.309–312.

Kaprielian, R.R. et al., 2000. Distinct Patterns of Dystrophin Organization in Myocyte Sarcolemma and Transverse Tubules of Normal and Diseased Human Myocardium. *Circulation*, 100, pp.2586–2594.

Karalis, K. et al., 1997. CRH and the immune system. *Journal of Neuroimmunology*, 72, pp.131–136.

Kargacin, M. & Kargacin, G., 1996. The sarcoplasmic reticulum calcium pump is functionally altered in dystrophic muscle. *Biochim Biophys Actaq*, May 21(1290(1)), pp.4–8.

Karin, M. & Delhase, M., 2000. The IκB kinase (IKK) and NF-κB key elements of proinflammatory signalling. *Seminars in Immunology*, 12(1), pp.85–98.

Keep, N.H., 2000. Structural comparison of actin binding in utrophin and dystrophin. *Neurological sciences : official journal of the Italian Neurological Society and of the Italian Society of Clinical Neurophysiology*, 21(5 Suppl), pp.S929–37.

Kelles, A., Janssens, J. & Tack, J., 2000. IL-1beta and IL-6 excite neurones and suppress cholinergic neurotransmission in the myenteric plexus of the guinea pig. *Neurogastroenterology and Motility*, 12(6), pp.531–538.

Khairallah, M. et al., 2007. Metabolic and signaling alterations in dystrophin-deficient hearts precede overt cardiomyopathy. *Journal of molecular and cellular cardiology*, 43(2), pp.119–29.

Kishimoto, T. et al., 1995. A sauvagine/corticotropin-releasing factor receptor expressed in heart and skeletal muscle. *Proceedings of the National Academy of Sciences of the United States of America*, 92(4), pp.1108–12.

Klingler, W. et al., 2012. The role of fibrosis in Duchenne muscular dystrophy. *Acta myologica : myopathies and cardiomyopathies : official journal of the Mediterranean Society of Myology / edited by the Gaetano Conte Academy for the study of striated muscle diseases*, 31(3), pp.184–95.

Koenig, M. et al., 1987. Complete cloning of the Duchenne muscular dystrophy (DMD) cDNA and preliminary genomic organization of the DMD gene in normal and affected individuals. *Cell*, 50(3), pp.509–17.

Koenig, M. et al., 1989. The molecular basis for Duchenne versus Becker muscular dystrophy: correlation of severity with type of deletion. *American journal of human genetics*, 45(4), pp.498–506.

Korman, S.H. et al., 1991. Orocaecal transit time in Duchenne muscular dystrophy. *Archives of disease in childhood*, 66, pp.143–144.

Kostek, M. et al., 2012. IL-6 signaling blockade increases inflammation but does not improve muscle function in the mdx mouse. *BMC musculoskeletal disorders*, 13(1), p.106.

Krag, T.O.B. et al., 2004. Heregulin ameliorates the dystrophic phenotype in mdx mice. *Proceedings of the National Academy of Sciences of the United States of America*, 101(38), pp.13856–60.

Kravchenco, I. V. & Furalev, V.A., 1994. Secretion of Immunoreactive Corticotrophin Releasng Factor and Adrenocorticotripic Hormone By T- and B- Lymphocytes in Response to Cellular Stress Factors. *Biochemical and biophysical research communications*, 204(2), pp.828–834.

Kubera, M. et al., 2000. The effect of repeated amitriptyline and desipramine administration on cytokine release in C57BL/6 mice. *Psychoneuroendocrinology*, 25(8), pp.785–97.

Kumar, A. & Boriek, A.M., 2003. Mechanical stress activates the nuclear factor-kappaB pathway in skeletal muscle fibers: a possible role in Duchenne muscular dystrophy. *FASEB journal*, 17(3), pp.386–96.

Kwon, H., Oh, S. & Kim, J., 2008. Glabridin, a functional compound of liquorice, attenuates colonic inflammation in mice with dextran sulphate sodium-induced colitis. *Clinical and experimental immunology*, 151(1), pp.165–73.

Lai, M. et al., 2003. Differential regulation of corticosteroid receptors by monoamine neurotransmitters and antidepressant drugs in primary hippocampal culture. *Neuroscience*, 118(4), pp.975–984.

Lapidos, K.A., Kakkar, R. & McNally, E.M., 2004. The dystrophin glycoprotein complex: signaling strength and integrity for the sarcolemma. *Circulation research*, 94(8), pp.1023–31.

Larson, S.J. & Dunn, A.J., 2001. Behavioral Effects of Cytokines. *Brain Behavior and Immunity*, 387(15), pp.371–387.

Lecarpentier, Y. et al., 1998. Mechanics , energetics , and crossbridge kinetics of rabbit diaphragm during congestive heart failure. *FASEB journal : official publication of the Federation of American Societies for Experimental Biology*, 12, pp.981–989.

Leduc, C. et al., 2002. The Effect of Local Anesthetics and Amitriptyline on Peroxidation In Vivo in an Inflammatory Rat Model: Preliminary Reports. *Anesthesia and Analgesia*, 95, pp.992–996.

Leon, S. et al., 1986. Chronic intestinal pseudoobstruction as a complication of Duchenne's muscular dystrophy. *Gastroenterology*, Feb(90(2)).

Leucht, C., Huhn, M. & Leucht, S., 2012. Amitriptyline versus placebo for major depressive disorder (Review). *The Cochrane Collaboration*, (12).

Lewis, C. & Ohlendieck, K., 2010. Proteomic profiling of naturally protected extraocular muscles from the dystrophin-deficient mdx mouse. *Biochemical and biophysical research communications*, 396(4), pp.1024–9.

Libermann, T.A. & Baltimore, D., 1990. Activation of Interleukin-6 Gene Expression through the NF-KB Transcription Factor. *Molecular and Cellular Biology*, 10(5), pp.2327–2334.

Lidov, H., Byers, T. & Kunkel LM, 1993. The distribution of dystrophin in the murine central nervous system: an immunocytochemical study. *Neuroscience*, May(54(1)), pp.167–87.

Lim, J.-H., Kim, D.-Y. & Bang, M.S., 2004. Effects of exercise and steroid on skeletal muscle apoptosis in the mdx mouse. *Muscle & nerve*, 30(4), pp.456–62.

Liu, G.-X. et al., 2007. Reduced anxiety and depression-like behaviors in mice lacking GABA transporter subtype 1. *Neuropsychopharmacology : official publication of the American College of Neuropsychopharmacology*, 32(7), pp.1531–9.

Lochmüller, H. & Bushby, K., 2013. Becker and Duchenne muscular dystrophy: a two-way information process for therapies. *Journal of neurology, neurosurgery, and psychiatry*, 0(0).

Love, D. et al., 1989. An autosomal transcript in skeletal muscle with homology to dystrophin. *Nature*, May(4;339(6219)), pp.55–8.

Lovering, R.M. et al., 2009. Malformed mdx myofibers have normal cytoskeletal architecture yet altered EC coupling and stress-induced Ca2 + signaling. *Am J Physiol Cell Physiol*, 297(3), pp.571–580.

Lu, Q.L. et al., 2003. Functional amounts of dystrophin produced by skipping the mutated exon in the mdx dystrophic mouse. *Nature medicine*, 9(8), pp.1009–14.

Lu, Q.L. et al., 2005. Systemic delivery of antisense oligoribonucleotide restores dystrophin expression in body-wide skeletal muscles. *Proceedings of the National Academy of Sciences of the United States of America*, 102(1), pp.198–203.

Lu, Q.-L. et al., 2011. The status of exon skipping as a therapeutic approach to duchenne muscular dystrophy. *Molecular therapy : the journal of the American Society of Gene Therapy*, 19(1), pp.9–15.

Luethi, M., Meier, B. & Sandi, C., 2008. Stress effects on working memory, explicit memory, and implicit memory for neutral and emotional stimuli in healthy men. *Frontiers in behavioral neuroscience*, 2, p.5.

Lust, J. et al., 1992. Isolation of an mRNA encoding a soluble form of the human interleukin-6 receptor. *Cytokine1*, Mar(4(2)), pp.96–100.

Lydiard, R., 1991. Coexisting depression and anxiety special. *J Clin*, Jun(52), pp.48–54.

Lydiard RB, 1991. Coexisting depression and anxiety: special diagnostic and treatment issues. *J Clin Psychiatry*, June(52), pp.48–52.

Lynch, G.S. et al., 2001. Force and power output of fast and slow skeletal muscles from mdx mice 6-28 months old. *The Journal of physiology*, 535(Pt 2), pp.591–600.

Maes, M. et al., 2012. Depression and sickness behavior are Janus-faced responses to shared inflammatory pathways. *BMC medicine*, 10(66), pp.1–19.

Maes, M., 2008. The cytokine hypothesis of depression: inflammation, oxidative & nitrosative stress (IO&NS) and leaky gut as new targets for adjunctive treatments in depression. *Neuro endocrinology letters*, 29(3), pp.287–91.

Maillot, L. et al., 2002. Human urocortin II , a new CRF-related peptide , displays selective CRF 2 - mediated action on gastric transit in rats. *Am J Physiol Gastrointest Liver Physiol*, 282, pp.34–40.

Mallouk, N., Jacquemond, V. & Allard, B., 2000. Elevated subsarcolemmal Ca2+ in mdx mouse skeletal muscle fibers detected with Ca2+-activated K+ channels. *Proceedings of the National Academy of Sciences of the United States of America*, 97(9), pp.4950–5.

Mancinellia, R. et al., 1995. Analysis of peristaltic reflex in young mdx dystrophic mice. *Neuroscience Letters*, 192(1), pp.57–60.

Manzur, A. et al., 2007. Glucocorticoid corticosteroids for Duchenne muscular dystrophy (Review). *The Cochrane Collaboration*, (4).

Marques, M.J. et al., 2009. Long-term therapy with deflazacort decreases myocardial fibrosis in mdx mice. *Muscle & nerve*, 40(3), pp.466–8.

Mart, V. et al., 2004. Central CRF , urocortins and stress increase colonic transit via CRF 1 receptors while activation of CRF 2 receptors delays gastric transit in mice. *j Phsiol*, 1(556), pp.221–234.

Martinez, V. et al., 2004. Urocortins and the regulation of gastrointestinal motor function and visceral pain. *Peptides*, 25(10), pp.1733–44.

Martínez, V. et al., 2002. Differential actions of peripheral corticotropin-releasing factor (CRF), urocortin II, and urocortin III on gastric emptying and colonic transit in mice: role of CRF receptor subtypes 1 and 2. *The Journal of pharmacology and experimental therapeutics*, 301(2), pp.611–7.

März, P. et al., 1998. Sympathetic neurons can produce and respond to interleukin 6. *Proceedings of the National Academy of Sciences of the United States of America*, 95(6), pp.3251–6.

Matsumura, C.Y. et al., 2011. Stretch-activated calcium channel protein TRPC1 is correlated with the different degrees of the dystrophic phenotype in mdx mice. *American journal of physiology. Cell physiology*, 301(6), pp.C1344–50.

Matsumura, K. et al., 1992. Association of dystrophin-related protein with dystrophin-associated proteins in mdx mouse muscle. *Nature1*, Dec 10(360(6494)), pp.588–91.

McKay, B.R. et al., 2009. Association of interleukin-6 signalling with the muscle stem cell response following muscle-lengthening contractions in humans. *PloS one*, 4(6), p.e6027.

Meléndez, G.C. et al., 2010. Interleukin 6 mediates myocardial fibrosis, concentric hypertrophy, and diastolic dysfunction in rats. *Hypertension*, 56(2), pp.225–31.

Menazza, S. et al., 2010. Oxidative stress by monoamine oxidases is causally involved in myofiber damage in muscular dystrophy. *Human molecular genetics*, 19(21), pp.4207–15.

Meneses, A., Terrón, J. & Hong, E., 1997. Effects of the 5-HT receptor antagonists GR127935 (5-HT1B/1D) and MDL100907 (5-HT2A) in the consolidation of learning. *Behav Brain Res*, Dec(89 (1-2)), pp.217–23.

Messina, S. et al., 2011. Activation of NF-kappaB pathway in Duchenne muscular dystrophy: relation to age. *Acta myologica : myopathies and cardiomyopathies : official journal of the Mediterranean Society of Myology / edited by the Gaetano Conte Academy for the study of striated muscle diseases*, 30(1), pp.16–23.

Michele, D.E. & Campbell, K.P., 2003. Dystrophin-glycoprotein complex: post-translational processing and dystroglycan function. *The Journal of biological chemistry*, 278(18), pp.15457–60.

Miles, M.T. et al., 2011. Reduced resting potentials in dystrophic (mdx) muscle fibers are secondary to NF-κB-dependent negative modulation of ouabain sensitive Na+-K+ pump activity. *Journal of the neurological sciences*, 303(1-2), pp.53–60.

Mizunoya, W. et al., 2011. Nitric oxide donors improve prednisone effects on muscular dystrophy in the mdx mouse diaphragm. *American journal of physiology. Cell physiology*, 300(5), pp.C1065–77.

Moens, P., Baatsen, P.H. & Maréchal, G., 1993. Increased susceptibility of EDL muscles from mdx mice to damage induced by contractions with stretch. *Journal of muscle research and cell motility*, 14(4), pp.446–51.

Monaco, A.P. et al., 1986. Isolation of candidate cDNAs for portions of the Duchenne muscular dystrophy gene. *Nature*, 323(6089), pp.646–50.

Mosqueira, M. et al., 2013. Cardiac and Respiratory Dysfunction in Duchenne Muscular Dystrophy and the Role of Second Messengers. *Medicinal Research Revies*, 33(5), pp.1174–1213.

Moss, A.C. et al., 2007. Urocortin II mediates pro-inflammatory effects in human colonocytes via corticotropin-releasing hormone receptor 2alpha. *Gut*, 56(9), pp.1210–7.

Mulé, F. et al., 1999. Mechanical activity of small and large intestine in normal and mdx mice: a comparative analysis. *Neurogastroenterology and motility : the official journal of the European Gastrointestinal Motility Society*, 11(2), pp.133–9.

Mulè, F., Amato, A. & Serio, R., 2010. Gastric emptying, small intestinal transit and fecal output in dystrophic (mdx) mice. *The journal of physiological sciences : JPS*, 60(1), pp.75–9.

Muntoni, F. et al., 1994. Deletions in the 5' region of dystrophin and resulting phenotypes. *Journal of medical genetics*, 31(11), pp.843–7.

Muntoni, F., Mateddu, a & Serra, G., 1991. Passive avoidance behaviour deficit in the mdx mouse. *Neuromuscular disorders : NMD*, 1(2), pp.121–3.

Muntoni, F., Torelli, S. & Ferlini, A., 2003. Dystrophin and mutations : one gene , several proteins , multiple phenotypes. *Neurology*, 44, pp.731–740.

Nakae, Y. et al., 2012. Quantitative evaluation of the beneficial effects in the mdx mouse of epigallocatechin gallate, an antioxidant polyphenol from green tea. *Histochemistry and cell biology*, 137(6), pp.811–27.

Nakae, Y. et al., 2008. Subcutaneous injection, from birth, of epigallocatechin-3-gallate, a component of green tea, limits the onset of muscular dystrophy in mdx mice: a quantitative histological, immunohistochemical and electrophysiological study. *Histochemistry and cell biology*, 129(4), pp.489–501.

Nakamura, A. & Takeda, S., 2011. Mammalian models of Duchenne Muscular Dystrophy: pathological characteristics and therapeutic applications. *Journal of biomedicine & biotechnology*, 2011, p.184393.

Nasir, G.A. et al., 2013. Mesenchymal stem cells and Interleukin-6 attenuate liver fibrosis in mice. *Journal of Translational Medicine*, 11(78), pp.1–9.

Natale, L. et al., 2003. Interleukins 1 beta and 6 induce functional alteration of rat colonic motility: an in vitro study. *European journal of clinical investigation*, 33(8), pp.704–12.

Naughton, M., Mulrooney, J. & Leonard, B., 2000. A review of the role of serotonin receptors in psychiatric disorders. *Hum Psychpharmacol*, Aug(15(6)), pp.397–415.

Nicholson, L. V et al., 1993. Functional significance of dystrophin positive fibres in Duchenne muscular dystrophy. *Archives of disease in childhood*, 68(5), pp.632–6.

Nigro, G. et al., 1990. The incidence and evolution of cardiomyopathy in Duchenne muscular dystrophy. *Int J Cardiol*, Mar(26(3)), pp.271–7.

Nijsen, M. et al., 2005. Divergent role for CRF1 and CRF2 receptors in the modulation of visceral pain. *Neurogastroenterology and motility : the official journal of the European Gastrointestinal Motility Society*, 17(3), pp.423–32.

Nishimoto, N. & Kishimoto, T., 2004. Inhibition of IL-6 for the treatment of inflammatory diseases. *Current opinion in pharmacology*, 4(4), pp.386–91.

Nishio, H. et al., 1994. Identification of a novel first exon in the human dystrophin gene and of a new promoter located more than 500 kb upstream of the nearest known promoter. *The Journal of clinical investigation*, 94(3), pp.1037–42.

Nudel, U. et al., 1989. Duchenne muscular dystrophy gene product is not identical in muscle and brain. *Nature*, Jan 5(6202), pp.76–8.

O' Malley, D., Quigley, E.M.M., et al., 2011. Do interactions between stress and immune responses lead to symptom exacerbations in irritable bowel syndrome ? *Brain Behavior and Immunity*, 25(7), pp.1333–1341.

O' Malley, D., Liston, M., et al., 2013. Colonic soluble mediators from the maternal separation model of irritable bowel syndrome activate submucosal neurons via an interleukin-6-dependent mechanism. *American journal of physiology. Gastrointestinal and liver physiology*, 300(2), pp.G241–52.

O' Malley, D., Cryan, J.F. & Dinan, T.G., 2013. Crosstalk between interleukin-6 and corticotropin-releasing factor modulate submucosal plexus activity and colonic secretion. *Brain Behavior and Immunity*, 30, pp.115–124.

O' Malley, D., Dinan, T.G. & Cryan, J.F., 2011a. Altered expression and secretion of colonic Interleukin-6 in a stress-sensitive animal model of brain-gut axis dysfunction. *Journal of Neuroimmunology*, 235(1-2), pp.48–55.

O' Malley, D., Dinan, T.G. & Cryan, J.F., 2011b. Neonatal maternal separation in the rat impacts on the stress responsivity of central corticotropin-releasing factor receptors in adulthood. *Psychopharmacology*, 214, pp.221–229.

O'Brien, S.M. et al., 2007. Plasma cytokine profiles in depressed patients who fail to respond to selective serotonin reuptake inhibitor therapy. *Journal of psychiatric research*, 41(3-4), pp.326–31.

O'Malley, D., Dinan, T.G., et al., 2010. Alterations in colonic corticotropin-releasing factor receptors in the maternally separated rat model of irritable bowel syndrome : Differential effects of acute psychological and physical stressors. *Peptides*, 31(4), pp.662–670.

O'Malley, D., Julio-Pieper, M., et al., 2010. Distinct alterations in colonic morphology and physiology in two rat models of enhanced stress-induced anxiety and depression-like behaviour. *Stress (Amsterdam, Netherlands)*, 13(2), pp.114–22.

Ohama, T., Hori, M. & Ozaki, H., 2007. Mechanism of abnormal intestinal motility in inflammatory bowel disease: how smooth muscle contraction is reduced? *Journal of smooth muscle research = Nihon Heikatsukin Gakkai kikanshi*, 43(2), pp.43–54.

Olivier M, D. et al., 2006. Green tea extract and its major polyphenol (-)-epigallocatechin gallate improve muscle function in a mouse model for Duchenne muscular dystrophy. *American journal of physiology. Cell physiology*, 290(2), pp.C616–25.

Pan, Y. et al., 2008. Curcumin alleviates dystrophic muscle pathology in mdx mice. *Molecules and cells*, 25(4), pp.531–7.

Passamano, L. et al., 2012. Improvement of survival in Duchenne Muscular Dystrophy: retrospective analysis of 835 patients. *Acta myologica : myopathies and cardiomyopathies : official journal of the Mediterranean Society of Myology / edited by the Gaetano Conte Academy for the study of striated muscle diseases*, 31(2), pp.121–5.

Pastoret, C. & Sebille, a, 1995. mdxMice Show Progressive Weakness and Muscle Deterioration With Age. *Journal of the neurological sciences*, 129(2), pp.97–105.

Payne, E.T. et al., 2006. Nutritional therapy improves function and complements corticosteroid intervention in mdx mice. *Muscle & nerve*, 33(1), pp.66–77.

Pedersen, B.K. & Febbraio, M.A., 2008. Muscle as an Endocrine Organ : Focus on Muscle-Derived Interleukin-6. *Physiol rev*, 88, pp.1379–1406.

Peterson, J.M. et al., 2011. Peptide-Based Inhibition of NF- κ B Rescues Diaphragm Duchenne Muscular Dystrophy. *Mol Med*, 17(5-6), pp.508–515.

Petrof, B., Stedman, H., et al., 1993. Adaptations in myosin heavy chain expression and contractile function in dystrophic mouse diaphragm. *1Am J Physiol*, Sep(365 (3 Pt 1)), pp.834–41.

Petrof, B., Shrager, J.B., et al., 1993. Dystrophin protects the sarcolemma from stresses developed during muscle contraction. *Proceedings of the National Academy of Sciences of the United States of America*, 90(8), pp.3710–4.

Pierno, S. et al., 2007. Role of tumour necrosis factor alpha, but not of cyclo-oxygenase-2-derived eicosanoids, on functional and morphological indices of dystrophic progression in mdx mice: a pharmacological approach. *Neuropathology and applied neurobiology*, 33(3), pp.344–59.

Plomgaard, P., Penkowa, M. & Pedersen, B.K., 2005. Fiber type specific expression of TNF-alpha , IL-6 and IL-18 in human skeletal muscles Running title : Cytokine Expression is Fiber Type Dependent. *Exerc Immunol Rev*, 11, pp.53–63.

Podhorska-Okolow, M. et al., 1998. Apoptosis of myofibres and satellite cells: exercise-induced damage in skeletal muscle of the mouse. *Neuropathology and …*.

Porsolt, R.D. et al., 2001. Rodent Models of Depression : Forced Swimming and Tail Suspension Behavioral. *Current Protocols in Neuroscience*, Supplement, pp.1–10.

Porter, J.D. et al., 2002. A chronic inflammatory response dominates the skeletal muscle molecular signature in dystrophin-deficient mdx mice. *Human molecular genetics*, 11(3), pp.263–72.

Prut, L. & Belzung, C., 2003. The open field as a paradigm to measure the effects of drugs on anxiety-like behaviors: a review. *European Journal of Pharmacology*, 463(1-3), pp.3–33.

Radley, H.G., Davies, M.J. & Grounds, M.D., 2008. Reduced muscle necrosis and long-term benefits in dystrophic mdx mice after cV1q (blockade of TNF) treatment. *Neuromuscular disorders : NMD*, 18(3), pp.227–38.

Rall, J., 1985. Energetic aspects of skeletal muscle contraction:implications of fibre types. *Exerc Sport Sci Rev*, 13, pp.33–74.

Rando, T.A., 2001. The dystrophin–glycoprotein complex, cellular signaling, and the regulation of cell survival in the muscular dystrophies. *Muscle & Nerve*, 24(112), pp.1575–1594.

Reutenauer-Patte, J. et al., 2012. Urocortins improve dystrophic skeletal muscle structure and function through both PKA- and Epac-dependent pathways. *The American journal of pathology*, 180(2), pp.749–62.

Reyes, T.M. et al., 2001. Urocortin II: a member of the corticotropin-releasing factor (CRF) neuropeptide family that is selectively bound by type 2 CRF receptors. *Proceedings of the National Academy of Sciences of the United States of America*, 98(5), pp.2843–8.

Rifai, Z. et al., 1995. Effect of prednisone on protein metabolism in Duchenne dystrophy. *The American journal of physiology*, 268(1 Pt 1), pp.E67–74.

Robertson, D.A.F. et al., 1989. Personality profile and affective state of patients with inflammatory bowel disease. *Gut*, 30, pp.623–626.

Roccella, M., Pace, R. & De Gregorio, M., 2003. Psychopathological assessment in children affected by Duchenne de Boulogne muscular dystrophy. *Minerva Pediatr*, Jun(55 (3)), pp.267–73, 273–6.

Romfh, A. & McNally, E.M., 2010. Cardiac assessment in duchenne and becker muscular dystrophies. *Current heart failure reports*, 7(4), pp.212–8.

Rose-John, S., 2012. IL-6 trans-signaling via the soluble IL-6 receptor: importance for the pro-inflammatory activities of IL-6. *International journal of biological sciences*, 8(9), pp.1237–47.

Rosen, J.B. & Schulkin, J., 1998. From normal fear to pathological anxiety. *Psychological Revew*, 105(2)(Apr 1998), pp.325–350.

Rubinsztein, J.S. et al., 1998. Apathy and hypersomnia are common features of myotonic dystrophy. *Journal of neurology, neurosurgery, and psychiatry*, 64(4), pp.510–5.

Ruegg, U.T. et al., 2002. Pharmacological control of cellular calcium handling in dystrophic skeletal muscle. *Neuromuscular disorders : NMD*, 12 Suppl 1, pp.S155–61.

Rufo, A. et al., 2011. Mechanisms inducing low bone density in Duchenne muscular dystrophy in mice and humans. *Journal of bone and mineral research : the official journal of the American Society for Bone and Mineral Research*, 26(8), pp.1891–903.

Rybakova, I.N. et al., 2006. Dystrophin and utrophin bind actin through distinct modes of contact. *The Journal of biological chemistry*, 281(15), pp.9996–10001.

Sabharwal, R., 2014. The link between stress disorders and autonomic dysfunction in muscular dystrophy. *Frontiers in physiology*, 5(January), p.25.

Sali, A. et al., 2012. Glucocorticoid-treated mice are an inappropriate positive control for long-term preclinical studies in the mdx mouse. *PloS one*, 7(4), p.e34204.

Salinthone, S., Singer, C. a & Gerthoffer, W.T., 2004. Inflammatory gene expression by human colonic smooth muscle cells. *American journal of physiology. Gastrointestinal and liver physiology*, 287(3), pp.G627–37.

Sang-Jun, N. et al., 2013. Clinical , immunohistochemical , Western blot , and genetic analysis in dystrophinopathy. *Journal of Clinical Neuroscience*, 20(8), pp.1099–1105.

Sarna, S., 2010. *Colonic Motility Dysfunction - Colonic Motility - NCBI Bookshelf*,

Schara, U. & Mortier, W., 2001. Long-term steroid therapy in Duchenne muscular dystrophy-positive results versus side effects. *Journal of Clinical Neuromuscular …*.

Schreiber, A. et al., 1987. Magnetic resonance imaging of children with Duchenne muscular dystrophy. *Pediatric Radiology …*, (17), pp.495–497.

Schuster, B. et al., 2003. The human interleukin-6 (IL-6) receptor exists as a preformed dimer in the plasma membrane. *FEBS Letters*, 538(1-3), pp.113–116.

Seidman, R., 1983. Skeletal Muscle Pathology. *The American Journal of Surgical Pathology*, 7(8), p.871. Available at: http://content.wkhealth.com/linkback/openurl?sid=WKPTLP:landingpage&an=00000478-198307080-00015.

Sekiguchi, M. et al., 2009. A deficit of brain dystrophin impairs specific amygdala GABAergic transmission and enhances defensive behaviour in mice. *Brain : a journal of neurology*, 132(Pt 1), pp.124–35.

Serio, R., Bonvissuto, F. & Mulè, F., 2001. Altered electrical activity in colonic smooth muscle cells from dystrophic (mdx) mice. *Neurogastroenterol Motil*, Apr(13(2)), pp.169–75.

Shima, Y. et al., 2010. The skin of patients with systemic sclerosis softened during the treatment with anti-IL-6 receptor antibody tocilizumab. *Rheumatology*, (September), pp.2408–2412.

Siegel, A.L. et al., 2009. Treatment with inhibitors of the NF-kappaB pathway improves whole body tension development in the mdx mouse. *Neuromuscular disorders : NMD*, 19(2), pp.131–9.

Simonds, A.K. et al., 1998. Impact of nasal ventilation on survival in hypercapnic Duchenne muscular dystrophy. *Thorax*, 53(11), pp.949–952.

Spencer, M.J., Croal, l D.E. & Tidball, J.G., 1995. Calpains Are Activated in Necrotic Fibers from mdxDystrophic Mice. *The Journal of Biological Chemistry*, 270(18), pp.10909–10914.

Spurney, C. et al., 2009. Preclinical drug trials in the mdx mouse Assessment of reliable and sensitive outcome measures. *Muscle & Nerve*, May(39(5)), pp.591–602.

Squire, S. et al., 2002. Prevention of pathology in mdx mice by expression of utrophin: analysis using an inducible transgenic expression system. *Human molecular genetics*, 11(26), pp.3333–44.

Stedman, H.H. et al., 1991. The mdx mouse diaphragm reproduces the degenerative changes of Duchenne muscular dystrophy. *Nature*, 352(6335), pp.536–9.

Steru, L. et al., 1985. The tail suspension test: A new method for screening antidepressants in mice. *Psychopharmacology*, 85(3), pp.367–370.

Stevens, E.D. & Faulkner, J.A., 2000. The capacity of mdx mouse diaphragm muscle to do oscillatory work. *Journey of Physiology*, 522(3), pp.457–466.

Strik, J.J.M.H., Honig, A. & Maes, M., 2001. Depression and Myocardial Infarction: Relationship between heart and mind. *Progress in neuro-psychopharmacology & biological psychiatry*, 25, pp.879–892.

Stuckey, D.J. et al., 2012. In vivo MRI characterization of progressive cardiac dysfunction in the mdx mouse model of muscular dystrophy. *PloS one*, 7(1), p.e28569.

Summan, M. et al., 2006. Mechanisms of Tissue Repair Macrophages and skeletal muscle regeneration : a clodronate-containing liposome depletion study. *Am J Physiol Integr Comp Physiol*, 26505, pp.1488–1495.

Taché, Y. et al., 1993. Role of CRF in stress-related alterations of gastric and colonic motor function stress-related alterations o. *Ann N Y Anad Sci*, Oct 29(697), pp.233–43.

Taga, T., 1997. gp130 AND THE INTERLEUKIN-6 FAMILY OF CYTOKINES. *Immunology*, (15(1)), pp.797–81+.

Tai, Y.-H. et al., 2006. Amitriptyline suppresses neuroinflammation and up-regulates glutamate transporters in morphine-tolerant rats. *Pain*, 124(1-2), pp.77–86.

Tameyasu, T., Ogura, S. & Ogihara, K., 2004. The Effect of e- , i- , and n-Nitric Oxide Synthase Inhibition on Colonic Motility in Normal and Muscular Dystrophy (mdx) Mice. *Japanese Journal of Physiology*, 54(6), pp.555–566.

Tamura, T., 1993. Soluble interleukin-6 receptor triggers osteoclast formation by interleukin 6. *Proc Natl Acad Sci USA*, 90(December), pp.11924–11928.

Thanh, L.T. et al., 1995. Characterization of revertant muscle fibers in Duchenne muscular dystrophy, using exon-specific monoclonal antibodies against dystrophin. *American journal of human genetics*, 56(3), pp.725–31.

Thi, M., Spra, Y. & Hanani, M., 2008. Aquaporin-4 water channels in enteric neurons. *J Neurosci Res*, Feb 1(86(2)), pp.448–56.

Tinsley, J. et al., 1998. Expression of full-length utrophin prevents muscular dystrophy in mdx mice. *Nature medicine*, 4(12), pp.1441–4.

Tinsley, J.M., Blake, D.J. & Davies, K.E., 1993. Apo-dystrophin-3: a 2.2kb transcript from the DMD locus encoding the dystrophin glycoprotein binding site. *Human Molecular Genetic*, 2(5), pp.521–524.

Tonghui, M. & Verkman, A.S., 1999. Aquaporin water channels in gastrointestinal physiology. *Journal Of Physiology*, 517, pp.317–326.

Torelli, S. et al., 1999. Expression, regulation and localisation of dystrophin isoforms in human foetal skeletal and cardiac muscle. *Neuromuscular disorders : NMD*, 9(8), pp.541–51.

Tsatsanis, C. et al., 2007. Corticotropin Releasing Factor Receptor 1 (CRF 1) and CRF 2 Agonists Exert an Anti-Inflammatory Effect During the Early Phase of Inflammation Suppressing LPS-Induced TNF- a Release From Macrophages via Induction of COX-2 and PGE 2. *Journal Of Cellular Physiology*, 783(September 2006), pp.774–783.

Tsatsanis, C. et al., 2005. Urocortin 1 and Urocortin 2 induce macrophage apoptosis via CRFR2. *FEBS letters*, 579(20), pp.4259–64.

Turgeman, T. et al., 2008. Prevention of muscle fibrosis and improvement in muscle performance in the mdx mouse by halofuginone. *Neuromuscular disorders : NMD*, 18(11), pp.857–68.

Turner, P. et al., 1993. Proteolysis results in altered leak channel kinetics and elevated free calcium in mdx muscle. *J Membr Biol*, May(133(3)), pp.243–51.

Vaillend, C. & Ungerer, a, 1999. Behavioral characterization of mdx3cv mice deficient in C-terminal dystrophins. *Neuromuscular disorders : NMD*, 9(5), pp.296–304.

Vale, W. et al., 1981. Characterization of a 41-residue ovine hypothalamic peptide that stimulates secretion of corticotropin and beta-endorphin. *Science*, 18(213(4514)), pp.1394–7.

Vallières, L. et al., 2002. Reduced hippocampal neurogenesis in adult transgenic mice with chronic astrocytic production of interleukin-6. *The Journal of neuroscience : the official journal of the Society for Neuroscience*, 22(2), pp.486–92.

Vallières, L. & Rivest, S., 1999. Interleukin-6 is a needed proinflammatory cytokine in the prolonged neural activity and transcriptional activation of corticotropin-releasing factor during endotoxemia. *Endocrinology*, 140(9), pp.3890–903.

Vandebrouck, C. et al., 2002. Involvement of TRPC in the abnormal calcium influx observed in dystrophic (mdx) mouse skeletal muscle fibers. *The Journal of cell biology*, 158(6), pp.1089–96.

Vannucchi, M. et al., 2004. Functional activity and expression of inducible nitric oxide synthase (iNOS) in muscle of the isolated distal colon of mdx mice. *Muscle Nerve*, June(29(6)), pp.795–803.

Vannucchi, M.G. et al., 2001. Expression of dystrophin in the mouse myenteric neurones. *Neuroscience letters*, 300(2), pp.120–4.

Vannucchi, M.-G. et al., 2002. Interstitial cells of Cajal, enteric neurons, and smooth muscle and myoid cells of the murine gastrointestinal tract express full-length dystrophin. *Histochemistry and cell biology*, 118(6), pp.449–57.

Varghese, A.K. et al., 2006. Antidepressants attenuate increased susceptibility to colitis in a murine model of depression. *Gastroenterology*, 130(6), pp.1743–53.

Venihaki, M. et al., 2001. Corticotropin-releasing hormone regulates IL-6 expression during inflammation. *The Journal of clinical investigation*, 108(8), pp.1159–1166.

Vilquin, J.T. et al., 1998. Evidence of mdx mouse skeletal muscle fragility in vivo by eccentric running exercise. *Muscle & nerve*, 21(5), pp.567–76.

Vittorino, A. et al., 1994. Long-term Nasal Intermittent Positive Pressure Ventilation in Advanced Duchenne ' s Muscular Dystrophy. *Chest*, 105(2), pp.445–448.

Voorhees, J.L. et al., 2013. Prolonged restraint stress increases IL-6, reduces IL-10, and causes persistent depressive-like behavior that is reversed by recombinant IL-10. *PloS one*, 8(3), p.e58488.

Wagner, K.R., 2008. Approaching a new age in Duchenne muscular dystrophy treatment. *Neurotherapeutics : the journal of the American Society for Experimental NeuroTherapeutics*, 5(4), pp.583–91.

Waite, A. et al., 2009. The neurobiology of the dystrophin-associated glycoprotein complex. *Annals of medicine*, 41(5), pp.344–59.

Walker, J. et al., 2011. Psychiatric disorders in patients with immune-mediated inflammatory diseases: prevalence, association with disease activity, and overall patient well-being. *J Rheumatol Suppl*, Nov(88), pp.31–5.

Walsh, R.N. & Cummins, R.A., 1976. The Open-Field Test: a critical review. *Psychological bulletin*, 83(3), pp.482–504.

Wang, K., Grivennikov, S.I. & Karin, M., 2013. Implications of anti-cytokine therapy in colorectal cancer and autoimmune diseases. *Annals of the rheumatic diseases*, 72 Suppl 2, pp.ii100–3.

Wang, W. et al., 2013. Mutation analysis and prenatal diagnosis of families affected with Duchenne and Becker muscular dystrophy. *Zhonghua Yi Xue Yi Chuan Xue Za Zhi*, Feb(30(1)), pp.45–8.

Wehling-Henricks, M. et al., 2008. Major basic protein-1 promotes fibrosis of dystrophic muscle and attenuates the cellular immune response in muscular dystrophy. *Human molecular genetics*, 17(15), pp.2280–92.

Wehling-Henricks, M., Lee, J.J. & Tidball, J.G., 2004. Prednisolone decreases cellular adhesion molecules required for inflammatory cell infiltration in dystrophin-deficient skeletal muscle. *Neuromuscular disorders : NMD*, 14(8-9), pp.483–90.

Williams, B.Y.D.A. et al., 1993. Contractile properties of skinned muscle fibres from young and adult normal and dystophic (mdx) mice. *Journal Of Physiology*, (460), pp.51–67.

Winter, C.L. De et al., 2009. In vivo comparison of 2 -O-methyl phosphorothioate and morpholino antisense oligonucleotides for Duchenne muscular dystrophy exon skipping. *The journal of gene medicine*, (November 2008), pp.257–266.

Xia, Z., DePierre, J.W. & Nassberger, L., 1996. Tricyclic antidepressants inhibit IL-6, IL-113 and TNF-oL release in human blood monocytes and IL-2 and interferon- T in T cells. *Immunopharmacology*, 34, pp.27–37.

Yamasaki, K. et al., 1988. Cloning and expression of the human interleukin-6 (BSF-2/IFN beta 2) receptor. *Science*, Aug 12(241 (4867)), pp.825–8.

Yang, L., Luo, J. & Petrof, B.J., 1998. Corticosteroid Threapy does not alter the threshold for contraction-induced njury in dystrophic (MDX) mouse diaphragm. *Muscle and Nerve*, (March), pp.394–397.

Yiu, E. & Kornberg, A., 2008. Duchenne muscular dystrophy. *Neurol India*, 56(3), pp.236–247.

Yokota, T. et al., 2006. Expansion of revertant fibers in dystrophic mdx muscles reflects activity of muscle precursor cells and serves as an index of muscle regeneration. *Journal of cell science*, 119(Pt 13), pp.2679–87.

Yu, X.-W. et al., 2005. Inhibition of sarcoplasmic reticular function by chronic interleukin-6 exposure via iNOS in adult ventricular myocytes. *The Journal of physiology*, 566(Pt 2), pp.327–40.

Yusof, M. & Emery, P., 2013. Targeting Interleukin-6 in Rheumatoid Arthritis. *Drugs*, 73(4), pp.341–356.

Zeiger, U., Mitchell, C.H. & Khurana, T.S., 2010. Superior calcium homeostasis of extraocular muscles. *Experimental eye research*, 91(5), pp.613–22.

Zhang, L. et al., 2013. Exogenous interleukin-6 facilitated the contraction of the colon in a depression rat model. *Digestive diseases and sciences*, 58(8), pp.2187–96.

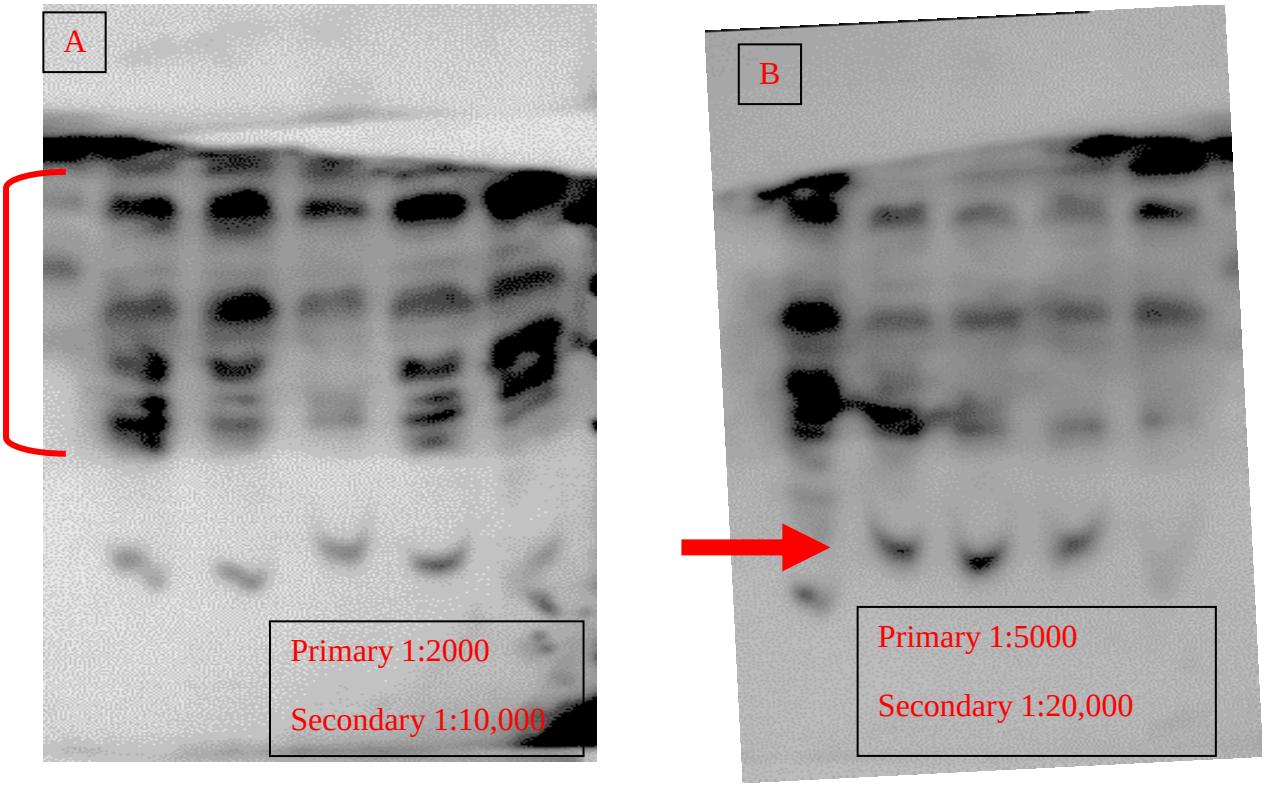
Zoumakis, E. et al., 2000. Corticotrophin-releasing hormone (CRH) interacts with inflammatory prostaglandins and interleukins and affects the decidualization of human endometrial stroma. *Molecular human reproduction*, 6(4), pp.344–51.

Appendix

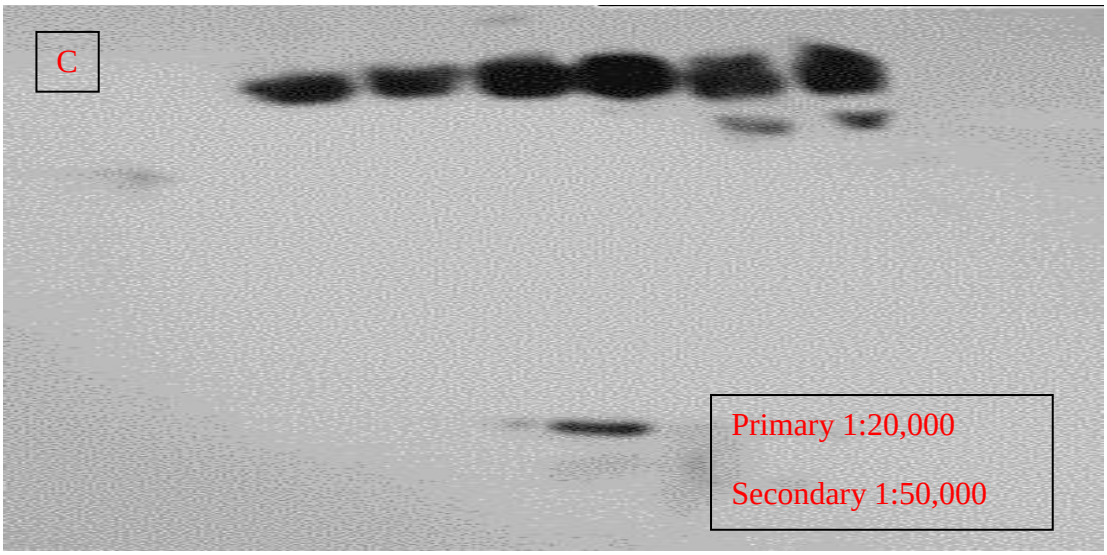
For our proteins of interest, therefore a starting point to prevent saturation of GAPDH (highly expressed, more so than IL-6 or IL-6R in tissues).

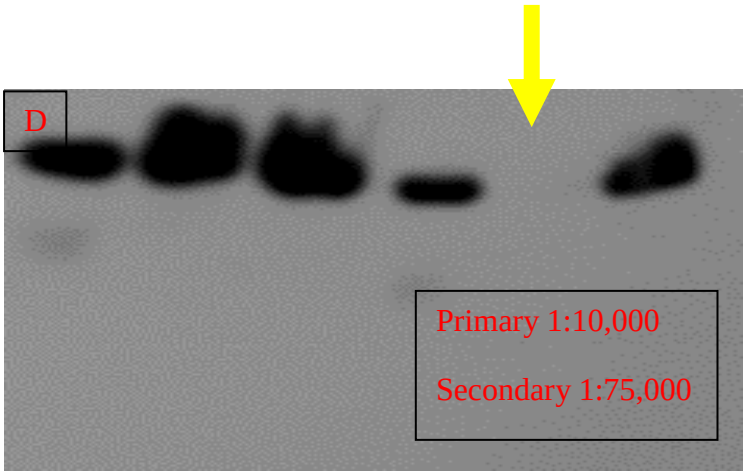
GAPDH

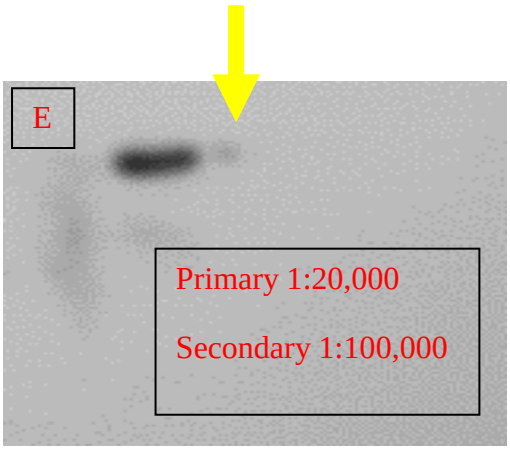
Protein expression per sample compared to GAPDH expression



Anti-GAPDH at 1:2000, secondary at 10:10,000 (A) produces a signal but high non-specific binding, as does a primary concentration of 1:5000, secondary at 1:20,000 (B), a reduction in current (optimised blots run for 90minutes at 100volts) to prevent unevening running of bands was performed at this stage.



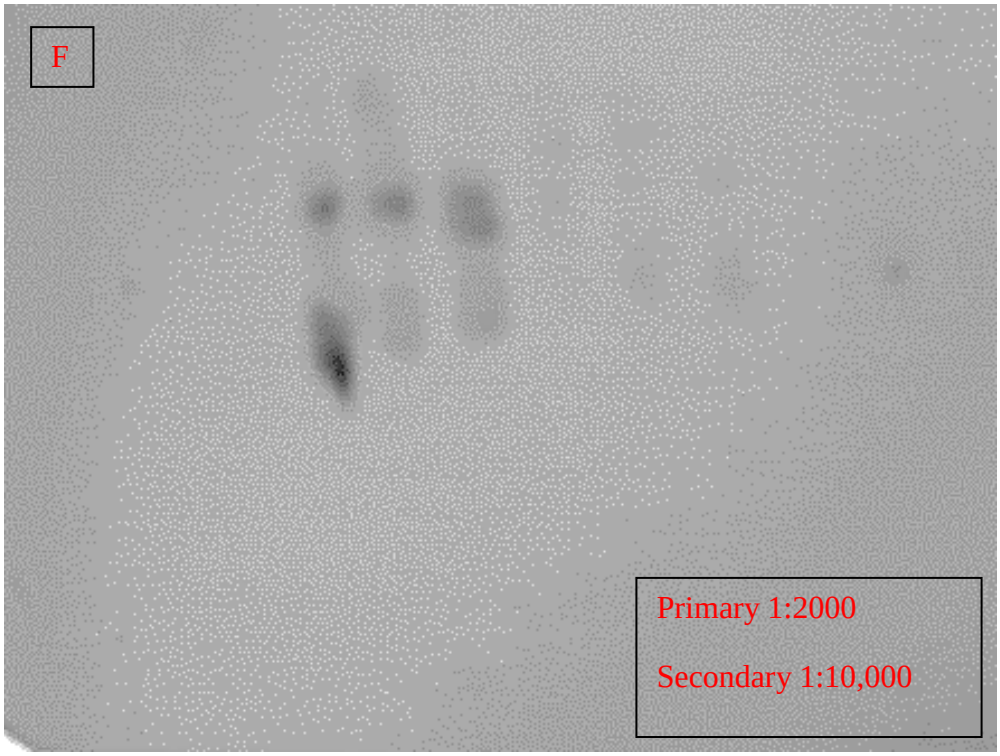


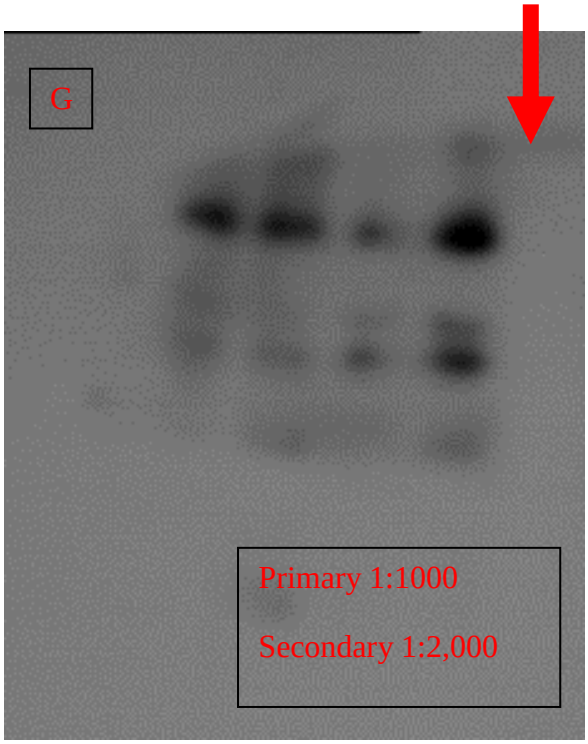


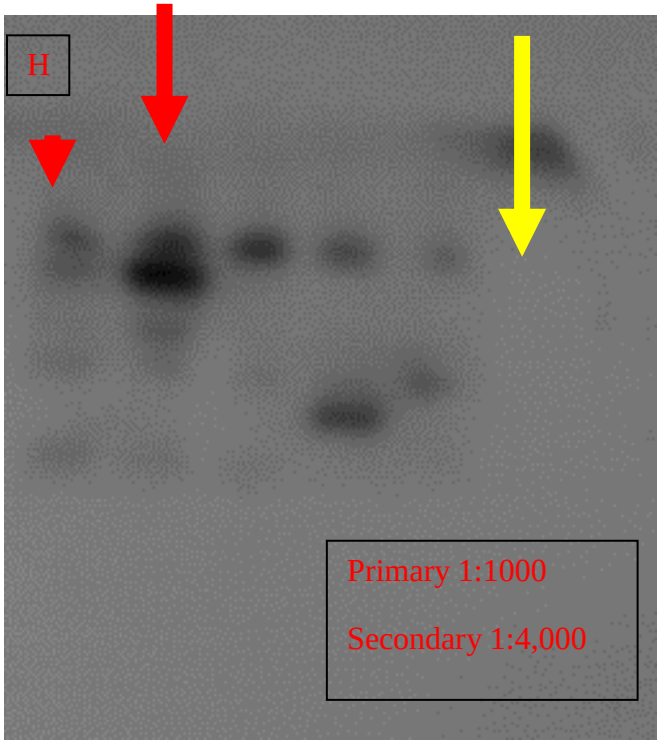
Final concentration used for GAPDH western blots was 1:20,000 with secondary concentration 1:100,000, reducing background, which is still apparent in 1:50,000 concentration in (C), in (D) a negative control (sample buffer without protein), and again in (E). (D) and (E) also reduce in antibody concentration.

IL-6R

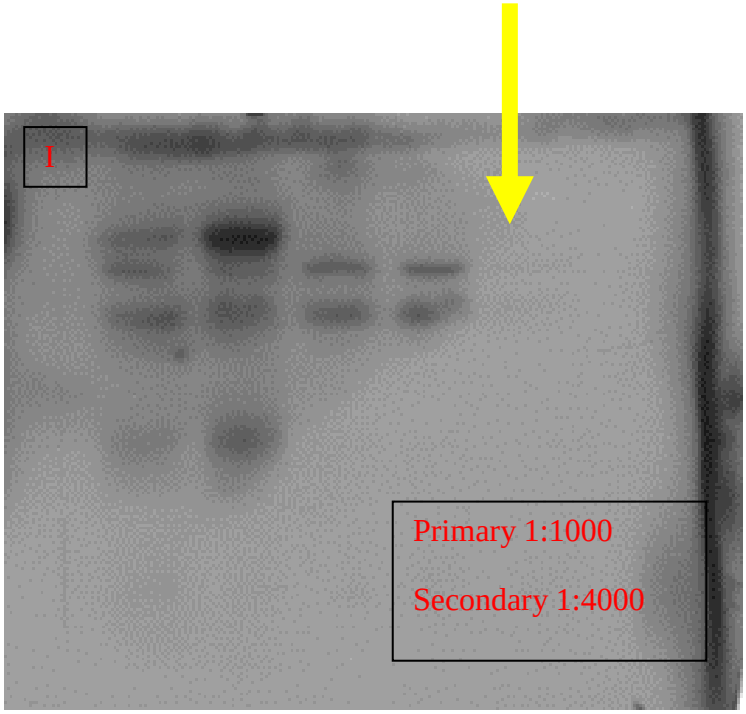
Previously optimised in laboratory with 40ug of protein at. 1:1000, secondary 1:5000.

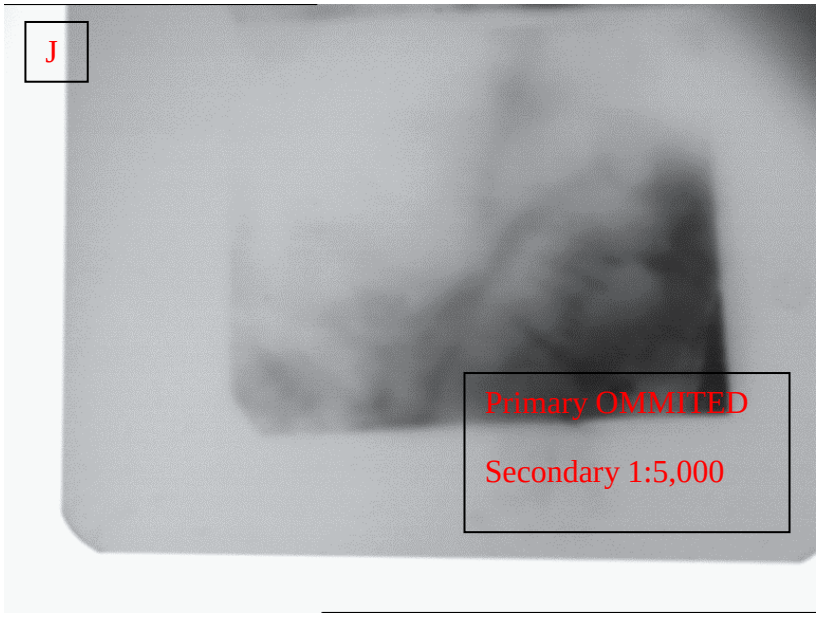






In (F), starting at a concentration of 1:2000 showed a faint signal and background, increasing concentration to 1:1000 and secondary of 1:2000 (G) produced high background as did 1:2000 and secondary of 1:4000, double banding (red arrows in (H)) represent dimerization of the IL-6 receptor at the predicted molecular weight, which is a result found in this specific protein (Schuster et al. 2003), yellow arrow represents a negative control lane (no protein in lane).

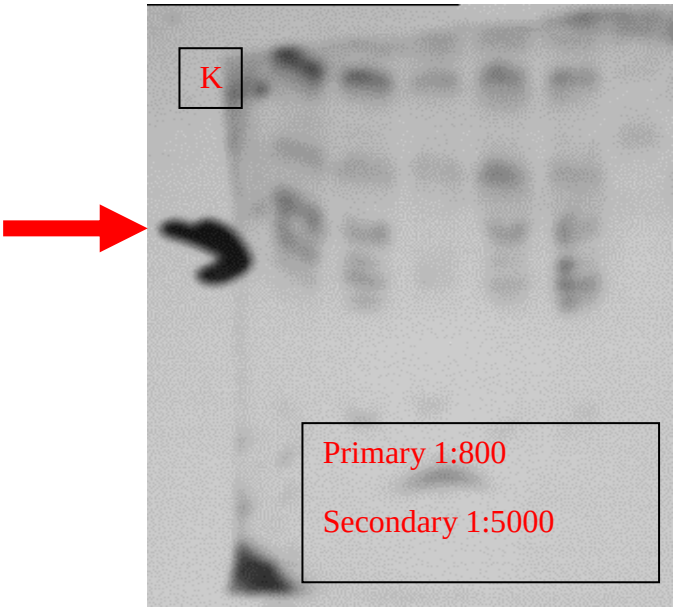


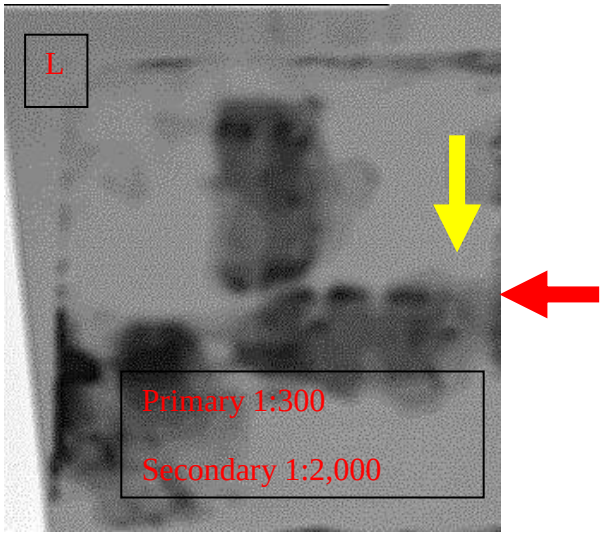


Yellow arrow in (I) represents a negative control, at this stage, washes were increased from 5X3 minutes to 10X3 minutes to remove any residual non-specific binding. (J) A primary omission was performed with secondary concentration of 1:5,000, no bands were visible.

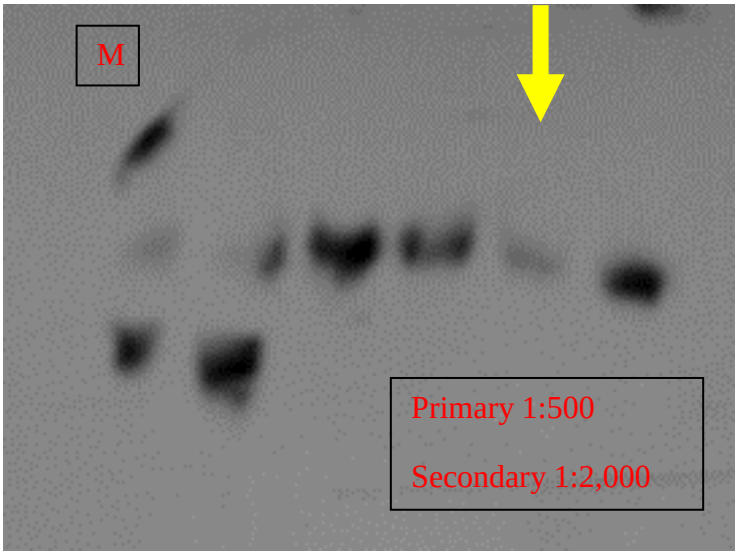
IL-6

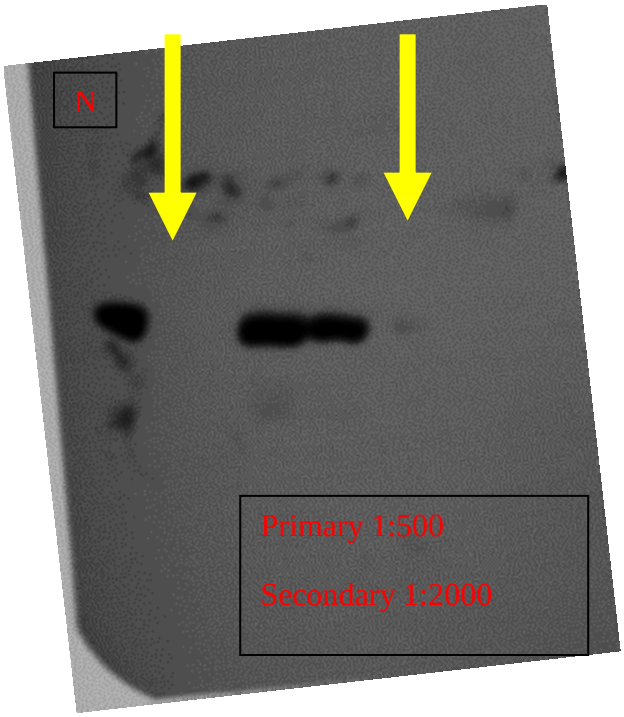
Previously used at 1:500 in rat tissue, secondary at 1:2000.





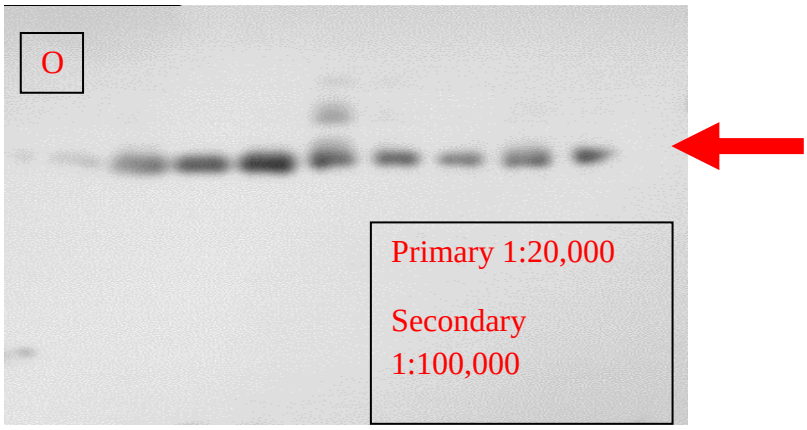
(K) and (L) show different antibody concentrations, arrows indicating IL-6 molecular weights, however high background signal was apparent and washes were increased (as with IL-6R) from 5X3 minutes to 10x3 minutes. The negative control in (L) is not obvious due to pooling of secondary antibody non-specific binding; this was overcome using a rotating incubation and an increase of volume of secondary antibody to reduce pooling in specific areas on the membrane.

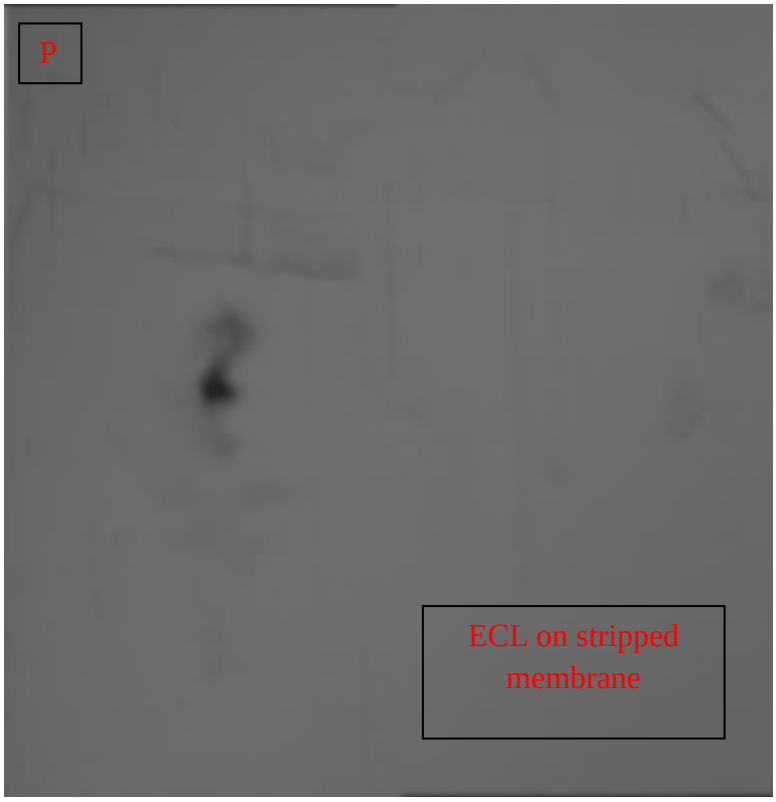




(M) and (N) are blots attempting to produce a signal with little background, negative controls (yellow arrow lanes) suggest low background, and bands at predicted molecular weights.

Loading control example





(O) is an example of loading controls, GAPDH 1:20,000, secondary 1:100,000. (P) is an example of a membrane which went through a stripping process to re-probe, in order to compare IL-6/IL-6R concentration to GAPDH expression, after membrane was stripped, it was re-ECLed, it is apparent no antibody producing signal is bound to the membrane.